Fundamental Studies Of Biomolecule Partitioning In Aqueous Polymer Two-phase Systems.

Order Number 9119351

Fundamental studies of biomolecule partitioning in aqueous polymer two-phase systems

Diamond, Alan David, Ph.D.

Lehigh University, 1991

U·M·I
300 N. Zeeb Rd.
Ann Arbor, MI 48106

Fundamental Studies of Biomolecule Partitioning in Aqueous Polymer Two-Phase Systems

by

Alan D. Diamond

A Dissertation
Presented to the Graduate Committee
of Lehigh University
in Candidacy for the Degree of
Doctor of Philosophy
in
Chemical Engineering

Lehigh University
1990

CERTIFICATE OF APPROVAL

Approved and recommended for acceptance as a dissertation in partial fulfillment of the requirements for the degree of Doctor of Philosophy.

James T. Hsu
Professor in Charge

Dec. 3, 1990
Date of Acceptance

Special committee directing
the doctoral work of
Alan D. Diamond

James T. Hsu
Dr. James T. Hsu

Arthur E. Humphrey
Dr. Arthur E. Humphrey

Janice A. Phillips
Dr. Janice A. Phillips

Michael J. Behe
Dr. Michael J. Behe

DEDICATION

to

my parents

Marvin and Sandra Diamond

with love

ACKNOWLEDGEMENT

During my studies at Lehigh University there were many people who influenced me and my research. Although I can not mention everyone's name who helped, I would like to express my sincere gratitude and appreciation to:

Professor James T. Hsu who provided me with the opportunity to do graduate research in the field of bioseparations. His guidance, knowledge, experience, creativity and strategies were the best of any person I encountered in my undergraduate and graduate studies. He taught me many lessons both in and out of the classroom, one of the most important of which was that working both smart and hard produces the best results. For these reasons and many more he commands my highest respect and admiration and sincere thanks.

Professors Arthur Humphrey, Janice Phillips and Mike Behe for their generous help and service on my Ph.D. committee.

My colleague and labmate Ulrich Ernst for providing insight into many chemical engineering problems and his comradery both in and out of the lab.

Kathleen Ferretti for proofreading and helping me prepare all of the figures for my dissertation.

Dr. Gary Poehlein at Georgia Tech for encouraging me to go to Lehigh University for graduate studies.

Xia Lei, a visiting scholar from China, and Kun Yu, a fellow graduate student, for help with laboratory experiments.

The National Science Foundation (through a research grant obtained by Professor Hsu), the National Institutes of Health, and the Department of Chemical Engineering at Lehigh University (through an Air Products Fellowship and a Teaching Assistantship) for financial support during my graduate studies.

TABLE OF CONTENTS

LIST OF TABLES

LIST OF FIGURES

ABSTRACT

Fundamental studies have been performed on aqueous two-phase systems with the goal of understanding the thermodynamics of their phase separation and biomolecule partitioning, thereby facilitating their selection and scale-up for the commercial purification of biological materials. The significant findings in this dissertation are as follows:

1. Phase diagrams have been measured for the poly(ethylene glycol) (PEG)/dextran/water and PEG/potassium phosphate/water systems at 4°C, 10°C and 22°C. The equilibrium data were correlated with first order semilogarithmic expressions derived from a modified form of the Flory-Huggins theory of polymer solution thermodynamics. The phase diagram data were then used for the prediction of biomolecule partitioning.

2. Utilizing a modified form of the Flory-Huggins theory, both first and second order semilogarithmic relationships were presented for correlation of biomolecule partition coefficients. The relations were verified by partitioning dipeptides and proteins covering a wide range of molecular weight in the PEG/dextran, PEG/potassium phosphate and ficoll/dextran aqueous two-phase systems. The first order relationship was found to be applicable to dipeptides and proteins with molecular weight below 25,000. The second order relationship was found to be applicable to peptides and proteins regardless of their molecular weight, when partitioned in the above systems. These correlating equations will be extremely powerful for the selection and

engineering scale-up of aqueous two-phase systems for biomolecule purification.

3. The effect of amino acid sequence on protein partitioning was investigated by partitioning twenty-three pairs of reversed sequence dipeptides, twenty amino acids, β-lactoglobulins A and B, horse and pig insulin, and horse, dog and pig cytochrome c in the PEG 3400/potassium phosphate/water phase diagram at 20°C. The dipeptide and amino acid partition data were utilized to obtain a predictive equation for peptide and protein partition coefficients based on amino acid sequence. The equation was used to successfully predict the partition of homogeneous glycine peptides containing two to five residues, and several tripeptides, and the ratio of β-lactoglobulin A and B partition coefficients, along with the ratio of horse to pig insulin partition coefficients.

CHAPTER I
AQUEOUS TWO-PHASE SYSTEMS: AN OVERVIEW

1.1 Introduction

The impetus for research in the field of bioseparations has been sparked by the difficulty and complexity in the downstream processing of pharmaceutical and biological products. There is a need for efficient, effective and economical large-scale bioseparation techniques which will achieve high purity and high recovery, while maintaining the biological activity of the molecule. One such purification technique which meets these criteria involves the partitioning of biomolecules between two or more immiscible phases in an aqueous system.

The multiphase aqueous system has been a topic of interest for some time, and was first reported in the literature by Beijerinck (1896, 1910). He discovered that when gelatin, agar and water were mixed at certain concentrations, an aqueous two phase system would result, the top phase being rich in gelatin, while the bottom phase rich in agar. In 1947, Dobry and Boyer-Kawenoki (1947) performed a systematic study on the miscibility of pairs of polymers in the presence of water or organic solvents. They found that phase separation was rather commonplace. In the 1940's and 50's Craig and Craig (1956) pioneered the use of organic/aqueous two phase systems for protein purification using countercurrent distribution. However, it was not until 1955 that Per-Åka Albertsson, a Swedish biochemist, discovered that poly(ethylene glycol) (PEG), potassium phosphate and water, and then PEG, dextran and water formed two-phases (Walter *et al.*, 1985).

Since their discovery in 1955, aqueous polymer two-phase systems have been studied at great length, and have been the topic of a number of interesting reviews (Albertsson, 1986; Walter *et al.* 1985; Abbot and Hatton, 1988; Carlson, 1988; Johansson, 1974; Kroner *et al.*, 1982). The systems depend on the immiscibility of aqueous solutions of incompatible polymers such as PEG and dextran. At appropriate concentrations, the solvated polymers cause a phase separation. The upper phase is rich in PEG whereas the lower phase is dextran rich. The phases offer different physical and chemical environments which allow for the partitioning of solutes such as proteins and nucleic acids. The differences in the phases are small (Albertsson, 1986), and therefore preclude the harsh treatment offered by traditional extraction systems. For example, the phases of PEG/dextran/water systems contain between 80% and 99% water by weight, possess extremely low interfacial tensions (on the order of 10^{-2} dyne/cm), and have been shown to provide a protective environment for biological materials (Albertsson, 1986). This compares rather favorably with organic solvent/water systems, such as butanol/water and ethanol/aqueous salt solutions pioneered by Craig and Craig (1956). Such systems have high interfacial tensions (on the order of 10^{1} dyne/cm) and organic phases containing only 40% to 50% water. These conditions lead to several problems, including precipitation and denaturation effects, and concentration of biological materials exclusively in the aqueous phase. These deleterious effects can be avoided through the use of aqueous polymer two-phase systems.

Aqueous polymer two-phase systems are extremely powerful for the separation and analysis of biological particles. Over the past three decades, many researchers have applied these systems to laboratory-scale separation of proteins, cells, cell organelles, viruses, cell membrane fragments and other

biological materials (Albertsson, 1986; Walter *et al.*, 1985; Fisher and Sutherland, 1989). Shanbhag, Walter, Zaslavsky and other researchers have utilized these systems as a means for determining surface properties of biomolecules such as charge and hydrophobicity (Shanbhag and Axelsson, 1975; Walter *et al.*, 1976; Zaslavsky *et al.*, 1979, 1978, 1982a,b, 1983). The application of aqueous polymer two-phase systems to large-scale purification of proteins has also been demonstrated using centrifuges as extractors (Hustedt *et al.*, 1978; Kroner *et al.*, 1982, 1984; Tjerneld *et al.*, 1987). The main advantages of using such systems include their gentleness toward biological materials, ability to offer good resolution factors and activity yields, high volume capacity, and ease of scale-up. In particular, the ease of scale-up is demonstrated by the fact that the partition coefficient is essentially independent of the volume of the system (Albertsson, 1986). However, the main disadvantages include the lack of a means for characterizing aqueous biphasic systems, the lack of a methodology for selecting the proper system for protein purification, the absence of a generalized method for correlating biomolecule partitioning, and the difficulty in separating the two phases due to a phase density difference of usually no more than 0.05 g/mL. The difficulty in separating the two phases may adequately be handled through the use of centrifugation.

In order to overcome the first three disadvantages listed above, a fundamental understanding of aqueous two-phase separation and biomolecule partitioning is necessary. Traditionally, selection of an aqueous two-phase system for purification, and prediction of partitioning therein, has been dealt with using empiricism and tedious experimentation (Albertsson, 1986). The variables affecting phase equilibrium and protein distribution include pH (Albertsson *et al.* 1970), salt type and concentration (Johansson, 1970;

Albertsson, 1971), hydrophobicity (Shanbhag and Axelsson, 1975; Zaslavsky *et al.* 1978) and biomolecule and polymer molecular weight (Hustedt *et al.*, 1978; Albertsson *et al.*, 1987) thus making the search for an optimal system extremely difficult. In this thesis, a means will be established for characterizing aqueous two-phase systems, and correlating partition coefficients based on the thermodynamic solution theory developed by Flory (1941) and Huggins (1941). In particular, simple semilogarithmic relationships will be obtained which permit the prediction of phase separation and biomolecule partitioning in aqueous two-phase systems. In addition, a means for correlating a protein's primary structure with its partition coefficient will be presented.

1.2 Research Objectives

In this thesis, an investigation of phase separation and solute partitioning in aqueous two-phase systems will be presented. The results of these studies will strengthen our understanding of the molecular mechanisms, thermodynamics, and kinetics of aqueous two-phase systems. The distribution of the phase forming polymers will be investigated and serve as a means for predicting biomolecule partitioning based on the Flory-Huggins theory of solution thermodynamics and protein structure.

Hence, the proposed research will proceed along three tracts which are as follows:

1. Determination of phase diagrams for aqueous two-phase systems not available in the open literature and characterization of these systems using the Flory-Huggins theory of polymer solution thermodynamics.

2. Correlation of biomolecule partitioning using the above phase equilibrium data and the Flory-Huggins theory.

3. Investigation of the effect of protein structure on the partition phenomenon.

The background and research plan for each stage will now be discussed.

1.2.1 Experimental Determination and Characterization of Aqueous Two-Phase Systems.

1.2.1.1 Background

There are several explanations in the literature for phase separation in aqueous systems containing either two polymers and water, or a polymer, an inorganic salt and water. The two most important views on phase separation are the one advocated by Brooks *et al.* (1984) and Gustafsson and Wennerström (1986), and the other proposed by Zaslavsky *et al.* (1989). The reason for their existence is the lack of a comprehensive, aqueous two-phase system, phase diagram data base for their analysis. The most extensive source of phase diagram data is that provided by Albertsson (1986), but this is still far from complete particularly with regard to the PEG/dextran/water and PEG/potassium phosphate/water phase systems.

Brooks, Gustafsson and co-workers have based their explanation for phase separation upon the polymer solution thermodynamics theory developed by Flory (1956) and Huggins (1956). This theory is the simplest and most basic for describing phase separation in polymeric systems. The simplest way to discuss their hypothesis is to first present the general expression for the Gibbs free energy of mixing at constant temperature and pressure:

$$\Delta G_m = \Delta H_m - T\Delta S_m \tag{1.1}$$

where ΔG_m, ΔH_m, ΔS_m and T refer to the Gibbs free energy of mixing, the enthalpy of mixing, the entropy of mixing, and absolute temperature, respectively. If ΔG_m is negative when the two polymers are mixed with water, a solution will result without phase separation. If ΔG_m is positive, phase separation will occur. The Flory-Huggins theory suggests that if polymer solution concentrations are low, then there will only be a small gain in entropy upon mixing the polymers in water. However, since polymer chains have a much higher surface area per molecule than do low molecular weight compounds, the interaction between segments of the two polymer molecules, which are generally unfavorable, will lead to a positive ΔH_m which will dominate the ΔG_m expression (Flory, 1956). The positive ΔG_m will result in phase separation.

Zaslavsky *et al.* (1989) have advocated a different explanation for phase separation. They point out that the structure of water molecules will be different in the presence of the two polymers. In other words the interactions of the polymers with water are extremely important in governing whether or not phase separation will occur. This reasoning was based on the fact that they found the physico-chemical properties of water (dielectric relaxation time, static dielectric constant, relative affinity of water for a CH_2 group and overall polarity) in the coexisting phases of the systems were different (Zaslavsky *et al.*, 1989).

In order to fully understand the phase separation phenomenon described above and develop a thermodynamic model for its prediction, the most

fundamental data needed are phase diagrams. Without these, the full potential of aqueous two-phase systems will never be realized since the phase diagrams and a sound thermodynamic theory are needed to predict protein and biomolecule partition coefficients.

1.2.1.2 Research Plan

A comprehensive set of phase diagram data is needed in order to understand the partition phenomenon, facilitate the use of aqueous polymer systems for protein purification and to aid in the development of thermodynamic models for their prediction. Furthermore, phase diagram data are needed for the eventual correlation of protein partitioning. The most extensive source of such data is that presented by Albertsson (1971, 1986). However these data are far from complete, particularly with regard to the PEG/dextran/water and PEG/potassium phosphate/water systems at 4°C, 10°C and 22°C. Since purification of labile biomolecules frequently occurs at low temperatures, the data at 4°C and 10°C are of extreme importance for biochemical research. Aqueous two-phase systems may also be used at room temperature due to the fact that the polymers tend to stabilize the partitioning biomolecules. Hence, the specific objective of this research is to obtain phase equilibrium concentrations for the above systems at these three temperatures and use these data to develop a thermodynamic model based on the Flory-Huggins theory of thermodynamics for phase separation.

1.2.2 Biomolecule Partitioning in Aqueous Two-Phase Systems

1.2.2.1 Background

The partition coefficient of a biomolecule has empirically been found to be a function on numerous parameters. Albertsson (1986) proposed the following relationship for complex macromolecules such as proteins:

$$\ln K = \ln K^{\circ} + \ln K_{elec} + \ln K_{hfob} + \ln K_{size} + \ln K_{biosp} + \ln K_{conf} \quad (1.2)$$

where hyfob, size, biosp, conf stand for hydrophobic, size, biospecific and conformational contributions to the partition coefficient and K° includes other factors. Alternatively, the partition coefficient may be expressed as:

$$\ln K = \ln K_{environment} + \ln K_{structure} \quad (1.3)$$

The partition coefficient of a biomolecule is a function of the environmental conditions, such as phase forming polymer type, concentration and molecular weight, salt type and concentration, pH and temperature, and the structural properties of the biomolecule, such as its primary, secondary, tertiary and quaternary structure, molecular weight, net charge, hydrophobicity and surface properties. In order to predict biomolecule partitioning in aqueous two-phase systems, a fundamental understanding of each of the above factors is ultimately needed.

Several theoretical models have been proposed for the thermodynamic behavior protein partitioning in aqueous two-phase systems. Brooks *et al.* (1985) and Albertsson (1987) have shown that the lattice model of Flory (1941) and Huggins (1941) could be used to qualitatively predict protein partition trends. Baskir *et al.* (1987) have modified the theory of Scheutjens and Fleer (1979, 1980) to predict protein partitioning, while King *et al.* (1988) extended

the solution theory of Edmond and Ogston (1968) by taking into account the electrostatic potential difference between the phases. The advantages and disadvantages of the above models has been discussed in detail by Baskir *et al.* (1989). Gustafsson and Wennerström (1986) attempted to predict a binodial of the PEG/dextran aqueous two-phase system using Flory-Huggins theory, while Kang and Sandler (1987) attempted to analyze PEG/dextran binodials using both the Flory-Huggins theory and the UNIQUAC equation (Abrams and Prausnitz, 1975). However, a generalized correlation for protein partitioning, which is needed in order to facilitate the use of aqueous two-phase systems, has not resulted.

1.2.2.2 Research Plan

In order to predict solute partitioning in aqueous two-phase systems an expression must be obtained for the partition coefficient as a function of measurable parameters. According to Flory-Huggins theory, the natural logarithm of the partition coefficient for a partitioning species (3), in a system composed of water (0), PEG (1) and dextran (2), can be expressed as a function of the volume fraction of the phase forming components. If it is assumed that the partitioning molecule is present in low concentrations relative to PEG and dextran, the Flory-Huggins expression for the partition coefficient of component (3), K_3, may be expressed as (Diamond and Hsu, 1989a; Diamond and Hsu, 1990a,b):

$$\ln(K_3) = A(w_1'' - w_1') \tag{1.4}$$

or,

$$\frac{\ln(K_3)}{(w_1'' - w_1')} = A^* + b^*(w_1'' - w_1') \qquad (1.5)$$

where w refers to the weight fraction of phase forming polymer number 1, the symbols A, A^* and b^* are constants which are a function of phase forming polymer molecular weight, the interactions among the protein, polymers and water, pH, salt type and concentration, and the single and double prime superscripts refer to the bottom and top phase, respectively.

The validity of these relationship will be tested by partitioning dipeptides and proteins in PEG/dextran/water, PEG/potassium phosphate/water and ficoll/dextran/water systems. Ficoll, which is a synthetic polymer of sucrose available from Pharmacia-LKB, will form two phases with dextran. The upper phase is rich in dextran and the lower phase is rich in ficoll (Albertsson, 1986). The dipeptides glycylglycine, glycylalanine, glycyl-α-aminobutyric acid, and glycylnorvaline, which differ from one another by the addition of a CH_2 group on the c-terminal residue, will be utilized in the study. In other words, the dipeptides contain 0, 1, 2, and 3 CH_2 groups on the c-terminal residue, respectively. These dipeptides have been chosen because they enable the determination of the effect of a CH_2 on the partition coefficient of a biomolecule.

Proteins covering a range of molecular weights will also be partitioned in the aqueous two-phase systems according to the above relationships. The proteins to be used and their molecular weights are as follows : lipase (6,669 MW), cytochrome c (12,400 MW), ribonuclease (12,600 MW), lysozyme (13,900 MW), myoglobin (16,900 MW), trypsin (23,300 MW), rhodanese (37,570 MW), ovalbumin (44,000 MW), α-amylase (45,000 MW), bovine serum albumin (67,500 MW), transferrin (77,000 MW), conalbumin (86,810 MW), hexokinase

(102,000 MW), alcohol dehydrogenase (145,000 MW), invertase (270,000 MW) and thyroglobulin (669,000 MW).

The effects of phase forming polymer concentration, molecular weight, biomolecule molecular weight and system temperature on the partition coefficient will be investigated for the dipeptide and protein partitioning.

1.2.3 Investigation of the Effect of Protein Structure on the Partition Phenomenon

1.2.3.1 Background

The partition coefficient of a protein will ultimately be a function of its primary, secondary, tertiary and quaternary structures, which in turn are a function of the environmental conditions. Sasakawa and Walter (1971, 1972, 1974) first examined the behavior in aqueous two-phase systems of some closely related proteins of known structure and chemical and physiological properties. They found that, while the molecular weights of homologous hemoglobins are essentially the same, significant differences in the partitioning of hemoglobins A and F as well as mammalian hemoglobins were evident in PEG/dextran/water systems. Human hemoglobin A had the highest K, 0.43; dog hemoglobin, 0.36; horse, 0.29; rabbit, 0.27 and pig hemoglobin the lowest, 0.20.

Previously, aqueous two-phase systems have been used to study protein secondary and tertiary structure. Andreasen (1981) had used aqueous two-phase partitioning to characterize the transformation process of the rat liver glucocorticoid receptor and to characterize aberrant receptor properties from cultured mouse lymphoma cells (Andreasen and Gehring, 1981). Recently, Hansen and Gorski (1985) have shown that the unoccupied estrogen receptor

(ER) has a higher partition coefficient (more hydrophobic) than the nontransformed (without heat treatment) ER.

In order to gain a fundamental understanding of the effect of protein or biomolecule primary structure on the partition coefficient, amino acids (which are the building blocks of peptides and proteins), reversed sequence dipeptides, homologous and structurally related proteins, and reversed sequence dinucleotides will be partitioned in aqueous two-phase systems. These data will be used to develop a model for predicting protein partitioning based on primary structure.

1.2.3.2 Research Plan

In this section of the proposed research, light will be shed on the effect of protein structure on the partition coefficient. First, twenty-three pairs of dipeptides which differ from one another by reversing the amino acid sequence will be partitioned in a variety of aqueous two-phase systems to determine which systems are sensitive enough to distinguish between these molecules. Particular effort will be focused on the PEG/dextran/water and PEG/potassium phosphate/water systems, since preliminary work has demonstrated that they are rather sensitive to slight changes in protein structure.

In the next stage of the research, twenty amino acids which make up the dipeptides will be partitioned in the selected systems. Their partition coefficients, along with that of the dipeptides, will be used for the development of an expression that can be used for the prediction of protein partition coefficients based on primary structure. After devlopment of the predictive

equation, partition coefficients for similar proteins such as β-lactoglobulins A and B, and homologous proteins such as horse, dog and pig cytochrome c and horse and pig insulin will be measured in the sensitive aqueous two-phase systems. The correlating equation will then be used to predict the partition coefficients of these molecules based on their amino acid sequence.

CHAPTER II
THERMODYNAMICS OF AQUEOUS TWO-PHASE SYSTEMS AND BIOMOLECULE PARTITIONING

In this chapter, the thermodynamic expressions for aqueous two-phase systems which will be used in subsequent chapters for the description of phase diagram behavior and biomolecule partitioning will be developed.

2.1 Introduction

In order to predict solute partitioning in aqueous two-phase systems, an expression must be obtained for the partition coefficient as a function of measurable parameters. The Flory-Huggins theory, though simplistic in nature, represents the classical approach for describing the thermodynamics of phase separation in polymer systems. According to this theory, the polymers are linear (monodisperse), long chained random coils, while the solvent is monomeric. The geometry of the polymer and solvent are considered essentially identical. The polymer and solvent molecules exist in the form of a single lattice scheme, each cell of which may be occupied by either a solvent molecule or the segment on a linear polymer. The entropy change on mixing is a combinatorial term reflecting the variety of ways of arranging the polymers and solvent in the lattice, while the heat of mixing represents the energy change associated with the formation of contacts between unlike neighbors in the lattice.

Various workers have applied the Flory-Huggins theory to aqueous two-phase systems and have shown that it provides a satisfactory quantitative

description of phase separation (Kang and Sandler, 1987; Gustafsson and Wennerström, 1986) as well as a qualitative description of the solute partitioning phenomena (Brooks *et al.*, 1985; Albertsson *et al.* 1987). In order to apply this theory to aqueous polymer systems, several simplifying assumptions must be made, the most important of which are as follows: The first assumption is that the phase forming polymers and partitioning solutes (biologicals) can be treated as linear (monodisperse), homogeneous, polymeric species in which the tertiary structure is that of a random coil. This assumption has been demonstrated to be valid for PEG and dextran (Gustafsson and Wennerström, 1986). Since proteins may consist of one, two, or possibly several polypeptide chains connected by disulfide bonds, the degree of branching is generally small, and the proteins may only be crudely approximated as linear polymers. One must keep in mind that proteins tend to be globular in nature with their structures being held together by intrachain covalent bonding, hydrogen bonding, ionic interactions and hydrophobic interactions (Lehninger, 1982). The dipeptides may be approximated as small linear polymers in the sense that they consist of only a single chain containing two amino acid residues. The second assumption is that the partitioning solute concentration is small relative to the phase forming polymers and water. This is usually the case when working with proteins. It should be pointed out that, in this work, peptide and protein concentrations were 0.03 and 0.10 %(w/w), respectively, while PEG and dextran concentrations were on the order of 2 to 11 %(w/w) in the total system. The third assumption is that the phase compositions do not significantly change in the presence of the partitioning solute. This assumption stems from the second assumption, in which the solute concentration will be small enough so as not to have an effect on the

distribution of the phase forming polymers.

2.2 The Thermodynamics of Phase Diagrams

The generalized expression for the entropy and enthalpy of mixing in a multicomponent system may be expressed as (Flory, 1953)

$$\Delta S_m = -k \sum n_i \ln v_i \tag{2.1}$$

and

$$\Delta H_m = kT \sum_{i<j} n_i v_j \chi_{ij} \tag{2.2}$$

where k is Boltzman's constant, n_i is the number of molecules of species i, T refers to absolute temperature, v_j is the volume fraction of species j, and χ_{ij} represents the Flory-Huggins interaction parameter for species i and j. In aqueous two-phase systems, the meaning of the interaction parameter will be modified to include hydrogen bonding and ionic and hydrophobic interactions, in addition to van der Waals forces. Using these two expressions, the Gibbs free energy of mixing at constant temperature and pressure can be expressed as:

$$\Delta G_m = kT\left(\sum_{i<j} n_i v_j \chi_{ij} + \sum n_i \ln v_i\right) \tag{2.3}$$

The chemical potential of a species can then be calculated by the partial differential:

$$\mu_i - \mu_i^{\circ} = N_A\left(\frac{\partial \Delta G_m}{\partial n_i}\right)_{n_j, T, P} \tag{2.4}$$

where μ_i is the chemical potential of species i, $\mathring{\mu_i}$ is the chemical potential in the standard state taken as the pure component species at the temperature and pressure of the mixture, N_A is Avogadro's number, T is absolute temperature and P refers to pressure. At equilibrium, the following condition must be satisfied:

$$\mu_i' = \mu_i'' \tag{2.5}$$

where single and double prime superscripts refer to the bottom and top phase, respectively. Substituting equation (2.4) into (2.5) gives:

$$N_A\left(\frac{\partial\, \Delta G_m'}{\partial n_i}\right)_{n_j,T,P} = N_A\left(\frac{\partial\, \Delta G_m''}{\partial n_i}\right)_{n_j,T,P} \tag{2.6}$$

Equations (2.4), (2.5) and (2.6) will serve as the starting point for the derivation of solute partition coefficient expressions in aqueous two-phase systems. First, a three component system composed of water (0), polymer (1) and polymer, or solute (2) will be considered. Later on in the chapter, the addition of protein will be explored (four component system). The subscripts 1 and 2 refer to PEG and dextran, respectively, for the PEG/dextran/water systems, and PEG and potassium phosphate, respectively, for the PEG/potassium phosphate/water systems. For the ficoll/dextran/water systems, 1 and 2 refer to dextran and ficoll, respectively. It should be pointed out that in the PEG/dextran/water system, dextran is enriched in the bottom phase and PEG in the top, while for the ficoll/dextran/water systems, ficoll predominates in the bottom and dextran in the top. For this reason, dextran is

given the subscript 2 in the PEG/dextran/water systems and 1 in the ficoll/dextran/water systems. For the three component system, the Gibbs free energy of mixing based on equation (2.3) may be expressed as:

$$\Delta G_m = kT(n_0 v_1 \chi_{01} + n_0 v_2 \chi_{02} + n_1 v_2 \chi_{12} + n_0 \ln v_0 + n_1 \ln v_1 + n_2 \ln v_2) \tag{2.7}$$

With the substitution of ΔG_m into equation (2.6), a series of three equations may be obtained, one for each of the components. For species (1), the result of the above substitution will yield, upon rearrangement, the following expression for the partition coefficient, K_1:

$$\ln (K_1) = m_1(v_0'' - v_0') + (v_1'' - v_1') + \frac{m_1}{m_2}(v_2'' - v_2') - \chi_{10}(v_0''^2 - v_0'^2)$$

$$+ (-\chi_{10} + m_1\chi_{02} - \chi_{12})(v_0'' v_2'' - v_0' v_2') - \chi_{12}(v_2''^2 - v_2'^2) \tag{2.8}$$

where $K_1 = (v_1''/v_1')$, m_i is the molar volume ratio of species i to water, and v_i and χ_{ij} have previously been defined. Equation (2.8) may be expanded by expressing v_0 as a function of v_1 and v_2 using the relations:

$$v_0'' = 1 - v_1'' - v_2'' \tag{2.9}$$

and

$$v_0' = 1 - v_1' - v_2' \tag{2.10}$$

Substituting equations (2.9) and (2.10) into equation (2.8) gives:

$$\ln(K_1) = m_1(v_1' - v_1'' + v_2' - v_2'') + (v_1'' - v_1') + \frac{m_1}{m_2}(v_2'' - v_2')$$

$$- \chi_{10}\Big((1 - v_1'' - v_2'')^2 - (1 - v_1' - v_2')^2\Big) + (-\chi_{10}$$

$$+ m_1\chi_{02} - \chi_{12}\Big)\Big((1 - v_1'' - v_2'')v_2'' - (1 - v_1' - v_2')v_2'\Big)$$

$$- \chi_{12}(v_2''^2 - v_2'^2) \tag{2.11}$$

Equation (2.11) may be simplified by making the assumption that second order terms containing v_1 and v_2 (i.e., v_1^2, v_2^2 and v_1v_2) may be neglected. This assumption is based on the fact that polymer concentrations (i.e., for species 1 and 2) are typically low, on the order of 0.5 to 10.0 %(w/w), in comparison to water which typically has a concentration between 85.0 and 95.0 %(w/w). With this assumption, equation (2.11) becomes:

$$\ln(K_1) = (1 - m_1 + 2\chi_{10})(v_1'' - v_1') + \Big(\frac{m_1}{m_2} - m_1 + \chi_{10}$$

$$+ m_1\chi_{02} - \chi_{12}\Big)(v_2'' - v_2') \tag{2.12}$$

Factoring m_1 from the right hand side of equation (2.12) and letting the interaction parameter χ_{ij} refer to the interaction intensity per segment, the following relation is obtained:

$$\ln(K_1) = m_1\Bigg(\Big(\frac{1}{m_1} - 1 + 2\chi_{01}\Big)(v_1'' - v_1')$$

$$+ \Big(\frac{1}{m_2} - 1 + \chi_{01} + \chi_{02} - \chi_{12}\Big)(v_2'' - v_2')\Bigg) \tag{2.13}$$

The phase compositions for the aqueous polymer phase diagrams presented in the literature (Albertsson, 1986) and in Chapter III are expressed as weight percent rather than volume percent. However, the Flory-Huggins theory utilizes volume rather than weight fractions. In order to facilitate the correlation of these phase data, it would be beneficial to express equation (2.13) in terms of weight fraction. This may be accomplished by first noting that

$$v_i = \rho \overline{V}_i w_i \tag{2.14}$$

where ρ is the density of the aqueous polymer phase, $\overline{V}_i$ is the partial specific volume of species i, and w_i is the weight fraction of species i. Therefore, the volume fraction difference between the phases for species i is given by :

$$v_i'' - v_i' = \rho'' \overline{V}_i w_i'' - \rho' \overline{V}_i w_i' \tag{2.15}$$

The densities of the top and bottom phases in aqueous two-phase systems are similar to that of water (approximately 1.0 g/ml) and usually differ from one another by no more than 0.05 g/ml (Albertsson, 1986). Therefore, if it is assumed that the densities of the top and bottom phases are equivalent, equation (2.15) may be expressed as :

$$v_i'' - v_i' \doteq 1.0 \overline{V}_i (w_i'' - w_i') \tag{2.16}$$

According to Edmond and Ogston (1968), the partial specific volume of dextran and PEG are constant over a broad range of molecular weight fractions.

Therefore, equation (2.16) may be rewritten as:

$$v_i'' - v_i' \doteq \alpha_i(w_i'' - w_i') \tag{2.17}$$

where $\alpha_i = 1.0\overline{V}_i$ and is assumed to be constant. Substituting equation (2.17) into equation (2.13) for both dextran and PEG yields:

$$\ln(K_1) = m_1\left(\left(\frac{1}{m_1} - 1 + 2\chi_{01}\right)\alpha_1(w_1'' - w_1') + \left(\frac{1}{m_2} - 1 + \chi_{01} + \chi_{02} - \chi_{12}\right)\alpha_2(w_2'' - w_2')\right) \tag{2.18}$$

In order to further simplify equation (2.18), the weight percent ratio ϕ may be defined as:

$$\phi = \frac{w_2'' - w_2'}{w_1'' - w_1'} \tag{2.19}$$

In Figure 2.1, the quantity ϕ has been plotted versus the PEG concentration difference between the phases for the PEG/dextran/water systems at 4°C. The phase compositions used for this plot are presented in Chapter III (Figures 3.1–3.9). In Figure 2.2 similar plots are shown for the PEG 3400/potassium phosphate/water system at 20°C and the Ficoll 400/Dextran T-500/water system at 23°C, the data for both systems being obtained from Albertsson (1986). The above three system types have been selected since future partitioning studies will be done with these systems. Figures 2.1 and 2.2 reveal that ϕ is relatively constant, with an average value of –2.1, for the PEG/dextran/water, PEG 3400/potassium phosphate/water and Ficoll

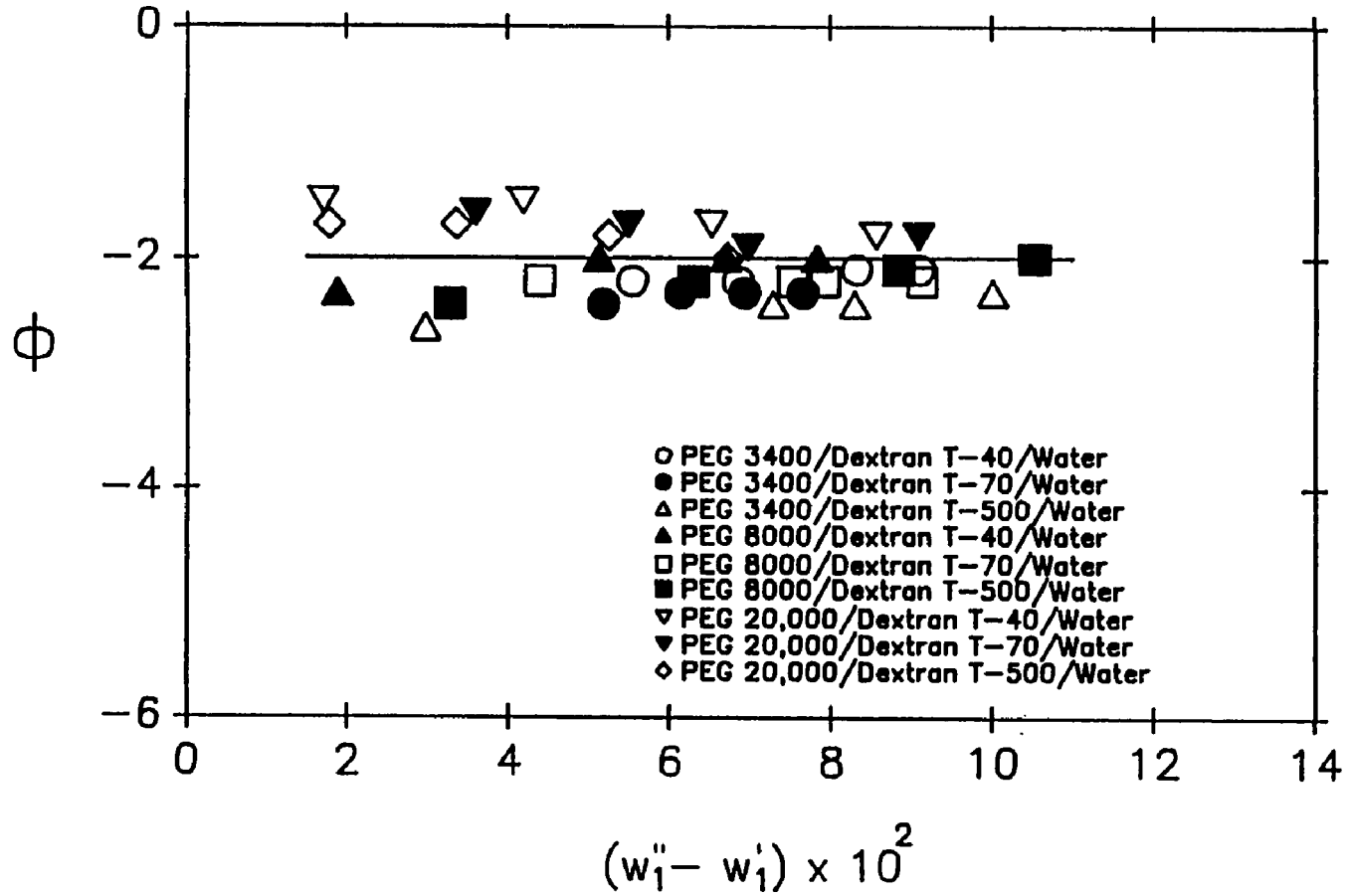

Figure 2.1 Weight Percent Ratio, ϕ, Versus PEG Concentration Difference in the PEG/Dextran/Water Systems at 4°C.

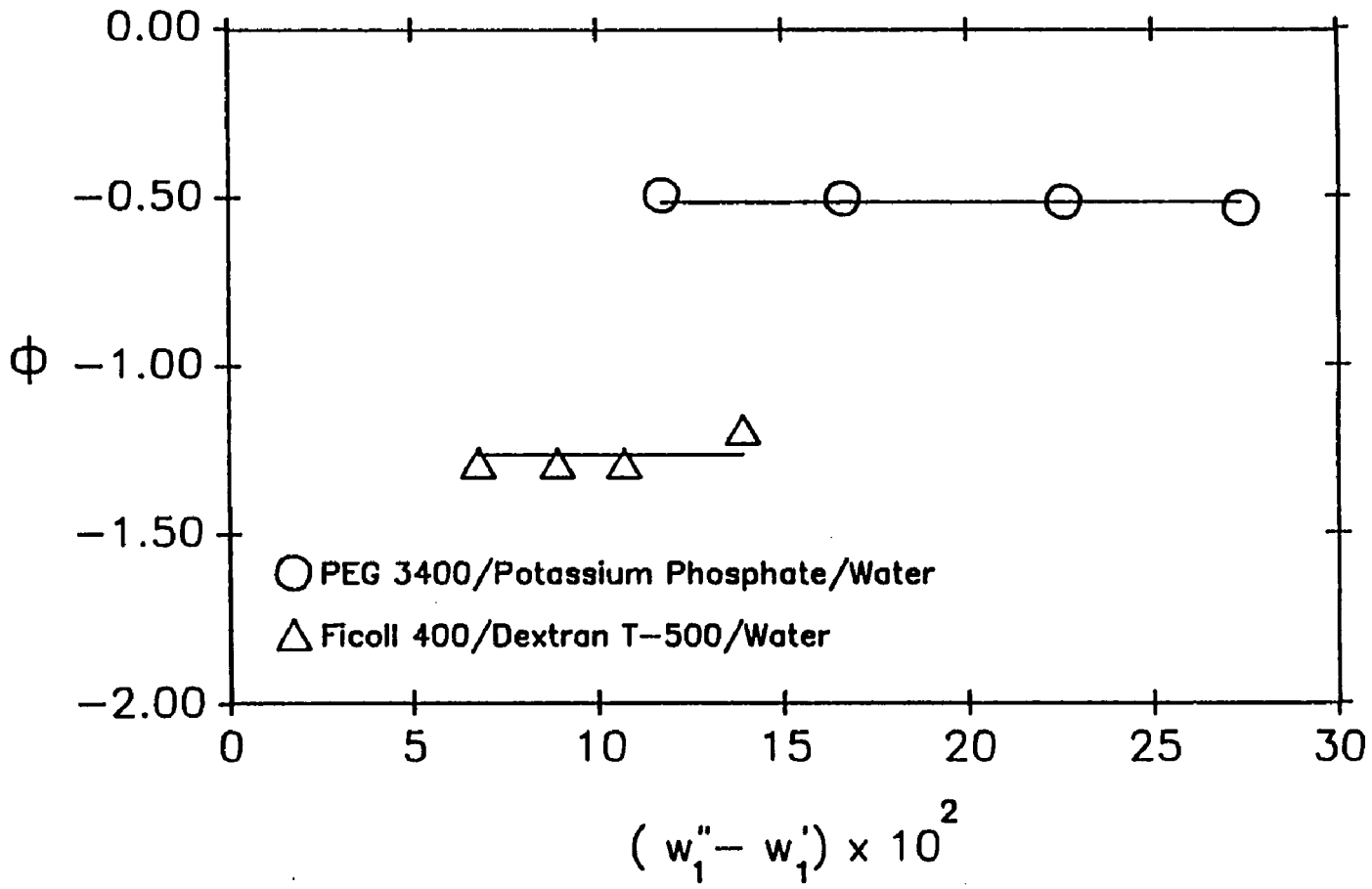

Figure 2.2 Weight Percent Ratio, ϕ, Versus PEG Concentration Difference in the PEG 3400/Potassium Phosphate/Water System at 20°C and the Ficoll 400/Dextran T-500/Water System at 23°C.

400/Dextran T-500/water systems, respectively. This interesting observation permits a further simplification of equation (2.18) through introduction of the constant ratio ϕ:

$$\ln (K_1) = m_1\Big(\alpha_1\big(\frac{1}{m_1} - 1 + 2\chi_{01}\big) + \alpha_2\phi\big(\frac{1}{m_2} - 1 + \chi_{01} + \chi_{02} - \chi_{12}\big)(w_1'' - w_1')\Big) \tag{2.20}$$

Thus, a simple linear semilogarithmic relationship is obtained between ln (K_1) and the polymer (1) concentration difference between the phases. A similar equation may be derived for the partition coefficient of polymer (2):

$$\ln (K_2) = m_2\Big(\alpha_2\phi\big(\frac{1}{m_2} - 1 + 2\chi_{02}\big) + \alpha_1\big(\frac{1}{m_1} - 1 + \chi_{02} + \chi_{01} - \chi_{12}\big)(w_1'' - w_1')\Big) \tag{2.21}$$

The above linear semilogarithmic relationships may be simplified by defining their slopes as follows:

$$A_1 = m_1\Big(\alpha_1\big(\frac{1}{m_1} - 1 + 2\chi_{01}\big) + \alpha_2\phi\big(\frac{1}{m_2} - 1 + \chi_{01} + \chi_{02} - \chi_{12}\big)\Big) \tag{2.22}$$

and

$$A_2 = m_2\Big(\alpha_2\phi\big(\frac{1}{m_2} - 1 + 2\chi_{02}\big) + \alpha_1\big(\frac{1}{m_1} - 1 + \chi_{02} + \chi_{01} - \chi_{12}\big)\Big) \tag{2.23}$$

Equations (2.20) and (2.21) then become:

$$\ln (K_1) = A_1(w_1'' - w_1') \tag{2.24}$$

and

$$\ln (K_2) = A_2(w_1'' - w_1') \tag{2.25}$$

where A_1 and A_2 are a function of the polymer molecular weights and the interactions between the polymers and water. As will be demonstrated in Chapter III, equations (2.24) and (2.25) will provide a means for correlating phase equilibrium data for aqueous polymer systems.

2.3 Low Molecular Weight Solute Partitioning

Having established linear semilogarithmic relationships for three component systems, the next step is to extend the Flory-Huggins theory to include a fourth component such as a biomolecule. The Gibbs free energy of mixing, based on equation (2.3), for a system composed of biomolecule water (component 0), polymer (1), polymer (2) and biomolecule (component 3) can be expressed as:

$$\begin{aligned}\Delta G_m = kT(&n_0v_1\chi_{01} + n_0v_2\chi_{02} + n_0v_3\chi_{03} + n_1v_2\chi_{12} + n_1v_3\chi_{13} \\ &+ n_2v_3\chi_{23} + n_0 \ln v_0 + n_1 \ln v_1 + n_2 \ln v_2 + n_3 \ln v_3)\end{aligned} \tag{2.26}$$

Substituting ΔG_m into equation (2.26) yields a series of four equations, one for each of the components. For the biomolecule (species 3), the result of the above substitution will produce the following relationship for its partition

coefficient, K_3:

$$\ln (K_3) = (v_3'' - v_3') + m_3\Big((1 - \chi_{03})(v_0'' - v_0') + \Big(\frac{1}{m_1} - \chi_{13}\Big)(v_1'' - v_1')$$

$$+ \Big(\frac{1}{m_2} - \chi_{23}\Big)(v_2'' - v_2') + \chi_{01}(v_0''v_1'' - v_0'v_1') + \chi_{02}(v_0''v_2'' - v_0'v_2')$$

$$+ \chi_{03}(v_0''v_3'' - v_0'v_3') + \chi_{12}(v_1''v_2'' - v_1'v_2') + \chi_{13}(v_1''v_3'' - v_1'v_3')$$

$$+ \chi_{23}(v_2''v_3'' - v_2'v_3')\Big) \qquad (2.27)$$

where $K_3 = (v_3''/v_3')$. It was stated earlier in the chapter that the concentration of the partitioning solute (or biomolecule) can be considered small and negligible. In the partition experiments to be discussed in Chapters IV and V, the concentration of the biomolecule is on the order of 0.1 %(w/w) while phase forming polymer concentrations are typically on the order of 5.0 to 10.0 %(w/w). Therefore, setting v_3 equal to zero and substituting the following relationships for v_0'' and v_0' into equation (2.27),

$$v_0'' \doteq 1 - v_1'' - v_2'' \qquad (2.28)$$

and

$$v_0' \doteq 1 - v_1' - v_2' \qquad (2.29)$$

yields the following relationship for the biomolecule partition coefficient:

$$\ln (K_3) = m_3\Big(\Big(\frac{1}{m_1} - 1 + \chi_{03} - \chi_{13} + \chi_{01}\Big)(v_1'' - v_1')\Big)$$

$$+\left(\frac{1}{m_2}-1+\chi_{03}-\chi_{23}+\chi_{02}\right)\left(v_2''-v_2'\right)$$

$$-\chi_{01}\left(\left(v_1''^{2}-v_1'^{2}\right)+\left(v_1''v_2''-v_1'v_2'\right)\right)-\chi_{02}\left(\left(v_2''^{2}-v_2'^{2}\right)\right.$$

$$\left.+\left(v_1''v_2''-v_1'v_2'\right)\right)+\chi_{12}\left(v_1''v_2''-v_1'v_2'\right)\Bigg) \qquad (2.30)$$

Equation (2.30) may be simplified once again by making the assumption that second order terms containing v_1 and v_2 are negligible:

$$\ln\left(K_3\right)=m_3\Bigg(\left(\frac{1}{m_1}-1+\chi_{03}-\chi_{13}+\chi_{01}\right)\left(v_1''-v_1'\right)$$

$$+\left(\frac{1}{m_2}-1+\chi_{03}-\chi_{23}+\chi_{02}\right)\left(v_2''-v_2'\right)\Bigg) \qquad (2.31)$$

Assuming a proportionality between weight and volume fractions and introducing the weight ratio, ϕ, equation (2.31) then becomes:

$$\ln\left(K_3\right)=m_3\Bigg(\alpha_1\left(\frac{1}{m_1}-1+\chi_{03}-\chi_{13}+\chi_{01}\right)+\alpha_2\phi\left(\frac{1}{m_2}-1+\chi_{03}\right.$$

$$\left.-\chi_{23}+\chi_{02}\right)\left(w_2''-w_2'\right)\Bigg) \qquad (2.32)$$

If a biomolecule is partitioned in the tie line compositions of a particular phase diagram, then m_1 and m_2 are constant, along with χ_{01}, χ_{02}, χ_{03}, χ_{13} and χ_{23}. Therefore, equation (2.32) may be expressed as:

$$\ln(K_3)=A(w_1''-w_1') \qquad (2.33)$$

where,

$$A = m_3\left(\alpha_1\left(\frac{1}{m_1} - 1 + \chi_{03} - \chi_{13} + \chi_{01}\right) + \alpha_2\phi\left(\frac{1}{m_2} - 1 + \chi_{03} - \chi_{23} + \chi_{02}\right)\right) \tag{2.34}$$

The slope A is a function of biomolecule and polymer molecular weight, and the interaction among the biomolecule, polymers and water. Hence, equation (2.33) represents a simple linear semilogarithmic relationship for correlating biomolecule partition coefficients in aqueous two phase systems. Equation (2.33) is the starting point for the correlation of biomolecule partitioning, and will be shown in Chapter IV to be applicable to dipeptides and low molecular weight proteins (i.e., proteins below molecular weight 25,000).

2.4 General Partition Expression

In the following part of this chapter, a general partition expression will be developed which can account for both high and low molecular weight protein partitioning in a variety of aqueous two-phase systems. This will be accomplished by modifying the chemical potential expression of the Flory-Huggins theory, i.e., equation (2.4), to take into account the electrostatic potential between the phases.

The chemical potential expression, equation (2.4), may be taken one step further by noting that many researchers (Johansson, 1974; Zaslavsky *et al.*, 1982a,b; Brooks *et al.*, 1984; King *et al.*, 1988; Albertsson, 1986) have found that the addition of salts to aqueous two-phase systems induced an electrical potential difference between the phases. The contribution of an electrostatic term to the chemical potential in an aqueous polymer two-phase system may be expressed in a general form as (Albertsson, 1986):

$$\mu_i - \mathring{\mu_i} = N_A\left(\frac{\partial\, \Delta G_m}{\partial n_i}\right)_{n_j,T,P} + z_b F\psi \tag{2.35}$$

where z_b is the net charge of the species, F is the Faraday constant, and ψ is the electric potential. Substituting equation (2.35) into the equilibrium relation, equation (2.5), yields

$$N_A\left(\frac{\partial\, \Delta G'_m}{\partial n_i}\right)_{n_j,T,P} + z_b F\psi' = N_A\left(\frac{\partial\, \Delta G''_m}{\partial n_i}\right)_{n_j,T,P} + z_b F\psi'' \tag{2.36}$$

Then, by substituting the Gibbs free energy of mixing expression for the four component system, equation (2.26), into equation (2.36) and rearranging, we can obtain an expression for the partition coefficient of a biomolecule (component 3), K_3:

$$\begin{aligned} \ln(K_3) = (v''_3 - v'_3) + m_3\Big(& (1 - \chi_{03})(v''_0 - v'_0) + \left(\frac{1}{m_1} - \chi_{13}\right)(v''_1 - v'_1) \\ & + \left(\frac{1}{m_2} - \chi_{23}\right)(v''_2 - v'_2) + \chi_{01}(v''_0 v''_1 - v'_0 v'_1) + \chi_{02}(v''_0 v''_2 - v'_0 v'_2) \\ & + \chi_{03}(v''_0 v''_3 - v'_0 v'_3) + \chi_{12}(v''_1 v''_2 - v'_1 v'_2) + \chi_{13}(v''_1 v''_3 - v'_1 v'_3) \\ & + \chi_{23}(v''_2 v''_3 - v'_2 v'_3)\Big) + \frac{z_b F \Delta\psi}{RT} \end{aligned} \tag{2.37}$$

Equation (2.37) may be simplified by performing the following manipulations which have been described in sections 2.2 and 2.3 of this chapter: a) assume the biomolecule concentration v_3 is small and negligible, b) express v_0 as a function of v_1 and v_2, c) assume a proportionality constant, α_i, exists for the volume and

weight fraction differences between the phases for species i, and d) introduce the weight fraction ratio ϕ. The following simplified relationship is then obtained:

$$\ln (K_3) = m_3\Bigg(\left(\frac{\alpha_1}{m_1} + \frac{\alpha_2\phi}{m_2} + (\alpha_1 + \alpha_2\phi)(\chi_{03} - 1) - \alpha_1\chi_{13} - \alpha_2\phi\chi_{23}\right.$$

$$\left. + \alpha_1\chi_{01} + \alpha_2\phi\chi_{02}\right)(w_1'' - w_1') + (\chi_{02}\alpha_2^2\phi^2 - \chi_{01}\alpha_1^2)(w_1'' - w_1')^2$$

$$- 2\chi_{01}\alpha_1^2 w_1'(w_1'' - w_1') - 2\chi_{02}\alpha_2^2\phi w_2''(w_1'' - w_1')$$

$$\left. + (\chi_{12} - \chi_{01} - \chi_{02})\alpha_1\alpha_2(w_1''w_2'' - w_1'w_2')\right) + \frac{z_b F\Delta\psi}{RT} \qquad (2.38)$$

In order to further simplify equation (2.38), a comparison of the magnitude of the five terms $(w_1'' - w_1')$, $(w_1'' - w_1')^2$, $(w_1''w_2'' - w_1'w_2')$, $w_1'(w_1'' - w_1')$, and $w_2''(w_1'' - w_1')$ is appropriate. Each of these terms has been plotted versus w_2' in Figures 2.3, 2.4 and 2.5 for the PEG 8000/Dextran T-500/water phase diagram at 4°C, the PEG 3400/potassium phosphate/water phase diagram at 20°C, and the Ficoll 400/Dextran T-500/water system at 23°C, respectively. It is apparent from these three figures that $(w_1'' - w_1')$ and $(w_1'' - w_1')^2$ are of greatest importance, while the three remaining terms are negligible. This trend has also been found to be true for other PEG/dextran systems. The order of significance of the absolute value of the terms was found to be $(w_1'' - w_1') > (w_1'' - w_1')^2 > (w_1''w_2'' - w_1'w_2') > w_1'(w_1'' - w_1') > w_2''(w_1'' - w_1')$. Therefore, if $(w_1'' - w_1')$ and $(w_1'' - w_1')^2$ are maintained in the partition expression, while the remainder of the three terms are canceled, equation (2.38) becomes:

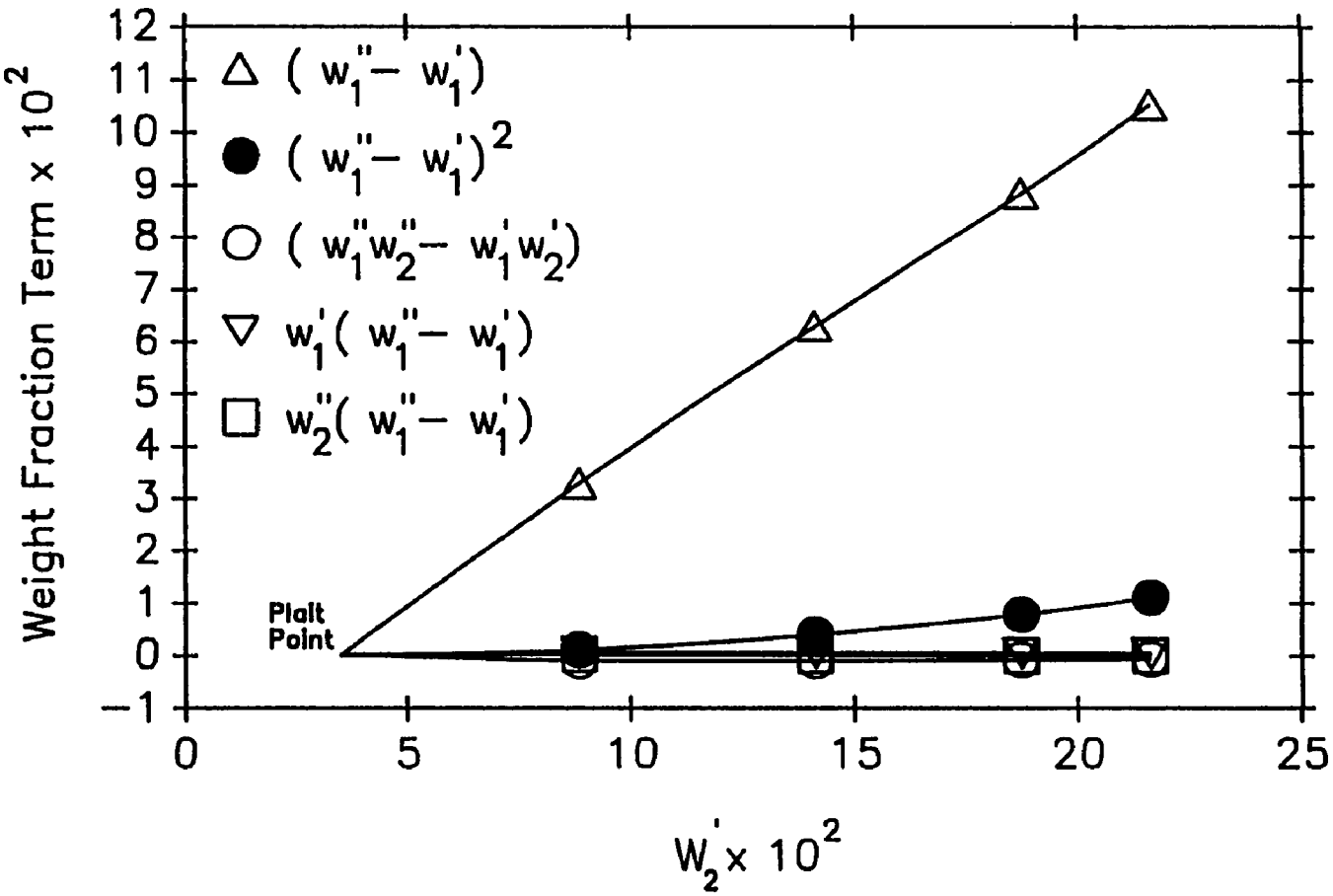

Figure 2.3 Comparison of the Magnitude of Weight Fraction Terms Present in the Flory-Huggins Partition Expression for the System Composed of PEG 8000/Dextran T-500/Water at 4°C.

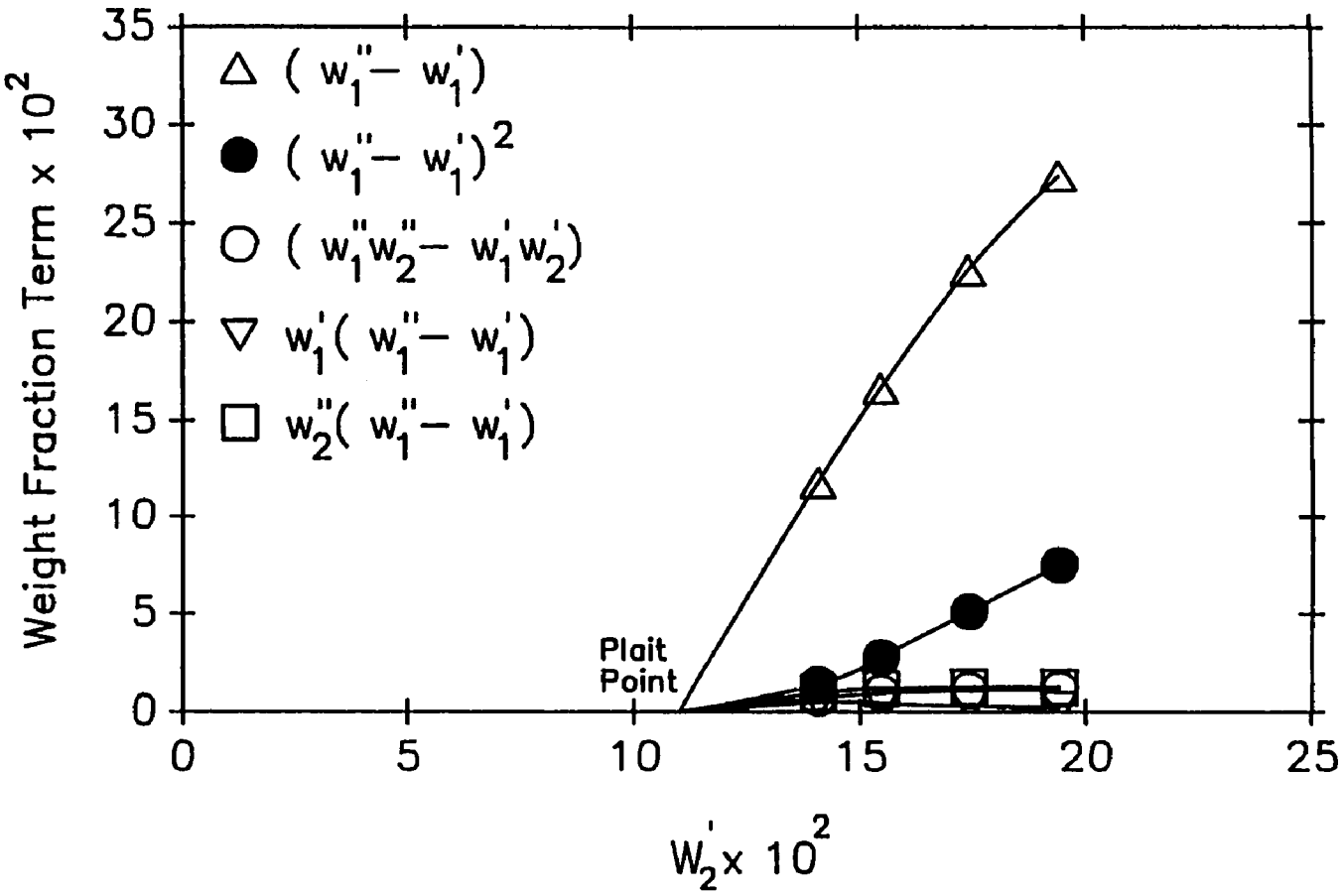

Figure 2.4 Comparison of the Magnitude of Weight Fraction Terms Present in the Flory-Huggins Partition Expression for the System Composed of PEG 3400/Potassium Phosphate/Water at 20°C.

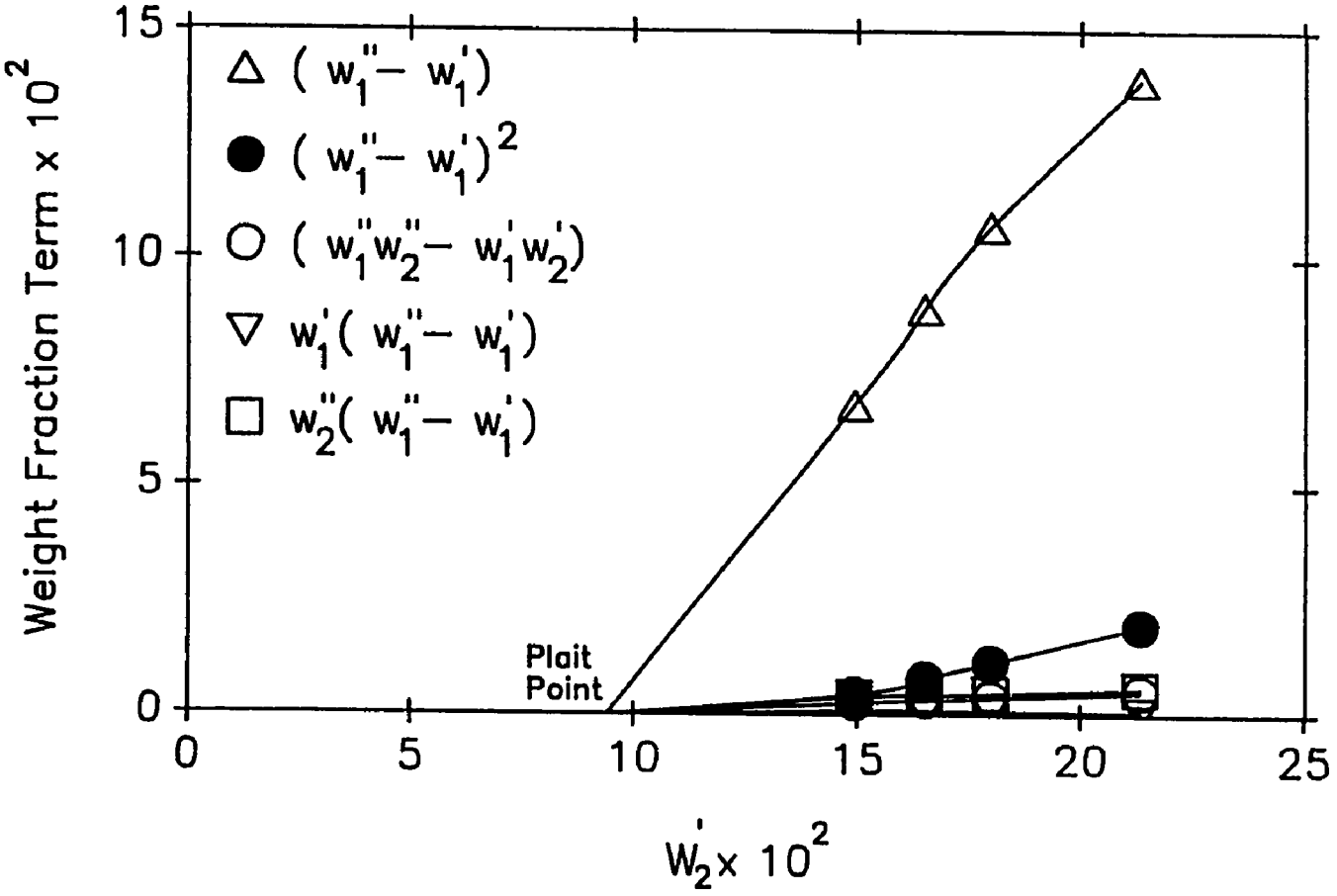

Figure 2.5 Comparison of the Magnitude of Weight Fraction Terms Present in the Flory-Huggins Partition Expression for the System Composed of Ficoll 400/Dextran T-500/Water at 23°C.

$$\ln (K_3) = m_3\Bigg(\left(\frac{\alpha_1}{m_1} + \frac{\alpha_2\phi}{m_2} + (\alpha_1 + \alpha_2\phi)(\chi_{03} - 1) - \alpha_1\chi_{13} - \alpha_2\phi\chi_{23}\right.$$

$$\left. + \alpha_1\chi_{01} + \alpha_2\phi\chi_{02}\right)(w_1'' - w_1') + (\chi_{02}\alpha_2^2\phi^2 - \chi_{01}\alpha_1^2)(w_1'' - w_1')^2\Bigg)$$

$$+ \frac{z_b F\Delta\psi}{RT} \qquad (2.39)$$

Equation (2.39) may be simplified by first noting that the collection of terms preceding $(w_1'' - w_1')$ is the parameter A given by equation (2.34). If we permit the letter b to represent the collection of terms preceding $(w_1'' - w_1')^2$, i.e.,

$$b = m_3(\chi_{02}\alpha_2^2\phi^2 - \chi_{01}\alpha_1^2) \qquad (2.40)$$

then equation (2.39) becomes:

$$\ln (K_3) = A(w_1'' - w_1') + b(w_1'' - w_1')^2 + \frac{z_b F\Delta\psi}{RT} \qquad (2.41)$$

In order to further simplify equation (2.41), a means is needed by which $\Delta\psi$ can be related to the PEG concentration difference between the phases, $(w_1'' - w_1')$. King *et al.* (1988) measured $\Delta\psi$ for various different phase compositions of the PEG 3350/Dextran T-70/salt-water and PEG 8000/Dextran T-500/salt-water systems at 25°C and plotted $\Delta\psi$ versus the tie line length (defined as $\sqrt{(w_1'' - w_1')^2 + (w_2'' - w_2')^2}$). For both phase diagrams, plots of $\Delta\psi$ versus tie line length showed a linear trend, with extrapolation of the data approximately originating at the point $\Delta\psi = 0$ at tie line length equal to zero, i.e., the plait point (King *et al.*, 1988). A different linear relationship was observed for the different salt types and concentrations. In Figures 2.6 and 2.7 King's data have

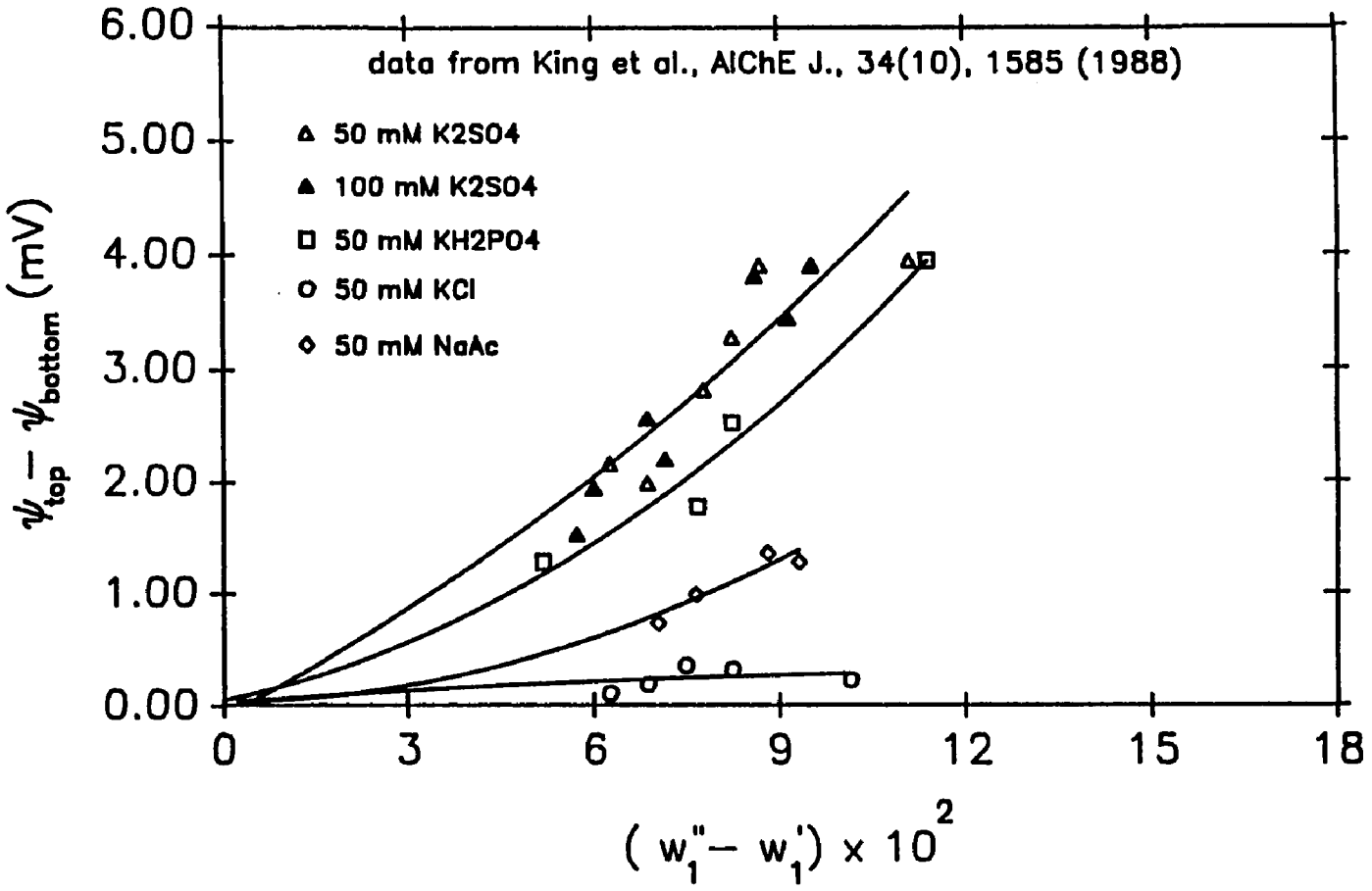

Figure 2.6 Potential Difference Versus PEG Concentration Difference Between the Phases for the PEG 8000/Dextran T-500/Water System at 25°C.

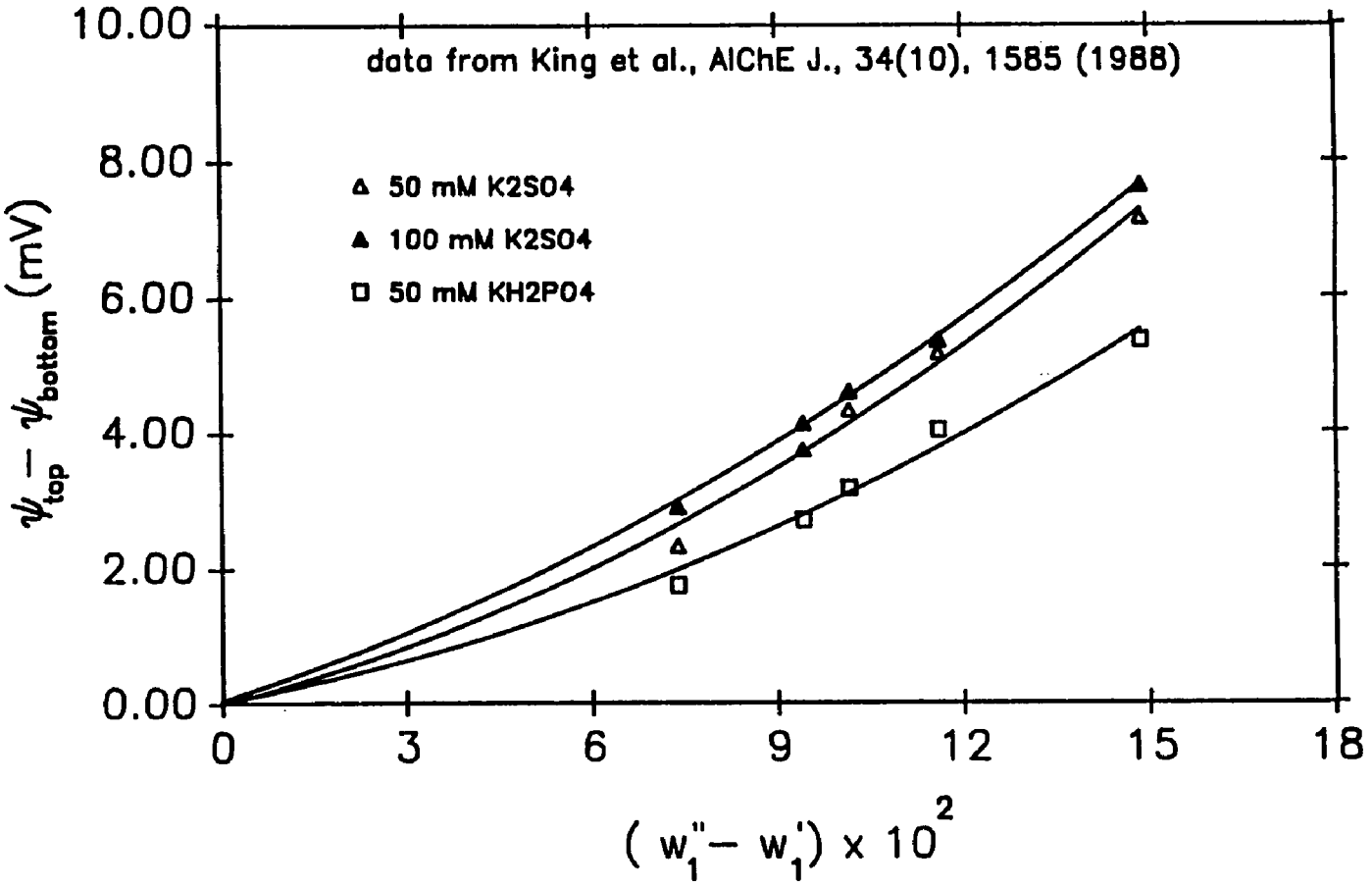

Figure 2.7 Potential Difference Versus PEG Concentration Difference Between the Phases for the PEG 3350/Dextran T-70/Water System at 25°C .

been replotted in the form $\Delta\psi$ versus $(w_1'' - w_1')$. Analysis of these data led to a correlation of the electrostatic potential difference with second order polynomials, which are indicated as the solid curves in Figures 2.6 and 2.7. The data utilized in the regression included the point (0,0). Based on the above electrostatic potential results, the following empirical relationship between $\Delta\psi$ and $(w_1'' - w_1')$ may be obtained:

$$\Delta\psi = g(w_i'' - w_i') + h(w_1'' - w_1')^2 \tag{2.42}$$

where g and h are regression constants, which are a function of salt type and concentration. These two parameters, as obtained from King's data, are presented in Table 2.1. Substituting equation (2.42) into (2.41) gives:

$$\ln (K_3) = \left(A + \frac{z_b F g}{RT}\right)(w_1'' - w_1') + \left(b + \frac{z_b F h}{RT}\right)(w_1'' - w_1')^2 \tag{2.43}$$

At a constant pH, temperature and pressure, the charge, z_b, of the biomolecule will be constant, and the terms, z_bFg/RT and z_bFh/RT, may be incorporated with A and b, respectively. The following relation is then obtained when equation (2.43) is divided through by $(w_1'' - w_1')$:

$$\frac{\ln (K_3)}{(w_1'' - w_1')} = A^* + b^*(w_1'' - w_1') \tag{2.44}$$

where,

$$A^* = A + \frac{z_b F g}{RT} \tag{2.45}$$

and

$$b^* = b + \frac{z_b F h}{RT} \tag{2.46}$$

Table 2.1 The Parameters g and h of Equation (2.42) Obtained from the Electrostatic Potential Data of King *et al.* (1988).

System	g x 10^{-2}	h x 10^{-4}	r^2
PEG 3350/Dextran T-70/water with:			
50 mM K_2SO_4	0.22	0.018	0.997
100 mM K_2SO_4	0.29	0.015	0.999
50 mM KH_2PO_4	0.15	0.014	0.996
PEG 8000/Dextant T-500/water with:			
50 mM K_2SO_4 and 100 mM K_2SO_4*	0.25	0.014	0.949
50 mM KH_2PO_4	0.11	0.020	0.991
50 mM KCl	0.038	0.0012	0.762
50 mM NaAc	0.0035	0.015	0.987

* The electrostatic potential data for these two salt concentrations were combined for the regression analysis. This was done because the two sets of data were very close to one another and overlapped at some points.

Equation (2.44) represents a simple second order semilogarithmic relationship for correlating protein partitioning in aqueous two-phase systems. The intercept A^* is a function of protein and phase forming polymer molecular weight, the protein-water, protein-polymer and polymer-water interaction parameters, pH and salt type and concentration. Similarly, the slope b^* is a function of protein molecular weight, the polymer-water interaction parameters, pH and the salt type and concentration. In Chapter V, equation (2.44) will be

shown to be applicable to proteins covering a wide range of molecular weight in a variety of aqueous two-phase systems.

It is quite interesting that A^* and b^* as well as the parameter A contain χ_{01} and χ_{02}, which represent the interactions between water and PEG, and water and dextran, respectively. Zaslavsky *et al.* (1989) have shown that phase separation in aqueous two-phase systems results from the structural effect on water provided by the PEG and dextran. The interaction parameters χ_{01} and χ_{02} range from 0.43 to 0.51. Therefore, it is not too surprising that a general partition expression would contain the phase forming polymer-solvent interaction parameters.

2.5 Conclusions

Utilizing the Flory-Huggins theory of polymer solution thermodynamics, expressions have been derived for correlating phase diagram behavior and biomolecule partitioning in aqueous polymer two-phase systems. The relations incorporate the polymer concentrations in the phases, the molecular weight of the species present, the interactions among the species present, and, in the case of the biomolecule correlation, the electrostatic potential difference between the phases. In the chapters that follow, these relationships will be verified through the use of aqueous polymer phase diagrams, and dipeptide and protein partitioning.

CHAPTER III
PHASE DIAGRAMS

This chapter provides the phase equilibrium data for the PEG/dextran/water and PEG/potassium phosphate/water systems, and the methodologies used to obtain them. The results are provided in both tabular and graphical form. The phase diagrams are then correlated using equations derived from Flory-Huggins theory.

3.1 Introduction

The most fundamental data for any type of liquid-liquid extraction process are the composition of the equilibrium phases. In the case of aqueous polymer two-phase systems, a comprehensive set of phase diagram data are needed in order to facilitate their use for protein purification and to aid in the development of thermodynamic models for their prediction. Furthermore, such data are needed for the eventual correlation of protein partitioning. The most extensive source of phase equilibrium data for aqueous two phase systems are that provided by Albertsson (1971, 1986). However, Albertsson's data are not yet complete, particularly with regard to PEG/dextran and PEG/potassium phosphate aqueous two-phase systems, which have the greatest potential for routine use in laboratory and large-scale bioseparations. Bamberger *et al.* (1984) and Schürch *et al.* (1981) present room temperature PEG/dextran phase diagrams without tabulating the phase compositions, thus making the data extremely difficult to use; King *et al.* (1988) provide phase compositions for two PEG/dextran systems at 25°C.

The PEG molecular weight fractions having the greatest potential for routine use in PEG/dextran aqueous two-phase systems include 3,400, 8,000 and 20,000. The most frequently used dextran fractions have weight average molecular weights of 40,000, 70,000 and 500,000. Phase diagrams using the above PEG and dextran molecular weight fractions have been obtained at 4°C and 22°C. In addition, the phase diagram at 10°C for the system composed of PEG 8,000 and dextran of molecular weight 70,000 and 500,000, and the system at 22°C with PEG and dextran of molecular weight 8,000 and 10,000, respectively, have been obtained.

Phase diagrams have been obtained at 4°C and pH 7.0 for the PEG/potassium phosphate/water system using PEG of molecular weight 400, 600, 1,000, 1,500, 3,400, 8,000, and 20,000. The effect of pH on phase separation at 4°C was also investigated for the PEG 3,400/potassium phosphate/water system over the pH range of 6.0 to 9.2. It should be noted that the pH of a system was changed by varying the ratio of monobasic to dibasic potassium phosphate. This ratio is maintained the same throughout a phase diagram which is at constant pH.

3.2 MATERIALS AND METHODS

3.2.1 Polymers and Salt

All dextran fractions used for the determination of PEG/dextran/water phase diagrams were obtained from Pharmacia Fine Chemicals, Piscataway, NJ. Dextran T-500 (Lot 05163), Dextran T-70 (Lot 02377), Dextran T-40 (Lot 01852), and Dextran T-10 (Lot 00985) which had weight average molecular weights of 507,000, 72,200, 40,200, and 10,900 and number average molecular weights of 234,200, 38,400, 24,400, and 5,300, respectively, were used for phase

diagrams at 22°C. Phase diagrams at 4°C were prepared with the same Dextran T-500 and Dextran T-70 lot numbers as the 22°C systems, except Dextran T-40 (Lot 03375) which had weight and number average molecular weights of 38,800 and 24,200, respectively. The PEG/dextran/water system at 10°C utilized Dextran T-500 (Lot 06905) which had weight and number average molecular weights of 497,000 and 180,300, respectively.

All PEG/dextran/water phase diagrams at 4°C, 10°C and 22°C utilized PEG of molecular weight 3,400 (Lot 00917 PT) and 8,000 (Lot 02521 LT) as purchased from Aldrich Chemical Company, Milwaukee, WI, and PEG of molecular weight 20,000 obtained as Carbowax 20M from Union Carbide, NY.

PEG/potassium phosphate/water phase systems were prepared with the following PEG molecular weight fractions as obtained from Aldrich Chemical Company: 400 (Lot 02166 TP), 600 (Lot 03403 HM), 1,000 (Lot 00404 HM), 3,400 (Lot 02607 HV), and 8,000 (Lot 1722 BW). PEG of molecular weight 20,000 was the same as indicated above. A.C.S. reagent grade mono- and dibasic potassium phosphate were obtained from Aldrich Chemical Company. Dowex 50-w cation exchange resin was purchased from Sigma Chemical Company, St. Louis, MO.

3.2.2 Experimental Techniques

3.2.2.1 PEG/dextran/water systems

Dextran stock solutions, ranging in concentration from 20%(w/w) to 30%(w/w), were prepared by mixing equal amounts of dextran and water to form a paste. Additional water was then added, and the resulting solution magnetically stirred approximately two hours. Dextran stock solution

concentration was then determined by measuring optical rotation with a Rudolph model 52 polarimeter assuming a specific rotation of $[\alpha]_D^{25}$=199° (Walter *et al.*, 1985). Since polarimetry gives concentration in weight per volume, the concentration in weight per weight was obtained by density measurements using pycnometry.

The biphasic systems constituting a phase diagram were prepared by weighing appropriate quantities of PEG (in the form of a solid), dextran stock solution and water. Typically, 30 grams of a system were prepared. The resulting solution was magnetically stirred approximately three hours, after which it was poured into a 50 mL polypropylene centrifuge tube. The tubes were tightly capped, and then allowed to settle by gravity for 24–48 hours either in a temperature controlled refrigerator for systems at 4°C and 10°C, or in the laboratory environment for systems at 22°C. A pasteur pipet was used to collect the top phase, while the lower phase was drained from the polypropylene tube by piercing a hole at its bottom.

The composition of each phase was determined through a combination of polarimetric and refractive index analysis as described by Walter *et al.* (1985). Since dextran is the only species in the system which possesses optical activity, its concentration was obtained by polarimetry. PEG content was determined by refractive index measurements based on the fact that concentration (in weight per volume) of total polymer present in the solution varies linearly with refractive index over the range of 0.0 to 10.0 %(w/v). The concentrations obtained on a weight per volume basis were converted to weight per weight by density measurements using pycnometry. Once the total polymer concentration in each phase was known, water content was calculated by subtraction.

3.2.2.2 PEG/potassium phosphate/water systems

The phase compositions of the PEG/potassium phosphate/water systems at 4°C were obtained according to the procedure described by Albertsson (1986). Potassium phosphate stock solutions of 20 %(w/w) at pH 6, 7, and 8 were prepared using a dibasic to monobasic weight ratio of 0.5, 1.82, and 15., respectively. The stock solution at pH 9.2 was prepared with pure dibasic potassium phosphate. The biphasic systems constituting a phase diagram were then prepared by weighing appropriate quantities of PEG, potassium phosphate solution and water into a 100 mL beaker. Typically, 40 grams of a system were prepared. The systems were magnetically stirred for 45 minutes, after which they were poured into 50 mL polypropylene centrifuge tubes. The tubes were tightly capped and then allowed to settle by gravity for 48–72 hours at 4°C in the temperature controlled refrigerator. A pasteur pipet was used to collect the top phase, while the lower phase was drained from the polypropylene tube by piercing a hole at its bottom.

Potassium phosphate concentration was determined by ion exchange chromatography and titration as described in detail by Svehla (1982). The chromatography column was filled with Dowex-50 cation exchange resin (8% cross linked), while titration was performed with 0.1 N sodium hydroxide and bromocresol green as the indicator. The concentrations obtained on a weight per volume basis were converted to weight per weight by density measurements using pycnometry. In order to determine water content, samples of about 2–3 grams from each phase were weighed into 20 mL polypropylene tubes, diluted with 5–7 mL water, and freeze dried for 24–72 hours. Having determined the potassium phosphate and water concentrations, PEG content was obtained by

subtraction.

3.3 RESULTS AND DISCUSSION

3.3.1 PEG/Dextran/Water Phase Diagrams

The phase diagrams at 4°C and 22°C for PEG/dextran/water systems utilizing Dextran T-40, T-70 and T-500 in combination with PEG 3,400, 8,000 and 20,000 are presented in Figures 3.1–3.9 and Figures 3.10–3.18, respectively (Diamond and Hsu, 1989a,b). The phase diagrams for the PEG 8000/dextran T-70/water and PEG 8000/Dextran T-500/water systems at 10°C are presented in Figures 3.19 and 3.20, respectively. The PEG 8000/Dextran T-10/water system at 22°C is presented in Figure 3.21. The phase compositions for the PEG/dextran/water systems at 4°C and 22°C (i.e., those in Figures 3.1–3.9 and 3.10–3.18) are recorded in Tables 3.1 and 3.2, respectively, while the compositions for the PEG/dextran/water systems at 10°C and the PEG 8000/Dextran T-10/water system at 22°C are recorded in Table 3.3.

The various factors that can influence phase equilibria include temperature, pressure, and, in the case of polymers, molecular weight, and polydispersity. We have focused primarily on the effects of PEG and dextran molecular weight . Examination of the set of binodial curves in Figures 3.1, 3.2 and 3.3; 3.4, 3.5 and 3.6; 3.7, 3.8 and 3.9; 3.21, 3.10, 3.11 and 3.12 (in that order); 3.13, 3.14 and 3.15; 3.16, 3.17 and 3.18; 3.19 and 3.20 reveals that as dextran molecular weight is increased, the binodial becomes more asymmetrical and distorted toward the PEG axis. This is in agreement with the experimental results of Albertsson (1986) and the theoretical predictions of Hsu and Prausnitz (1974). It can also be seen that at higher dextran molecular weights, lower polymer concentrations are required for phase separation and therefore a

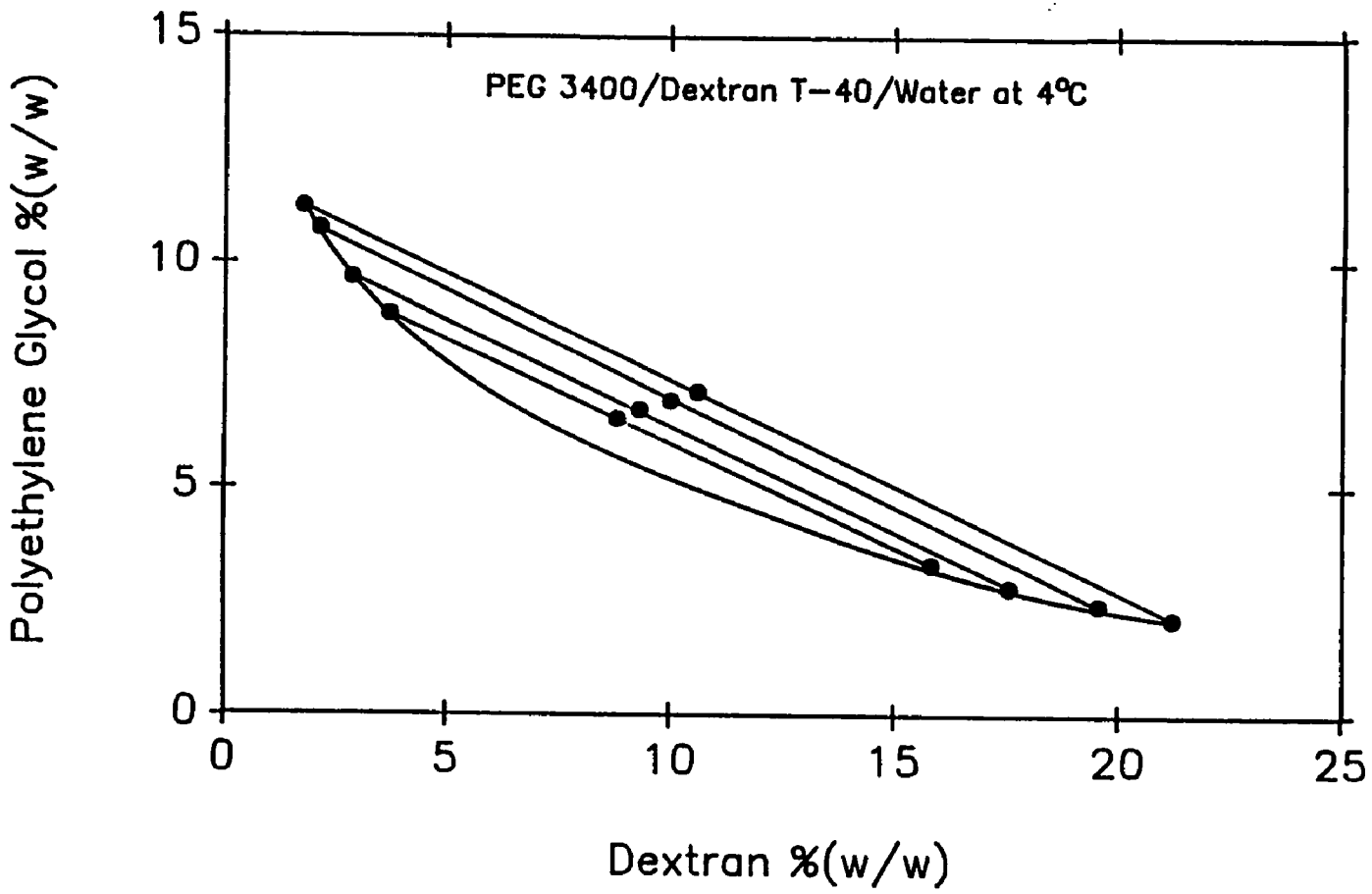

Figure 3.1 Phase Diagram for the PEG 3400/ Dextran T-40/Water System at 4°C.

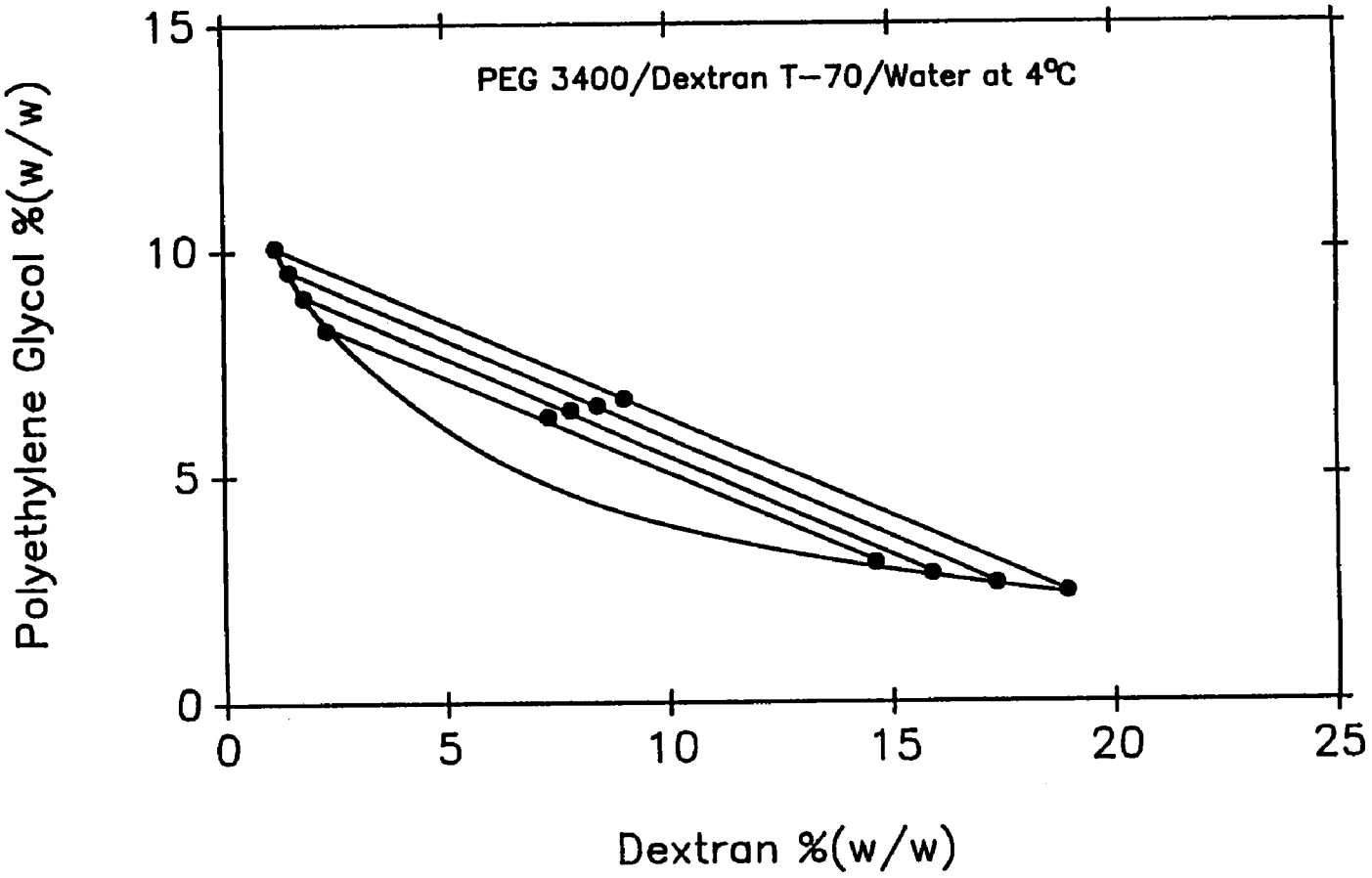

Figure 3.2 Phase Diagram for the PEG 3400/ Dextran T-70/Water System at 4°C.

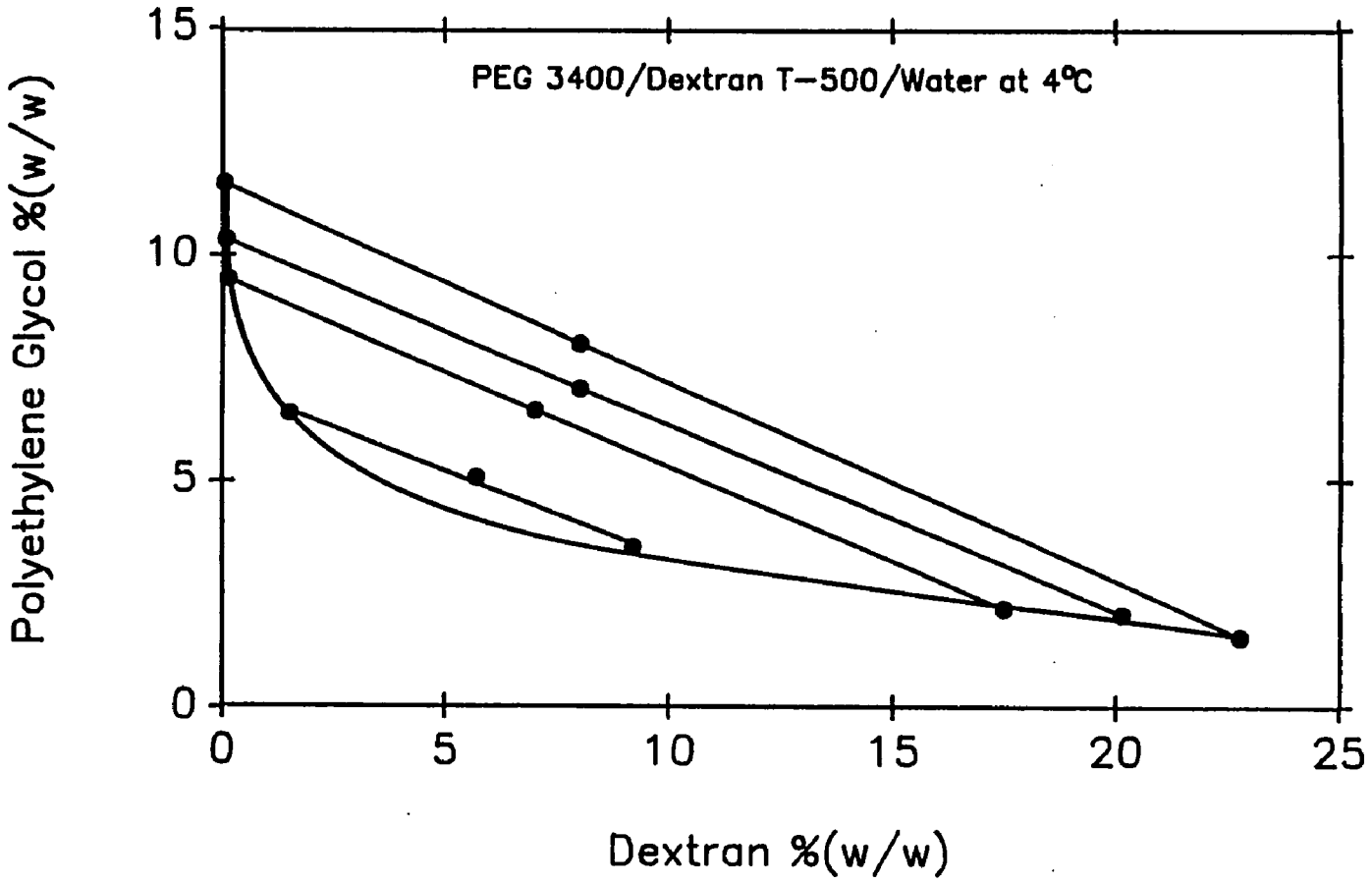

Figure 3.3 Phase Diagram for the PEG 3400/ Dextran T-500/Water System at 4°C.

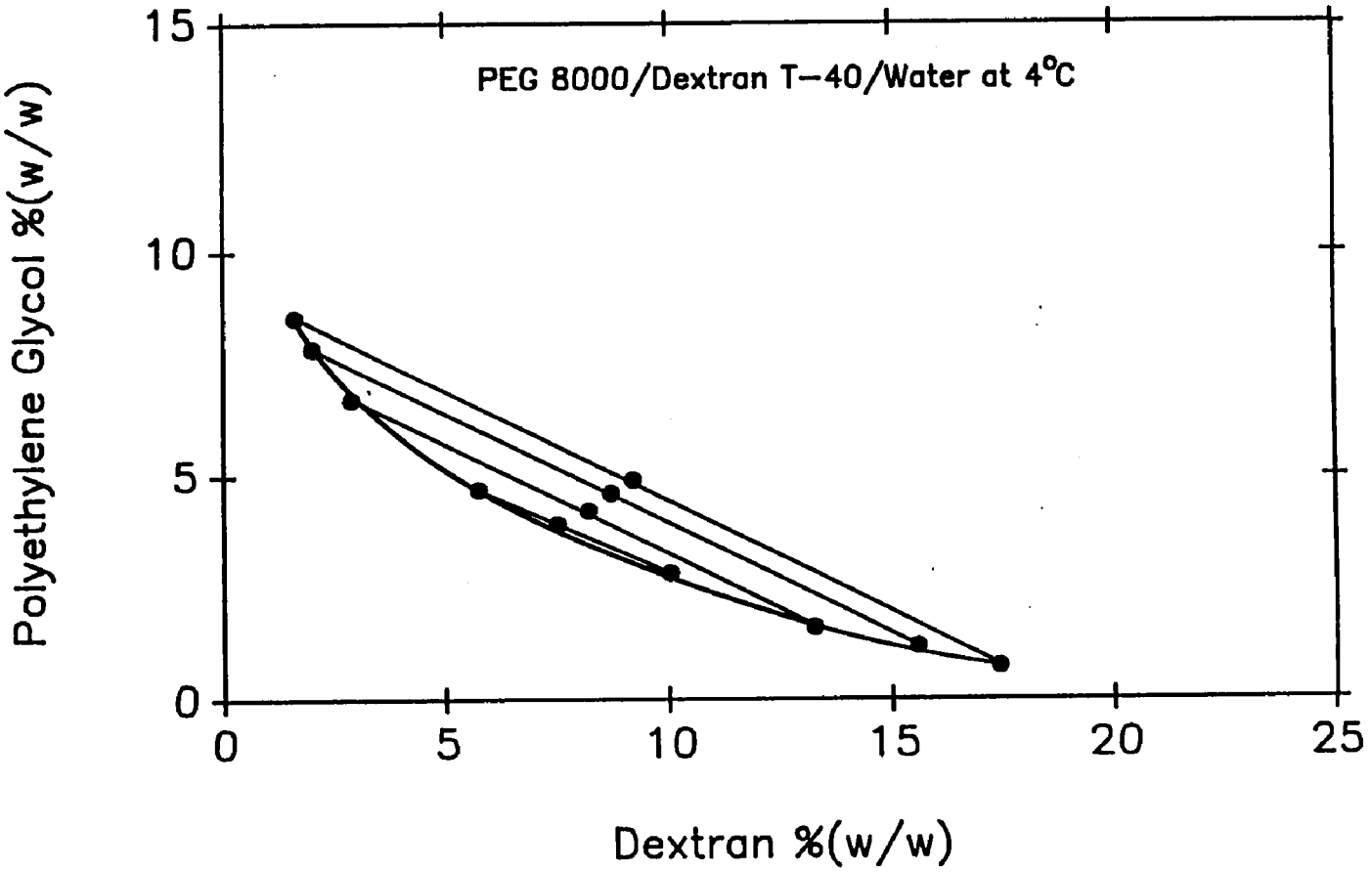

Figure 3.4 Phase Diagram for the PEG 8000/ Dextran T-40/Water System at 4°C.

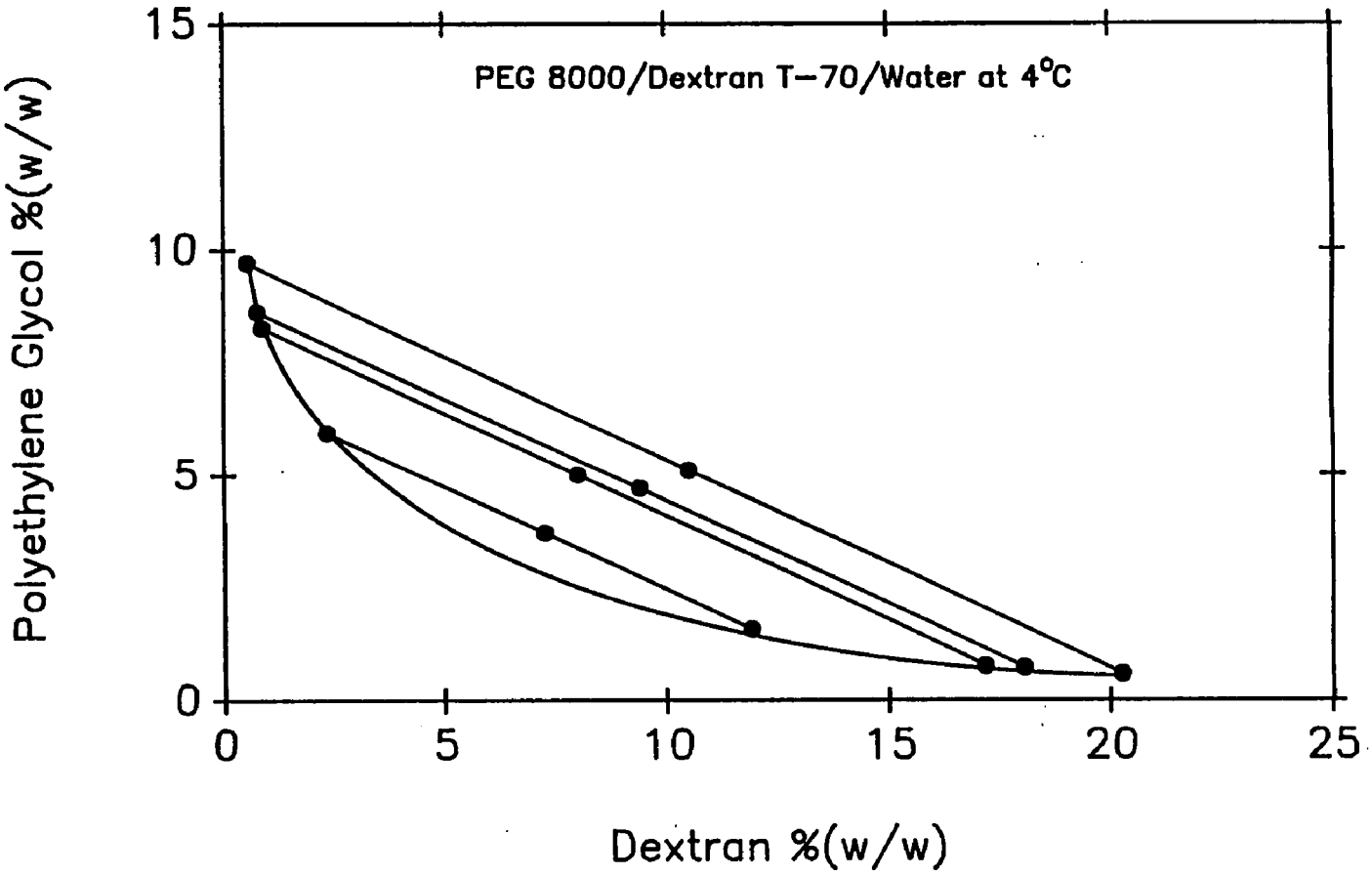

Figure 3.5 Phase Diagram for the PEG 8000/ Dextran T-70/Water System at 4°C.

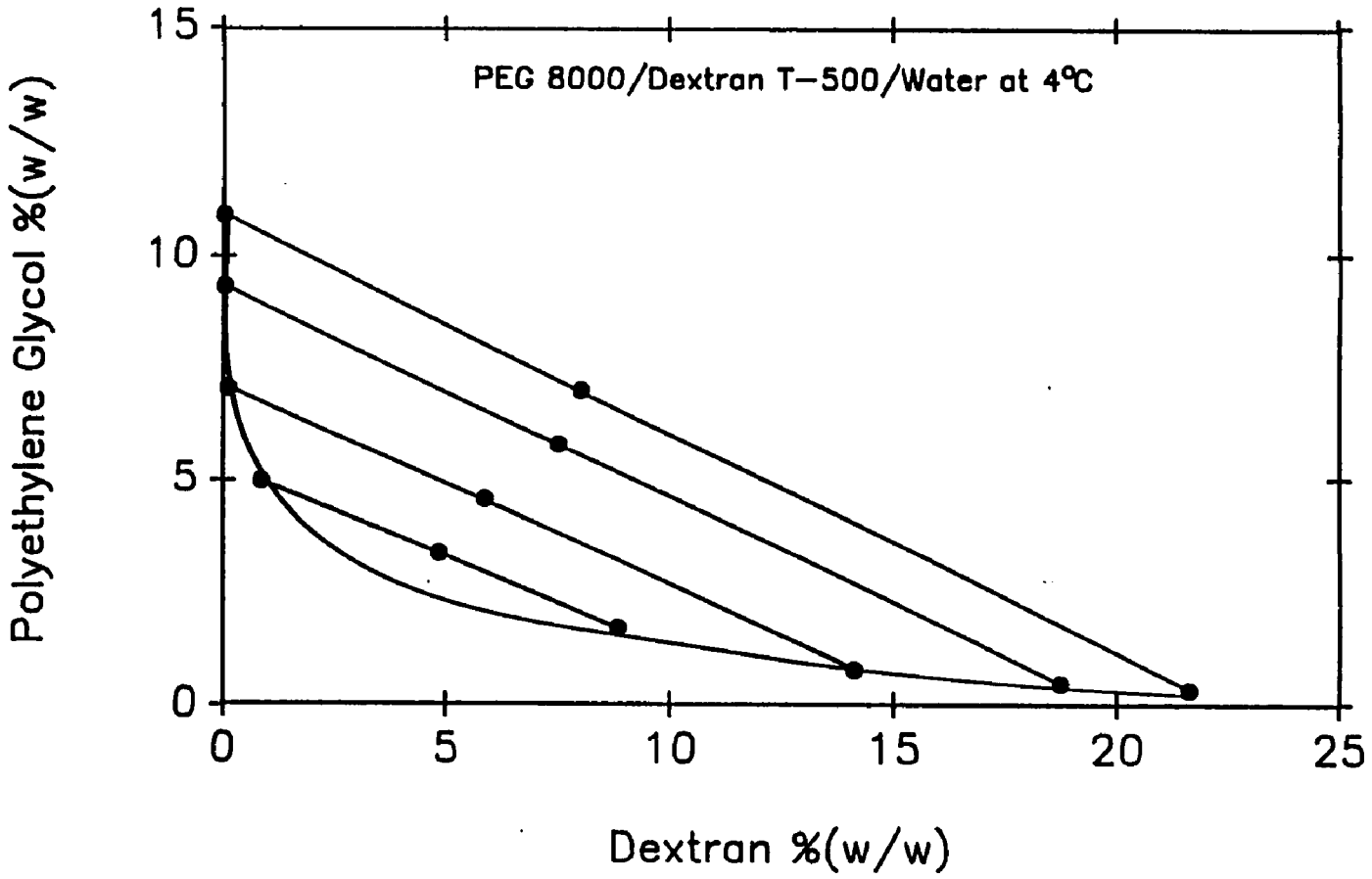

Figure 3.6 Phase Diagram for the PEG 8000/ Dextran T-500/Water System at 4°C.

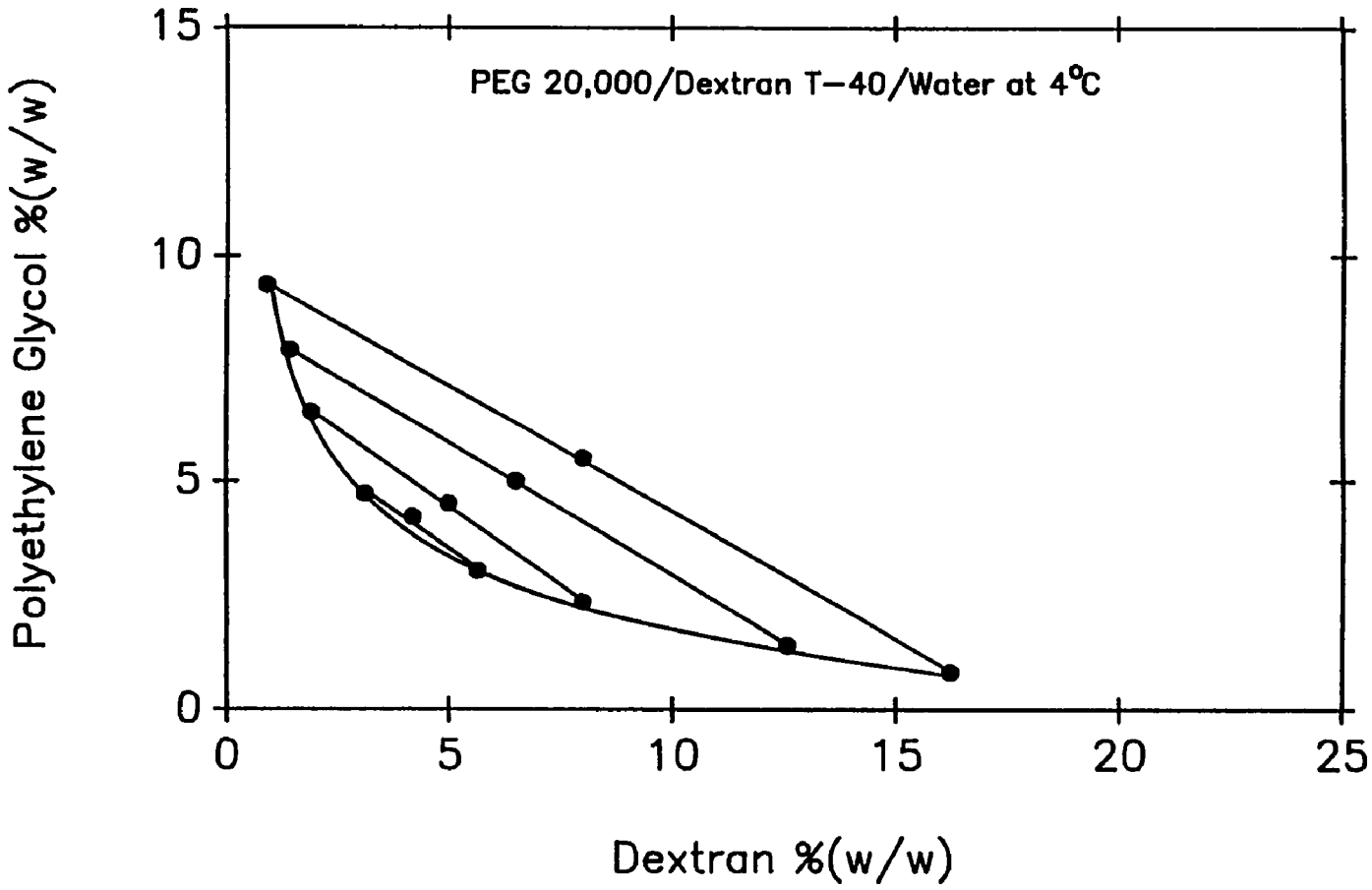

Figure 3.7 Phase Diagram for the PEG 20,000/ Dextran T-40/Water System at 4°C.

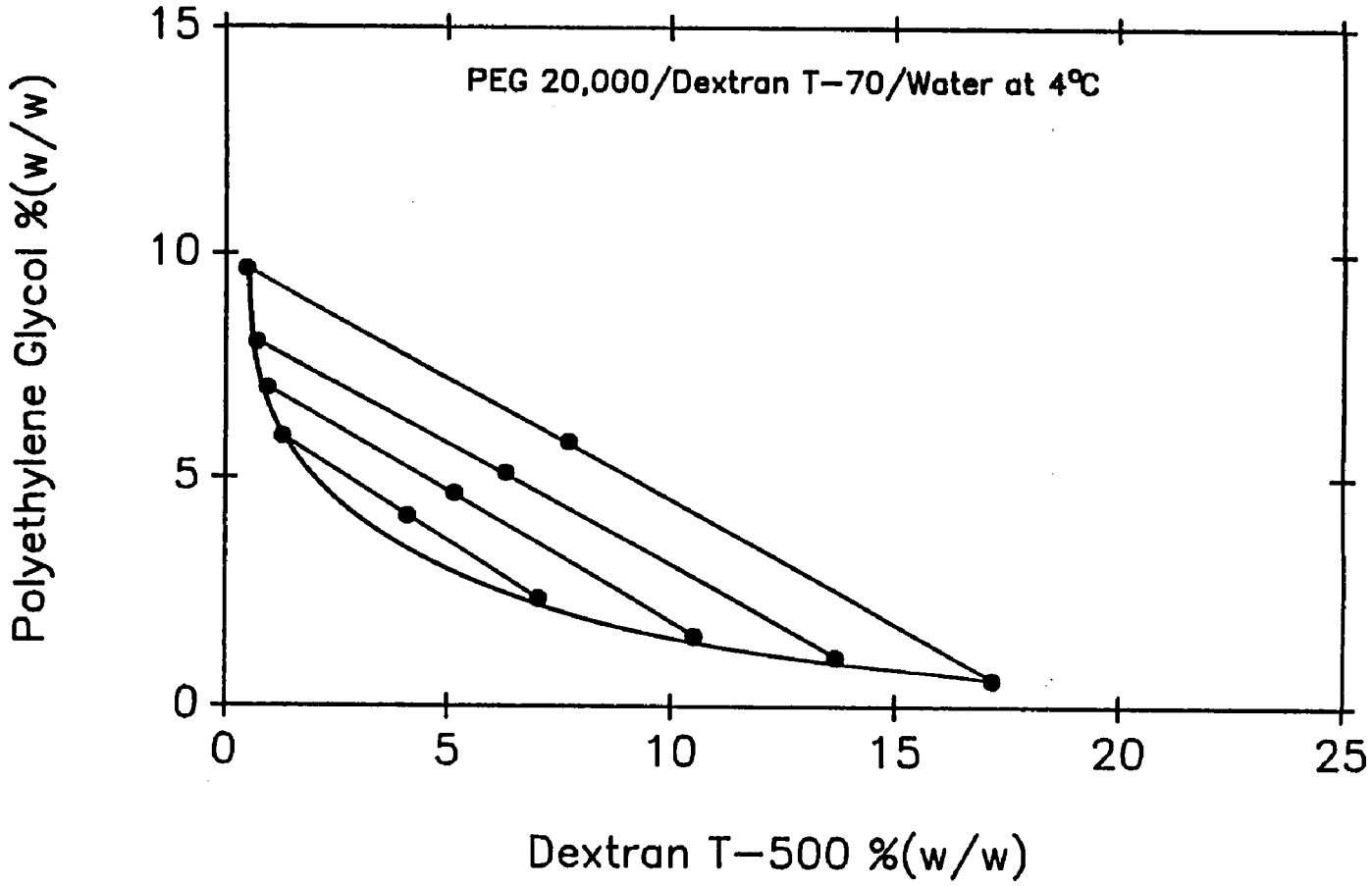

Figure 3.8 Phase Diagram for the PEG 20,000/ Dextran T-70/Water System at 4°C.

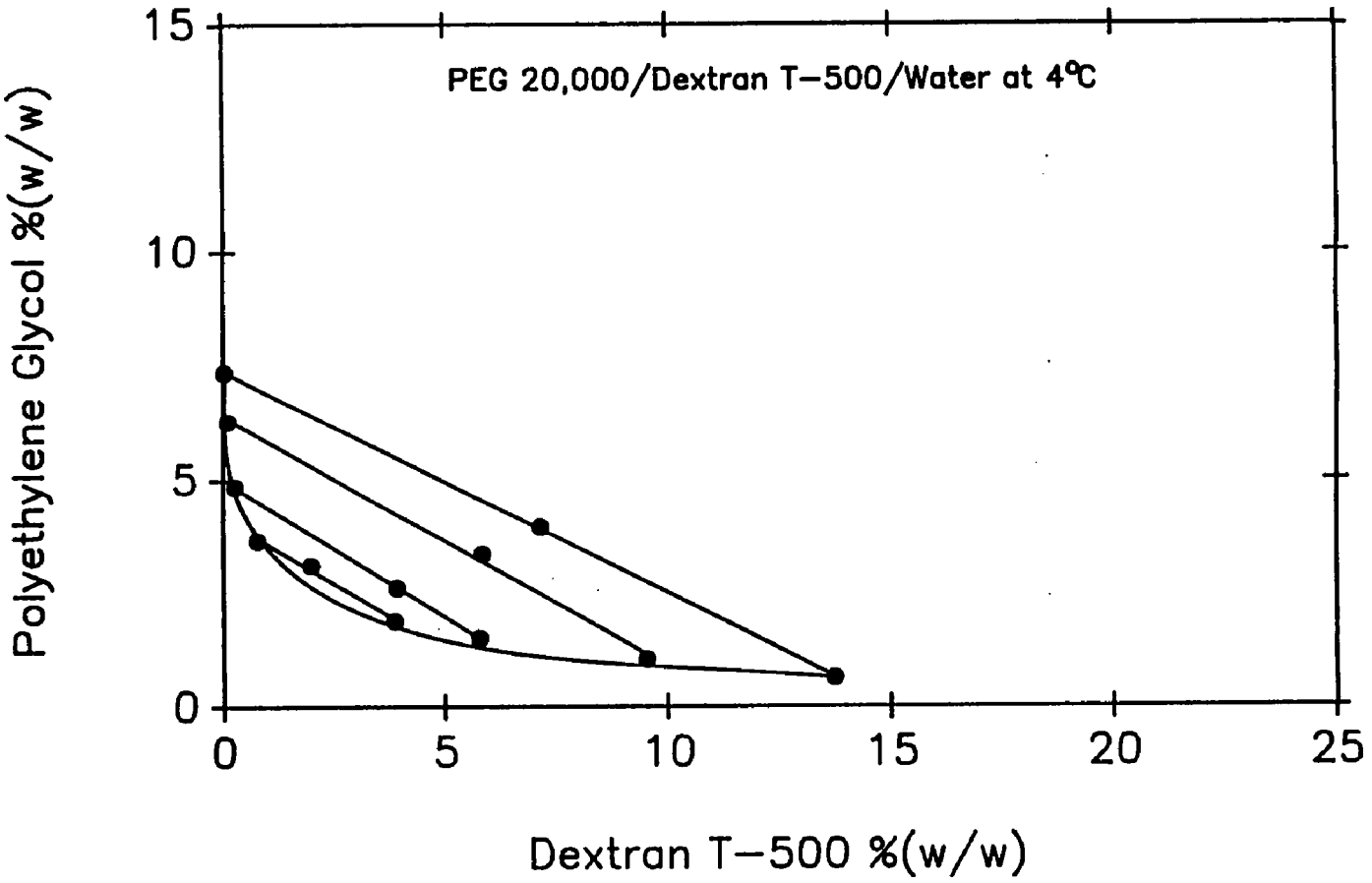

Figure 3.9 Phase Diagram for the PEG 20,000/ Dextran T-500/Water System at 4°C.

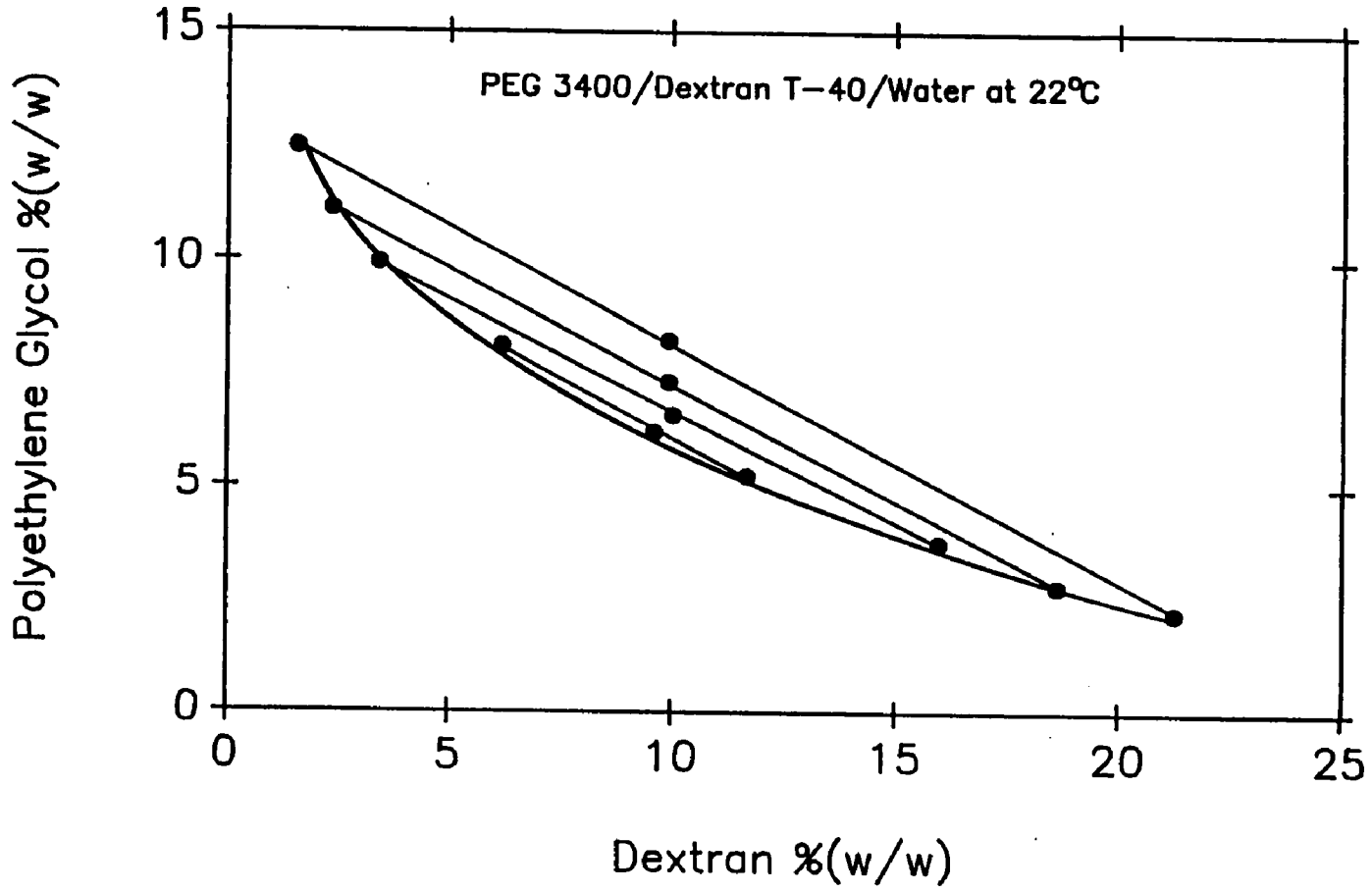

Figure 3.10 Phase Diagram for the PEG 3400/ Dextran T-40/Water System at 22°C.

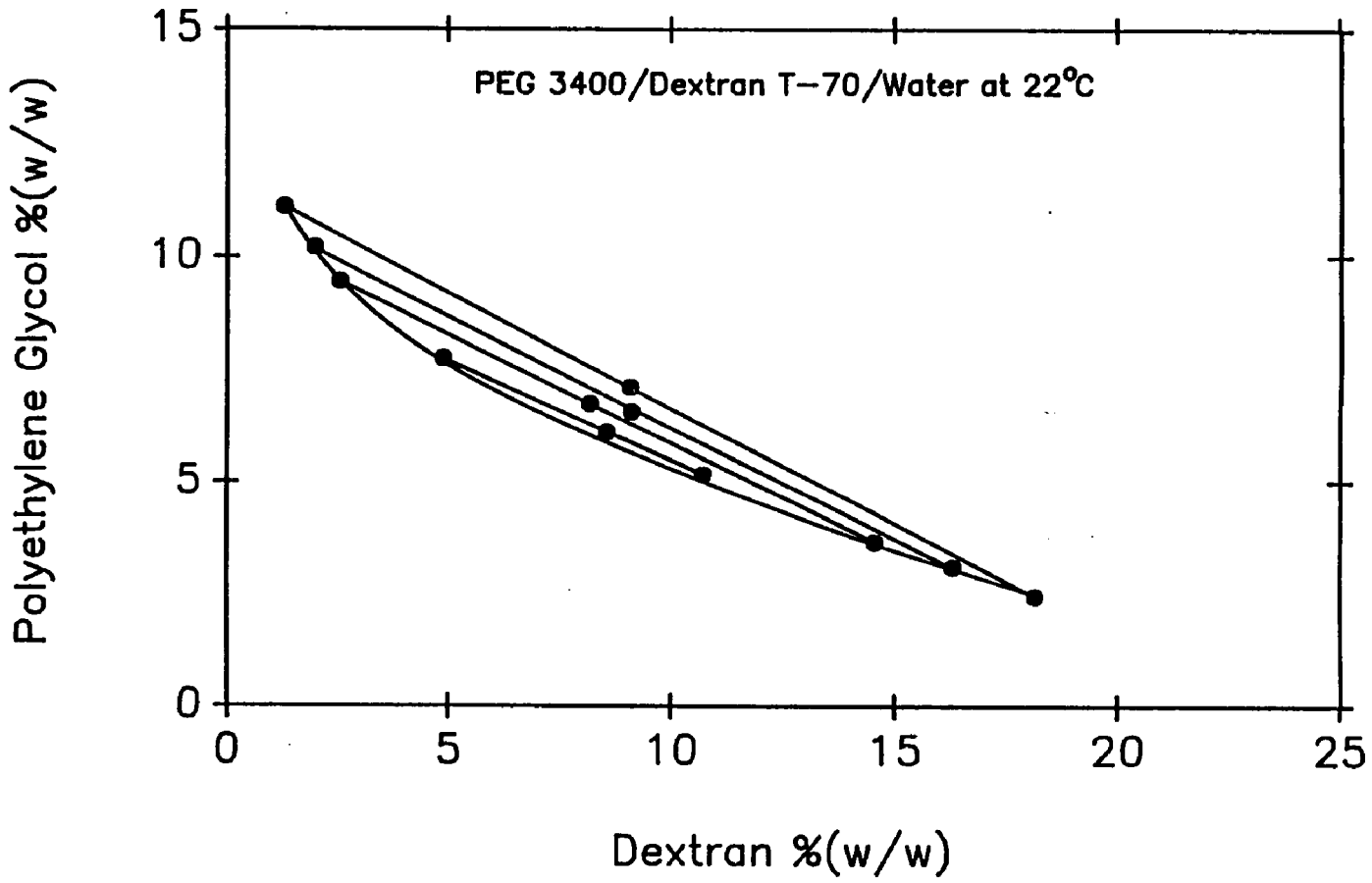

Figure 3.11 Phase Diagram for the PEG 3400/ Dextran T-70/Water System at 22°C.

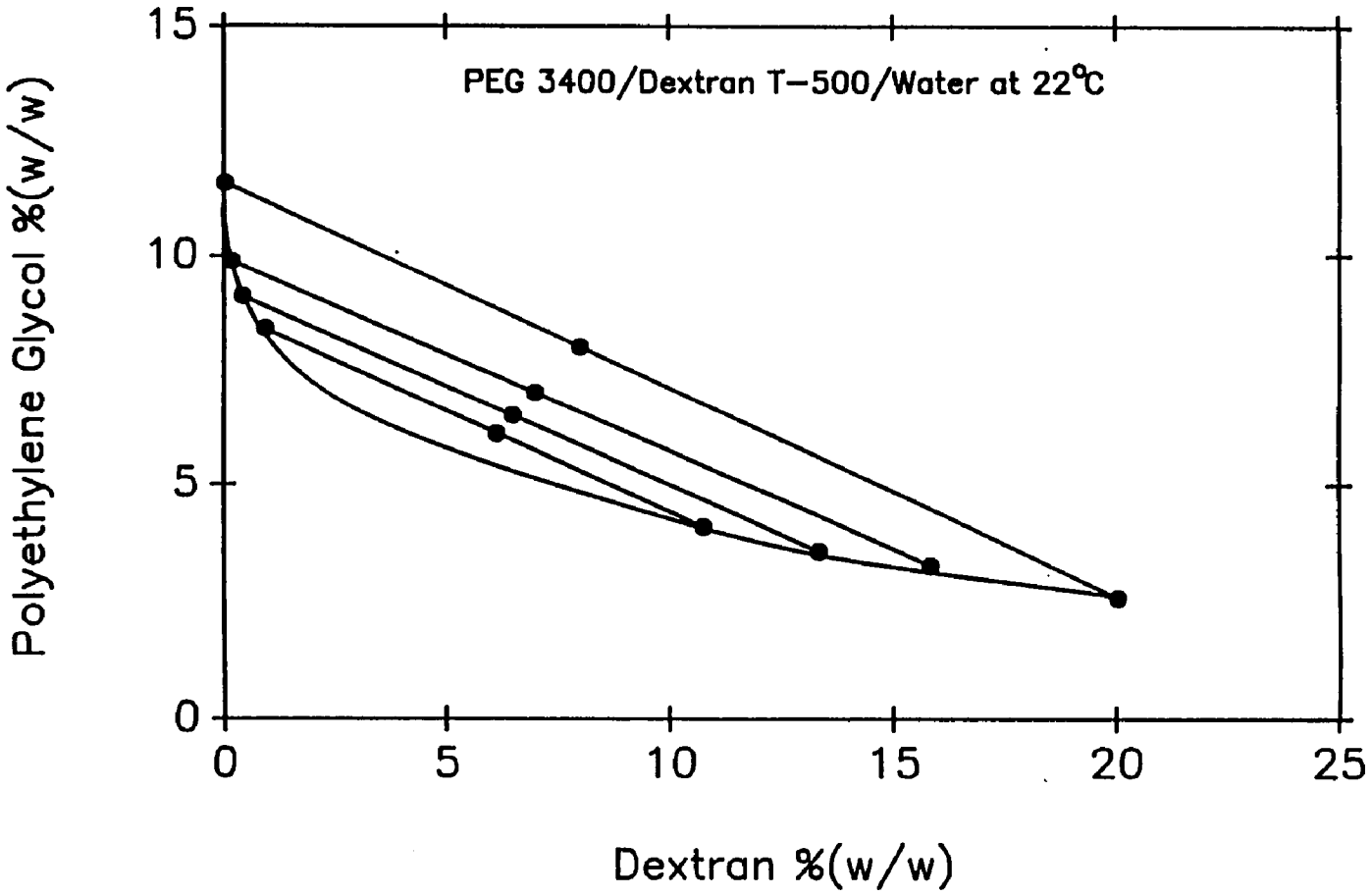

Figure 3.12 Phase Diagram for the PEG 3400/ Dextran T-500/Water System at 22°C.

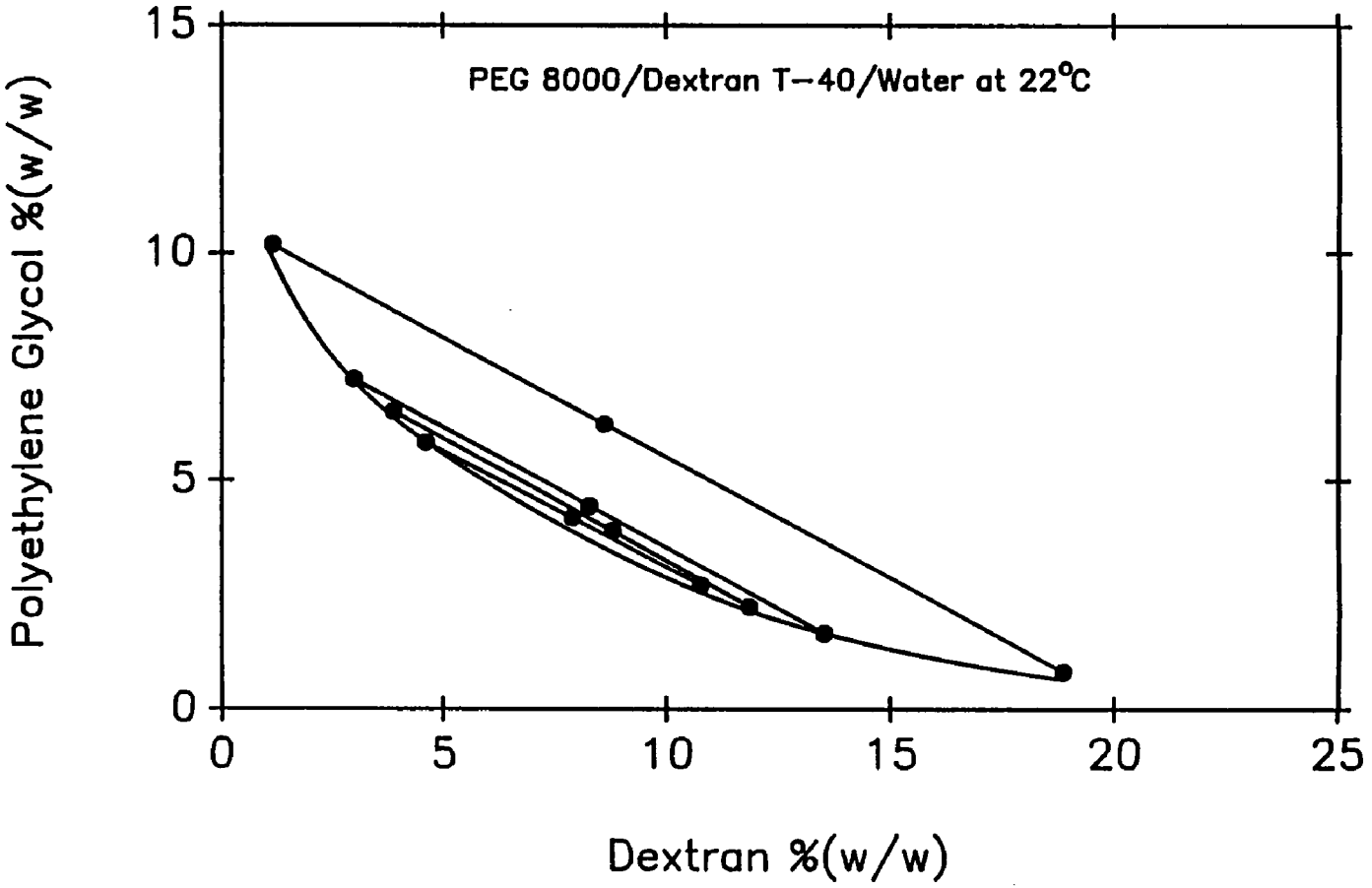

Figure 3.13 Phase Diagram for the PEG 8000/ Dextran T-40/Water System at 22°C.

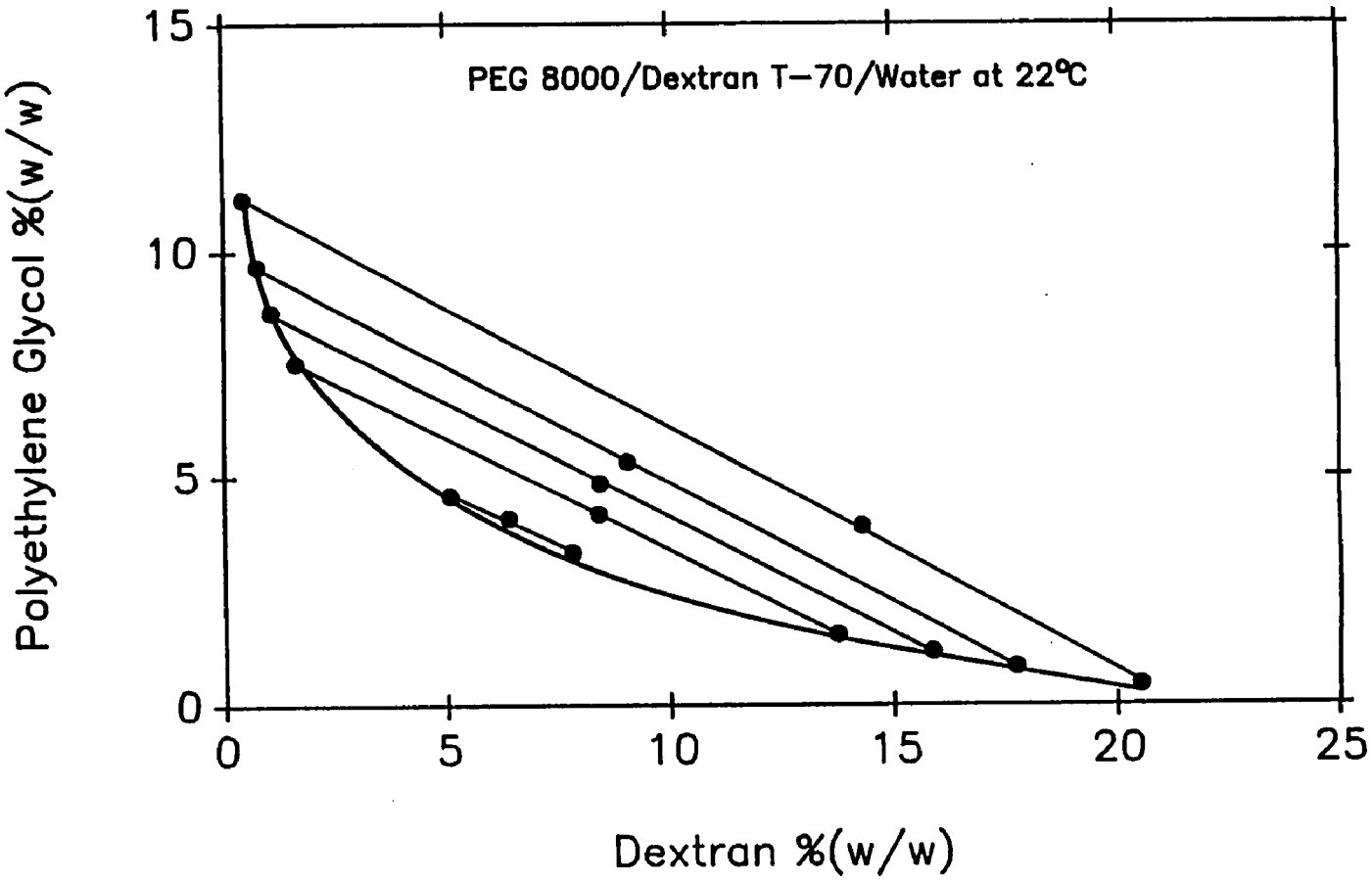

Figure 3.14 Phase Diagram for the PEG 8000/ Dextran T-70/Water System at 22°C.

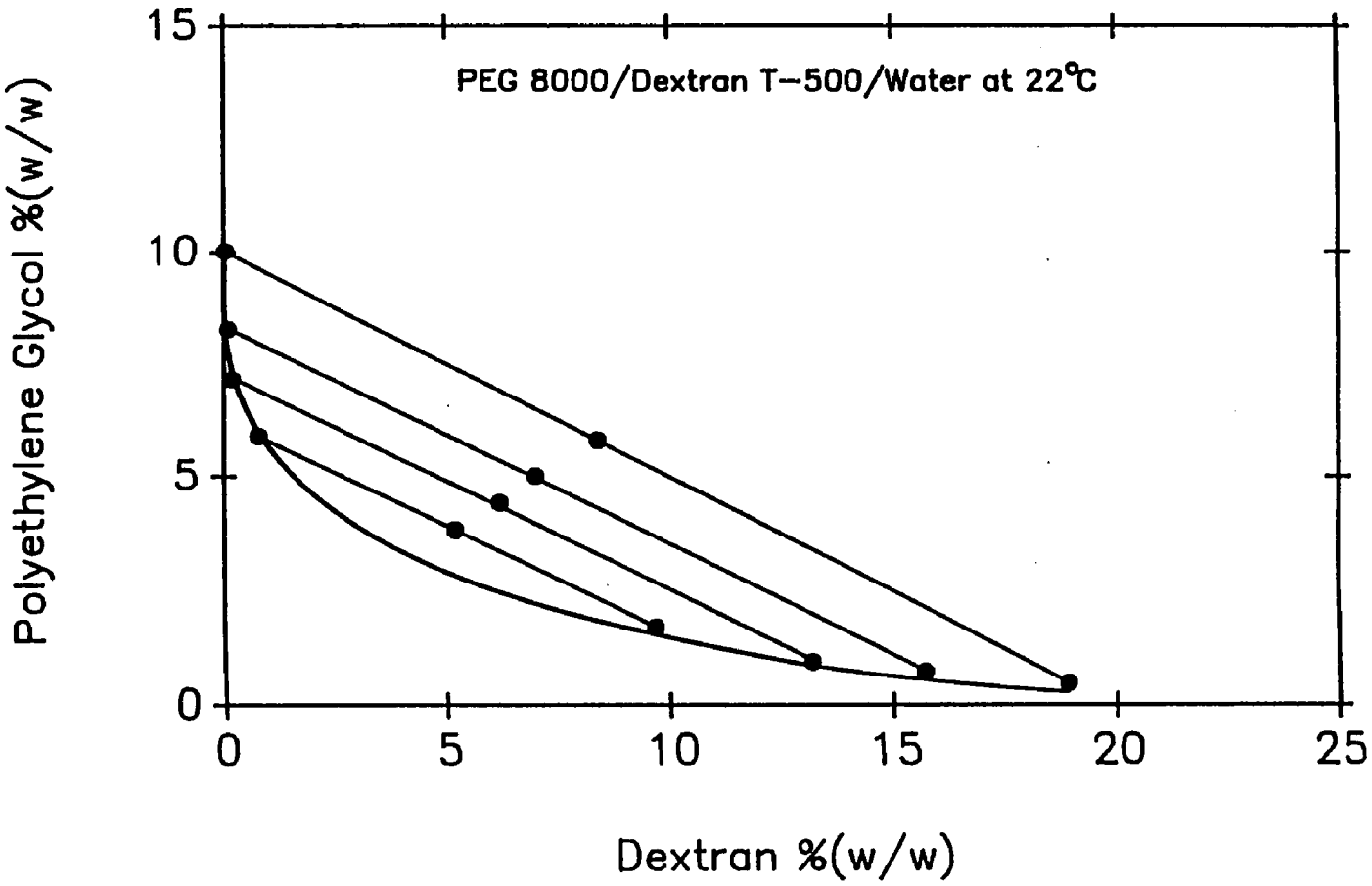

Figure 3.15 Phase Diagram for the PEG 8000/ Dextran T-500/Water System at 22°C.

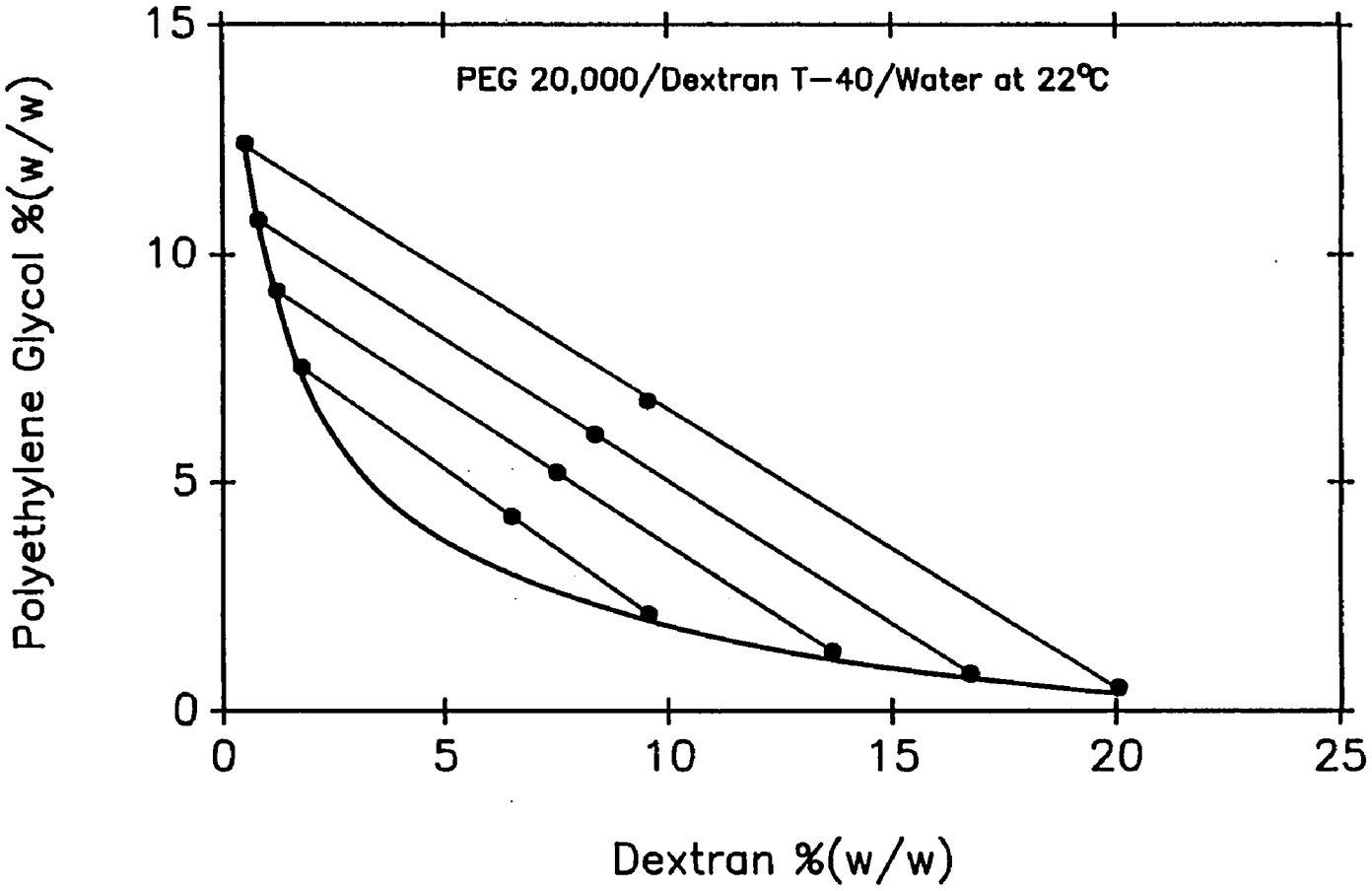

Figure 3.16 Phase Diagram for the PEG 20,000/ Dextran T-40/Water System at 22°C.

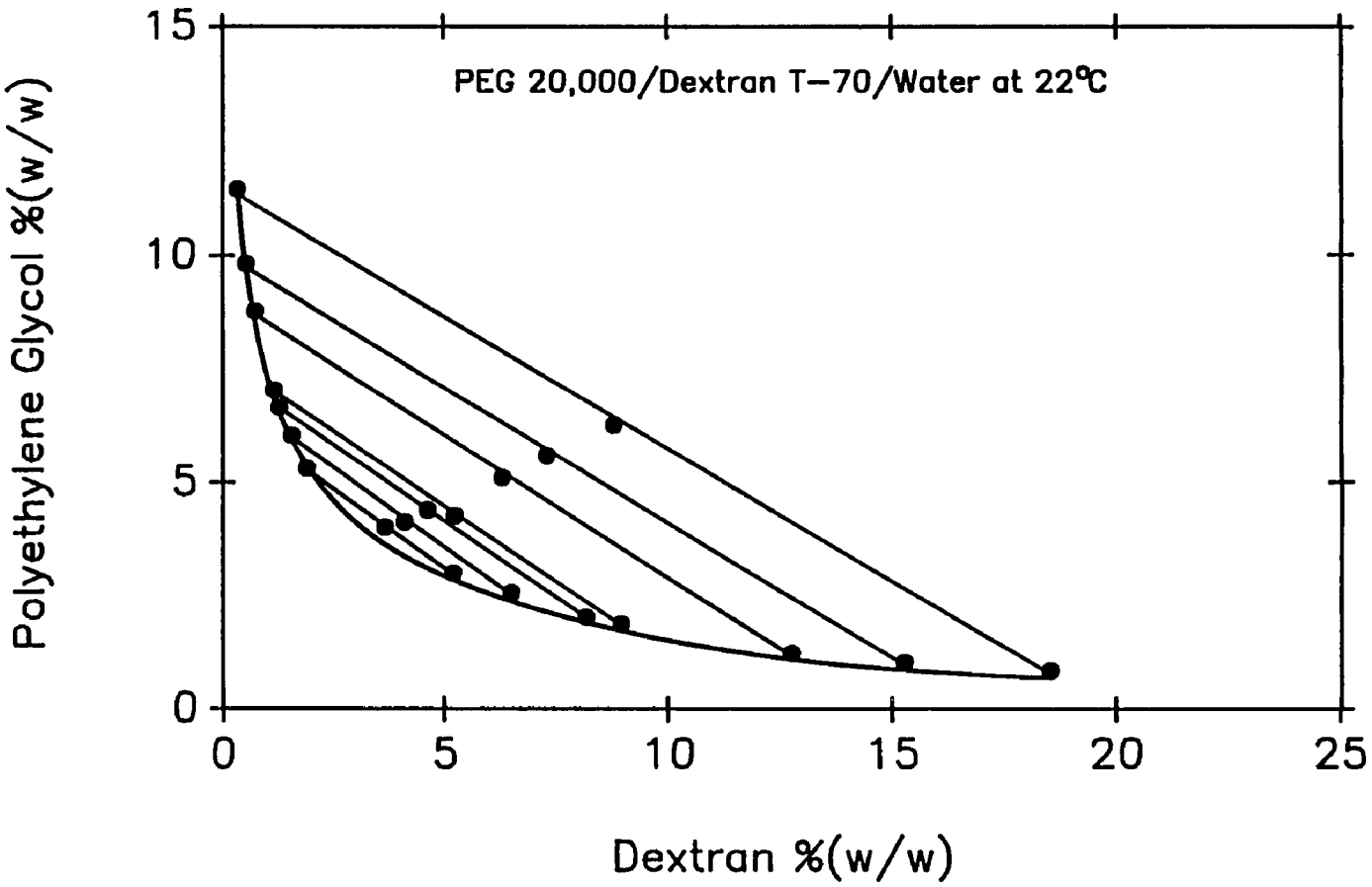

Figure 3.17 Phase Diagram for the PEG 20,000/ Dextran T-70/Water System at 22°C.

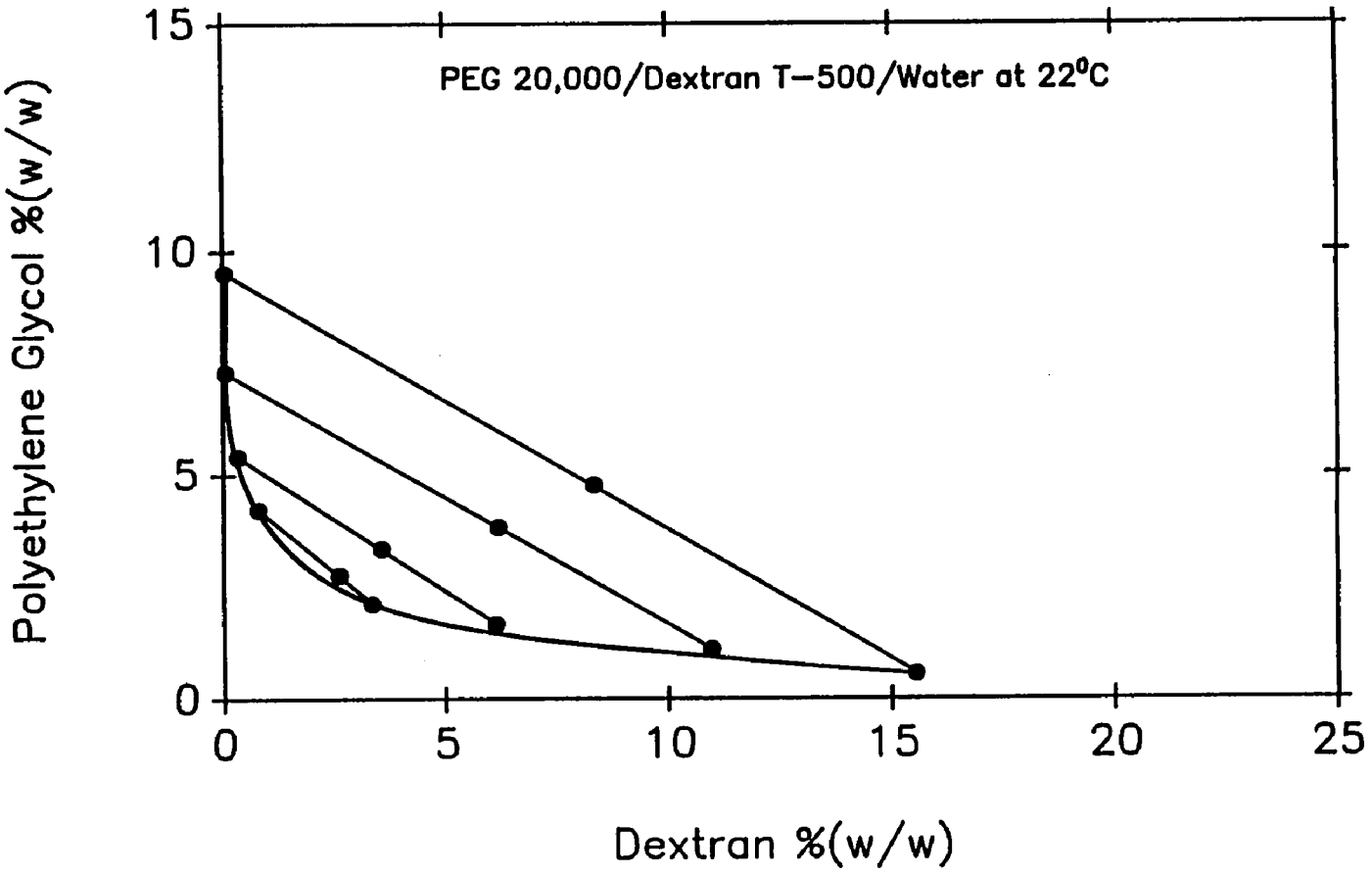

Figure 3.18 Phase Diagram for the PEG 20,000/ Dextran T-500/Water System at 22°C.

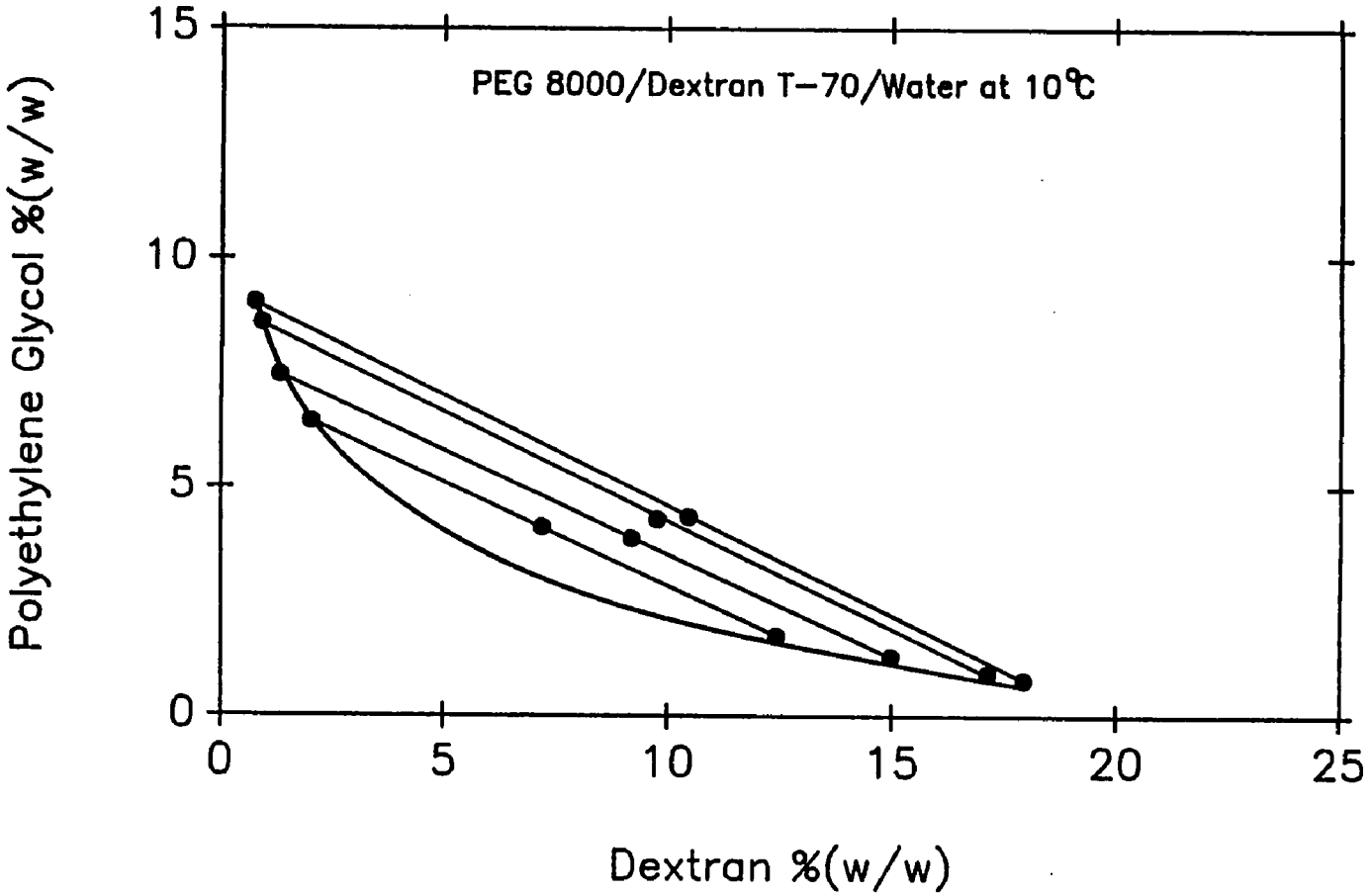

Figure 3.19 Phase Diagram for the PEG 8000/ Dextran T-70/Water System at 10°C.

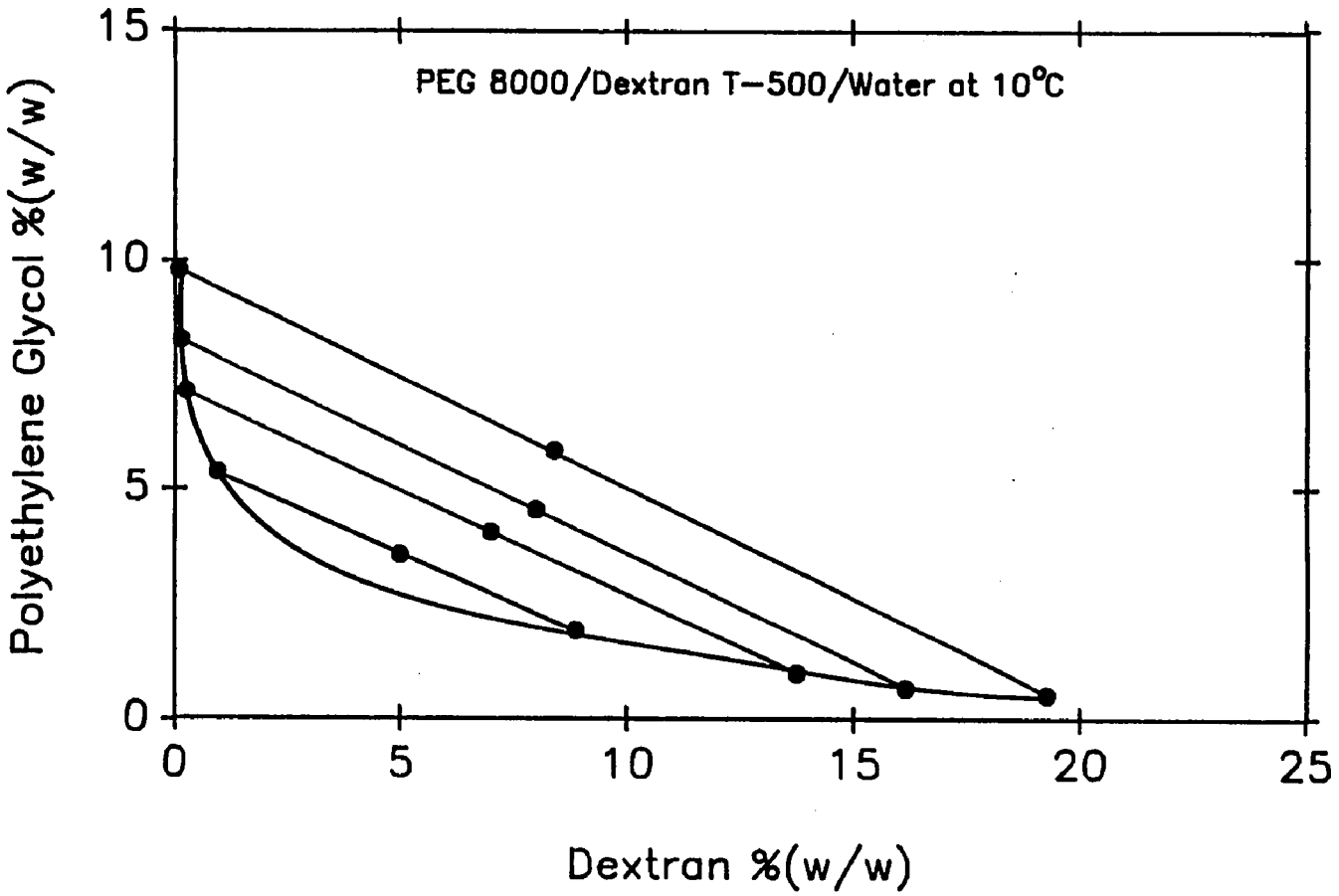

Figure 3.20 Phase Diagram for the PEG 8000/ Dextran T-500/Water System at 10°C.

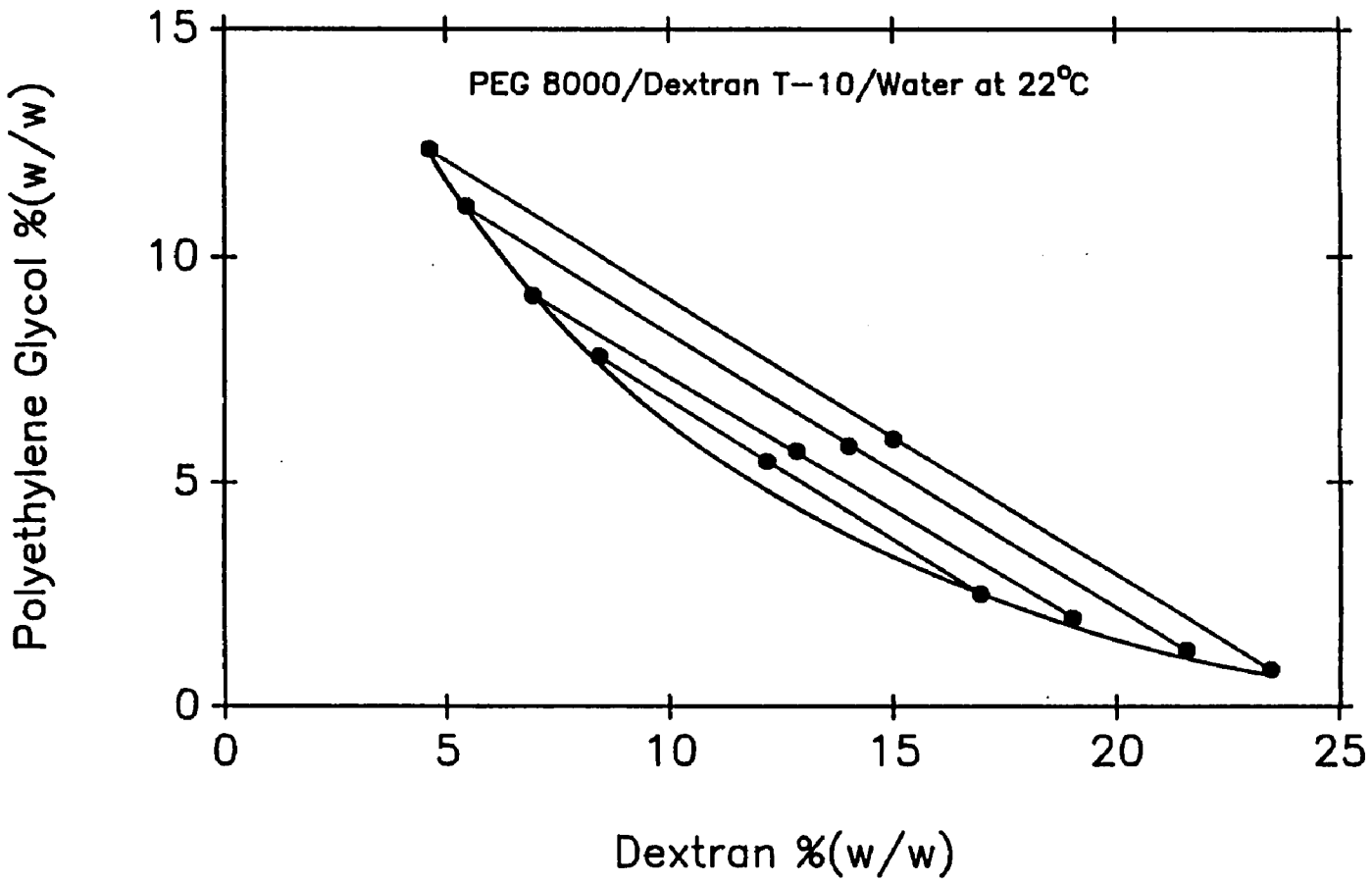

Figure 3.21 Phase Diagram for the PEG 8000/ Dextran T-10/Water System at 22°C.

Table 3.1 Phase Compositions for PEG/Dextran/Water Systems at 4°C.

Tie Line	Concentrations in %(w/w)								
	Total System			Bottom Phase			Top Phase		
No.	Dextran	PEG	Water	Dextran	PEG	Water	Dextran	PEG	Water
				PEG 3400/Dextran T-40/Water					
1	8.80	6.50	84.70	15.83	3.28	80.89	3.70	8.82	87.48
2	9.30	6.70	84.00	17.58	2.77	79.65	2.86	9.62	87.52
3	10.00	6.90	83.10	19.57	2.39	78.04	2.13	10.71	87.16
4	10.60	7.10	82.30	21.21	2.09	76.70	1.76	11.19	87.05
				PEG 3400/Dextran T-70/Water					
1	7.30	6.30	86.40	14.62	3.06	82.32	2.32	8.24	89.44
2	7.80	6.45	85.75	15.89	2.82	81.29	1.82	8.96	89.22
3	8.40	6.55	85.05	17.34	2.61	80.05	1.48	9.54	88.98
4	9.00	6.70	84.30	18.93	2.42	78.65	1.18	10.07	88.75
				PEG 3400/Dextran T-500/Water					
1	5.70	5.00	89.30	9.20	3.45	87.35	1.51	6.43	92.06
2	7.00	6.50	86.50	17.48	2.10	80.42	0.12	9.39	90.49
3	8.00	7.00	85.00	20.12	1.98	77.90	0.07	10.28	89.65
4	8.00	8.00	84.00	22.77	1.50	75.73	0.04	11.51	88.45
				PEG 8000/Dextran T-40/Water					
1	7.50	3.90	88.60	10.04	2.80	87.16	5.73	4.69	89.58
2	8.20	4.20	87.60	13.26	1.59	85.15	2.89	6.72	90.39
3	8.70	4.60	86.70	15.58	1.17	83.25	2.01	7.87	90.12
4	9.20	4.90	85.90	17.42	0.72	81.86	1.62	8.55	89.83
				PEG 8000/Dextran T-70/Water					
1	7.25	3.70	89.05	11.91	1.56	86.53	2.35	5.95	91.70
2	8.00	5.00	87.00	17.17	0.76	82.07	0.88	8.29	90.83
3	9.40	4.70	85.90	18.05	0.72	81.23	0.77	8.64	90.59
4	10.50	5.10	84.40	20.25	0.58	79.17	0.55	9.71	89.74
				PEG 8000/Dextran T-500/Water					
1	4.84	3.27	91.89	8.83	1.63	89.54	0.86	4.91	94.23
2	5.86	4.50	89.64	14.11	0.73	85.16	0.11	7.03	92.86
3	7.50	5.76	86.74	18.73	0.43	80.84	0.03	9.27	90.70
4	8.00	7.00	85.00	21.61	0.30	78.09	0.01	10.83	89.16
				PEG 20000/Dextran T-40/Water					
1	4.20	4.20	91.60	5.64	3.02	91.34	3.13	4.72	92.15
2	5.00	4.50	90.50	7.99	2.34	89.67	1.92	6.52	91.56
3	6.50	5.00	88.50	12.57	1.41	86.02	1.42	7.93	90.65
4	8.00	5.50	86.50	16.22	0.82	82.96	0.90	9.37	89.73
				PEG 20000/Dextran T-70/Water					
1	4.10	4.15	91.75	7.03	2.33	90.64	1.29	5.92	92.79
2	5.15	4.65	90.20	10.52	1.52	87.96	0.95	7.01	92.04
3	6.30	5.10	88.60	13.68	1.07	85.25	0.71	8.04	91.25
4	7.70	5.80	86.50	17.18	0.57	82.25	0.48	9.65	89.87
				PEG 20000/Dextran T-500/Water					
1	2.00	3.10	94.90	3.88	1.87	94.25	0.78	3.65	95.57
2	3.93	2.60	93.47	5.78	1.50	92.72	0.28	4.86	94.86
3	5.84	3.35	90.81	9.53	1.04	89.43	0.11	6.29	93.60
4	7.14	3.95	88.91	13.73	0.64	85.63	0.04	7.37	92.59

Table 3.2 Phase Compositions for PEG/Dextran/Water Systems at 22°C.

Tie Line	Concentrations in %(w/w) Total System			Bottom Phase			Top Phase		
No.	Dextran	PEG	Water	Dextran	PEG	Water	Dextran	PEG	Water
				PEG 3400/Dextran T-40/Water					
1	9.59	6.21	84.20	11.68	5.24	83.08	6.16	8.11	85.73
2	10.01	6.59	83.40	15.98	3.74	80.28	3.41	9.93	86.66
3	9.91	7.32	82.77	18.63	2.78	78.59	2.35	11.11	86.54
4	9.91	8.22	81.81	21.25	2.20	76.55	1.56	12.48	85.96
				PEG 3400/Dextran T-70/Water					
1	8.54	6.12	85.34	10.71	5.16	84.13	4.87	7.77	87.36
2	8.16	6.76	85.08	14.55	3.73	81.72	2.55	9.46	87.99
3	9.10	6.58	84.32	16.31	3.10	80.59	1.98	10.20	87.82
4	9.07	7.12	83.81	18.15	2.44	79.41	1.29	11.09	87.62
				PEG 3400/Dextran T-500/Water					
1	6.14	6.09	87.77	10.77	4.08	85.15	0.94	8.41	90.65
2	6.50	6.50	87.00	13.34	3.56	83.10	0.43	9.11	90.46
3	7.00	7.00	86.00	15.84	3.26	80.90	0.19	9.88	89.93
4	8.00	8.00	84.00	20.03	2.57	77.40	0.04	11.59	88.37
				PEG 8000/Dextran T-40/Water					
1	7.89	4.18	87.93	10.77	2.70	86.53	4.61	5.83	89.56
2	8.79	3.89	87.32	11.86	2.23	85.91	3.88	6.52	89.60
4	8.27	4.43	87.30	13.52	1.65	84.83	2.99	7.24	89.77
5	8.60	6.24	85.16	18.86	0.82	80.32	1.16	10.18	88.66
				PEG 8000/Dextran T-70/Water					
1	6.39	4.07	89.54	7.81	3.33	88.86	5.08	4.57	90.35
2	8.41	4.16	87.42	13.74	1.53	84.73	1.62	7.53	90.85
3	8.44	4.84	86.72	15.87	1.16	82.97	1.08	8.67	90.25
4	9.06	5.32	85.62	17.74	0.83	81.43	0.77	9.68	89.55
5	14.30	3.89	81.81	20.52	0.44	79.04	0.46	11.15	88.39
				PEG 8000/Dextran T-500/Water					
1	5.20	3.80	91.00	9.69	1.67	88.64	0.79	5.89	93.32
2	6.20	4.40	89.40	13.19	0.92	85.89	0.20	7.15	92.65
3	7.00	5.00	88.00	15.71	0.71	83.58	0.10	8.28	91.62
4	8.40	5.80	85.80	18.92	0.47	80.61	0.04	10.01	89.95
				PEG 20000/Dextran T-40/Water					
1	6.50	4.24	89.26	9.57	2.10	88.33	1.79	7.52	90.69
2	7.51	5.20	87.29	13.66	1.28	85.06	1.23	9.19	89.58
3	8.36	6.03	85.61	16.75	0.80	82.45	0.82	10.75	88.43
4	9.54	6.77	83.69	20.05	0.50	79.45	0.52	12.41	87.07
				PEG 20000/Dextran T-70/Water					
1	3.67	4.01	92.32	5.20	3.00	91.80	1.90	5.30	92.80
2	4.11	4.13	91.76	6.50	2.57	90.93	1.56	6.03	92.41
3	4.63	4.39	90.98	8.17	2.03	89.80	1.28	6.66	92.06
4	5.23	4.27	90.50	8.95	1.88	89.17	1.16	7.05	91.79
5	6.29	5.10	88.61	12.76	1.22	86.02	0.74	8.77	90.49
6	7.28	5.58	87.14	15.27	1.02	83.71	0.54	9.81	89.65
7	8.78	6.26	84.96	18.53	0.84	80.63	0.34	11.44	88.22
				PEG 20000/Dextran T-500/Water					
1	3.57	2.38	94.05	3.36	2.09	94.55	0.79	4.21	95.00
2	4.64	2.98	92.38	6.13	1.69	92.18	0.33	5.40	94.27
3	6.19	3.81	90.00	10.97	1.09	87.94	0.07	7.29	92.64
4	8.33	4.76	86.91	15.54	0.55	83.91	0.05	9.51	90.44

Table 3.3 Phase Compositions for PEG/Dextran/Water Systems at 10°C and the PEG 8000/Dextran T-10/Water System at 22°C.

	Concentrations in %(w/w)								
Tie Line	Total System			Bottom Phase			Top Phase		
No.	Dextran	PEG	Water	Dextran	PEG	Water	Dextran	PEG	Water
				PEG 8000/Dextran T-70/Water at 10°C					
1	7.19	4.13	88.68	12.43	1.75	85.82	2.02	6.43	91.55
2	9.19	3.89	86.92	14.98	1.29	83.73	1.32	7.45	91.23
3	9.77	4.22	86.01	17.14	0.92	81.94	0.91	8.59	90.50
4	10.47	4.35	85.18	17.95	0.79	81.26	0.75	9.03	90.22
				PEG 8000/Dextran T-500/Water at 10°C					
1	5.00	3.50	91.50	8.87	1.86	89.27	0.95	5.31	93.74
2	7.00	4.00	89.00	13.74	0.94	85.32	0.25	7.07	92.68
3	8.00	4.50	87.50	16.15	0.63	83.22	0.13	8.20	91.67
4	8.40	5.80	85.80	19.27	0.49	80.24	0.09	9.73	90.18
				PEG 8000/Dextran T-10/Water at 22°C					
1	12.18	5.47	82.35	16.96	2.50	80.54	8.42	7.82	83.76
2	12.84	5.70	81.46	19.01	1.96	79.03	6.92	9.16	83.92
3	14.00	5.81	80.19	21.56	1.25	77.19	5.44	11.11	83.45
4	15.00	5.96	79.04	23.46	0.82	75.72	4.63	12.37	83.00

decreased compatibility between the polymers.

Comparison of the set of binodial curves in Figures 3.1, 3.4 and 3.7; 3.2, 3.5 and 3.5; 3.3, 3.6 and 3.9; 3.10, 3.13 and 3.16; 3.11, 3.14 and 3.17; 3.12, 3.15 and 3.15 shows the effect of PEG molecular weight on phase separation. Increasing PEG molecular weight causes the binodial to shift toward the dextran axis and therefore become more symmetrical. Lower polymer concentrations are also required for phase separation as was observed above for increasing dextran molecular weight.

Examination of Figures 3.6, 3.15 and 3.20 reveals the effect of temperature on the PEG 8000/dextran T-500/water phase diagram. As the temperature is increased, the binodial moves to higher polymer concentrations, and results in a shorter tie-line length for the system. In other words, higher polymer concentrations are required for phase separation.

3.3.2 PEG/Potassium Phosphate/Water Phase Diagrams

The phase diagrams for the PEG/potassium phosphate/water systems at 4°C and pH 7.0 utilizing PEG of molecular weight 400, 600, 1,000, 1,500, 3,400, 8,000 and 20,000 are presented in Figures 3.22–3.28 (Lei *et al.*, 1990). The phase diagrams for the PEG 3400/potassium phosphate/water system at pH 6.0, 8.0 and 9.2 are provided in Figures 3.29–31. The binodials for the PEG 3400/potassium phosphate/water systems at pH 6.0, 7.0, 8.0 and 9.2 have also been provided in Figure 3.32. The phase compositions for the PEG/potassium phosphate aqueous systems at pH 7.0 are provided in Table 3.4, while the phase composition for the PEG/potassium phosphate aqueous systems at pH 6.0, 8.0 and 9.2 are provided in Table 3.5.

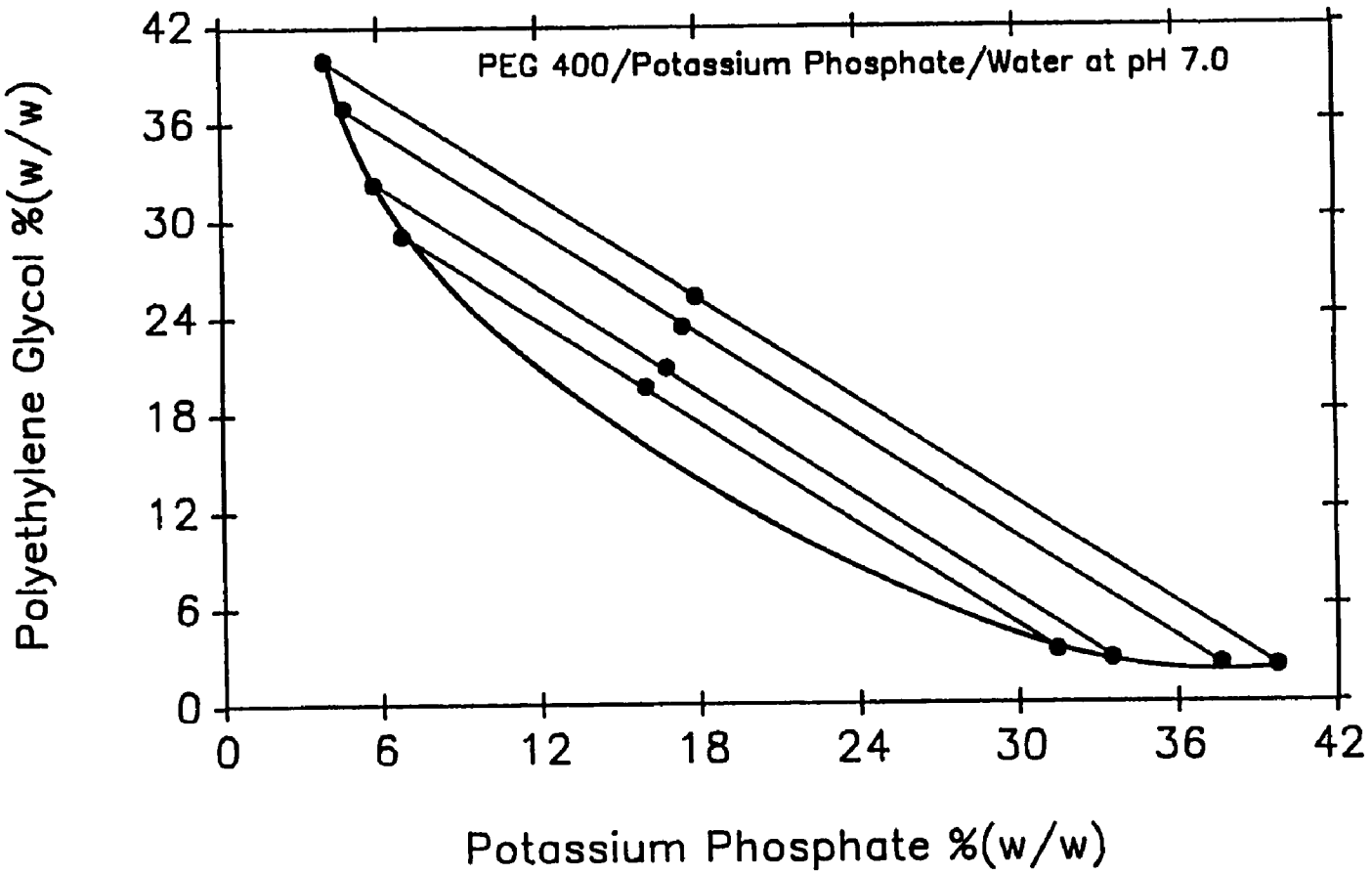

Figure 3.22 Phase Diagram for the PEG 400/Potassium Phosphate/Water System at 4°C and pH 7.0.

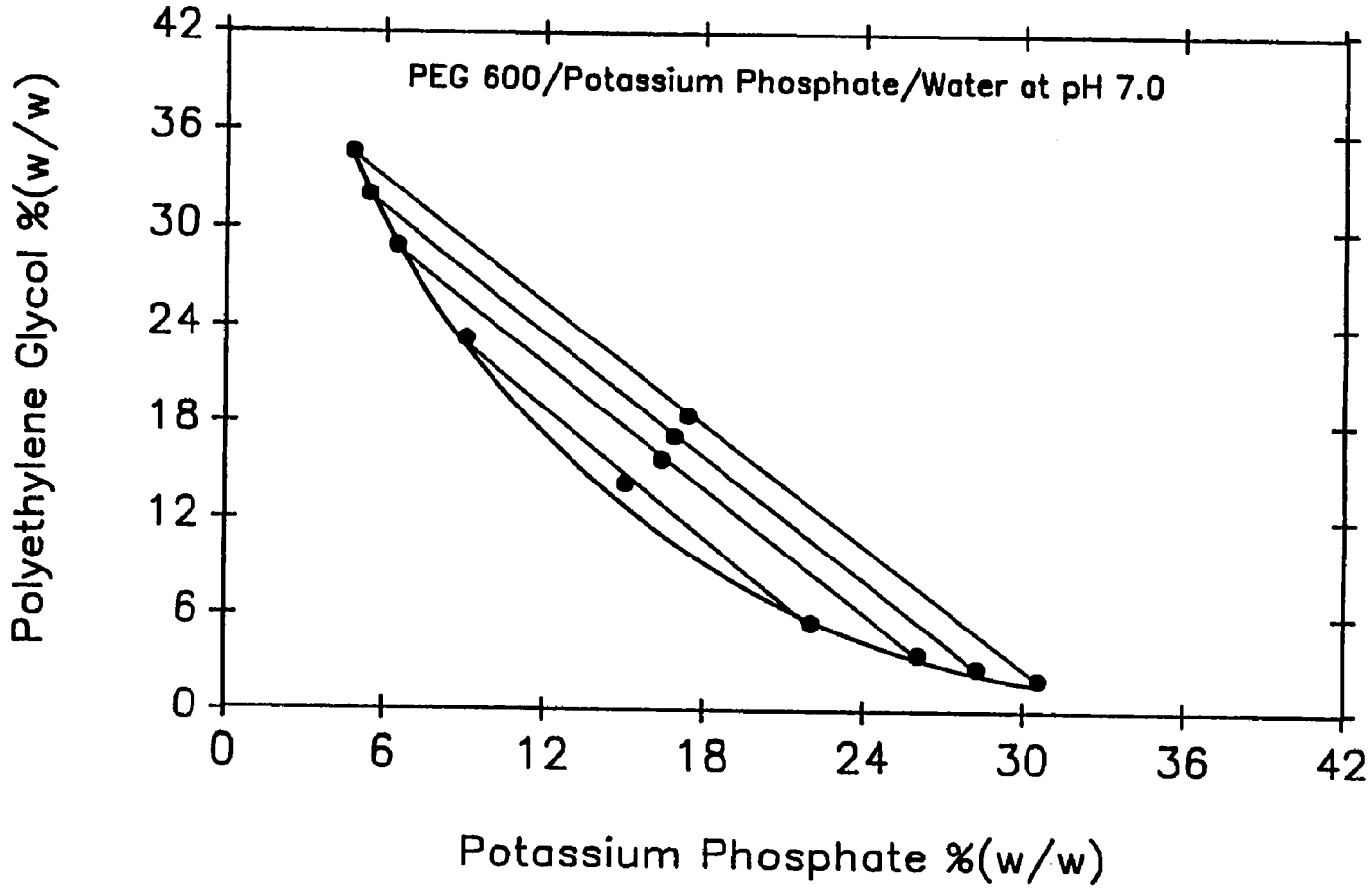

Figure 3.23 Phase Diagram for the PEG 600/Potassium Phosphate/Water System at 4°C and pH 7.0.

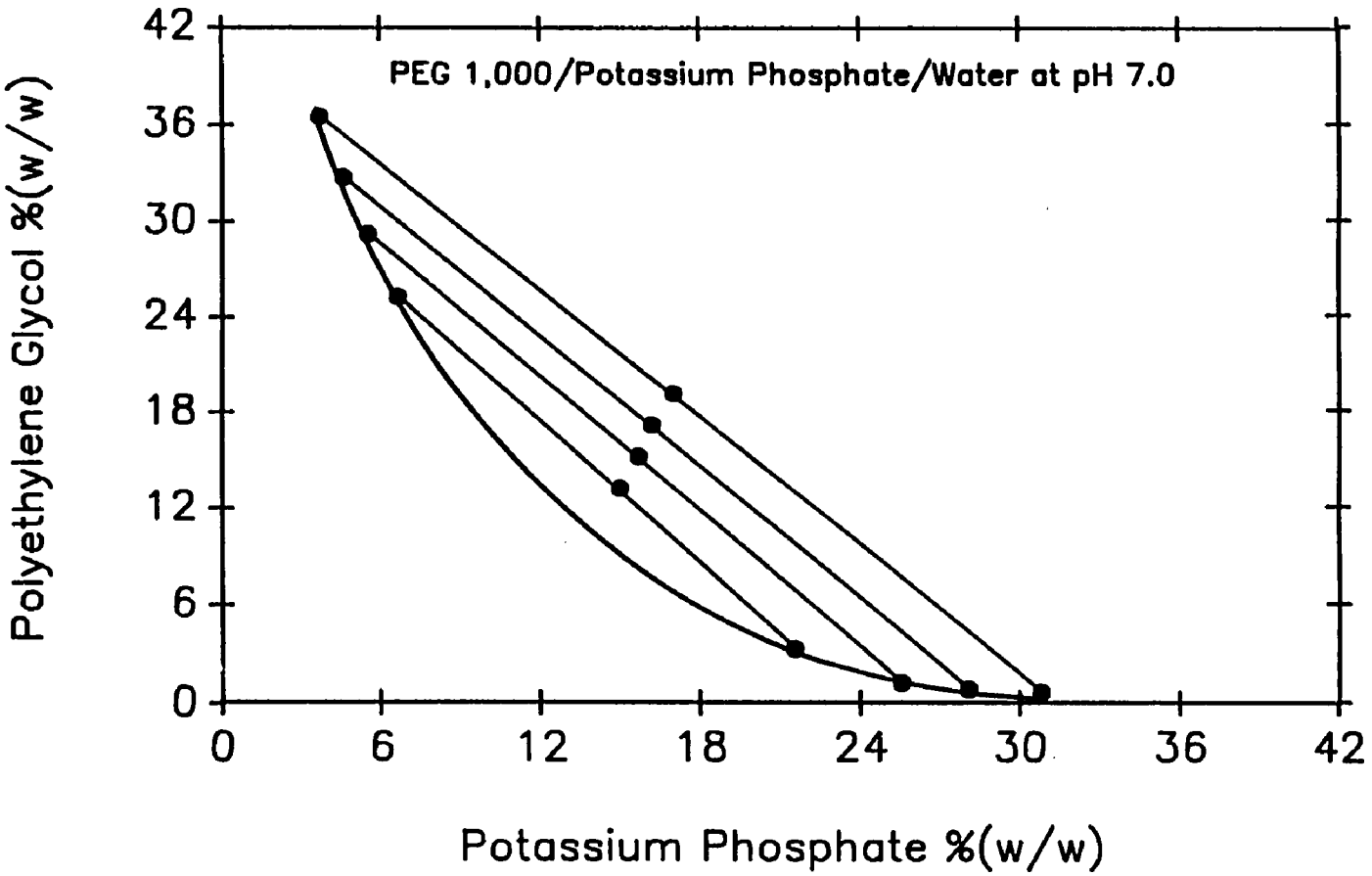

Figure 3.24 Phase Diagram for the PEG 1000/Potassium Phosphate/Water System at 4°C and pH 7.0.

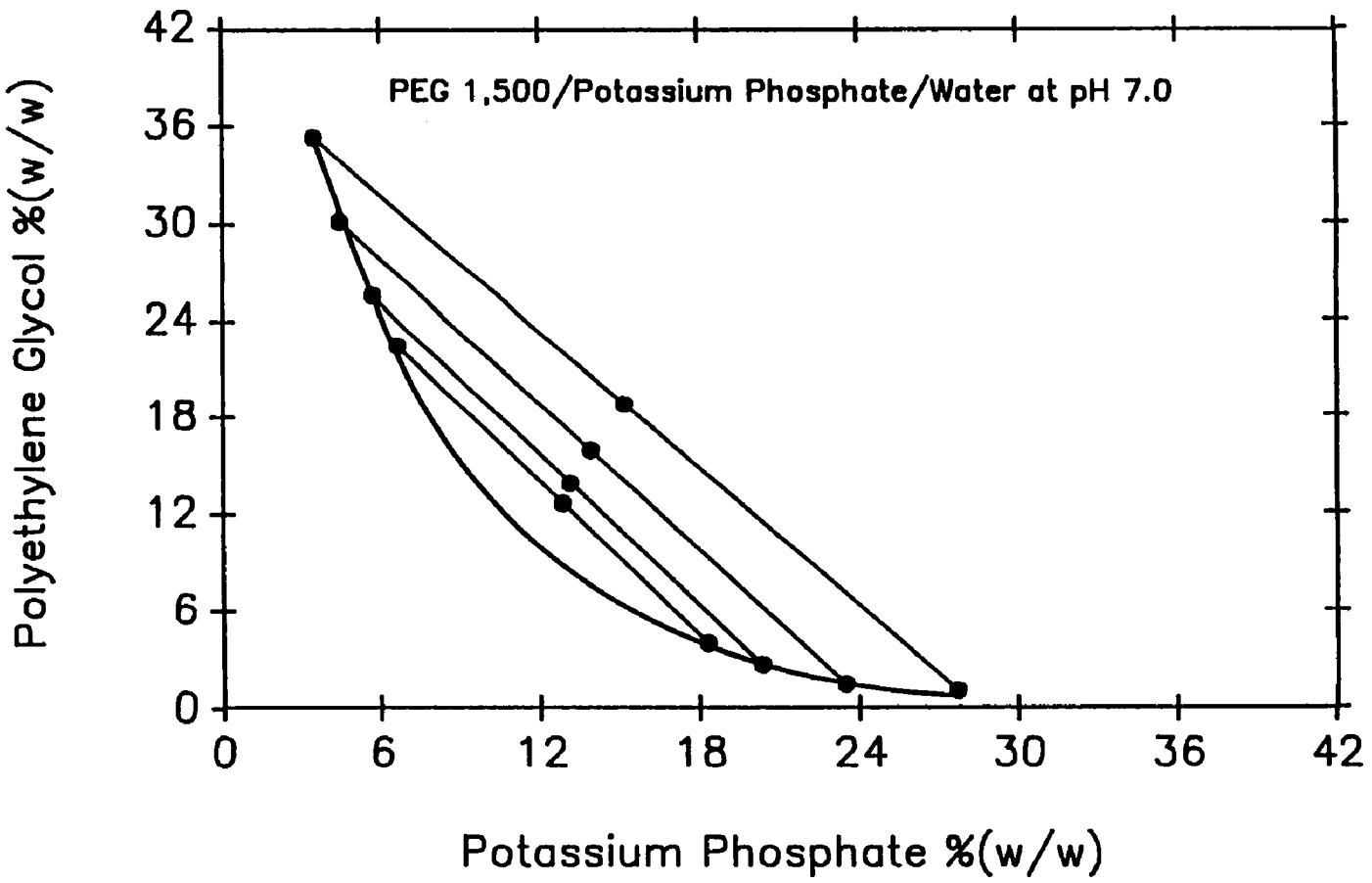

Figure 3.25 Phase Diagram for the PEG 1500/Potassium Phosphate/Water System at 4°C and pH 7.0.

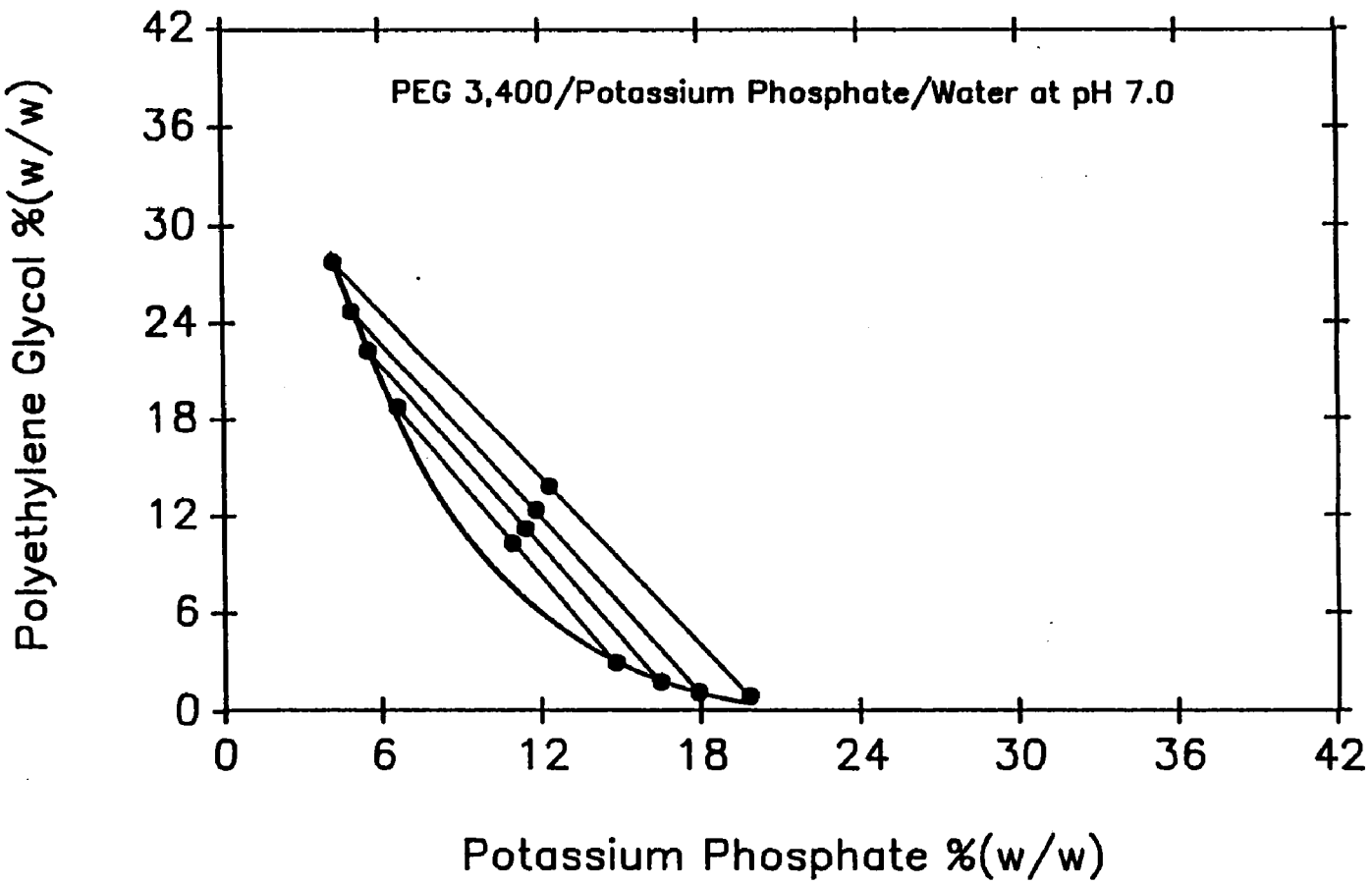

Figure 3.26 Phase Diagram for the PEG 3400/Potassium Phosphate/Water System at 4°C and pH 7.0.

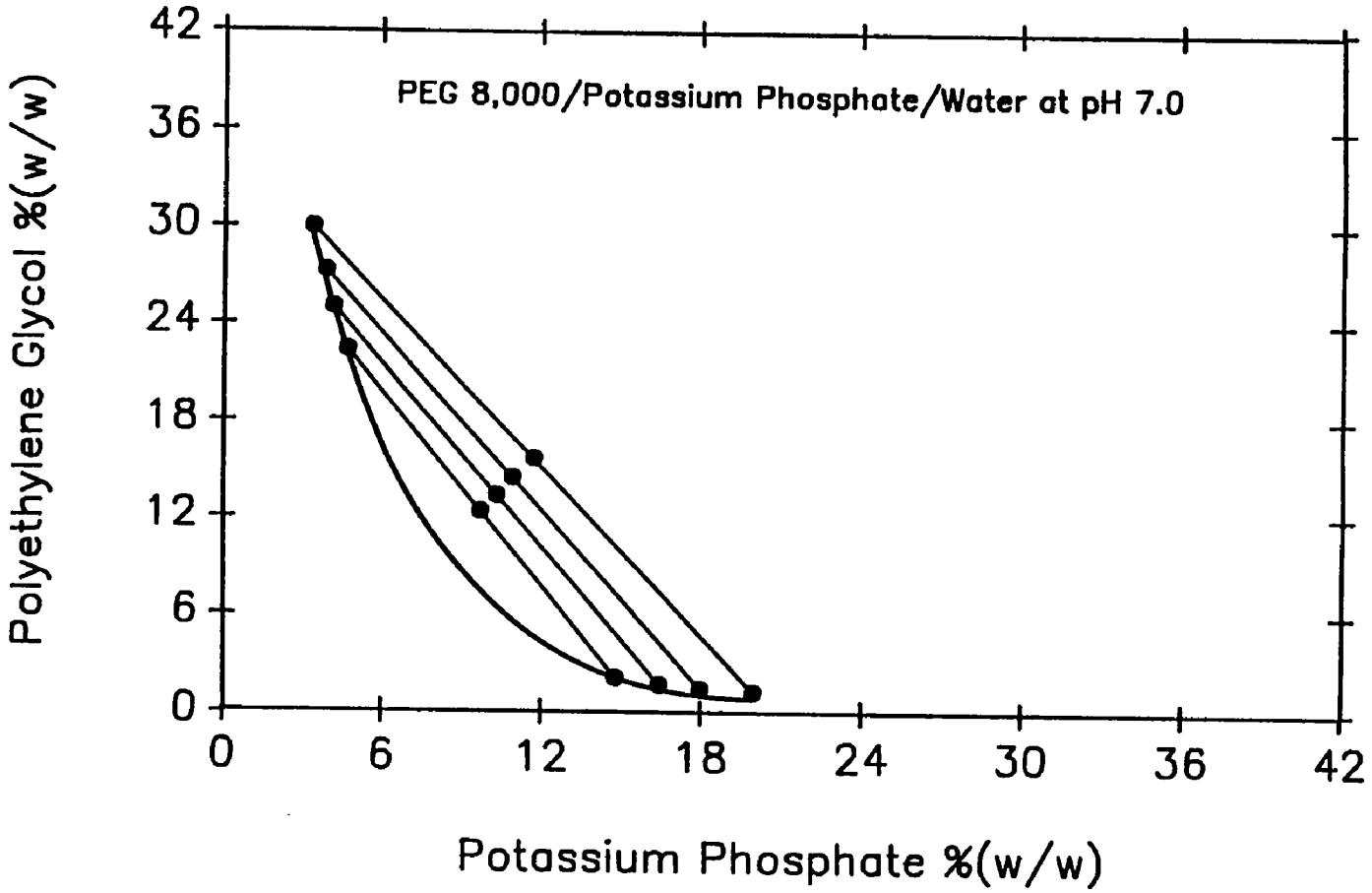

Figure 3.27 Phase Diagram for the PEG 8000/Potassium Phosphate/Water System at 4°C and pH 7.0.

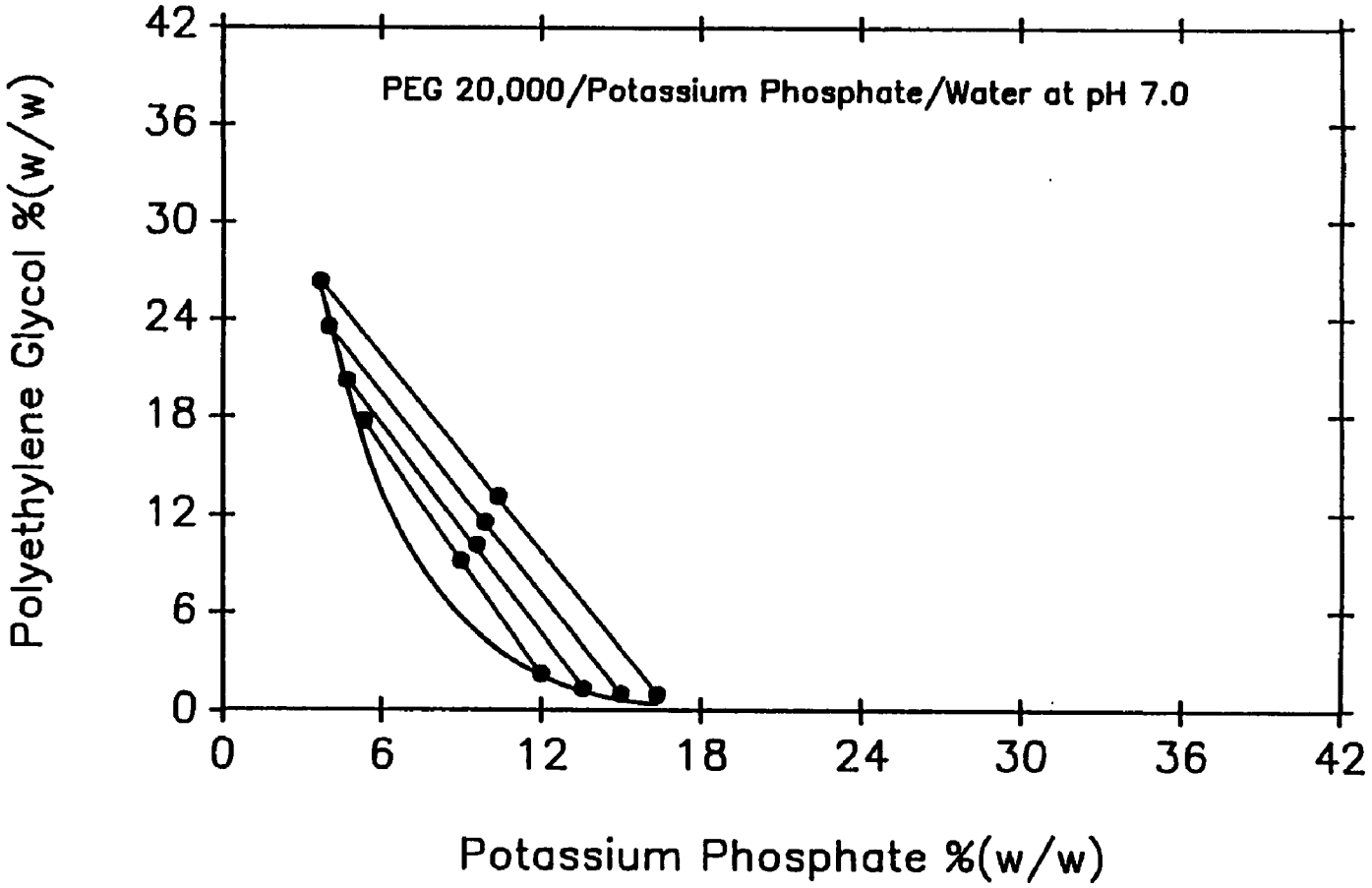

Figure 3.28 Phase Diagram for the PEG 20,000/Potassium Phosphate/Water System at 4°C and pH 7.0.

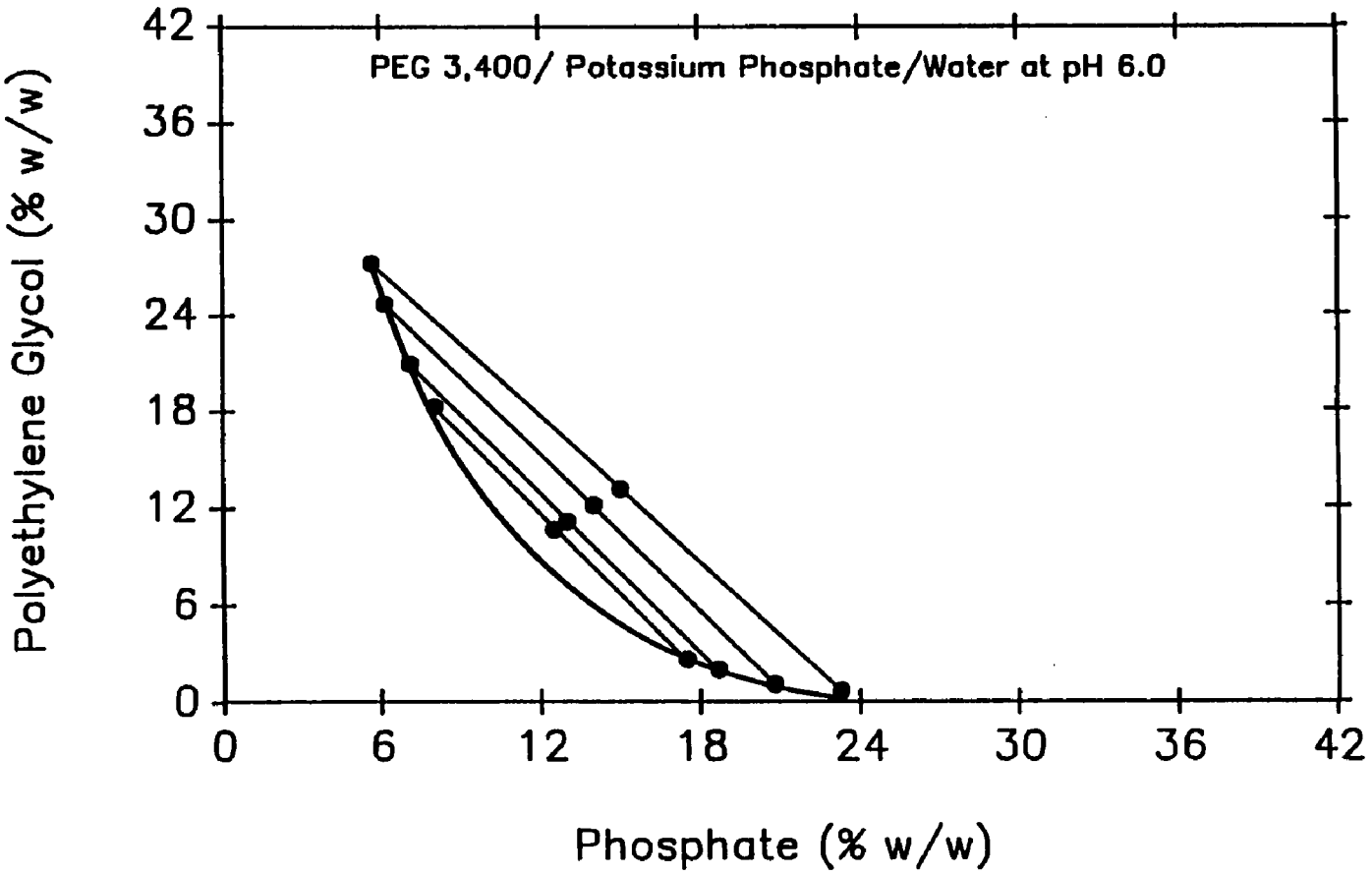

Figure 3.29 Phase Diagram for the PEG 3400/Potassium Phosphate/Water System at 4°C and pH 6.0.

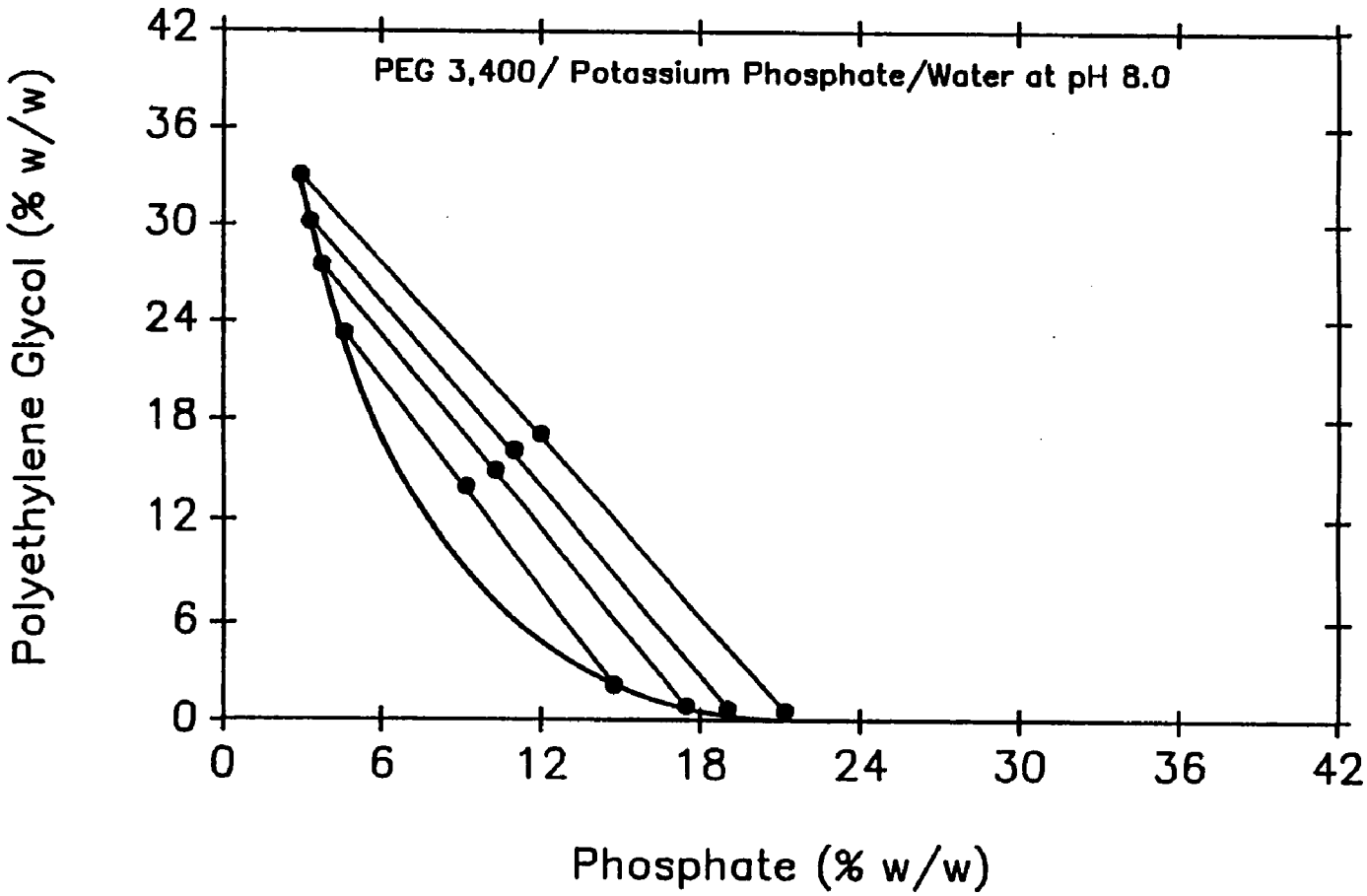

Figure 3.30 Phase Diagram for the PEG 3400/Potassium Phosphate/Water System at 4°C and pH 8.0.

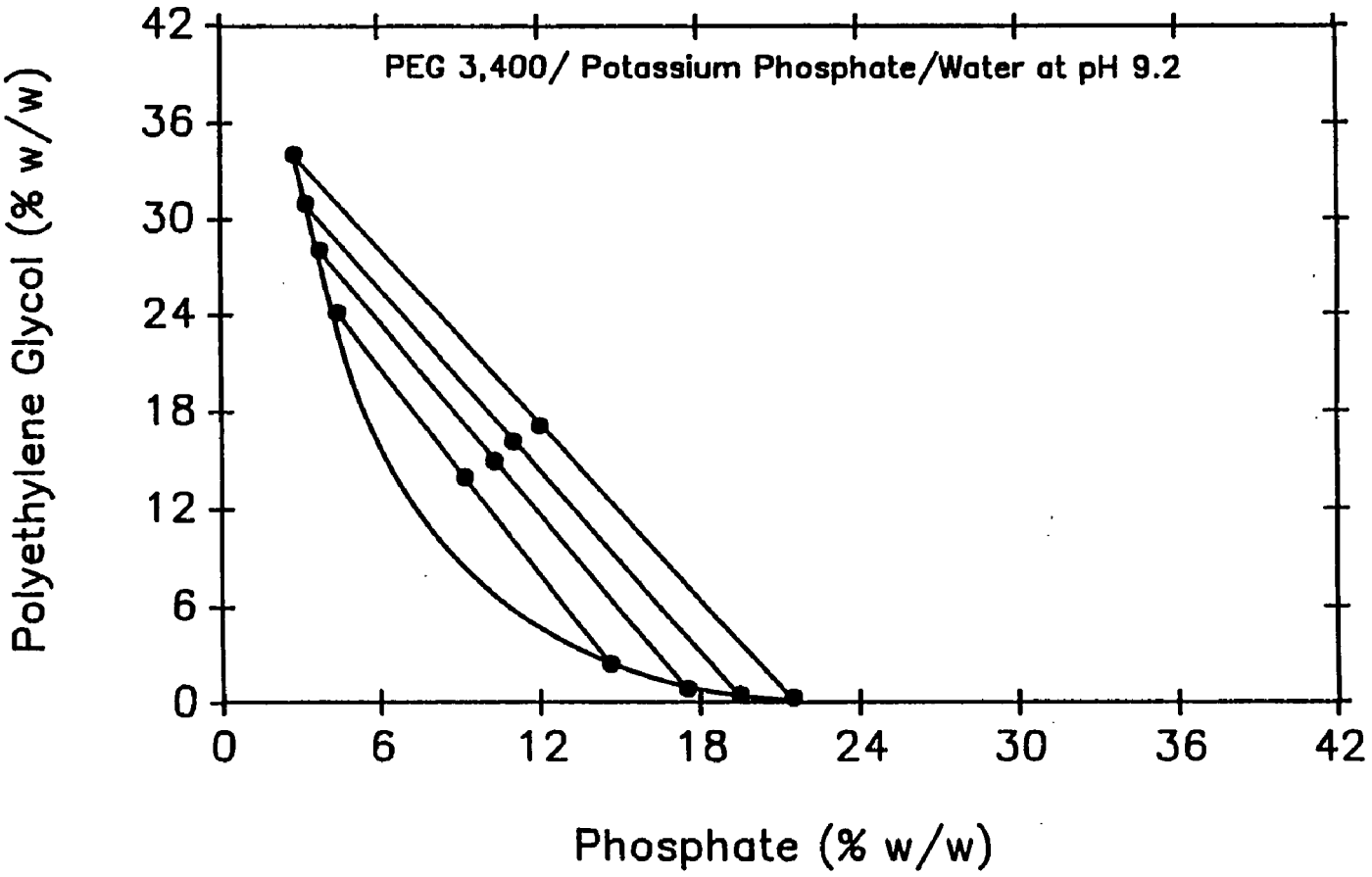

Figure 3.31 Phase Diagram for the PEG 3400/Potassium Phosphate/Water System at 4°C and pH 9.2.

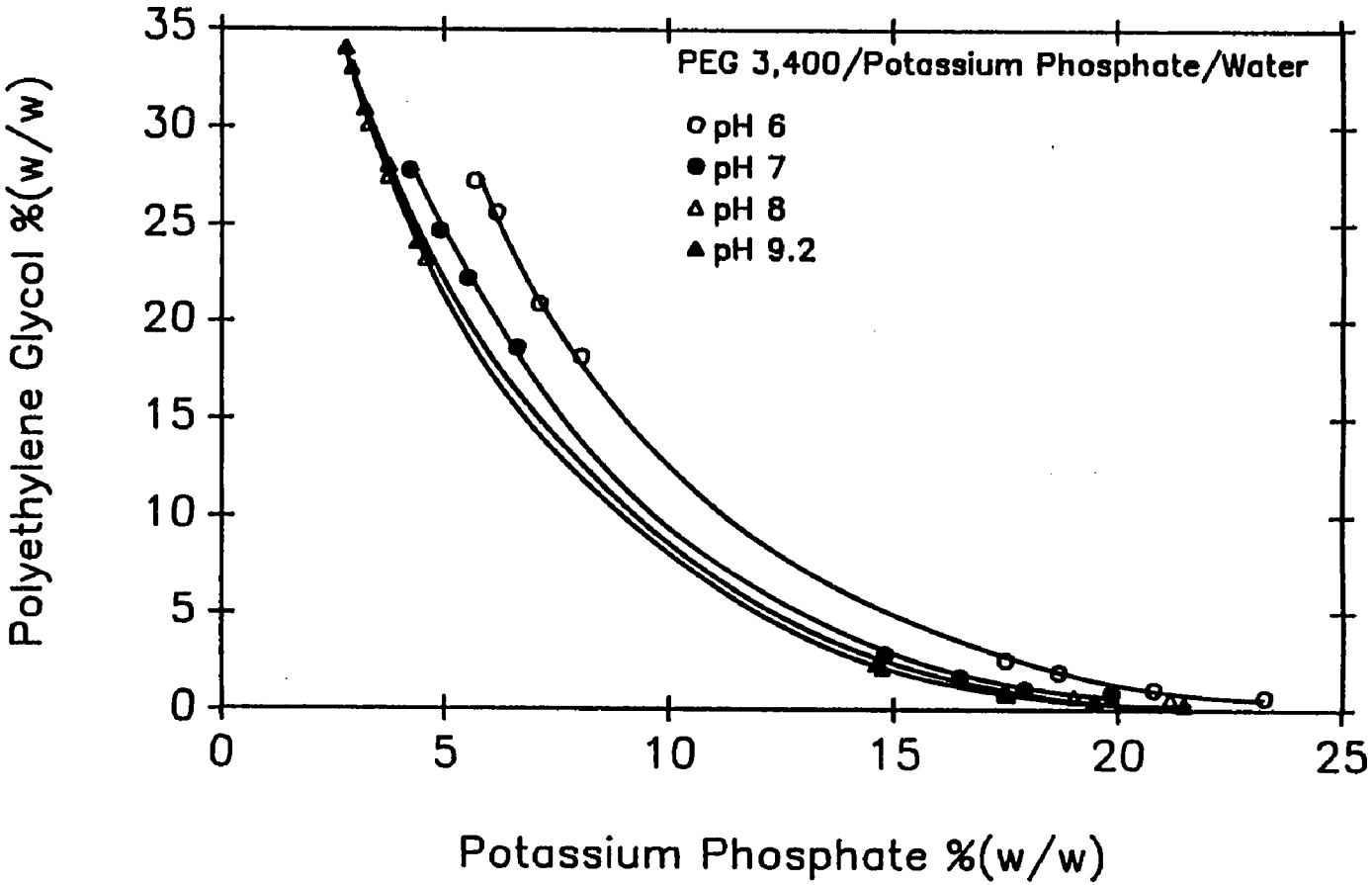

Figure 3.32 Binodial Curves for the PEG 3400/Potassium Phosphate/Water Systems at 4°C and pH 6.0–9.2.

Table 3.4 Phase Compositions for PEG/Potassium Phosphate/Water Systems at 4°C and pH 7.0.

Tie line No.	Concentrations in % (w/w) Total System KP*	PEG	Water	Bottom Phase KP*	PEG	Water	Top Phase KP*	PEG	Water
				PEG 400/Potassium Phosphate/Water					
1	16.00	19.40	64.60	31.45	3.05	65.50	6.85	28.75	64.40
2	16.80	20.60	62.60	33.51	2.54	63.95	5.78	32.02	62.20
3	17.40	23.20	59.40	37.61	2.24	60.15	4.69	36.79	58.52
4	17.90	25.10	57.00	39.73	2.12	58.15	3.95	39.73	56.32
				PEG 600/Potassium Phosphate/Water					
1	15.50	14.00	70.50	22.06	5.41	72.53	9.04	23.01	67.95
2	16.43	15.51	68.06	26.05	3.47	70.48	6.43	28.73	64.84
3	16.90	17.00	66.10	28.29	2.66	69.05	5.38	31.88	62.74
4	17.40	18.30	64.30	30.59	2.00	67.41	4.78	34.48	60.74
				PEG 1,000/Potassium Phosphate/Water					
1	15.00	13.00	72.00	21.56	3.08	75.36	6.64	25.02	68.34
2	15.70	15.00	69.30	25.56	1.08	73.36	5.53	29.02	65.45
3	16.20	17.00	66.80	28.08	0.71	71.21	4.60	32.56	62.84
4	17.00	19.00	64.00	30.81	0.56	68.63	3.70	36.37	59.93
				PEG 1,500/Potassium Phosphate/Water					
1	12.83	12.40	74.77	18.33	3.79	77.88	6.64	22.22	71.14
2	13.12	13.66	73.22	20.37	2.50	77.13	5.69	25.30	69.01
3	13.90	15.74	70.36	23.48	1.34	75.18	4.44	29.95	65.61
4	15.17	18.64	66.19	27.71	0.98	71.31	3.46	35.13	61.41
				PEG 3,400/Potassium Phosphate/Water					
1	10.90	10.10	79.00	14.80	2.76	82.44	6.60	18.55	74.85
2	11.40	11.00	77.60	16.48	1.61	81.91	5.51	22.14	72.35
3	11.80	12.20	76.00	17.92	1.01	81.07	4.88	24.58	70.54
4	12.30	13.70	74.00	19.85	0.78	79.37	4.21	27.66	68.13
				PEG 8,000/Potassium Phosphate/Water					
1	9.70	12.20	78.10	14.77	2.00	83.23	4.68	22.19	73.13
2	10.30	13.20	76.50	16.43	1.60	81.97	4.13	24.85	71.02
3	10.90	14.30	74.80	17.98	1.35	80.67	3.84	27.14	69.02
4	11.70	15.50	72.80	19.96	1.19	78.85	3.34	29.82	66.84
				PEG 20,000/Potassium Phosphate/Water					
1	9.00	9.00	82.00	11.99	2.10	85.91	5.36	17.55	77.09
2	9.60	10.00	80.40	13.56	1.20	85.24	4.70	20.06	75.24
3	9.90	11.40	78.70	14.99	0.90	84.11	4.01	23.39	72.60
4	10.40	13.00	76.60	16.36	0.88	82.76	3.69	26.21	70.10

* KP stands for potassium phosphate.

Table 3.5 Phase Compositions for PEG 3,400/Potassium Phosphate/Water Systems at 4°C and pH 6.0, 8.0 and 9.2.

Tie line No.	Concentrations in %(w/w) Total System KP*	PEG	Water	Bottom Phase KP*	PEG	Water	Top Phase KP*	PEG	Water
	PEG 3,400/Potassium Phosphate/Water at pH 6								
1	12.50	10.50	77.00	17.50	2.49	80.01	8.04	18.11	73.85
2	13.00	11.00	76.00	18.68	1.88	79.44	7.10	20.81	72.09
3	14.00	12.00	74.00	20.79	1.00	78.21	6.15	24.54	69.31
4	15.00	13.00	72.00	23.27	0.60	76.13	5.65	27.14	67.21
	PEG 3,400/Potassium Phosphate/Water at pH 8								
1	9.20	13.80	77.00	14.75	2.04	83.21	4.59	23.11	72.30
2	10.30	14.80	74.90	17.47	0.78	81.75	3.74	27.33	68.93
3	11.00	16.00	73.00	19.04	0.64	80.32	3.30	30.03	66.67
4	12.00	17.00	71.00	21.18	0.52	78.30	2.93	32.89	64.18
	PEG 1,000/Potassium Phosphate/Water at pH 9.2								
1	9.20	13.80	77.00	14.63	2.26	83.11	4.40	23.95	71.65
2	10.30	14.80	74.90	17.53	0.73	81.74	3.75	27.91	68.34
3	11.00	16.00	73.00	19.49	0.39	80.12	3.22	30.82	65.96
4	12.00	17.00	71.00	21.48	0.21	78.31	2.79	33.91	63.30

* KP stands for potassium phosphate.

Analysis of binodial curves in Figures 3.22–3.28 reveals the effect of PEG molecular weight on phase separation. As the molecular weight is increased, the binodial curve shifts to lower PEG and phosphate concentrations. This trend is in agreement with the experimental results of Albertsson (1986).

Examination of the binodial curves in Figures 3.29–3.32 demonstrates the effect of pH on separation at constant PEG molecular weight. As the system becomes more basic, the binodials shift to lower PEG and phosphate concentrations as was observed for the molecular weight effect. The difference in position between the binodials begins to diminish at high pH, with the binodials for pH 8.0 and 9.2 being almost identical. At the high pH, the phosphate is essentially deprotonated and negatively charged. Similarly, PEG, which has hydroxyl groups at either end of its chain, has a slight negative charge due to the loss of hydrogen from the hydroxyl groups. Since phosphate and PEG are both negatively charged at the high pH, they will tend to repel one another (more so than at lower pH) and lead to phase separation at low concentrations.

3.3.3 Flory-Huggins Analysis of Phase Diagram Data

In Chapter II the linear semilogarithmic relationships given by equations (2.24) and (2.25) were developed for correlating phase composition data in aqueous two-phase systems. These relationships were as follows:

$$\ln (K_1) = A_1(w_1'' - w_1') \tag{3.1}$$

and

$$\ln (K_2) = A_2(w_1'' - w_1') \tag{3.2}$$

where,

$$A_1 = m_1\left(\alpha_1\left(\frac{1}{m_1} - 1 + 2\chi_{01}\right) + \alpha_2\phi\left(\frac{1}{m_2} - 1 + \chi_{01} + \chi_{02} - \chi_{12}\right)\right) \qquad (3.3)$$

and

$$A_2 = m_2\left(\alpha_2\phi\left(\frac{1}{m_2} - 1 + 2\chi_{02}\right) + \alpha_1\left(\frac{1}{m_1} - 1 + \chi_{02} + \chi_{01} - \chi_{12}\right)\right) \qquad (3.4)$$

These relationships were tested using the PEG/dextran/water data at 4°C, 10°C and 22°C, and PEG/potassium phosphate/water systems at 4°C. In addition, Albertsson's (1986) phase diagrams for both system types and the Ficoll 400/Dextran T-500/water system at 23°C are correlated using the above relationships.

In Figure 3.33 the effect of dextran molecular weight on phase separation in PEG 3400/dextran/water systems at 4°C is presented. This figure reveals that the slope, A_1, for PEG 3400 is not effected as dextran molecular weight is changed. However, as dextran molecular weight is increased from 40,000 (T-40) to 500,000 (T-500), the slope, A_2, becomes more negative. Similar results are apparent in Figure 3.34, in which PEG 3400 has been replaced by PEG 8000 and the dextran fractions are the same. Comparing Figures 3.33 and 3.34 reveals that A_1 becomes slightly more positive and A_2 slightly more negative as PEG molecular weight is changed from 3400 to 8000.

In Figure 3.35, the effect of dextran molecular weight on phase separation in the PEG 3400/dextran/water system at 22°C is presented. As was the case in Figure 3.33, A_1 is essentially constant (PEG molecular weight

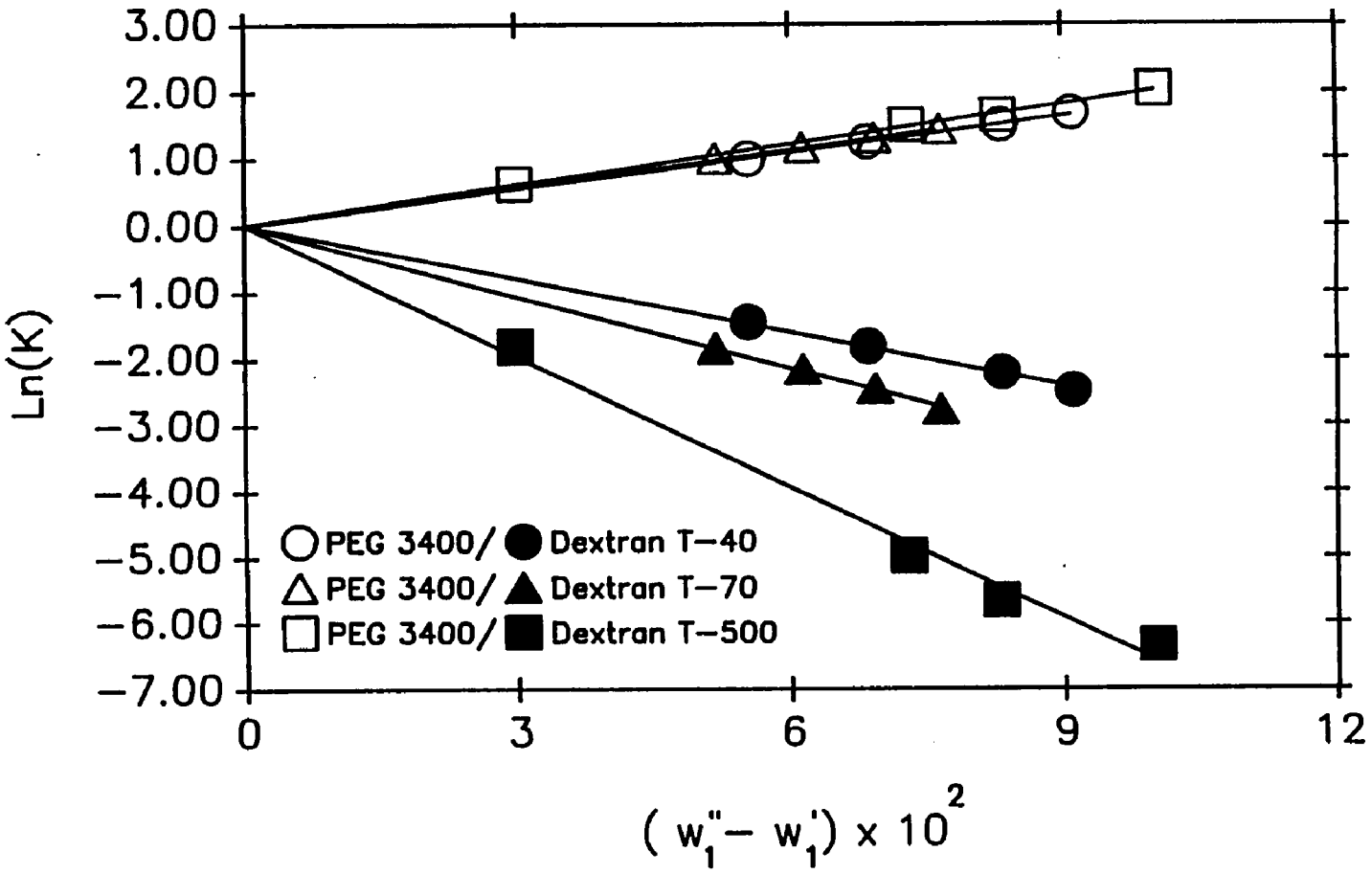

Figure 3.33 Correlation of PEG 3400/Dextran/Water Phase Diagram Data at 4°C According to Equations (3.1) and (3.2).

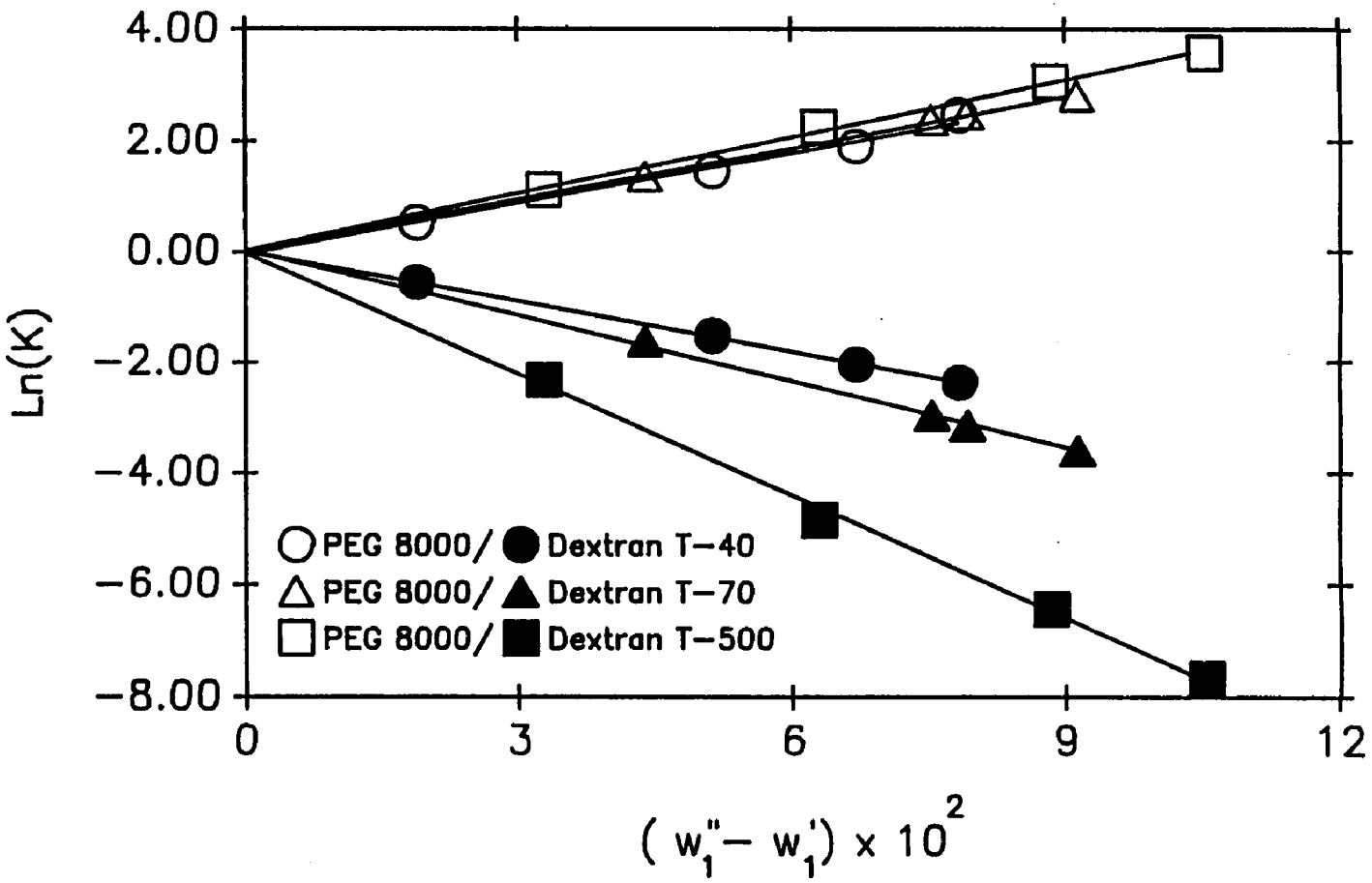

Figure 3.34 Correlation of PEG 8000/Dextran/Water Phase Diagram Data at 4°C According to Equations (3.1) and (3.2).

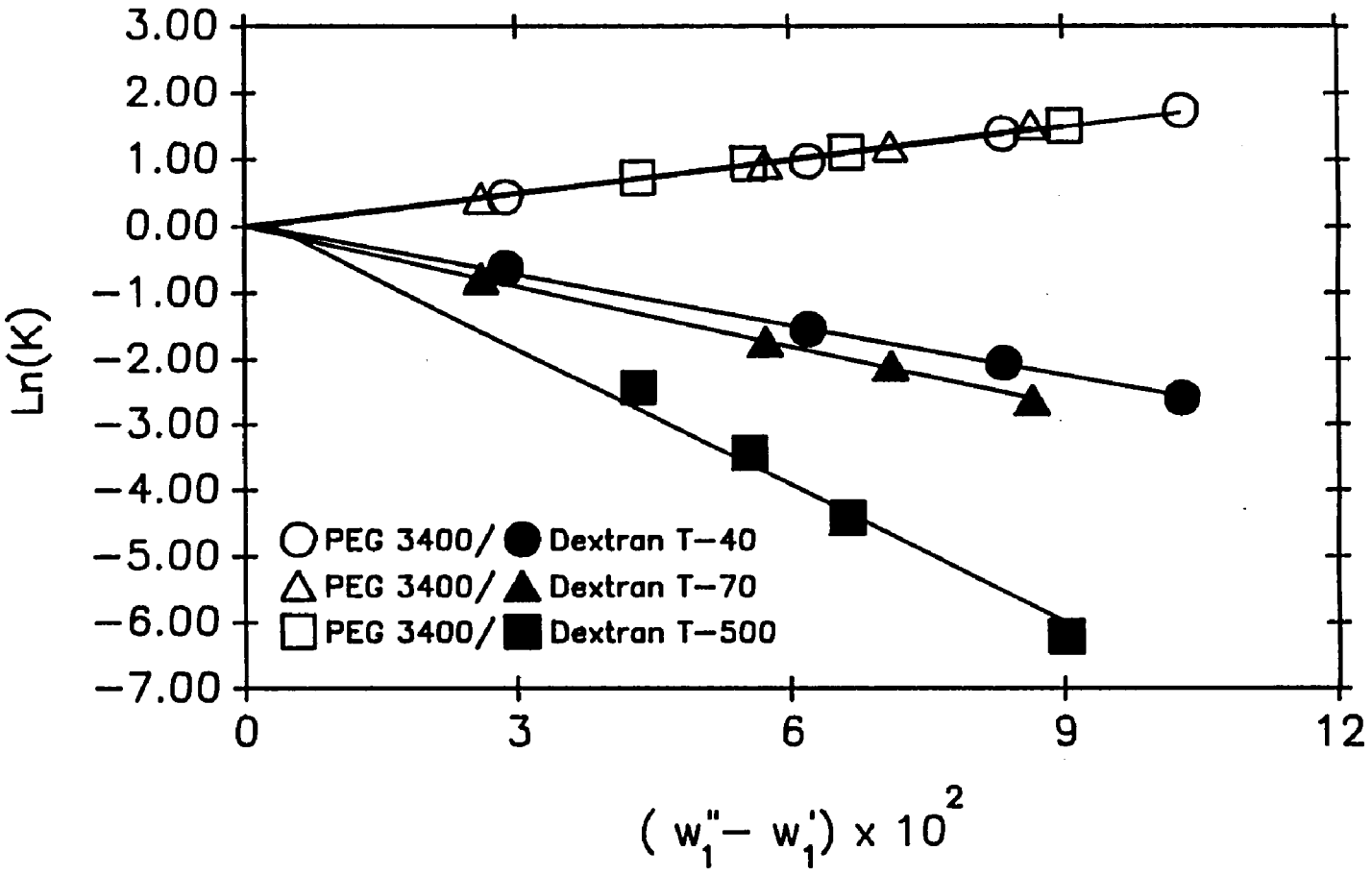

Figure 3.35 Correlation of PEG 3400/Dextran/Water Phase Diagram Data at 22°C According to Equations (3.1) and (3.2).

remains constant) and A_2 becomes more negative as dextran molecular weight is increased. Similar trends are observed in Figure 3.36, where PEG 3400 has been replaced by PEG 8000 and the temperature remains at 22°C.

The effect of PEG molecular weight on phase separation can be more readily observed in Figures 3.37–3.40. The PEG/Dextran T-70/water and PEG/Dextran T-500/water systems at 4°C with PEG of molecular weight 3400, 8000 and 20000 are revealed in Figures 3.37 and 3.38. The slope, A_1, increases as PEG molecular weight increases, with the difference between that for PEG 8000 and PEG 20000 being relatively small. The slope, A_2, becomes more negative as PEG molecular weight is increased. Similar trends are observed for the same systems at 22°C in Figures 3.39 and 3.40.

The effect of temperature on phase separation in the PEG 8000/Dextran T-500/water system is presented in Figure 3.41. As temperature is increased, A_1 remains essentially constant while A_2 becomes less negative.

The PEG/dextran/water phase diagram data from Albertsson (1986) were also tested using the relationships of equations (3.1) and (3.2), and the results are presented in Figures 3.42–3.44. Figures 3.42 and 3.43 demonstrate the effect of dextran molecular weight on the slopes A_1 and A_2, while Figure 3.44 shows the effect of PEG molecular weight. The trends revealed in each of these figures is in agreement with the previous PEG/dextran/water phase diagram data presented in this chapter.

Equations (3.1) and (3.2) were tested with the PEG/potassium phosphate/water data presented in this work and that of Albertsson (1986), and the results are presented in Figures 3.45–3.48. These figures reveal that the slope, A_2, remains constant regardless of PEG molecular weight, and the linear

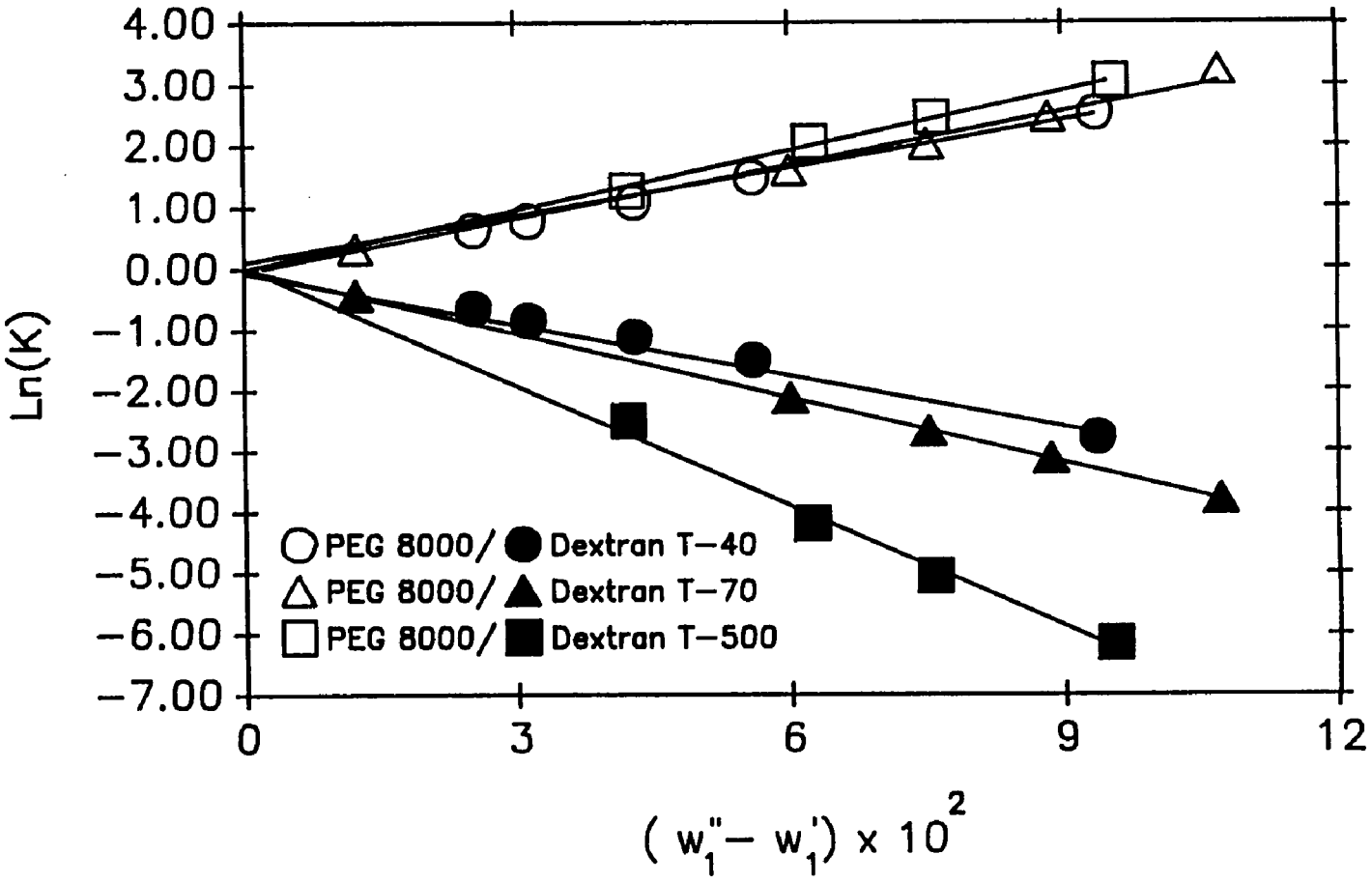

Figure 3.36 Correlation of PEG 8000/Dextran/Water Phase Diagram Data at 22°C According to Equations (3.1) and (3.2).

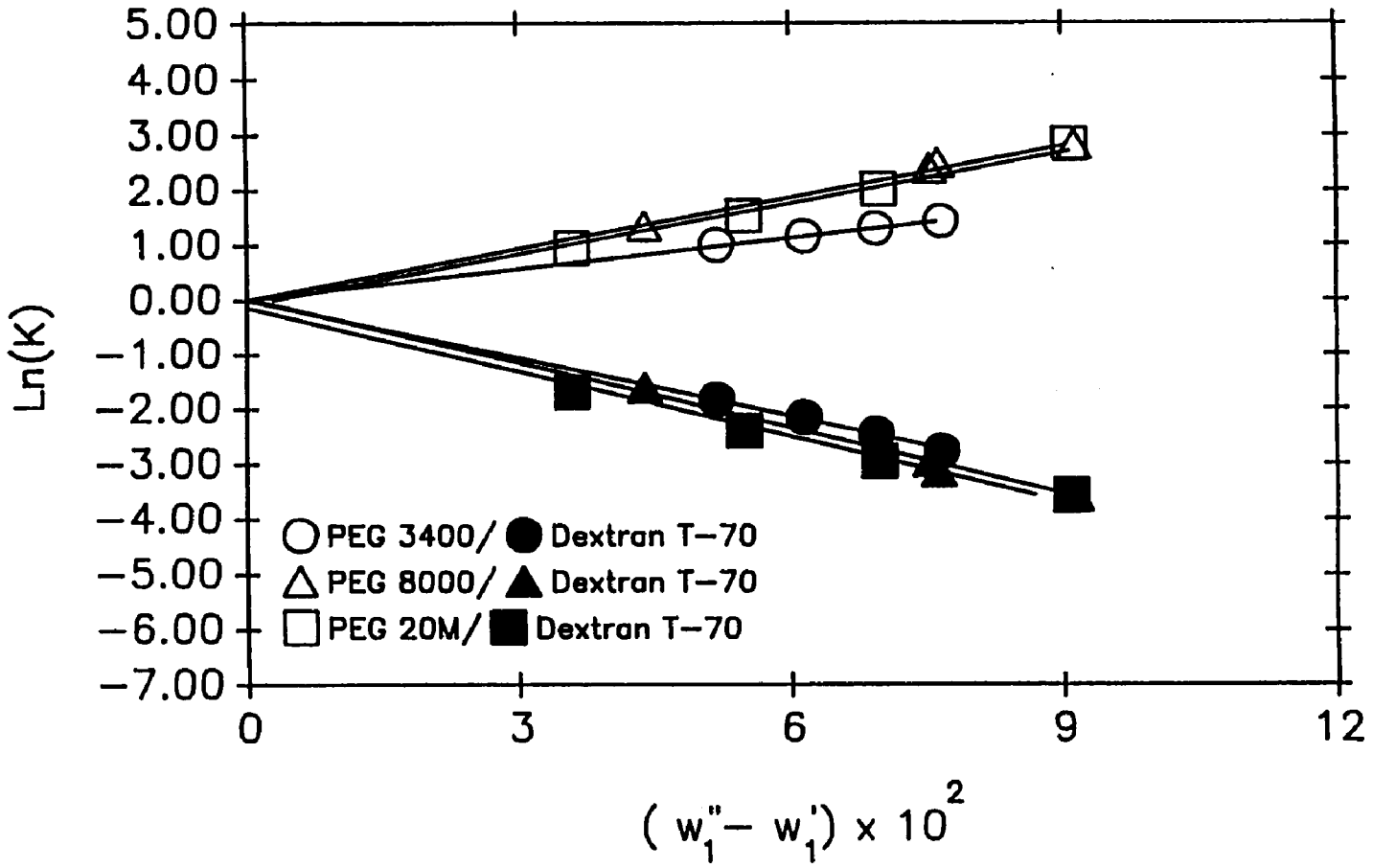

Figure 3.37 Correlation of PEG/Dextran T-70/Water Phase Diagram Data at 4°C According to Equations (3.1) and (3.2).

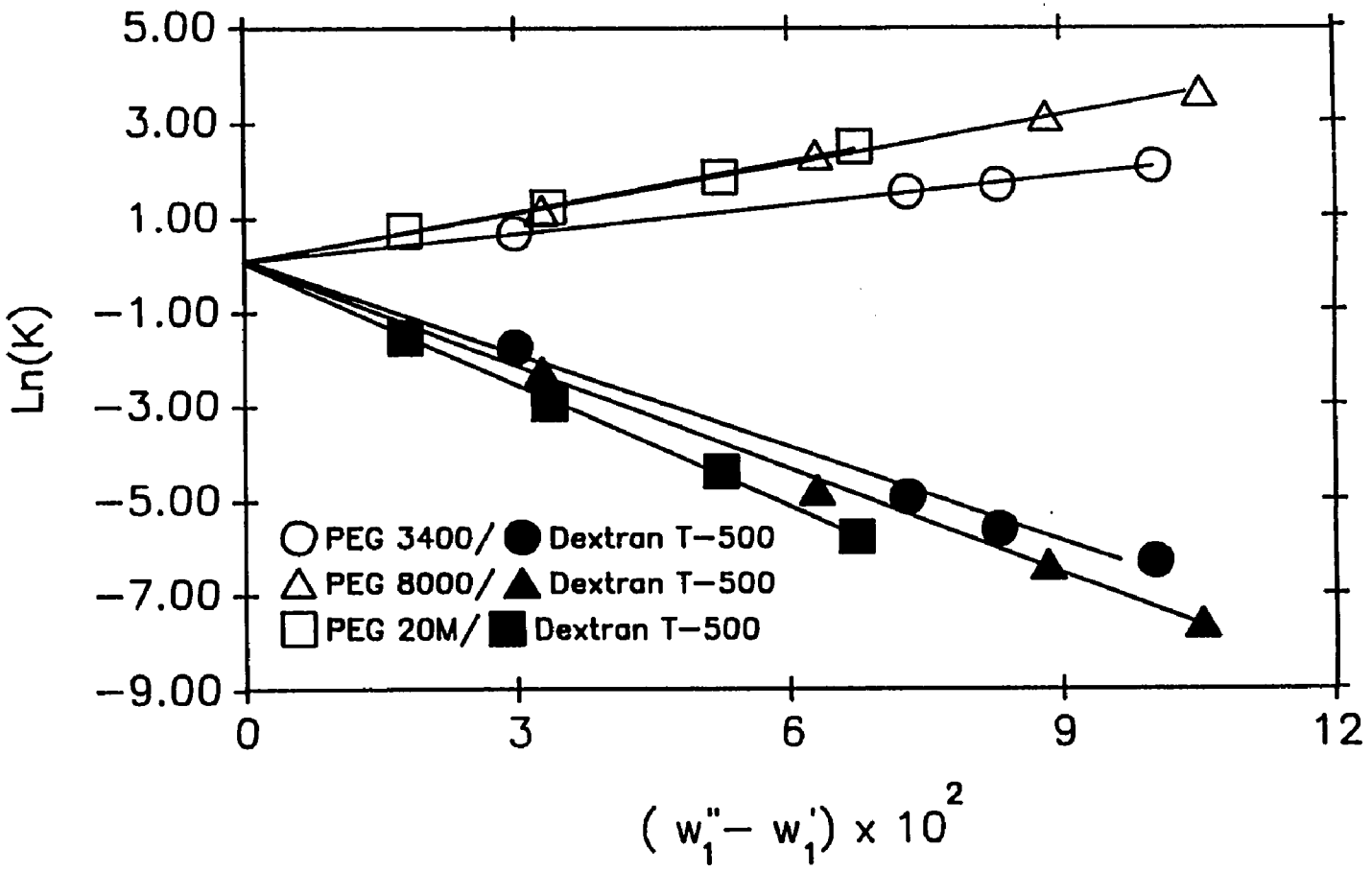

Figure 3.38 Correlation of PEG/Dextran T-500/Water Phase Diagram Data at 4°C According to Equations (3.1) and (3.2).

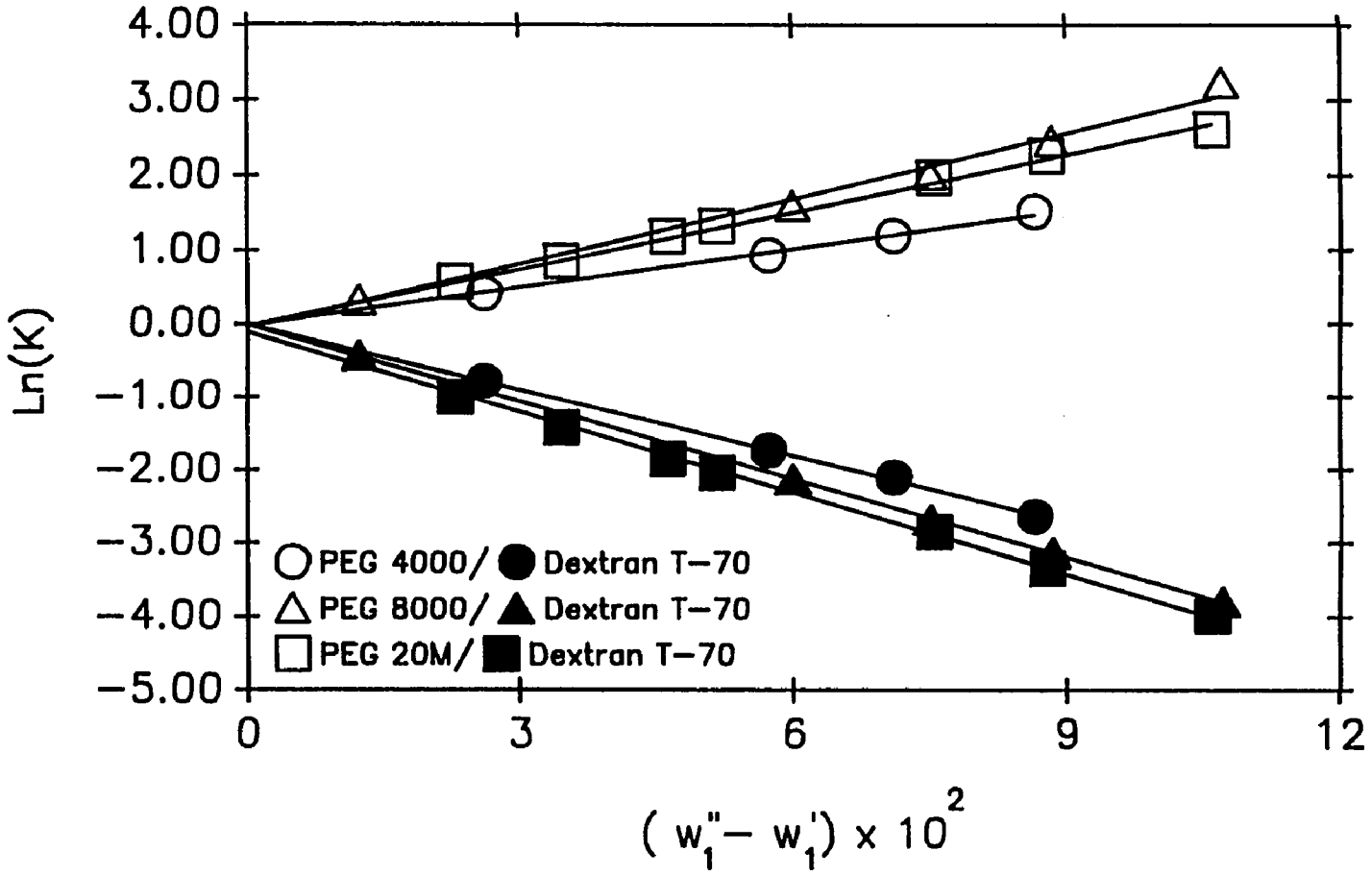

Figure 3.39 Correlation of PEG/Dextran T-70/Water Phase Diagram Data at 22°C According to Equations (3.1) and (3.2).

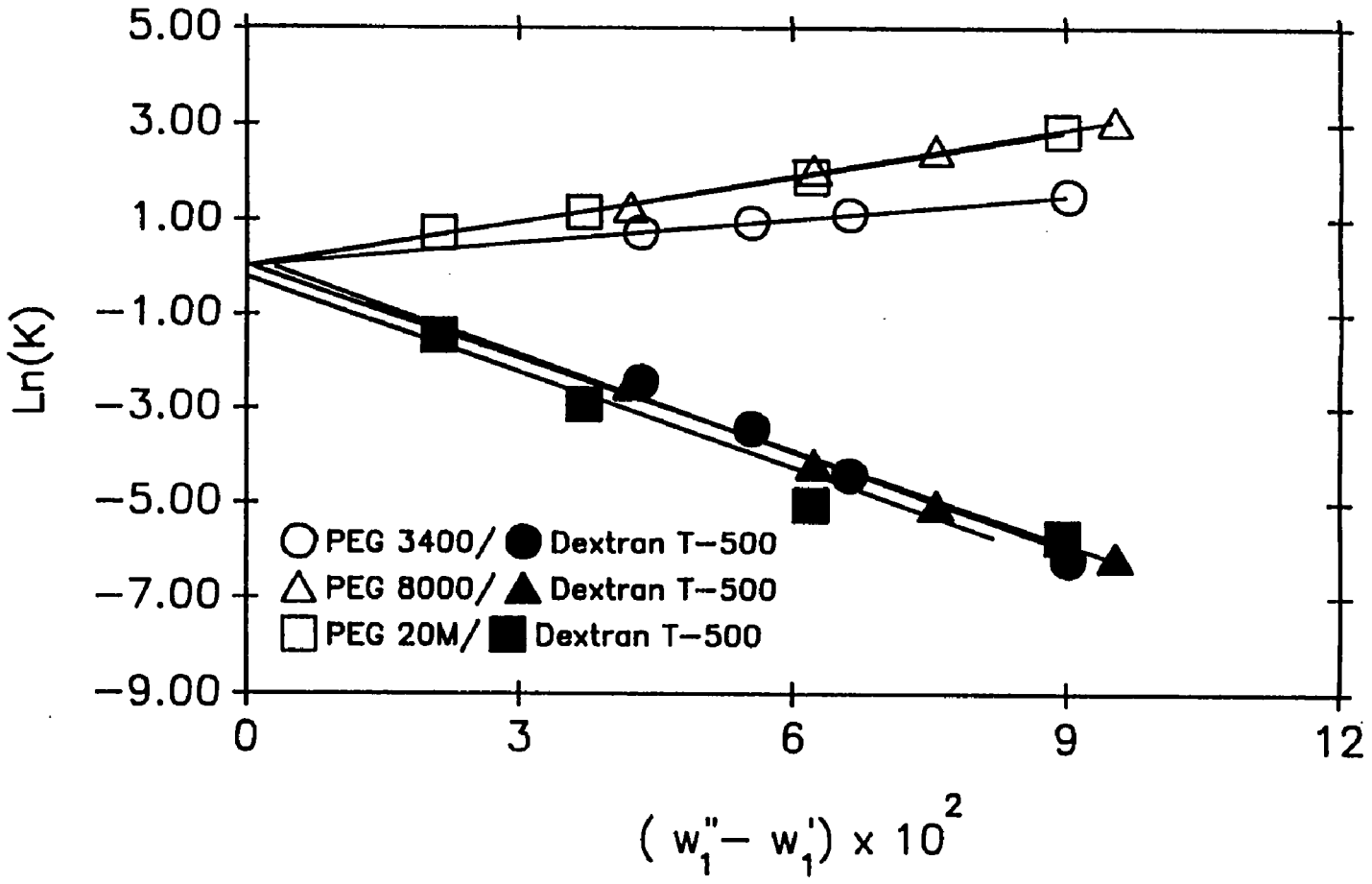

Figure 3.40 Correlation of PEG/Dextran T-500/Water Phase Diagram Data at 22°C According to Equations (3.1) and (3.2).

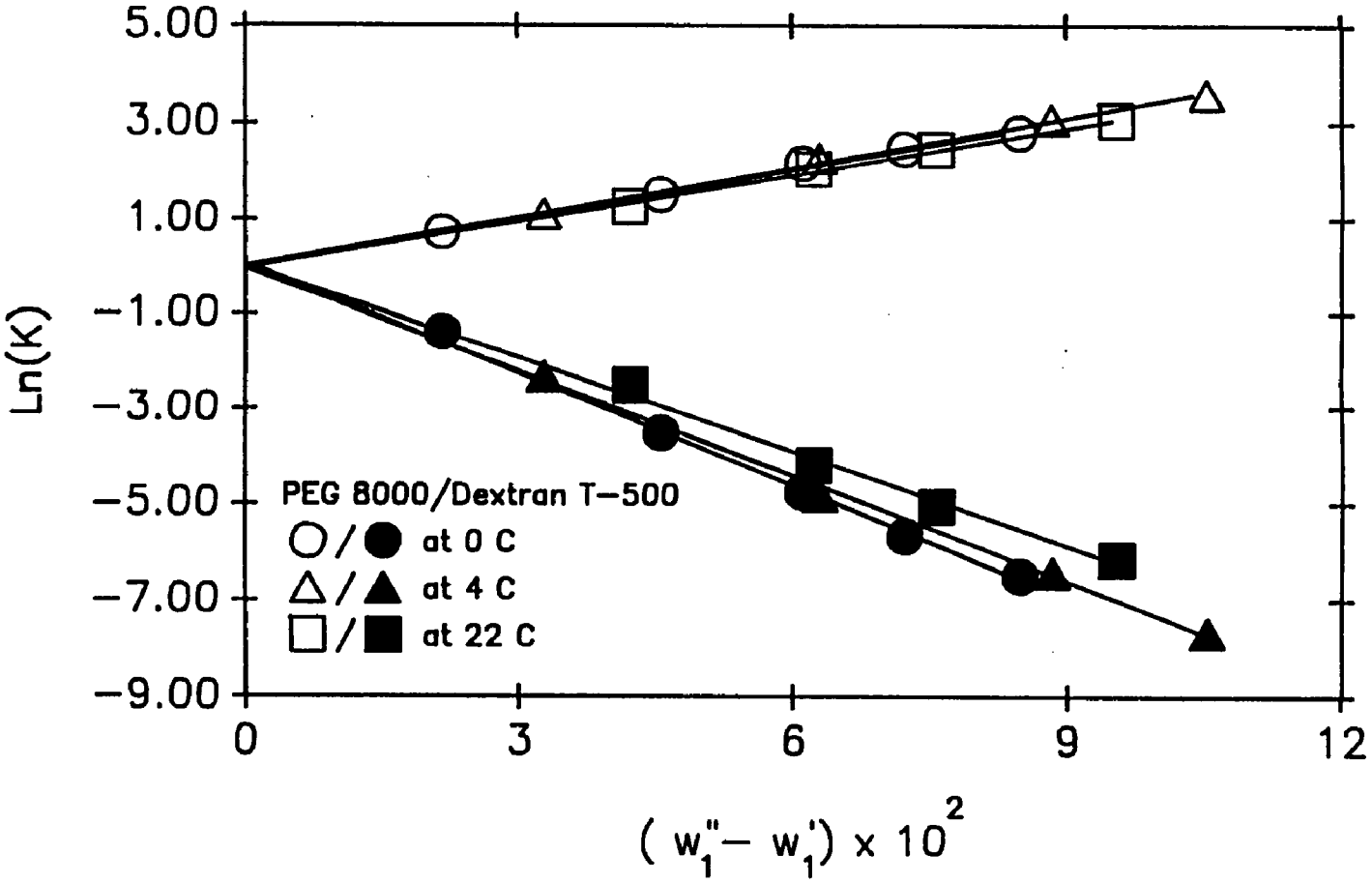

Figure 3.41 Correlation of PEG 8000/Dextran T-500/Water Phase Diagram Data at 0°C, 4°C and 22°C According to Equations (3.1) and (3.2). The Data at 0°C is from Albertsson (1986).

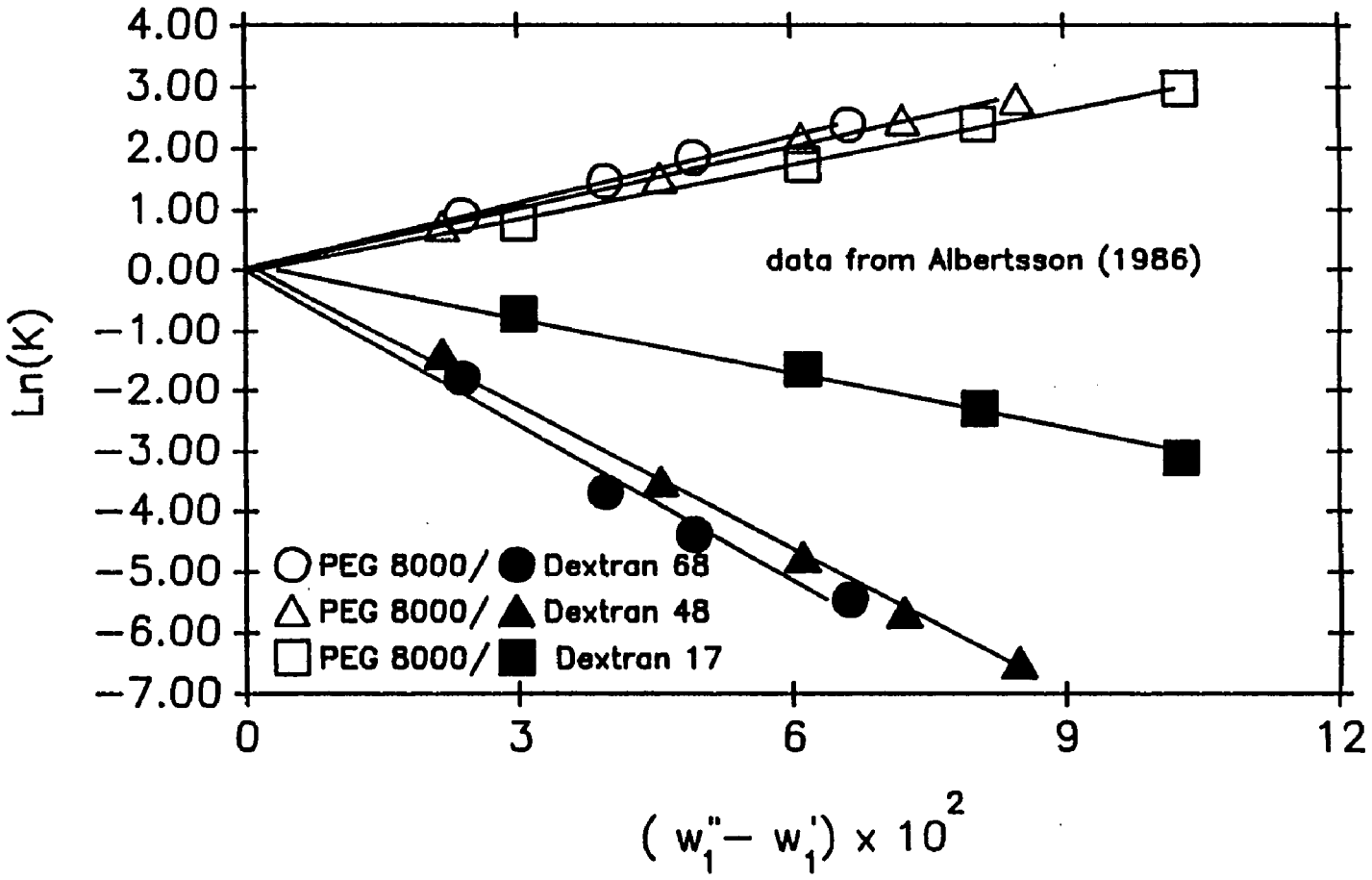

Figure 3.42 Correlation of PEG 8000/Dextran/Water Phase Diagram Data at 0°C According to Equations (3.1) and (3.2).

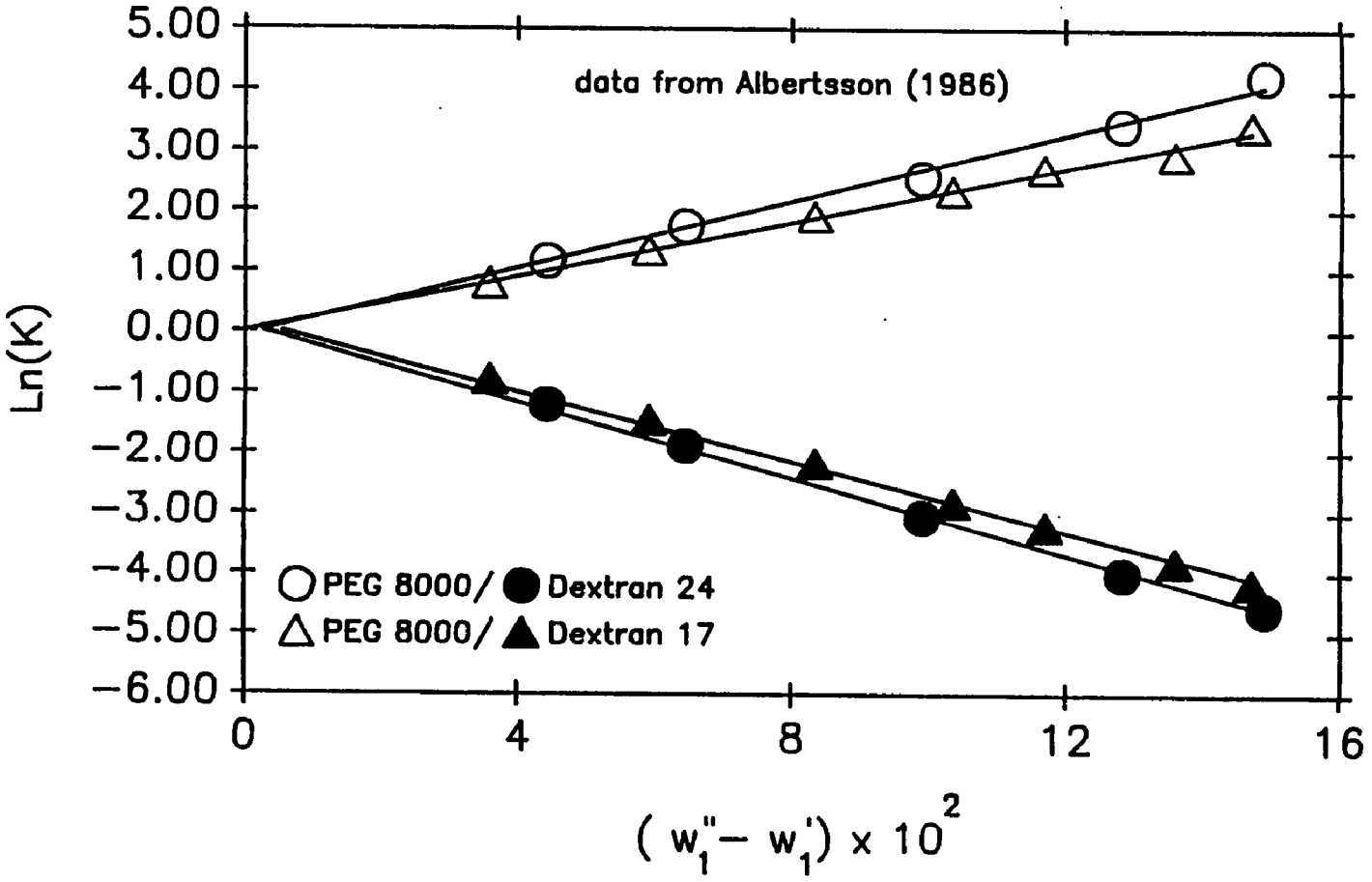

Figure 3.43 Correlation of PEG 8000/Dextran/Water Phase Diagram Data at 20°C According to Equations (3.1) and (3.2).

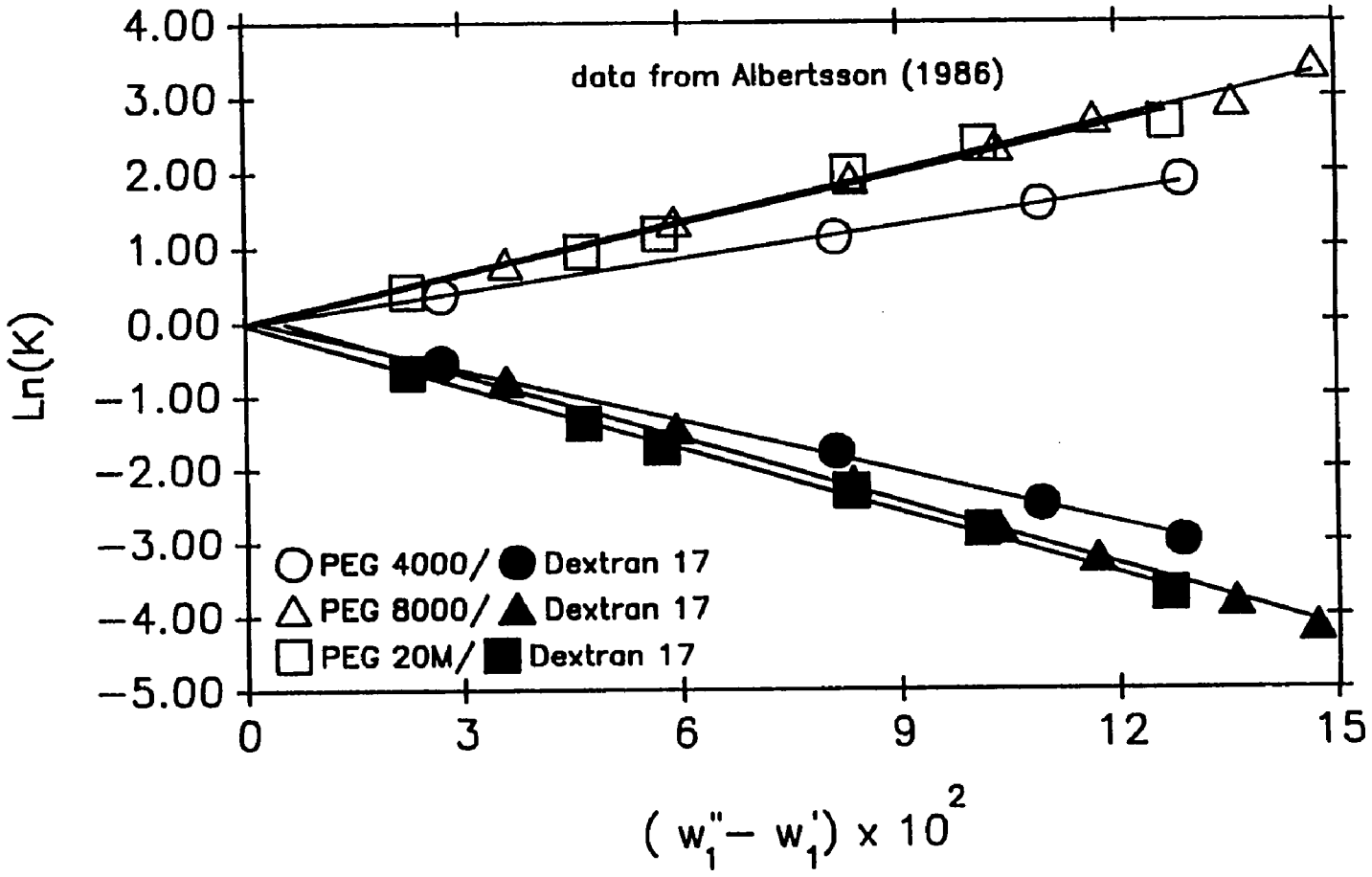

Figure 3.44 Correlation of PEG/Dextran 17/Water Phase Diagram Data at 20°C According to Equations (3.1) and (3.2).

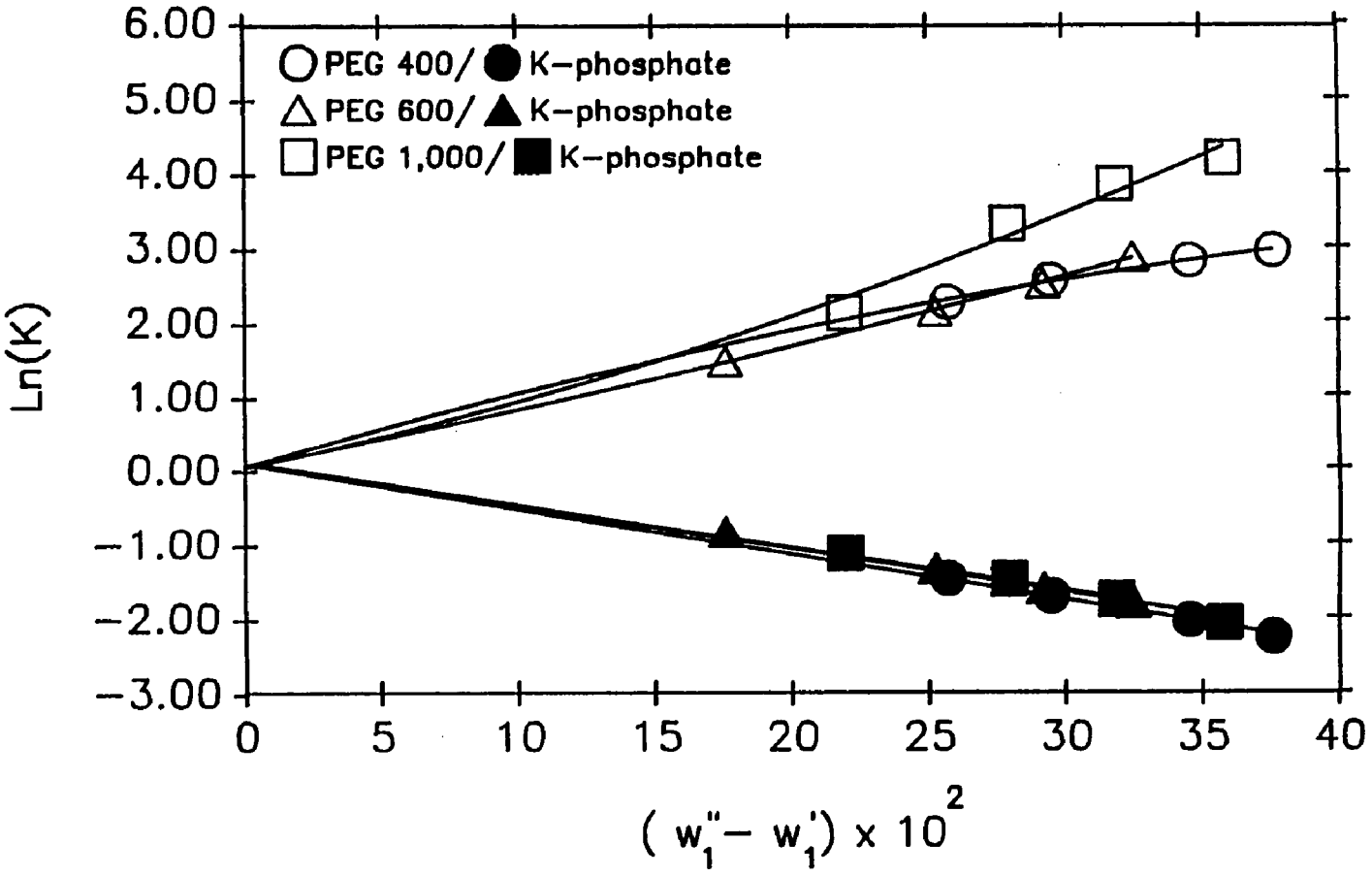

Figure 3.45 Correlation of PEG/Potassium Phosphate/Water Phase Diagram Data at 4°C and pH 7.0 According to Equations (3.1) and (3.2).

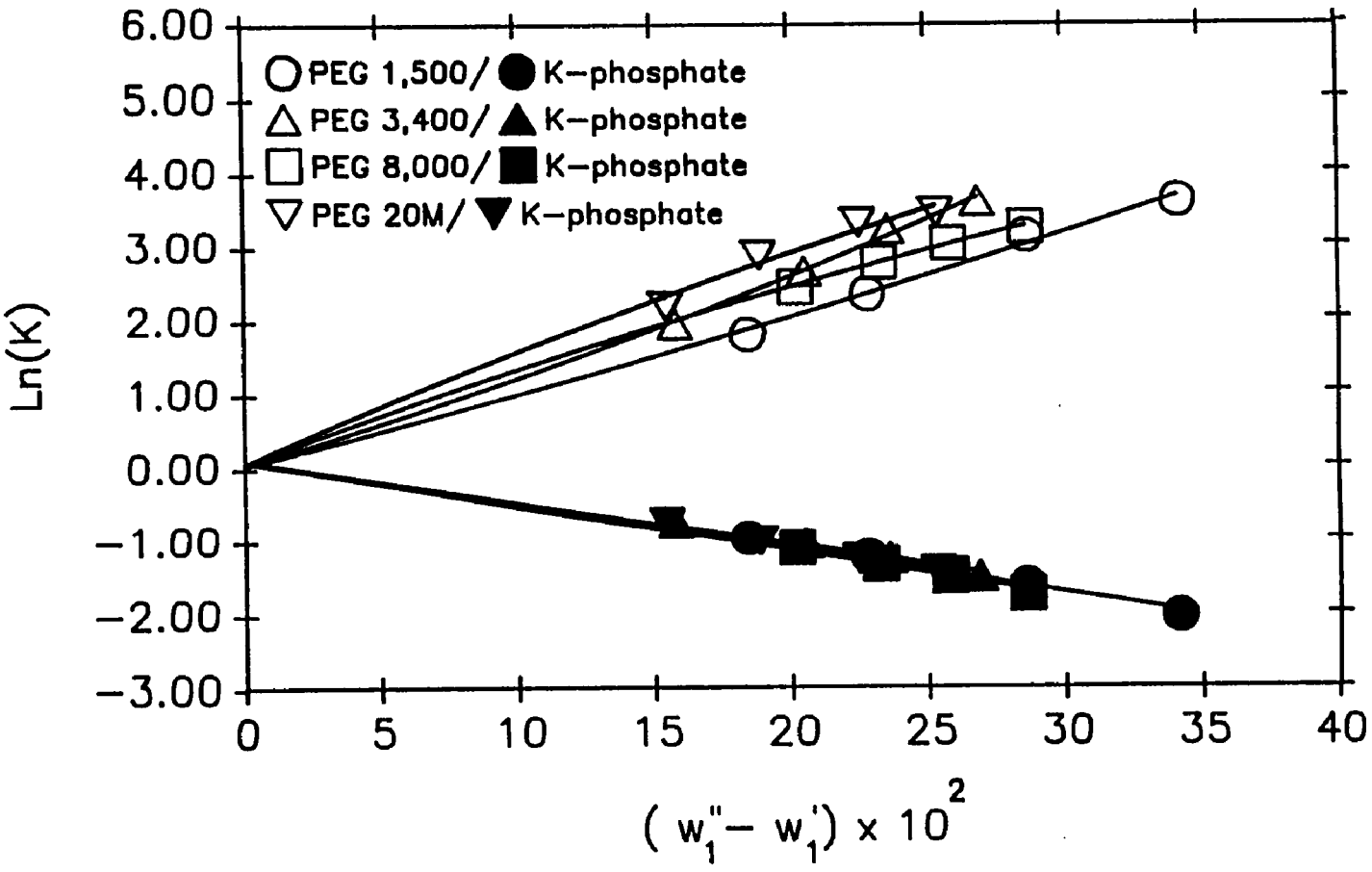

Figure 3.46 Correlation of PEG/Potassium Phosphate/Water Phase Diagram Data at 4°C and pH 7.0 According to Equations (3.1) and (3.2).

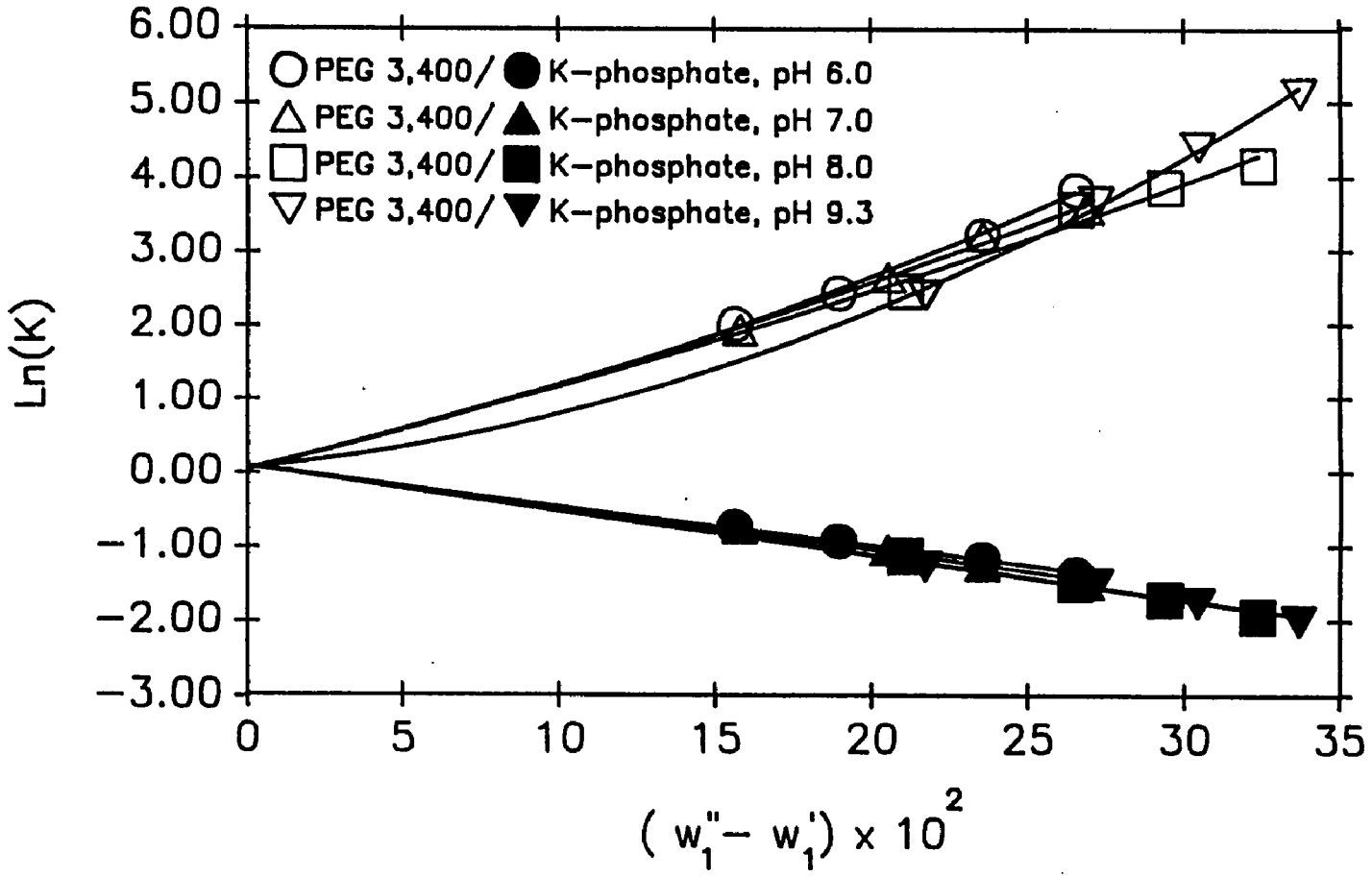

Figure 3.47 Correlation of PEG 3400/Potassium Phosphate/Water Phase Diagram Data at 4°C and pH 6.0–9.2 According to Equations (3.1) and (3.2).

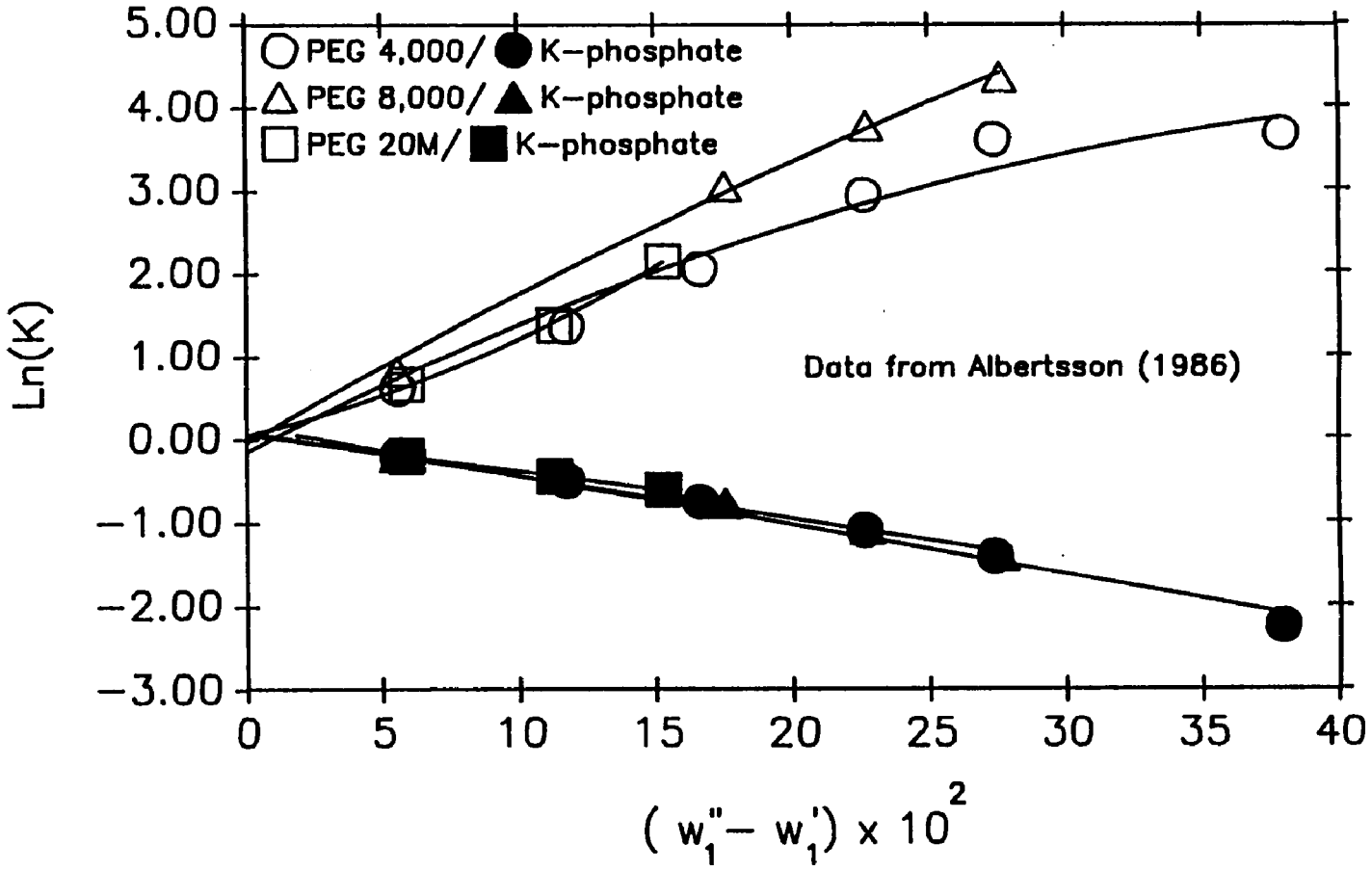

Figure 3.48 Correlation of PEG/Potassium Phosphate/Water Phase Diagram Data at 20°C and pH 7.0 According to Equations (3.1) and (3.2).

relationship is in agreement with equation (3.2). The slope, A_1, tends to increase as PEG molecular weight is increased. However, there is an apparent deviation from the linear relationship which is most probably due to the fact that the Flory-Huggins theory provides only a first approximation (and a good one at that) to the thermodynamic behavior of the PEG/potassium phosphate/water systems. These systems contain a relatively high interfacial potential (Albertsson, 1986) which is not readily accounted for with the Flory-Huggins theory.

In Figure 3.49, Albertsson's (1986) data for the Ficoll 400/Dextran T-500/water system at 23°C are shown to obey the relationships given by equations (3.1) and (3.2).

3.4 CONCLUSIONS

Phase diagram data have been obtained for PEG/dextran/water systems at 4°C, 10°C and 22°C, and PEG/potassium phosphate/water systems at 4°C and pH 6.0, 7.0, 8.0 and 9.2. These data are in agreement with experimental phase diagrams and qualitative predictions available in the literature. The PEG/dextran/water, PEG/potassium phosphate/water, and Ficoll 400/Dextran T-500/water phase diagram data presented in this chapter and obtained from the literature were also shown to correlate well with the Flory-Huggins equations for phase diagram separation developed in Chapter II.

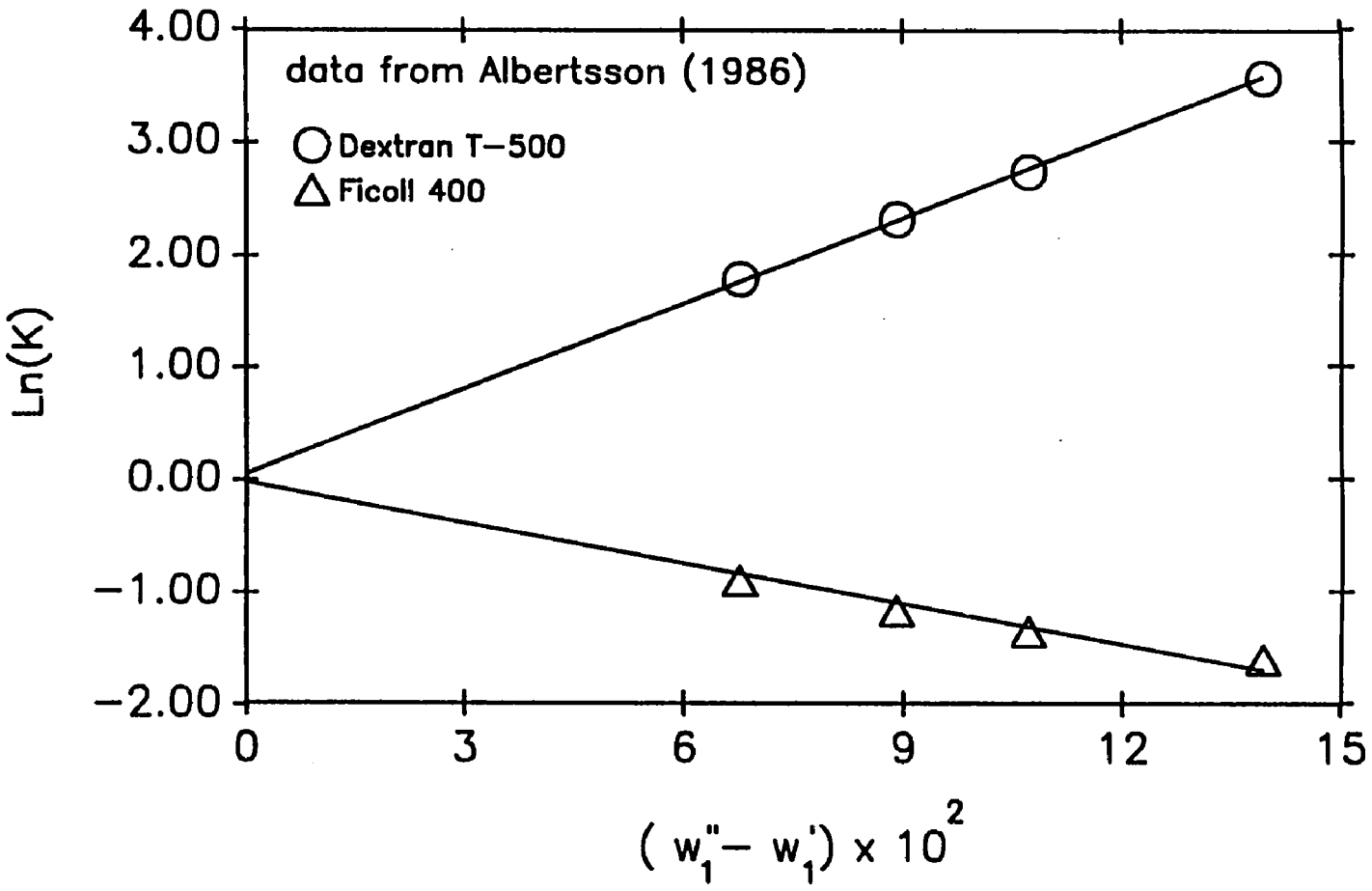

Figure 3.49 Correlation of Ficoll 400/Dextran T-500/Water Phase Diagram Data at 23°C According to Equations (3.1) and (3.2).

CHAPTER IV
LINEAR SEMILOGARITHMIC PARTITIONING OF BIOMOLECULES

In this chapter, a simple, linear semilogarithmic relationship derived from Flory-Huggins theory is used for correlating biomolecule partition coefficients. The relationship is verified for PEG/dextran/water systems by partitioning dipeptides and low molecular weight proteins.

4.1 Introduction

In Chapter II, the Flory-Huggins theory of polymer thermodynamics was used to develop a partition expression for biomolecules in aqueous two-phase systems. The result (equation (2.33) of Chapter II) was a simple linear relationship between the natural logarithm of the partition coefficient and the concentration of polymers in the two phases and was expressed as follows:

$$\ln (K_3) = A(w_1'' - w_1') \tag{4.1}$$

where,

$$A = m_3\left(\alpha_1\left(\frac{1}{m_1} - 1 + \chi_{03} - \chi_{13} + \chi_{01}\right) + \alpha_2\phi\left(\frac{1}{m_2} - 1 + \chi_{03} - \chi_{23} + \chi_{02}\right)\right) \tag{4.2}$$

This relationship will be verified for PEG/dextran/water systems by partitioning a series of dipeptides, which differ from one another by the addition

of a CH_2 group on the c-terminal amino acid residue, and by utilizing a set of low molecular weight proteins. The slope of the line can be expressed in terms of the interactions of the biomolecule with the phase forming polymers and water. The dipeptides will also be used for determination of the Gibbs free energy of transfer of a CH_2 group between the phases. This quantity will be correlated with polymer concentration, thus establishing a hydrophobicity profile for the PEG/dextran/water systems. Equation (4.1) is also extended to the correlation of low molecular weight protein partitioning.

4.2 Materials and Methods

4.2.1 Polymers

PEG of molecular weight 3,400 (Lot 00917 PT) and 8,000 (Lot 02521 LT) was purchased from Aldrich Chemical Company, Milwaukee, WI. Dextran T-500 (Lot 05163), Dextran T-70 (Lot 02377), and Dextran T-40 (Lot 03375) were obtained from Pharmacia Fine Chemicals, Piscataway, NJ.

4.2.2 Dipeptides and Proteins

Glycylglycine (gly-gly), glycylalanine (gly-ala), glycyl-α-aminobutyric acid (gly-α), and glycylnorvaline (gly-Nval) were purchased from Sigma Chemical Co., St. Louis, MO. Horse heart cytochrome c, ribonuclease a (from bovine pancreas), chicken egg lysozyme, trypsin, turkey egg ovalbumin, α-amylase, bovine serum albumin, human transferrin, and alcohol dehydrogenase (from bakers yeast) were also obtained from Sigma.

4.2.3 Partition Experiments

Phase systems were prepared by weighing appropriate quantities of PEG (in the form of a solid), dextran stock solution (prepared according to the procedure given in Chapter II), and water into a beaker, and then adding 0.02 molal potassium phosphate buffer to adjust the pH to 7.0. The resulting system contained the desired component concentrations in addition to 0.01 molal potassium phosphate buffer and was then magnetically stirred for three hours.

10 ml of the well mixed phase system was poured into 15 ml polypropylene centrifuge tubes. Either 3 mg of dipeptide or 10 mg of protein was then added, the tubes tightly capped, and then placed in a temperature controlled refrigerator at 4°C. The systems were allowed to settle by gravity for 24–48 hours. The top phase was then collected using a pasteur pipette, and the bottom phase drained by piercing a hole at the bottom of the polypropylene centrifuge tube.

Dipeptide and protein concentration were determined by measuring absorbance using a Shimadzu UV-Vis spectrophotometer according to the procedure of Sasakawa and Walter (1972, 1974). Absorbances of 220 and 280 nm were used for the dipeptides and proteins, respectively.

4.3 Results and Discussion

4.3.1 Dipeptide Partitioning

The validity of equation (4.1) was tested by partitioning a variety of biomolecules in PEG/dextran/water systems. The distribution of the dipeptides gly-gly, gly-ala, gly-α and gly-Nval, which differ from one another by the addition of a CH_2 group on the c-terminal amino acid residue, was investigated in the phase systems presented in Figures 3.1–3.9 of Chapter III.

In Figures 4.1–4.4, the natural logarithm of the partition coefficient for the dipeptides is plotted versus (w_1'' – w_1'), the PEG concentration difference between the phases. Several interesting trends are apparent in these figures. First, the natural logarithm of the partition coefficient for each of the dipeptides converged on a single line regardless of which PEG/dextran/water system was used, thus indicating the validity of equation (4.1), and that polymer molecular weight had little effect on the slope of the line for the low molecular weight solutes. Since the linear semilogarithmic relationship passes through the origin, corresponding to partitioning at the plait point, only one data point is required to obtain the slope of equation (4.1). This result leads to the conclusion that only a single partition coefficient need be measured in only one of the PEG/dextran/water systems in order to predict the partition coefficient in any of the systems.

Examination of the slopes of the lines in Figures 4.1–4.4 reveals a second trend in the dipeptide partitioning data. The slope, A, of equation (4.1) for gly-gly, gly-ala, gly-α and gly-Nval was –2.8, –2.3, –1.8, and –1.3, respectively. Therefore, as a CH_2 was added to the c-terminal residue, the molecule became more hydrophobic and the dipeptides partitioned to a greater extent in the PEG-rich phase, thus leading to an increase in the slope. The terms of the slope, A, in equation (4.1) dependent upon dipeptide structure are the molar volume ratio of the dipeptide (m_3) and the quantity $\alpha_1(\chi_{03}-\chi_{13}) + \alpha_2\phi(\chi_{03} - \chi_{23})$. Since the molar volume ratio is directly proportional to the molecular weight of the partitioning species, it should increase slightly as a CH_2 group is added to the dipeptide chain. Therefore, the quantity $\alpha_1(\chi_{03}-\chi_{13}) + \alpha_2\phi(\chi_{03} - \chi_{23})$ must also increase in order for A to become less negative. The constants α_1 and α_2 are positive quantities since they represent the product of the density of

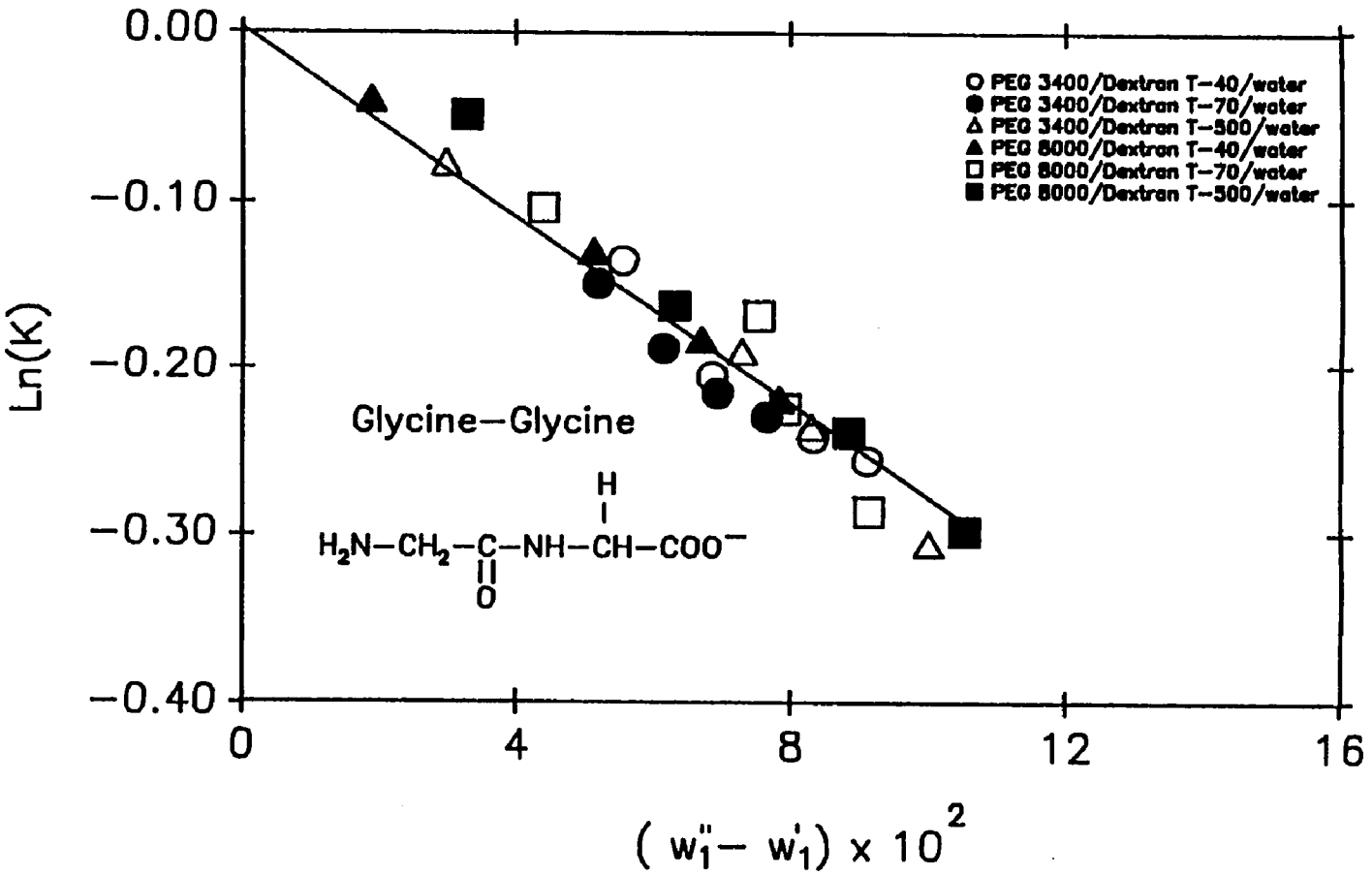

Figure 4.1 Effect of PEG Concentration Difference on the Natural Logarithm of the Partition Coefficient of Glycine-Glycine in PEG/Dextran/Water Systems at 4°C.

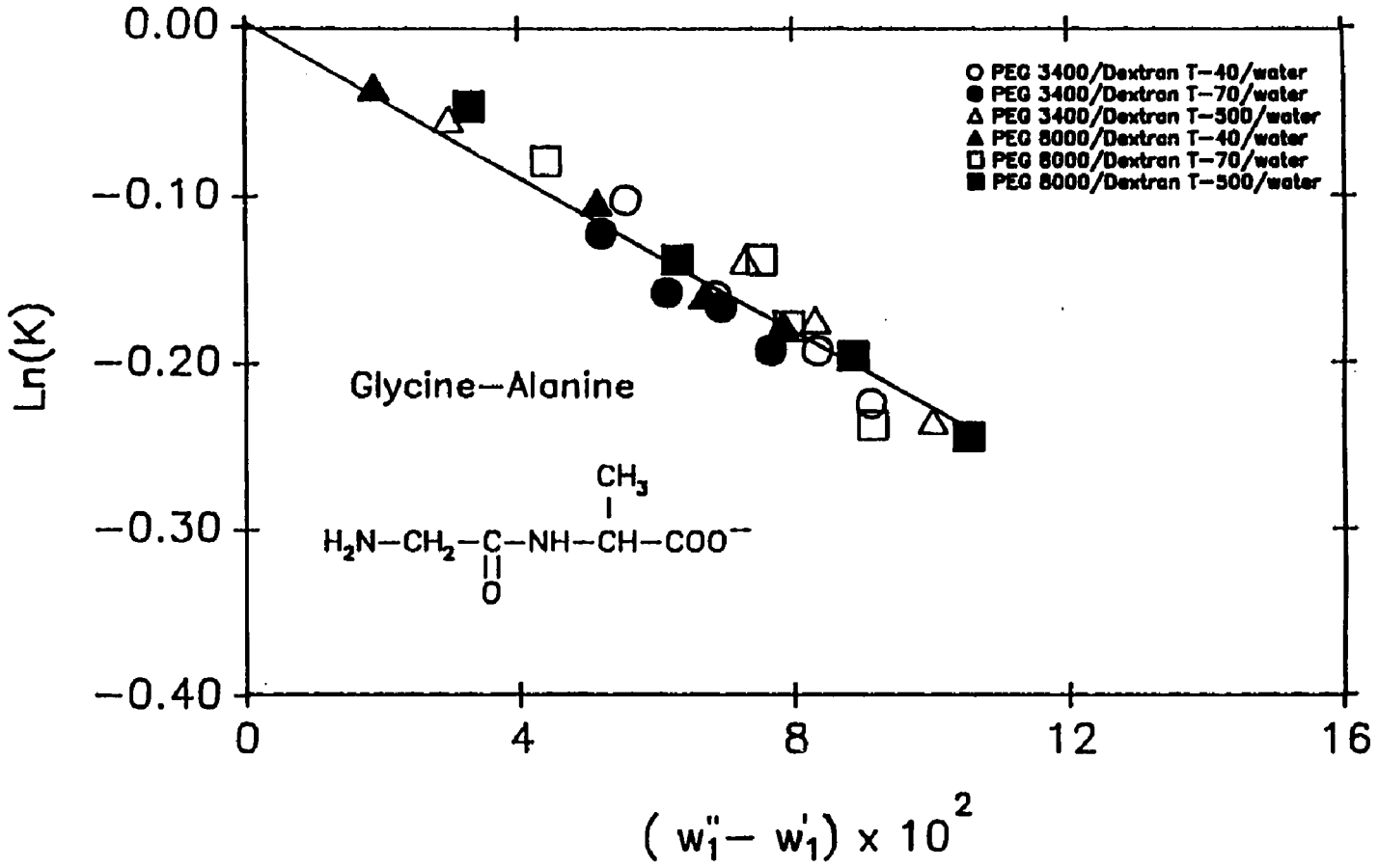

Figure 4.2 Effect of PEG Concentration Difference on the Natural Logarithm of the Partition Coefficient of Glycine-Alanine in PEG/Dextran/Water Systems at 4°C.

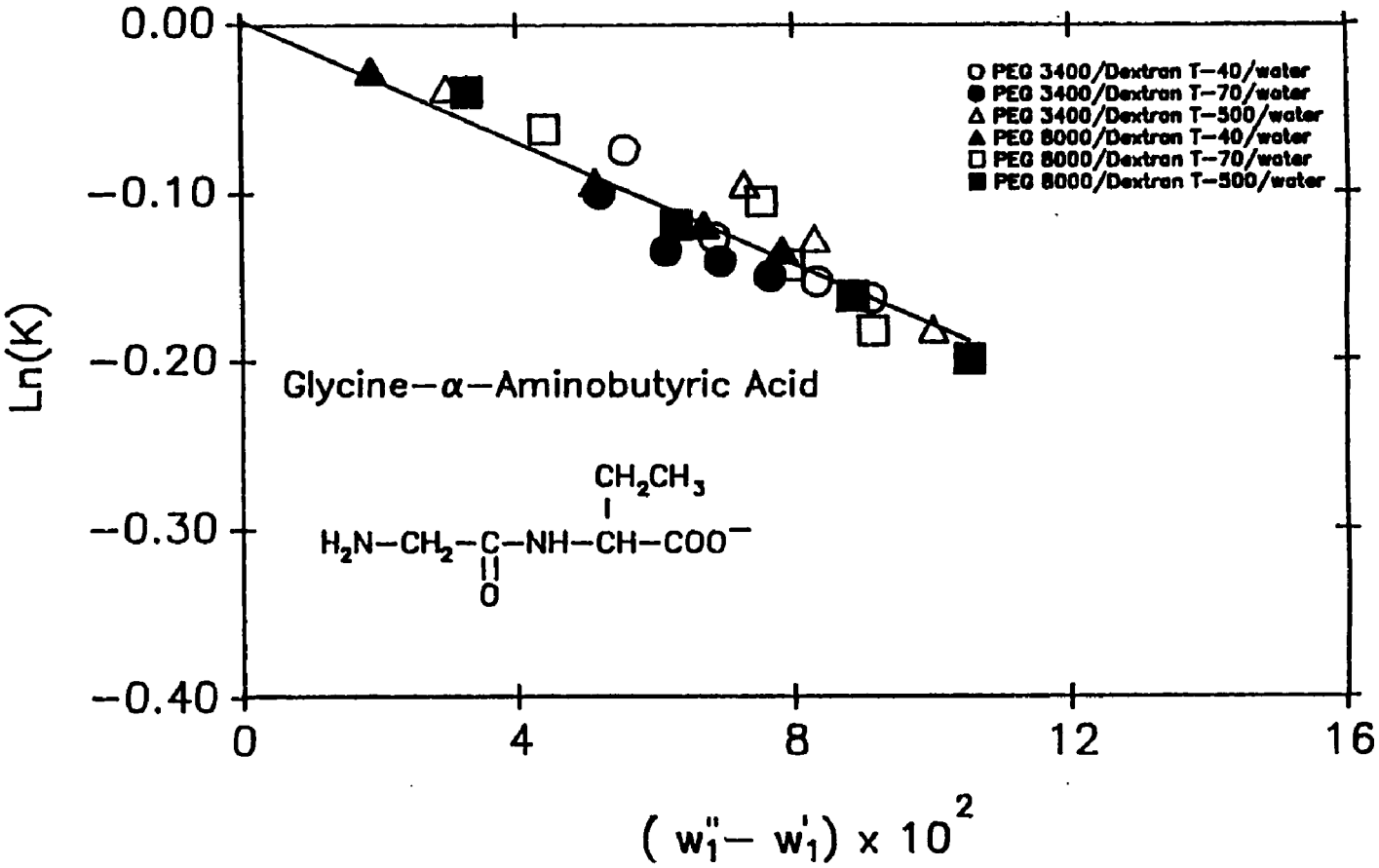

Figure 4.3 Effect of PEG Concentration Difference on the Natural Logarithm of the Partition Coefficient of Glycine-α-Aminobutyric Acid in PEG/Dextran/Water Systems at 4°C.

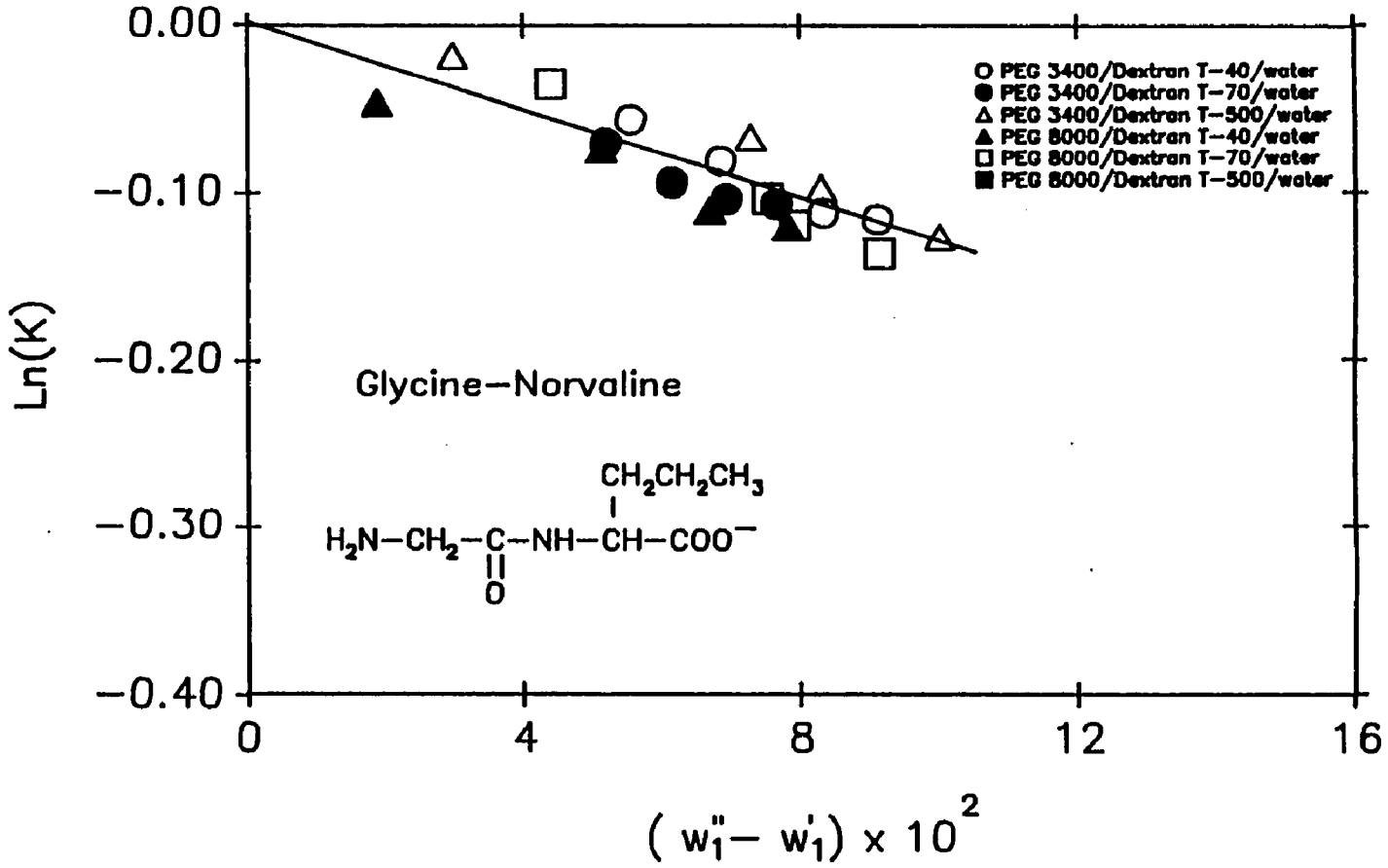

Figure 4.4 Effect of PEG Concentration Difference on the Natural Logarithm of the Partition Coefficient of Glycine-Norvaline in PEG/Dextran/Water Systems at 4°C.

the phase and partial specific volume of the polymer. The ratio ϕ was found to be −2.1 for PEG/dextran/water systems at 4°C, thus the interaction parameter term can be rewritten as $\alpha_1(\chi_{03}-\chi_{13}) - 2.1\alpha_2(\chi_{03} - \chi_{23})$. According to Flory (1953), the interaction parameter may be expressed as :

$$\chi_{ij} = \frac{z\Delta w_{ij} m_i}{kT} \tag{4.3}$$

where Δw_{ij} is the change in energy for the formation of a contact between species i and j, z is the lattice coordinate number, k is Boltzman's constant, T is absolute temperature, and m_i has previously been defined. From the definition of the interaction parameter, it is apparent that the greater the energy required to form a contact between species i and j and hence, the more repulsion between the two species, the larger the value of χ_{ij}. Therefore, since PEG is more hydrophobic than dextran or water (Albertsson, 1986), as a CH_2 group is added to the dipeptide chain, χ_{13} (interaction parameter for PEG and dipeptide) should increase the least while χ_{23} (interaction parameter for dextran and dipeptide) and χ_{03} (interaction between water and dipeptide) should show a higher increase than χ_{13}. This leads to an increase in the quantity $\alpha_1(\chi_{03}-\chi_{13}) - 2.1\alpha_2(\chi_{03} - \chi_{23})$ and hence a less negative slope in equation (4.1).

In addition to the correlation of equation (4.1), a second relationship may be obtained from the dipeptide partitioning. For a particular tie line composition on a phase diagram, a plot of $\ln(K_3)$ for the dipeptides versus number of CH_2 groups on the c-terminal residue gives a linear relationship, where gly-gly, gly-ala, gly-α, and gly-Nval correspond to 0, 1, 2, and 3 number of CH_2 groups, N_{CH_2}, respectively. According to Zaslavsky and coworkers (1982a,b, 1983, 1987) the slope of this line represents the $\ln(K_3)$ per N_{CH_2} for

the tie line. This quantity may be expressed in terms of equation (4.1) as follows :

$$\frac{\ln(K_3)}{N_{CH_2}} = \frac{A}{N_{CH_2}}(w_1'' - w_1') \tag{4.4}$$

Multiplying both sides of equation (4.4) by –RT, where R is the gas law constant and T is absolute temperature (277 K), gives :

$$-RT\,\frac{\ln(K_3)}{N_{CH_2}} = -RT\,\frac{A}{N_{CH_2}}(w_1'' - w_1') \tag{4.5}$$

or,

$$\Delta G_{tr}^{CH_2} = B(w_1'' - w_1') \tag{4.6}$$

where $\Delta G_{tr}^{CH_2} = -RT\frac{\ln(K_3)}{N_{CH_2}}$ represents the Gibbs free energy of transfer of a CH_2 group between the phases, and the slope $B = -RT\frac{A}{N_{CH_2}}$. Therefore, equation (4.6) provides a simple means for correlating the hydrophobicity difference between the phases with the PEG concentration difference (Zaslavsky and Miheeva, 1987).

The applicability of equation (4.6) was tested by plotting $\ln(K_3)$ of the dipeptides versus number of CH_2 groups for each of the tie lines in a phase diagram. The results for the PEG 3400/Dextran T-40, PEG 3400/Dextran T-70, PEG 3400/Dextran T-500, PEG 8000/Dextran T-40, PEG 8000/Dextran T-70 and PEG 8000/Dextran T-500/water systems at 4°C are provided in Figures 4.5–4.10, respectively. For each line, the $Ln(K_3)/N_{CH_2}$, and, therefore, the $\Delta G_{tr}^{CH_2}$ was calculated. In Figure 4.11, $\Delta G_{tr}^{CH_2}$ from Figures 4.5–4.10 were

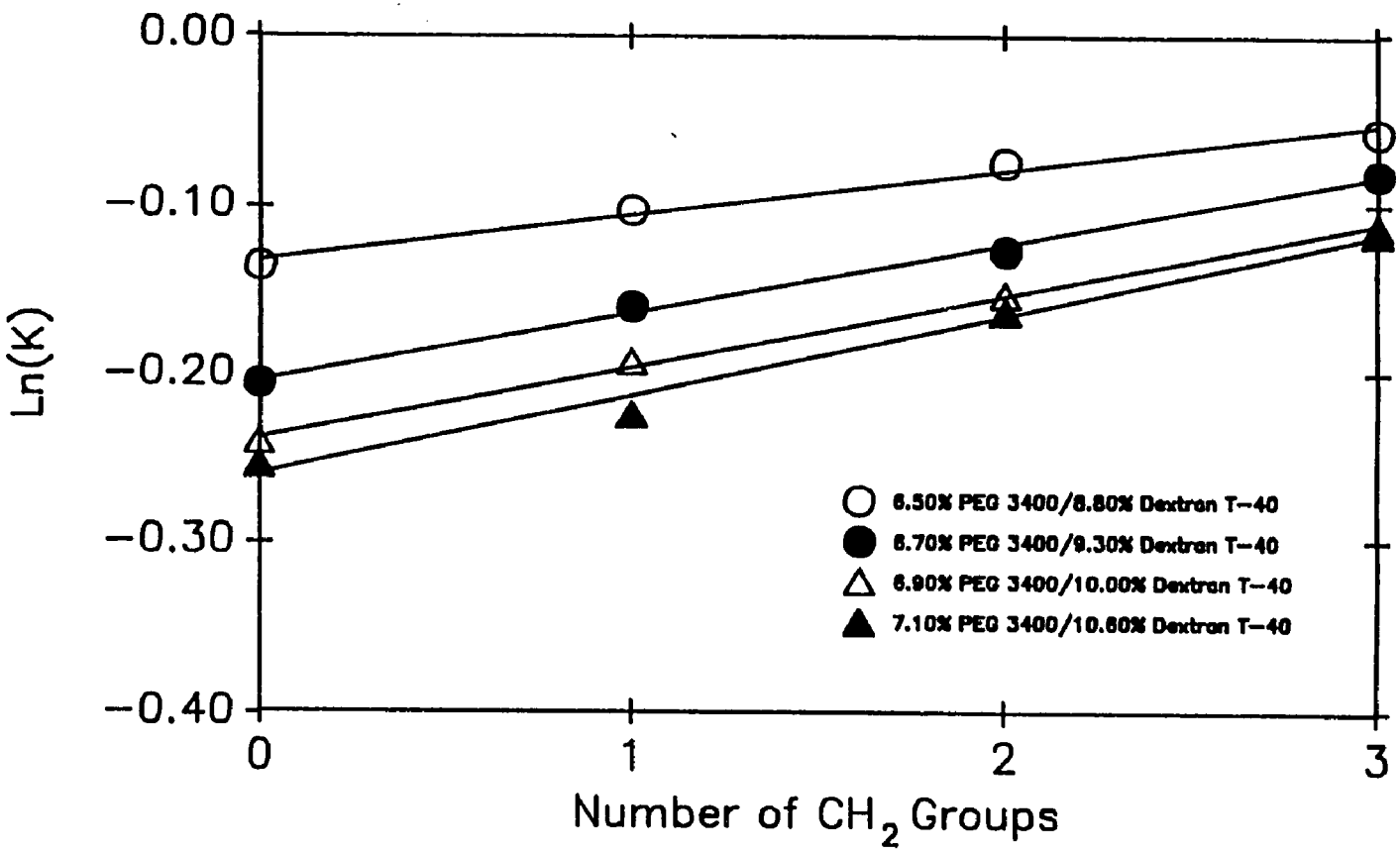

Figure 4.5 Natural Logarithm of the Partition Coefficient for the Dipeptides, Glycine-Glycine, Glycine-Alanine, Glycine-α-Aminobutyric Acid, and Glycine-Norvaline in PEG 3400/Dextran T-40/Water Systems at 4°C, as a Function of the Number of CH_2 Groups on the C-Terminal Residue. The dipeptides contain 0, 1, 2, and 3 number of CH_2 Groups, Respectively.

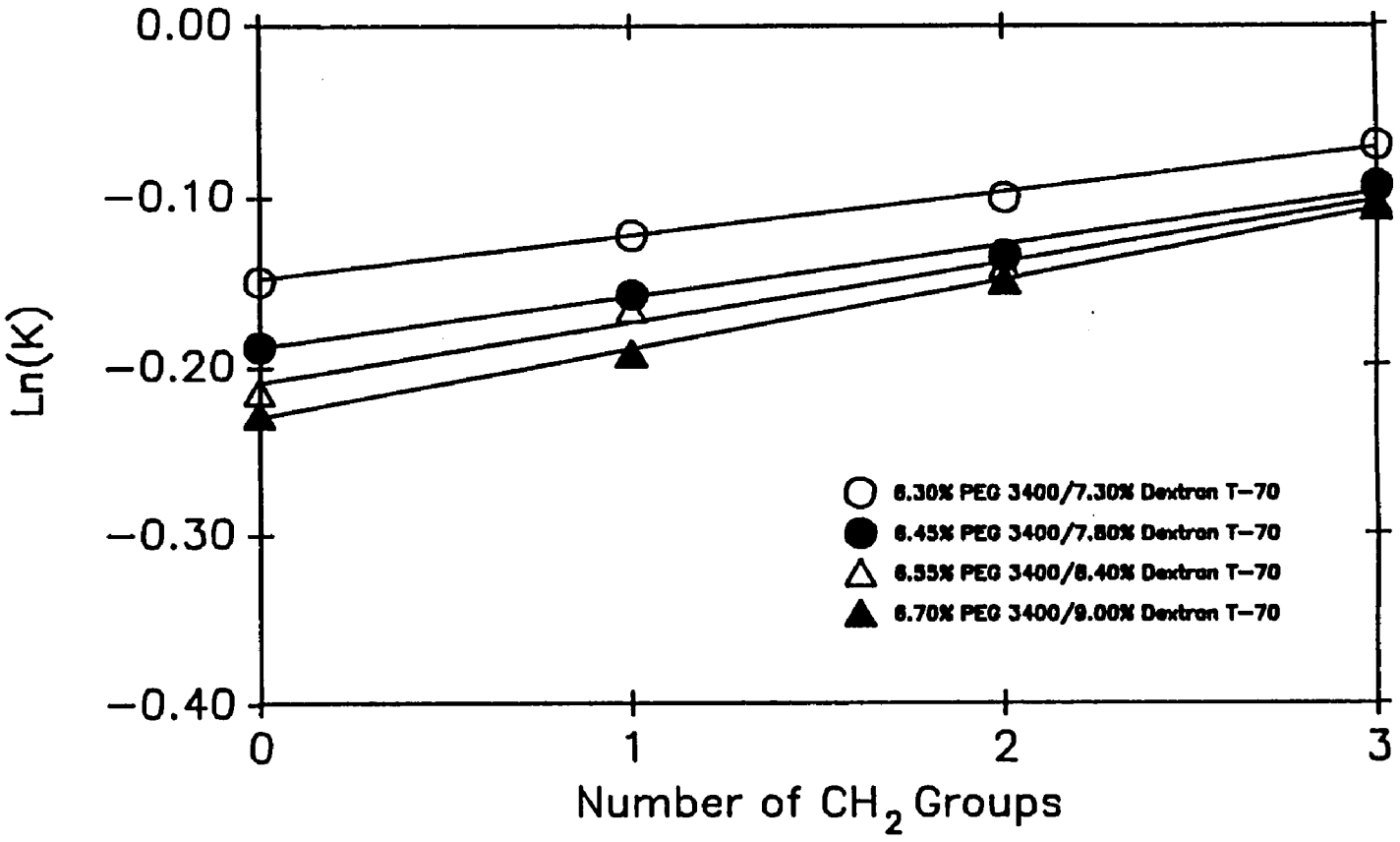

Figure 4.6 Natural Logarithm of the Partition Coefficient for the Dipeptides, Glycine-Glycine, Glycine-Alanine, Glycine-α-Aminobutyric Acid, and Glycine-Norvaline in PEG 3400/Dextran T-70/Water Systems at 4°C, as a Function of the Number of CH_2 Groups on the C-Terminal Residue.

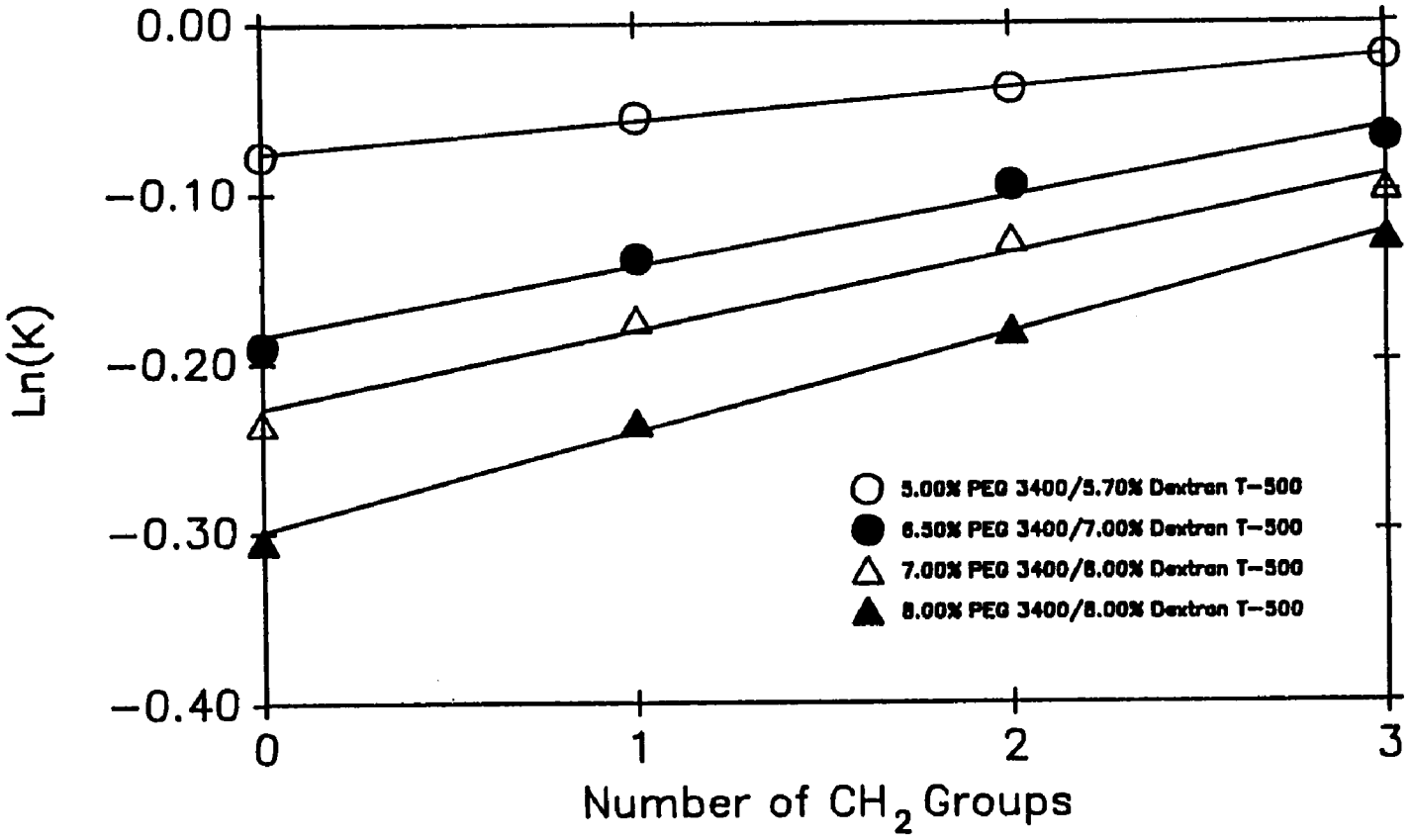

Figure 4.7 Natural Logarithm of the Partition Coefficient for the Dipeptides, Glycine-Glycine, Glycine-Alanine, Glycine-α-Aminobutyric Acid, and Glycine-Norvaline in PEG 3400/Dextran T-500/Water Systems at 4°C, as a Function of the Number of CH_2 Groups on the C-Terminal Residue.

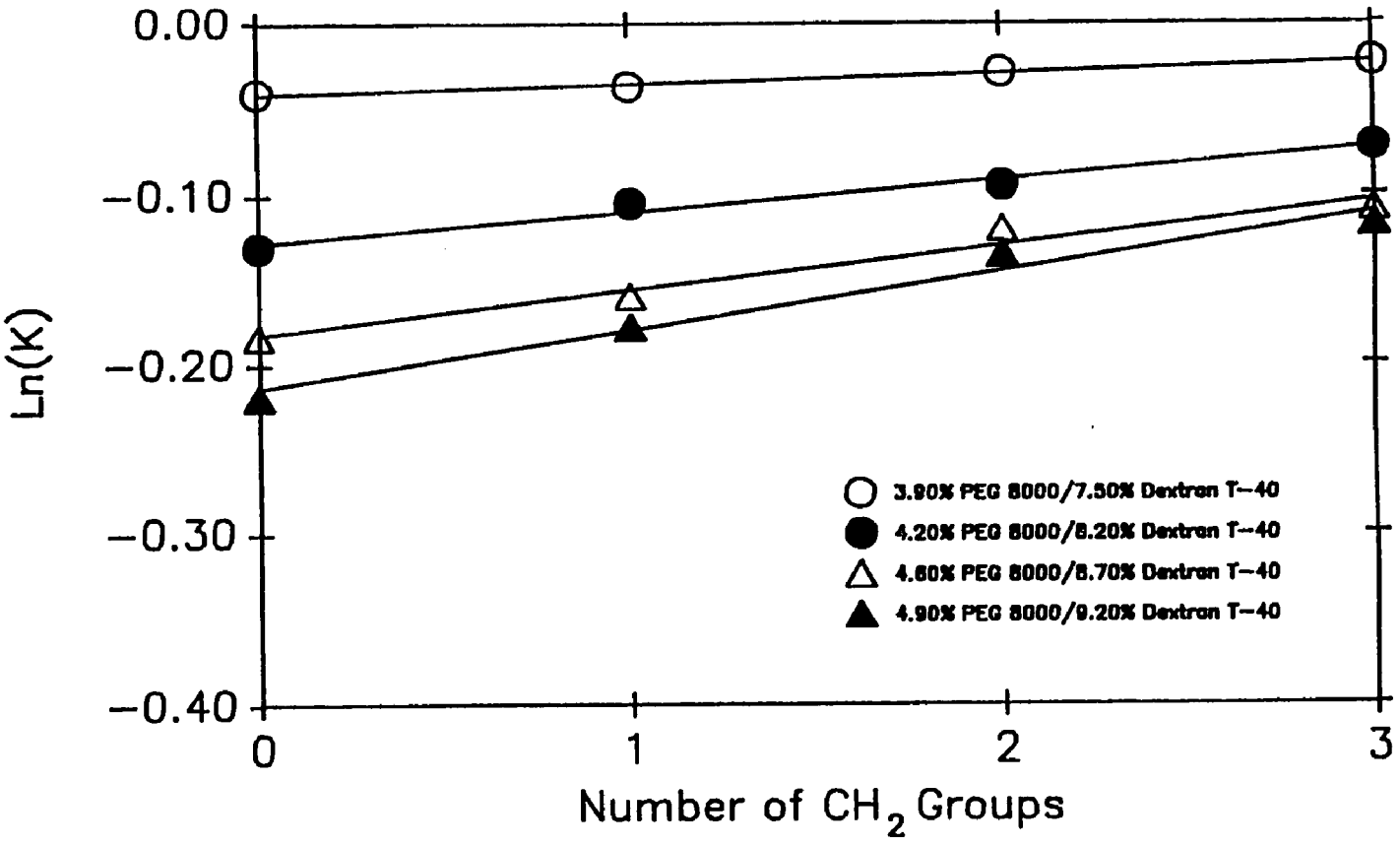

Figure 4.8 Natural Logarithm of the Partition Coefficient for the Dipeptides, Glycine-Glycine, Glycine-Alanine, Glycine-α-Aminobutyric Acid, and Glycine-Norvaline in PEG 8000/Dextran T-40/Water Systems at 4°C, as a Function of the Number of CH_2 Groups on the C-Terminal Residue.

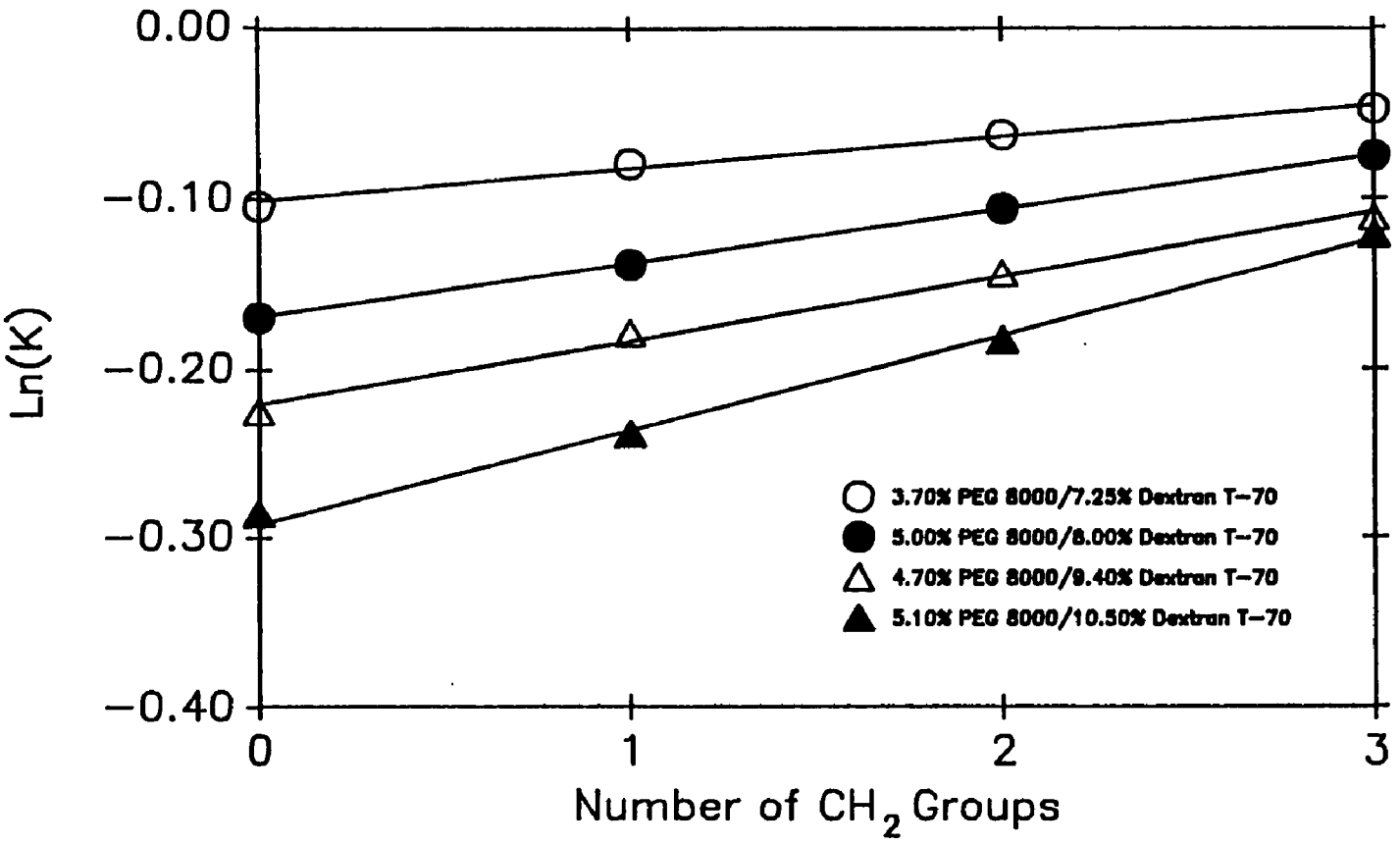

Figure 4.9 Natural Logarithm of the Partition Coefficient for the Dipeptides, Glycine-Glycine, Glycine-Alanine, Glycine-α-Aminobutyric Acid, and Glycine-Norvaline in PEG 8000/Dextran T-70/Water Systems at 4°C, as a Function of the Number of CH_2 Groups on the C-Terminal Residue.

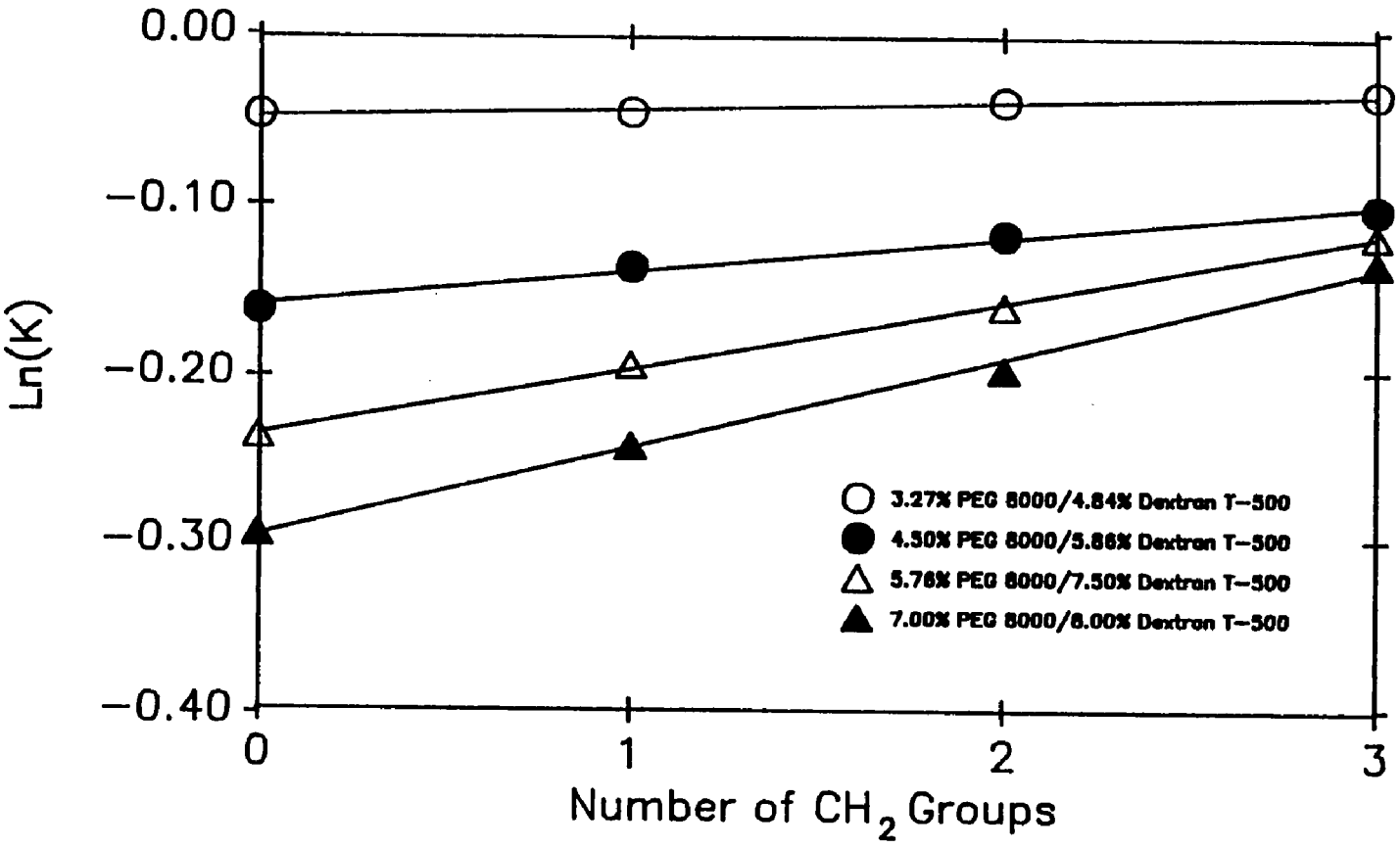

Figure 4.10 Natural Logarithm of the Partition Coefficient for the Dipeptides, Glycine-Glycine, Glycine-Alanine, Glycine-α-Aminobutyric Acid, and Glycine-Norvaline in PEG 8000/Dextran T-500/Water Systems at 4°C, as a Function of the Number of CH_2 Groups on the C-Terminal Residue.

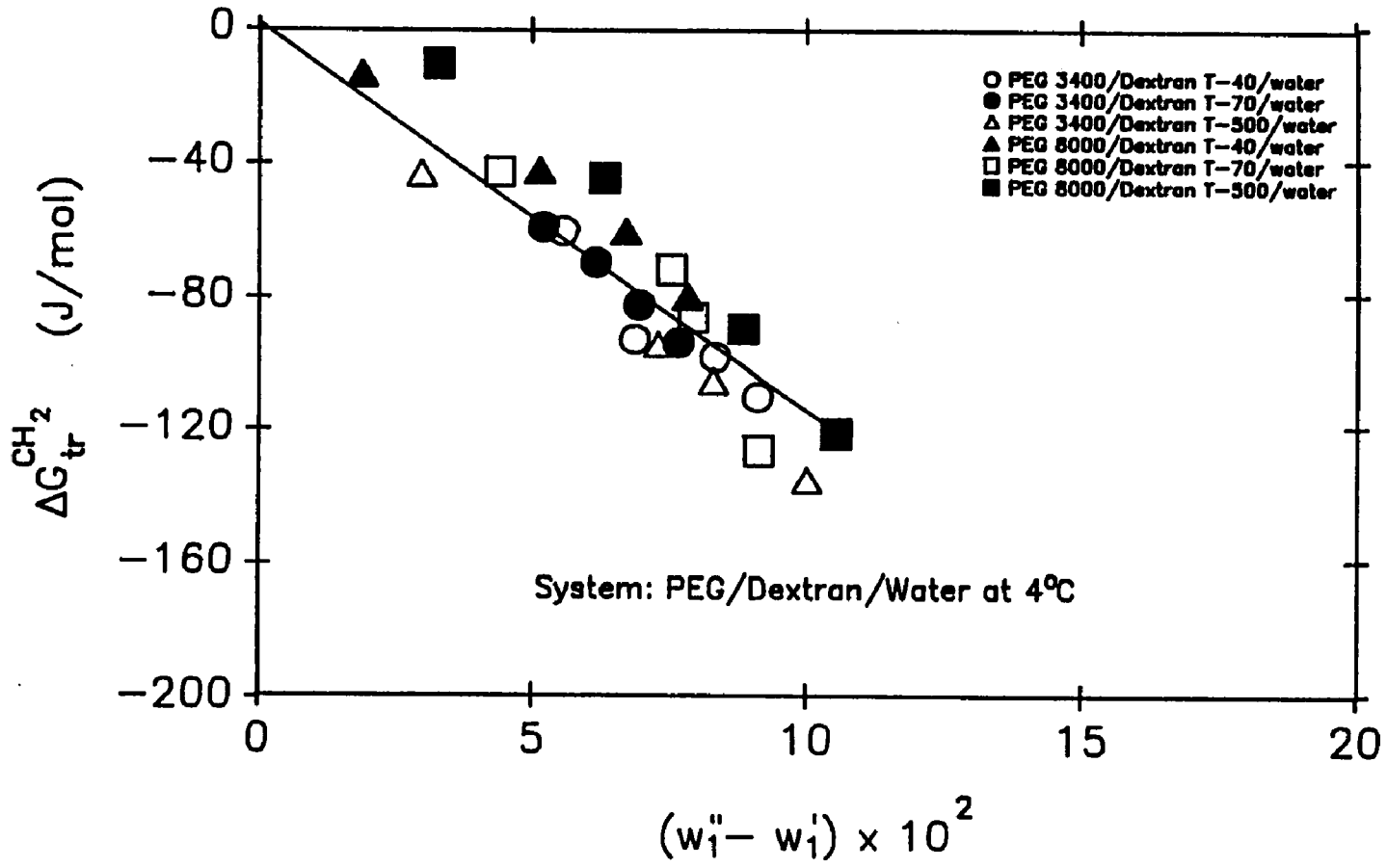

Figure 4.11 Effect of PEG Concentration Difference on the Gibbs Free Energy of Transfer of a CH_2 Group in PEG/Dextran/Water Systems at 4°C.

plotted versus the $(w_1'' - w_1')$ for the corresponding tie-line. The $\Delta G_{tr}^{CH_2}$ converge on a single line which represents the hydrophobicity profile for the PEG/dextran/water systems at 4°C. The greater the PEG concentration difference, the more negative the $\Delta G_{tr}^{CH_2}$, and hence the greater the hydrophobicity difference between the two phases.

From Figure 4.11, the value of the slope, B, in equation (4.6) was found to be −1161 J/mol. Dividing this value of B by −RT gives an A/N_{CH_2} of 0.5. The A/N_{CH_2} may have been obtained using a second method by plotting the values of A obtained for the dipeptides from Figures 4.1–4.4 versus the number of CH_2 groups on the c-terminal residue. Such a plot is provided in Figure 4.12 indicating a linear relationship was obtained according to the following equation:

$$A = -2.8 + 0.5(N_{CH_2}) \tag{4.7}$$

where the slope, 0.5, represents the A/N_{CH_2}, and −2.8 is the A value for gly-gly. Therefore, in order to obtain the value of A/N_{CH_2} and the slope of equation (4.6), only two partition coefficients need to be measured. One of these is gly-gly which enables the determination of its slope, A, and thus the intercept of equation (4.7), while the second partition coefficient may be from any of the other dipeptides. This second partition coefficient will give an additional value of A which will enable determination of the slope of equation (4.7).

4.3.2 Protein Partitioning

Having established the applicability of equation (4.1) for dipeptides, the next step was to investigate the partitioning of proteins. Nine different proteins

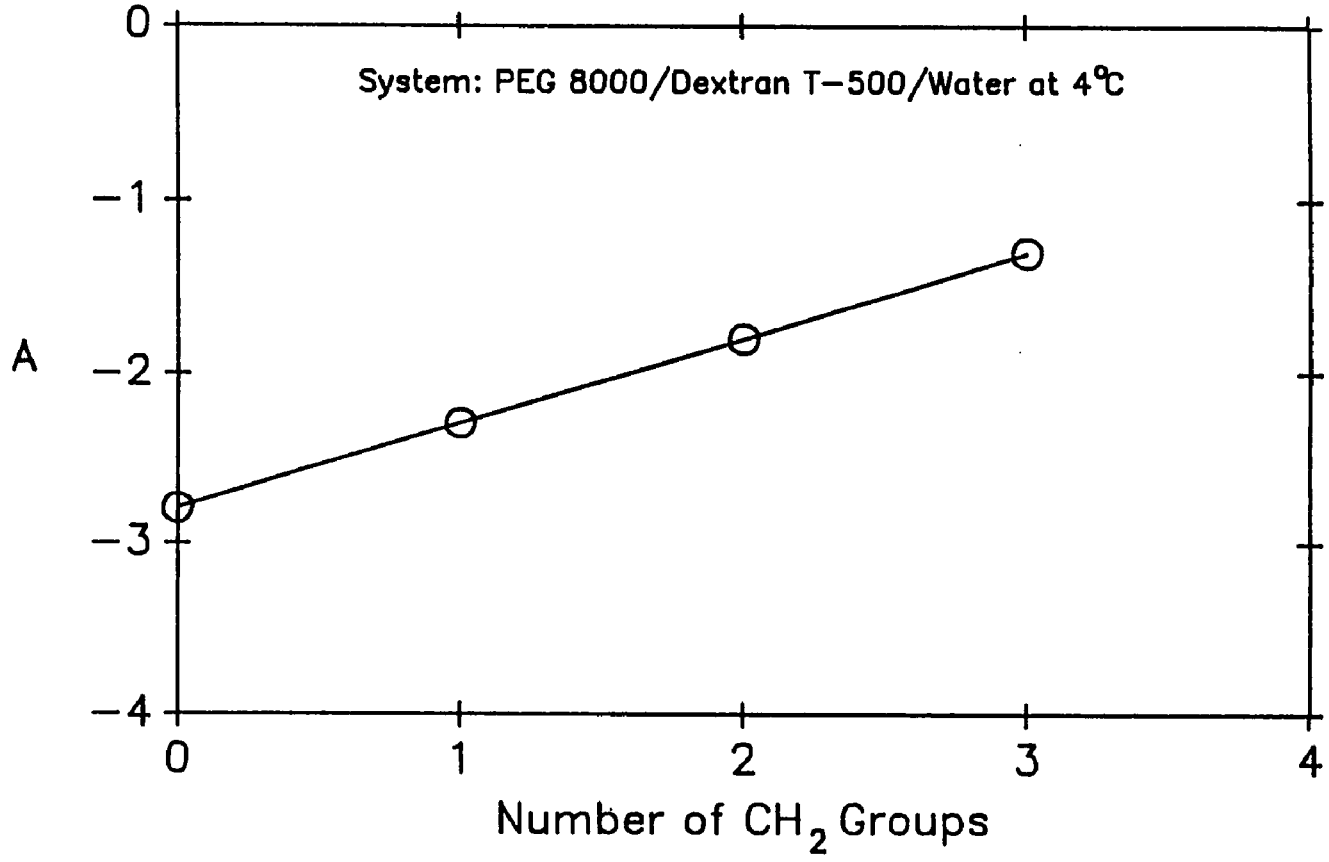

Figure 4.12 The Slope, A, of Equation (4.1) for Dipeptides as a Function of the Number of CH_2 Groups on the C-Terminal Amino Acid Residue.

with a range of molecular weights from 13,000 to 145,000 were partitioned in the PEG 8000/Dextran T-500/water at 4°C system, i.e., Figure 3.6 in Chapter III. The results appear in Figures 4.13 and 4.14. From these two figures it is apparent that proteins with molecular weights below approximately 25,000, ie, cytochrome c, lysozyme, ribonuclease, and trypsin, obeyed the linear semilogarithmic relationship of equation (4.1). The slope, A, of equation (4.1) for each of these proteins in phase diagram F was –21.2, –9.0, –13.4, and –6.1, respectively. However, for the proteins above this molecular weight (α-amylase, BSA, transferrin, ovalbumin, and alcohol dehydrogenase) the relationship became non-linear. In order to explain this trend the slope of equation (4.1) must be examined for the case where a single phase diagram is being utilized. The terms containing m_1 and m_2 should remain constant since the molecular weight of the phase forming polymers is unchanged. If the partitioning solute behaves ideally, the interaction parameters χ_{01}, χ_{02}, χ_{03}, χ_{13} and χ_{23} should not vary as long as the structure of the solute, phase forming polymers, and solvent remain the same. Therefore, the slope will be constant, and a linear relationship obtained, as was observed for the low molecular proteins. However, for the high molecular weight proteins, the slope does not remain constant. This was most probably due to a variation of the interaction parameters as phase forming polymer concentration was altered. The variation of the interaction terms may be due to a change in the tertiary structure of the large molecules at different tie line compositions of the phase diagram.

In order to view the effect of polymer molecular weight on the slope of equation (4.1), trypsin and lysozyme (two low molecular weight proteins), and BSA (a protein of moderate molecular weight) were partitioned in the phase diagrams of Figures 3.3, 3.4, 3.5 and 3.6 Chapter III. The phase diagrams in

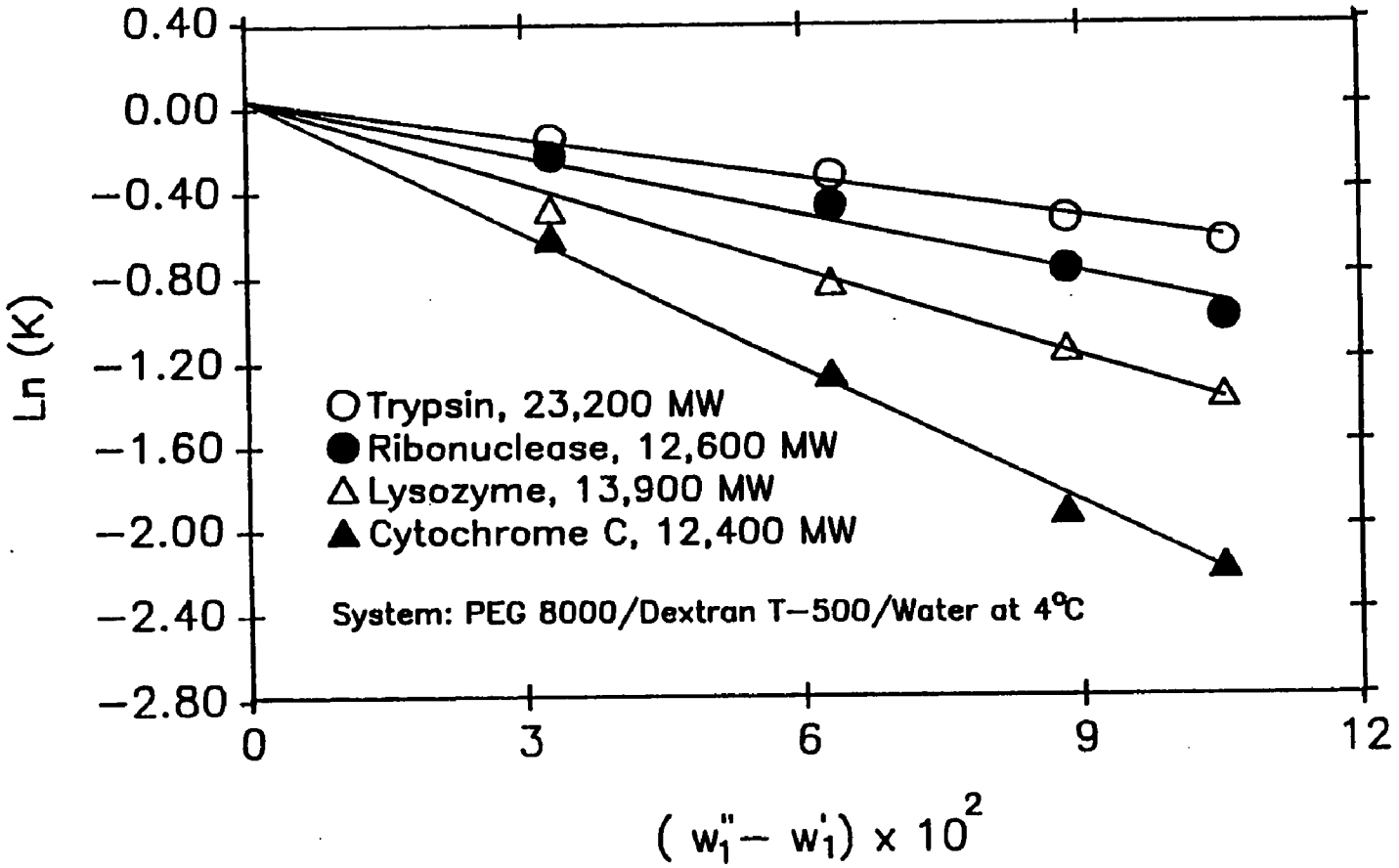

Figure 4.13 Natural Logarithm of the Partition Coefficient of Low Molecular Weight Proteins as a Function of PEG Concentration Difference in the PEG 8000/Dextran T-500/Water System at 4°C.

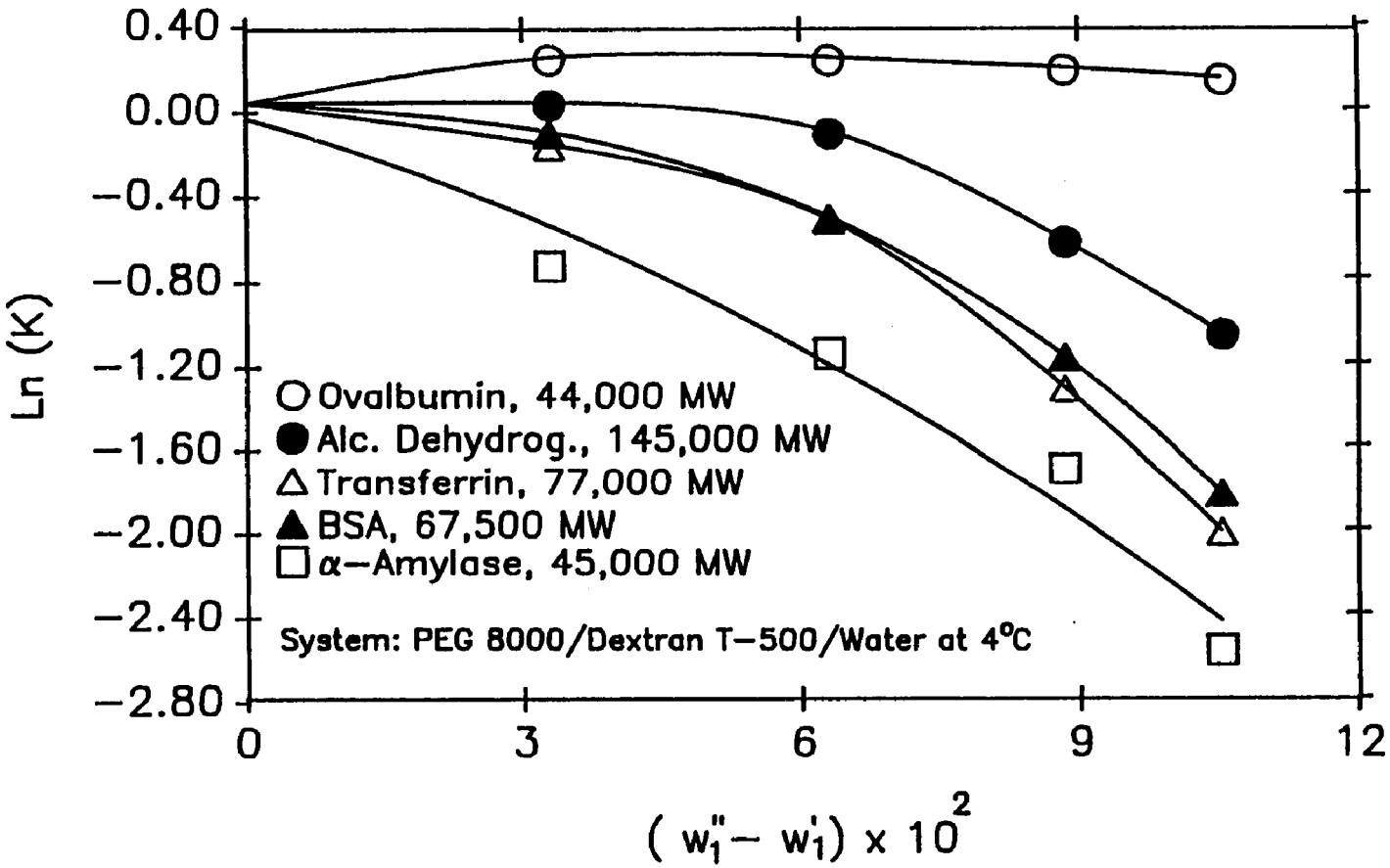

Figure 4.14 Natural Logarithm of the Partition Coefficient of High Molecular Weight Proteins as a Function of PEG Concentration Difference in the PEG 8000/Dextran T-500/Water System at 4°C.

Figures 3.4, 3.5 and 3.6 contain dextran of different molecular weight (covering the range of 40,000–500,000) while those in Figures 3.3 and 3.6 provide a variation of PEG molecular weight (from 3400–8000). The results were correlated according to equation (4.1) and are presented for the three proteins in Figures 4.15–4.17, respectively. Trypsin and lysozyme obeyed the linear semilogarithmic relationship of equation (4.1) in each of the phase diagrams, while BSA proved to be nonlinear. For each of the three proteins, it is apparent that as dextran molecular weight increased from 40,000 to 500,00 in systems and PEG is maintained at 8000, higher partition coefficients were obtained. The slope of equation (4.1) was –8.0, –7.2, and –6.1 for trypsin, and –15.5, –15.3, and –13.4 for lysozyme in the three phase diagrams. Therefore, as dextran molecular weight was increased, the slope became less negative. In a similar manner, it is seen that as PEG molecular weight was increased from 3400 to 8000, the partition coefficient decreased for all three proteins, and the slope of equation (4.1) decreased from –5.4 to –6.1 for trypsin, and –12.2 to –13.4 for lysozyme. The molecular weight effect of the phase forming polymers on partitioning has been observed by Albertsson (Albertsson, 1986; Albertsson *et al.*, 1987). The molecular weight effect on the slope of equation (4.1) can be explained by noting that the main term altered in the slope is $\left(\frac{\alpha_1}{m_1} - \frac{2.1\alpha_2}{m_2}\right)$. Increasing dextran molecular weight results in a decrease in $\frac{2.1\alpha_2}{m_2}$, thus causing the slope to become less negative. However, as PEG molecular weight is increased, $\frac{\alpha_1}{m_1}$ decreases, and the slope becomes more negative.

The main result of the protein partitioning study was that for proteins with molecular weights below 25,000 a linear relationship was established between the natural logarithm of the partition coefficient and the PEG concentration difference between the phases, for a particular phase diagram.

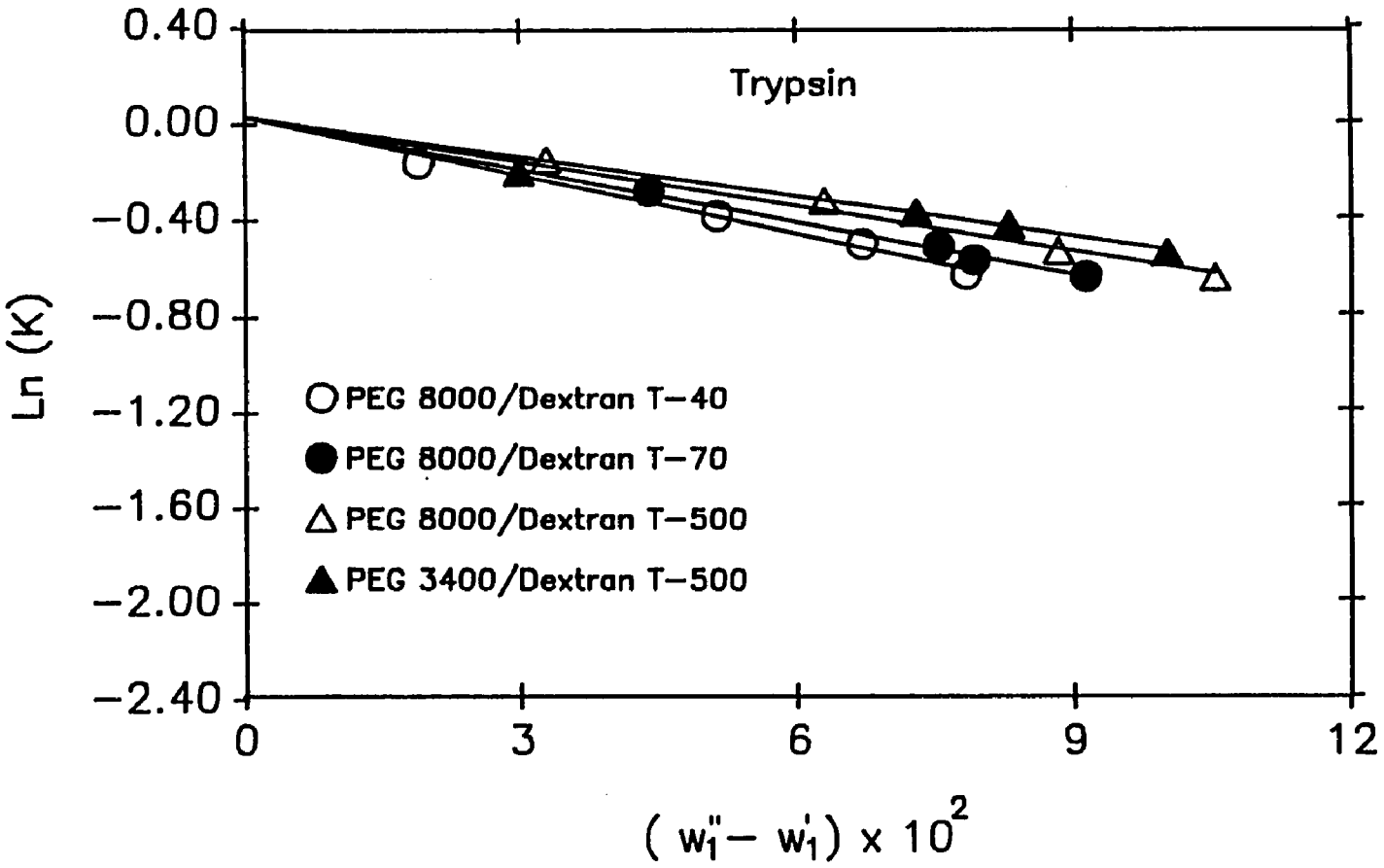

Figure 4.15 Natural Logarithm of the Partition Coefficient of Trypsin as a Function of PEG Concentration Difference in PEG/Dextran/Water Systems at 4°C.

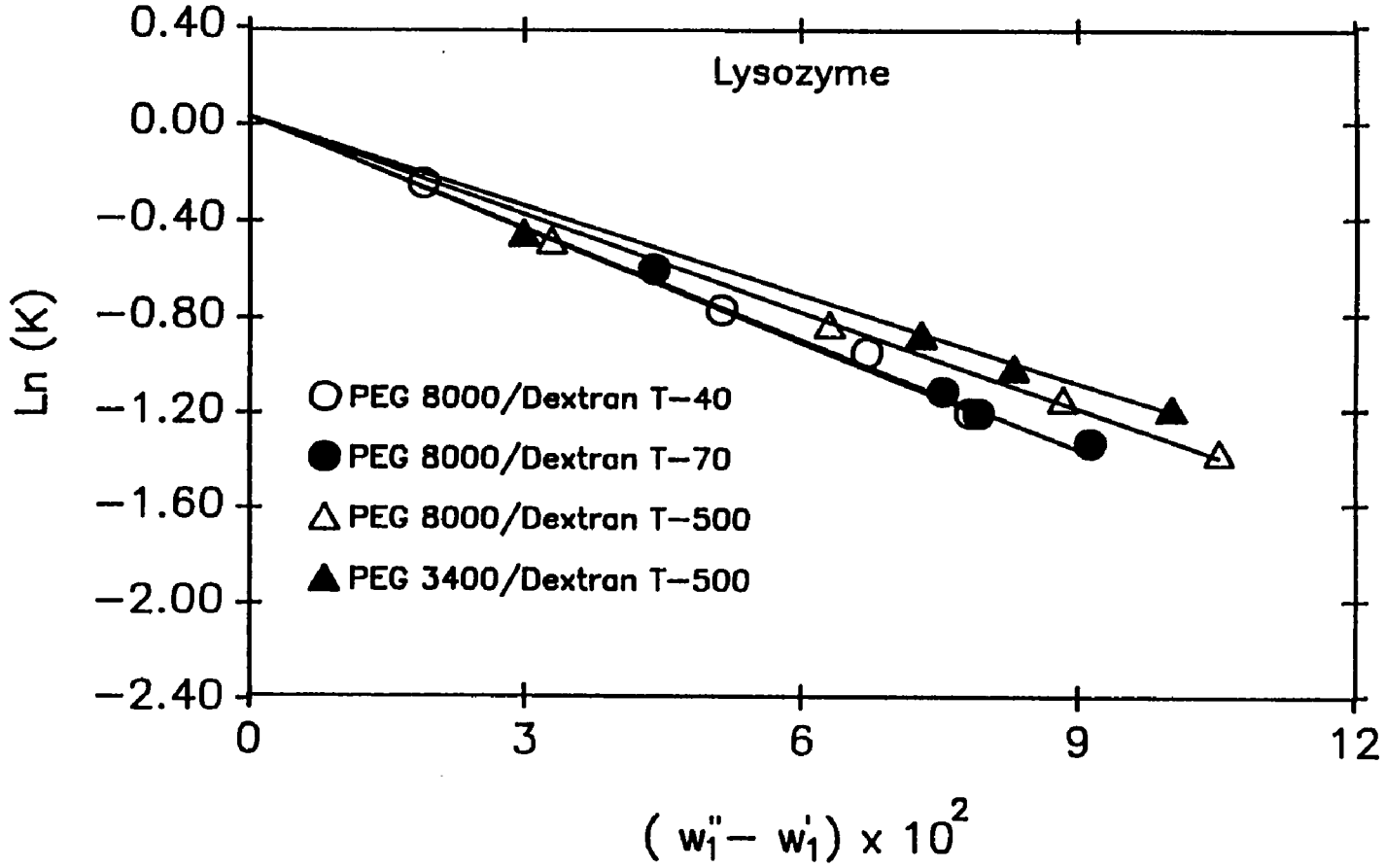

Figure 4.16 Natural Logarithm of the Partition Coefficient of Lysozyme as a Function of PEG Concentration Difference in PEG/Dextran/Water Systems at 4°C.

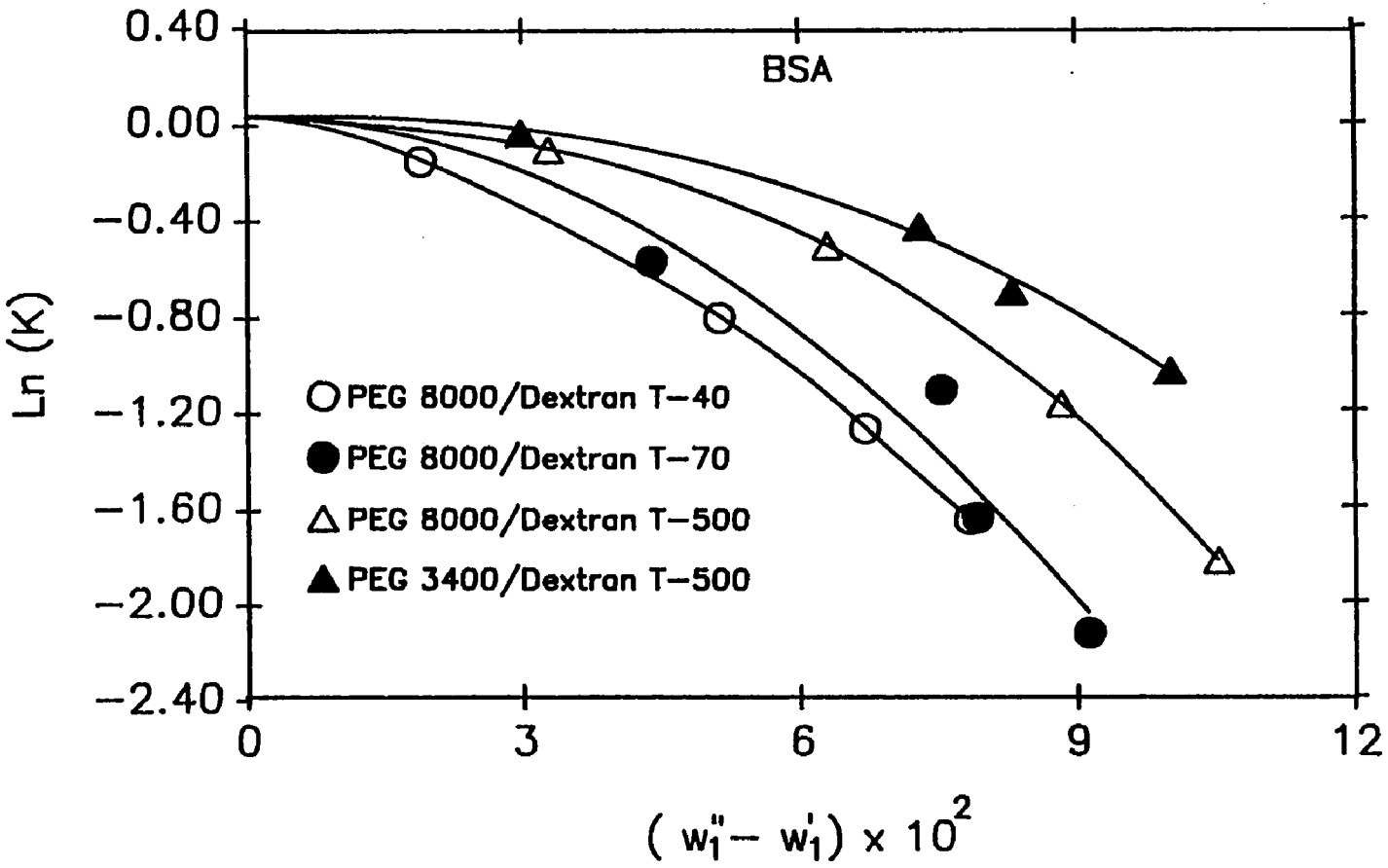

Figure 4.17 Natural Logarithm of the Partition Coefficient of BSA as a Function of PEG Concentration Difference in PEG/Dextran/Water Systems at 4°C.

The relationship may be obtained with knowledge of only a single partition coefficient at a tie line composition in the phase diagram. Therefore, only a single partition experiment is needed in order to have a clear picture of partitioning in the entire phase diagram.

4.4 Conclusions

Based on the linear semilogarithmic relationship of equation (4.1), which was derived from the Flory-Huggins theory, a simple means has been devised for correlating low molecular weight solute and protein partitioning. The relationship was verified for PEG/dextran/water systems utilizing dipeptides which differ from one another by a CH_2 group on the c-terminal residue and proteins as partitioning solutes. From the dipeptide partitioning, it was found that knowledge of the partition coefficient in only one of the PEG/dextran/water systems, regardless of polymer molecular weight, enabled prediction of the coefficient in all of the systems. The values of the slope A for the dipeptides permitted the determination of the Gibbs free energy of transfer for a CH_2 group and thus, the hydrophobicity in the PEG/dextran/water systems. As the tie line length increased the hydrophobicity was shown to increase. In addition, the effect of a CH_2 group on dipeptide partitioning could be qualitatively explained in terms of the interaction parameter, χ_{ij}. As a CH_2 group was added to the c-terminal residue, the slope A became less negative due to a small increase in χ_{13} (interaction between PEG and dipeptide) and a large increase in χ_{03} (interaction between water and dipeptide) and χ_{23} (interaction between dextran and dipeptide).

Protein distribution indicated that the relationship of equation (4.1) holds up to a molecular weight of approximately 25,000, above which

nonlinearities become important. The parameter A was shown to increase as dextran molecular weight increased, and increase as PEG dextran molecular weight decreased. For the low molecular weight proteins, knowledge of the partition coefficient at one tie line composition of a phase diagram enabled determination of the coefficient at other tie lines of the same diagram.

CHAPTER V
GENERALIZED PARTITION CORRELATION

In this chapter, a generalized expression, based on a modified form of the Flory-Huggins theory, is utilized for correlating biomolecule partitioning in PEG/dextran, PEG/potassium phosphate and ficoll/dextran aqueous two-phase systems. The relationship is verified by partitioning peptides and proteins covering a wide range of molecular weight in the tie lines of the above systems, along with data from the literature.

The parameters of the generalized relationship are a function of protein and phase forming polymer molecular weight, protein-water, protein-polymer, and polymer-water interaction parameters, and the electrostatic potential difference between the phases. The effects of phase forming polymer molecular weight on protein partitioning will be explained by careful examination of the partition data and the correlating parameters. Similarly, the effect of temperature on the correlating parameters is examined by partitioning proteins in PEG 8000/Dextran T-500 systems at 0°C, 4°C, 10°C, and 22°C.

5.1 Introduction

In Chapter IV, a simple linear semilogarithmic relationship was presented for correlating dipeptide and low molecular weight protein partitioning to the polymer concentration difference between the phases in the PEG 8000/Dextran T-500/water system based on Flory-Huggins polymer solution thermodynamics. However, the relationship was not applicable to high molecular weight proteins which exhibited nonlinear semilogarithmic

partitioning trends. The purpose of this chapter is to present a generalized correlation which is applicable to proteins partitioned in a variety of aqueous two-phase systems, and which can be used to facilitate the engineering scale-up of aqueous two phase systems for protein purification.

With this objective, proteins covering a broad range of molecular weight up to 669,000 were partitioned in the following three systems: PEG 8000/Dextran T-500/water at 4°C, PEG 3400/potassium phosphate/water at 20°C, and Ficoll 400/Dextran T-500/water at 23°C. In addition, the effect of phase forming polymer molecular weight on protein partitioning was investigated by using the PEG 8000/Dextran T-500/water system along with PEG 8000/Dextran T-40/water, PEG 8000/Dextran T-70/water, and PEG 3400/Dextran T-500/water systems at 4°C. The effect of temperature was investigated by using PEG 8000/Dextran T-500 systems at 0°C, 4°C, 10°C, and 22°C. A correlation was obtained which enabled the linearization of protein partitioning data regardless of protein molecular weight, or the system utilized. The correlating parameters were also shown to be a function of reciprocal absolute temperature.

5.2 Materials and Methods

5.2.1 Polymers and Proteins

Dextran T-500 (Lot 06905) and Ficoll 400 (Lot 07141) were purchased from Pharmacia, Piscataway, NJ. Polyethylene glycol of molecular weight 3,400 (Lot 00304 EV) and 8,000 (Lot 02316 EV) was obtained from Aldrich Chemical Company, Milwaukee, WI.

Ribonuclease (bovine pancreas), trypsin, lysozyme (chicken egg),

rhodanese (bovine liver), hexokinase (bakers yeast), invertase (bakers yeast), transferrin (human), bovine serum albumin (BSA), thyroglobulin (bovine), cytochrome c (horse heart), alcohol dehydrogenase (bakers yeast), ovalbumin (turkey egg), α-amylase (Bacillus species), lipase (wheat germ), conalbumin (chicken egg white), myoglobin (horse skeletal muscle), and protease were purchased from Sigma Chemical Company, St. Louis, MO.

5.2.2 Protein Partitioning

The phase compositions of the PEG 8000/Dextran T-40/water, PEG 8000/Dextran T-70/water, PEG 8000/Dextran T-500/water, and PEG 3400/Dextran T-500/water systems at 4°C, the PEG 8000/Dextran T-500/water systems at 10°C, and the PEG 8000/Dextran T-500/water systems at 22°C were presented in Chapter II. The phase compositions for the PEG 8000/Dextran T-500 systems at 0°C, the PEG 3400/potassium phosphate/water systems at 20°C, and the Ficoll 400/Dextran T-500/water systems at 23°C were obtained from Albertsson (1986).

Partition experiments were performed as previously described in Chapter IV. The PEG 3400/potassium phosphate/water and Ficoll 400/Dextran T-500/water systems were prepared according to Albertsson (1986), while the PEG/dextran/water systems were prepared as described in Chapter II. All experiments were performed at pH 7.0. In the PEG/dextran/water and Ficoll 400/Dextran T-500/water systems this pH was maintained by the addition of 0.01 molal potassium phosphate buffer, while the PEG/potassium phosphate/water systems contained a mono- to dibasic potassium phosphate ratio of 1.82. 10 mL of phase system was poured into 15 mL polypropylene centrifuge tubes. 10 mg of protein was added, and the tubes tightly sealed.

The phases of the PEG/dextran system were allowed to settle for 24–48 hours at either 0°C, 4°C, or 10°C in a temperature controlled refrigerator. Experiments at 22°C were permitted to settle for 24 hours in the laboratory environment. A pasteur pipet was used to collect the top phase, while the lower phase was drained from the tube by piercing a hole at its bottom.

Protein concentration was determined by diluting the phase aliquot with water, and measuring absorbance, by Shimadzu UV-VIS spectrophotometer, at 280 nm versus an appropriately diluted phase blank.

5.3 Results and Discussion

5.3.1 Correlation of Protein Partitioning

In Chapter II, the following relationship (equation (2.44)) was derived based on Flory-Huggins solution thermodynamics:

$$\frac{\ln(K_3)}{(w_1'' - w_1')} = A^* + b^*(w_1'' - w_1') \tag{5.1}$$

where,

$$A^* = A + \frac{z_b F g}{RT} \tag{5.2}$$

and

$$b^* = b + \frac{z_b F h}{RT} \tag{5.3}$$

Equation (5.1) is the generalized expression for correlating protein partitioning

in aqueous two-phase systems, where the intercept A^* is a function of protein and phase forming polymer molecular weight, and the protein-water, protein-polymer, polymer-water interaction parameters, pH and salt type and concentration. Similarly, the slope b^* is a function of protein molecular weight, the polymer-water interaction parameters, pH and the salt type and concentration. In order to verify the applicability of equation (5.1) for correlation of partition data, proteins covering a wide range of molecular weight were partitioned in four systems of the PEG 8000/Dextran T-500/water phase diagram at 4°C, the PEG 3400/potassium phosphate/water system at 20°C, and the Ficoll 400/Dextran T-500/water system at 23°C. In Figures 5.1–5.3, $\ln(K_3)$ for seventeen proteins partitioned in the PEG 8000/Dextran T-500/water system at 4°C is plotted versus $(w_1'' - w_1')$ according to equation (4.1) of Chapter IV. The data have first been plotted according to this equation to demonstrate the second order nature of the protein partition phenomena, and that equation (4.1) is mainly applicable to low molecular weight proteins (Diamond and Hsu, 1989a). Figure 5.1 contains low molecular weight protein partitioning (lipase, cytochrome c, ribonuclease, lysozyme, myoglobin, and trypsin), while Figures 5.2 and 5.3 contain high molecular weight proteins. We have established the distinction between low and high molecular weight proteins to be a molecular weight of 25,000. Similarly, in Figures 5.4 and 5.5 protein partitioning in the PEG 3400/potassium phosphate/water system at 20°C, and in Figures 5.6 and 5.7 protein partitioning partitioning in the Ficoll 400/Dextran T-500/water system at 23°C is presented according to equation (5.1). It should be pointed out that the curves drawn through the data in Figures 5.1–5.7 represent a second order regression which includes the point (0,0), i.e., the plait point. It should also be noted that not all of the proteins

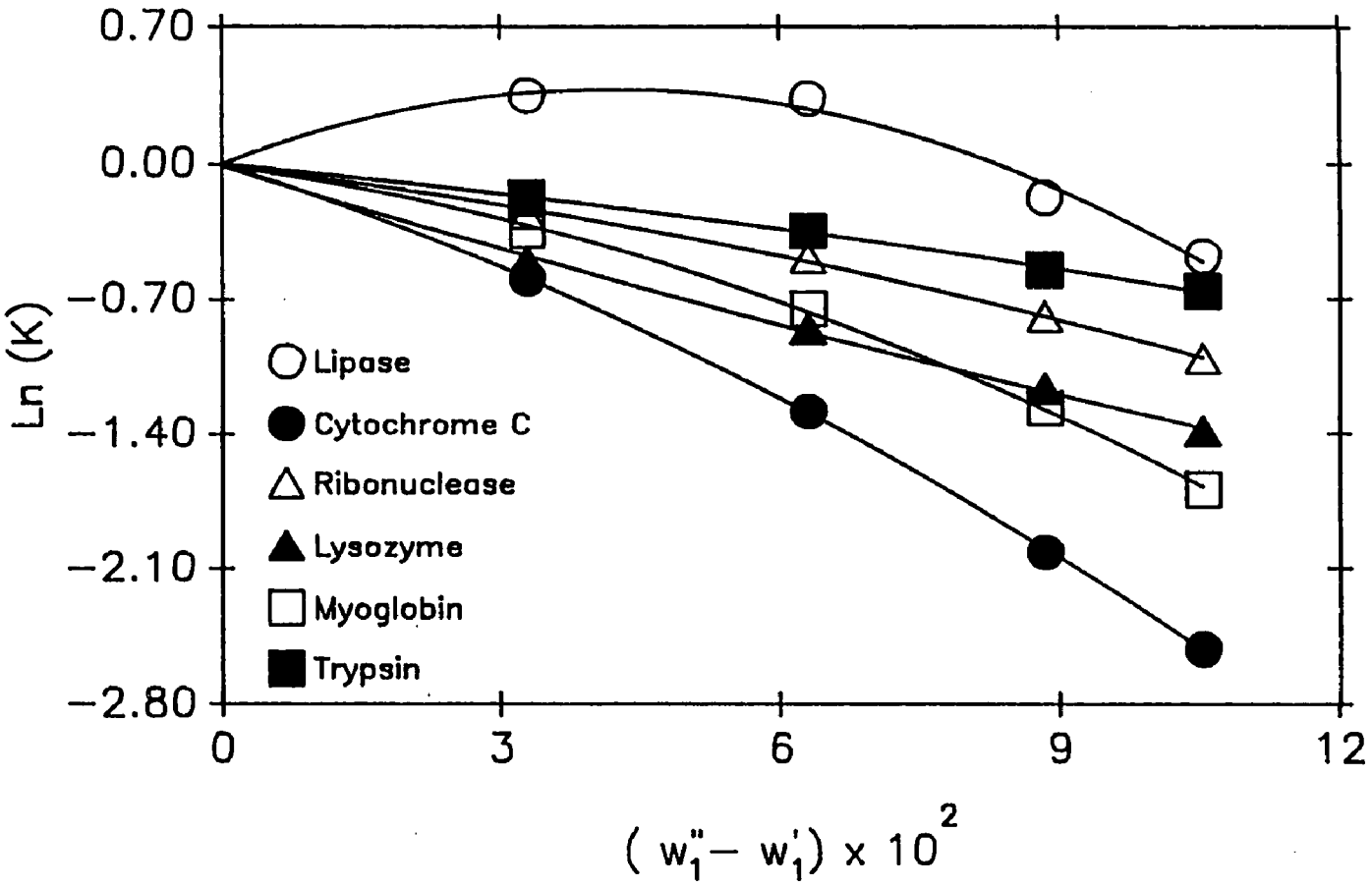

Figure 5.1 Correlation of Low Molecular Weight Protein Partitioning According to Equation (4.1) in the PEG 8000/Dextran T-500/Water System at 4°C.

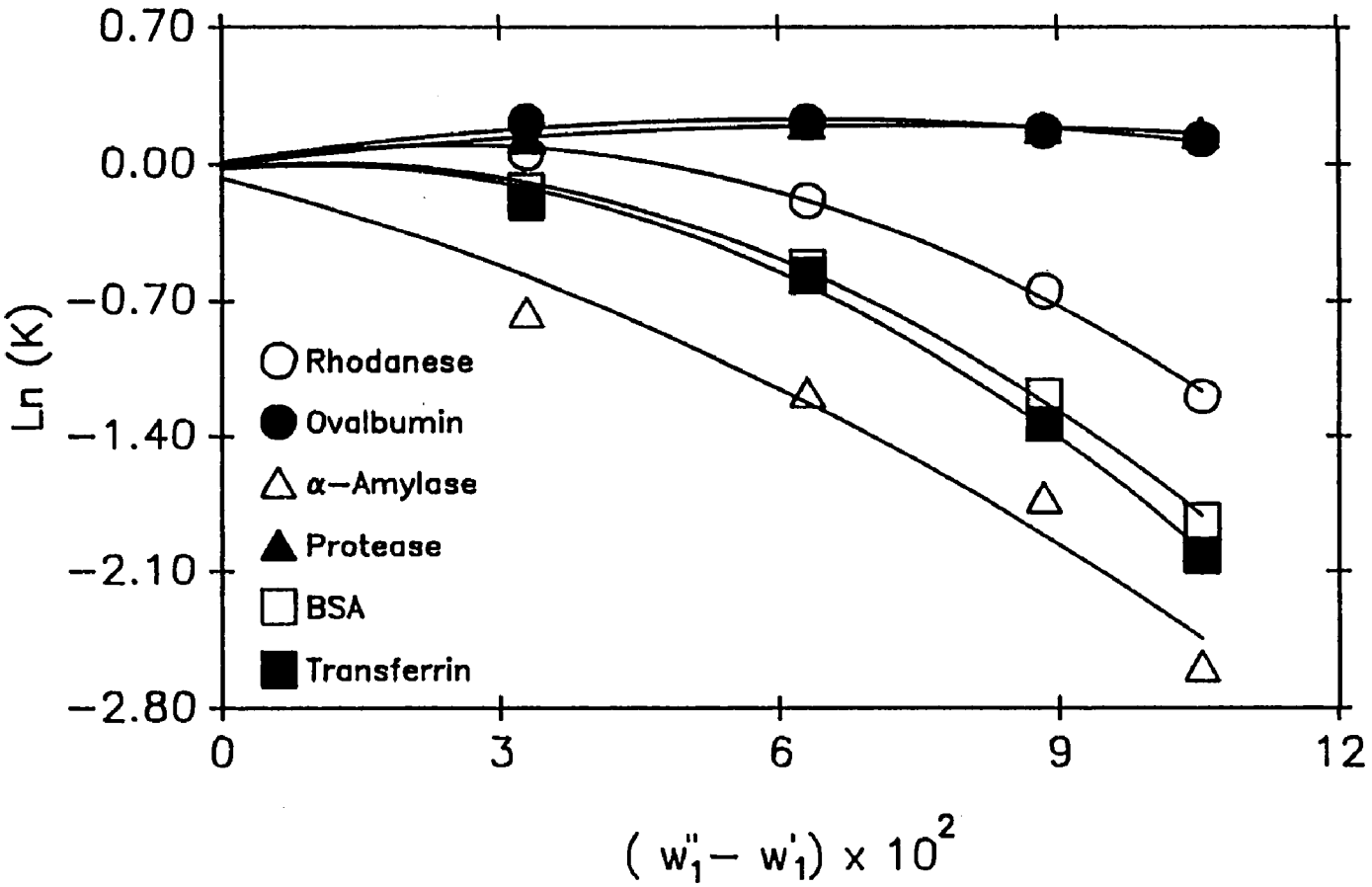

Figure 5.2 Correlation of High Molecular Weight Protein Partitioning According to Equation (4.1) in the PEG 8000/Dextran T-500/Water System at 4°C.

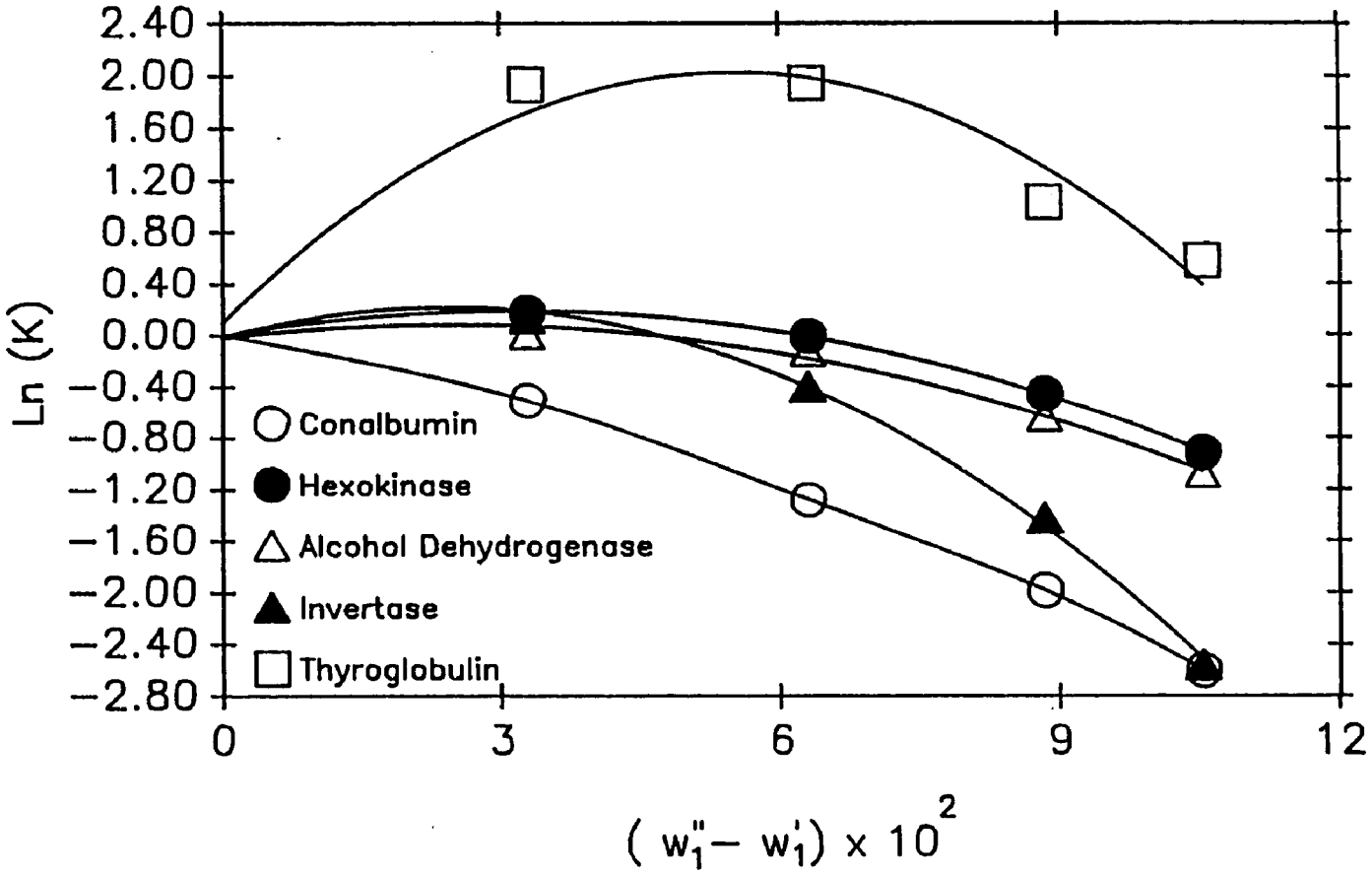

Figure 5.3 Correlation of High Molecular Weight Protein Partitioning According to Equation (4.1) in the PEG 8000/Dextran T-500/Water System at 4°C.

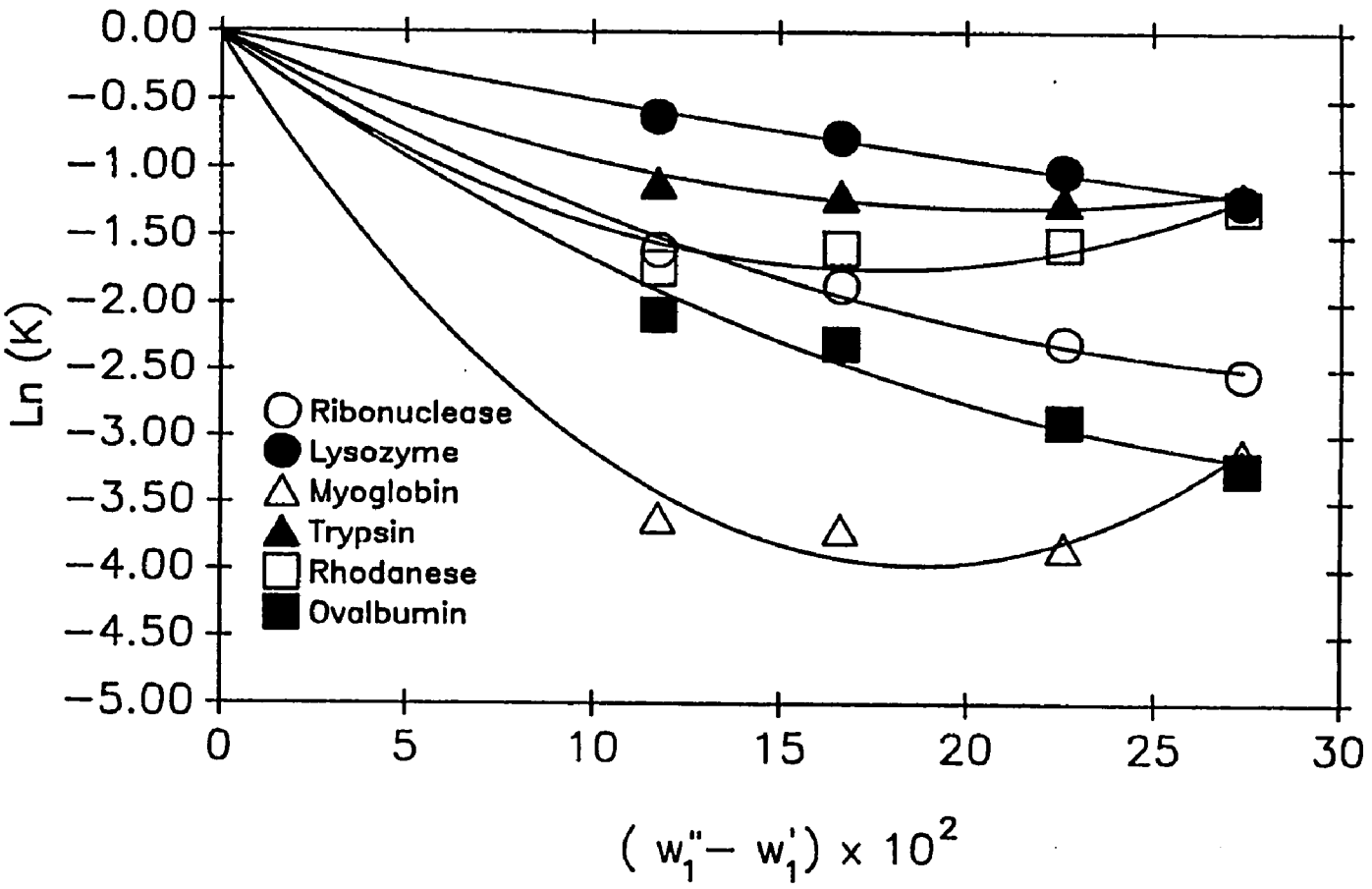

Figure 5.4 Correlation of Protein Partitioning According to Equation (4.1) in the PEG 3400/Potassium Phosphate/Water System at 20°C, pH 7.0.

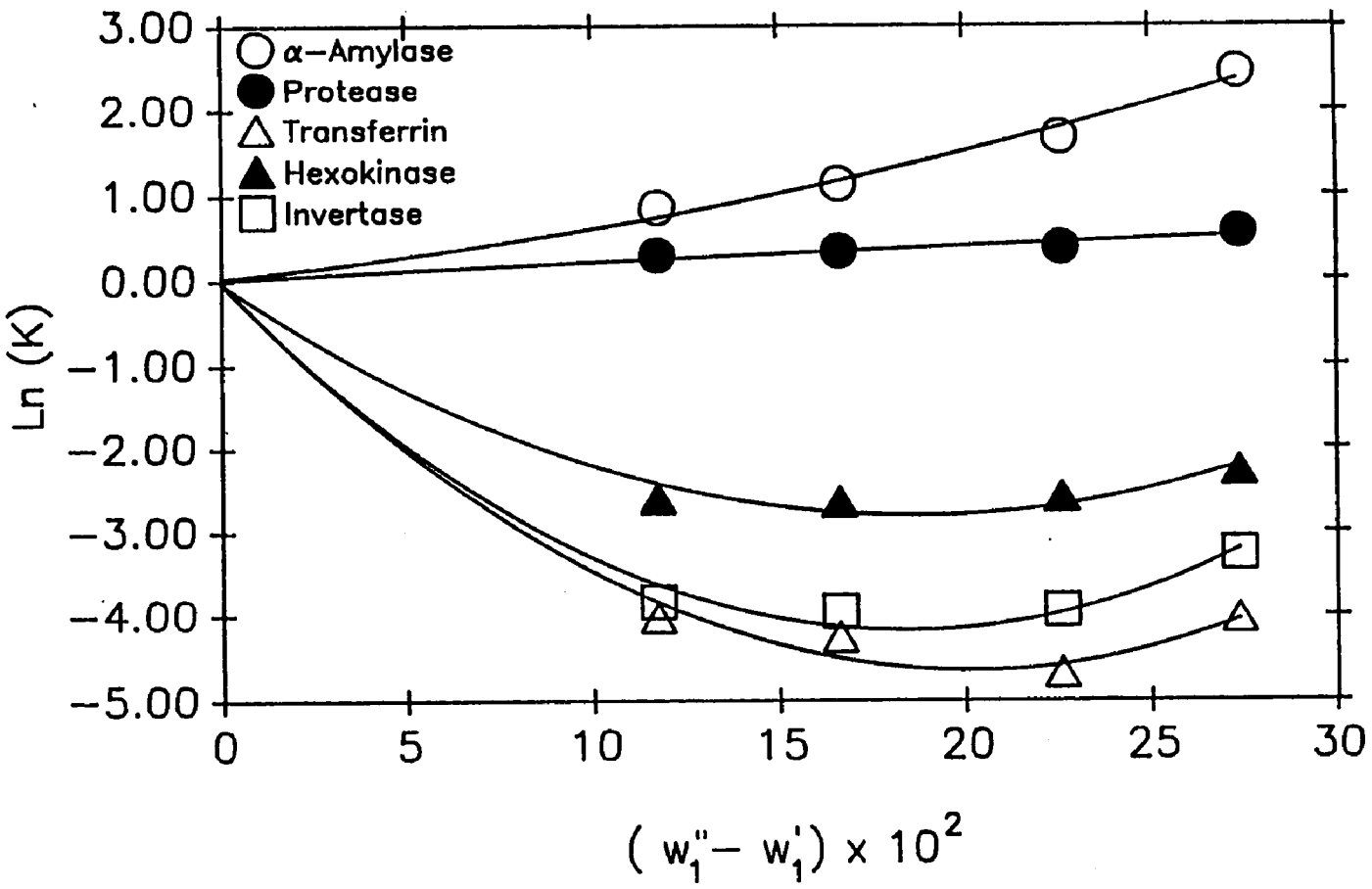

Figure 5.5 Correlation of Protein Partitioning According to Equation (4.1) in the PEG 3400/Potassium Phosphate/Water System at 20°C, pH 7.0.

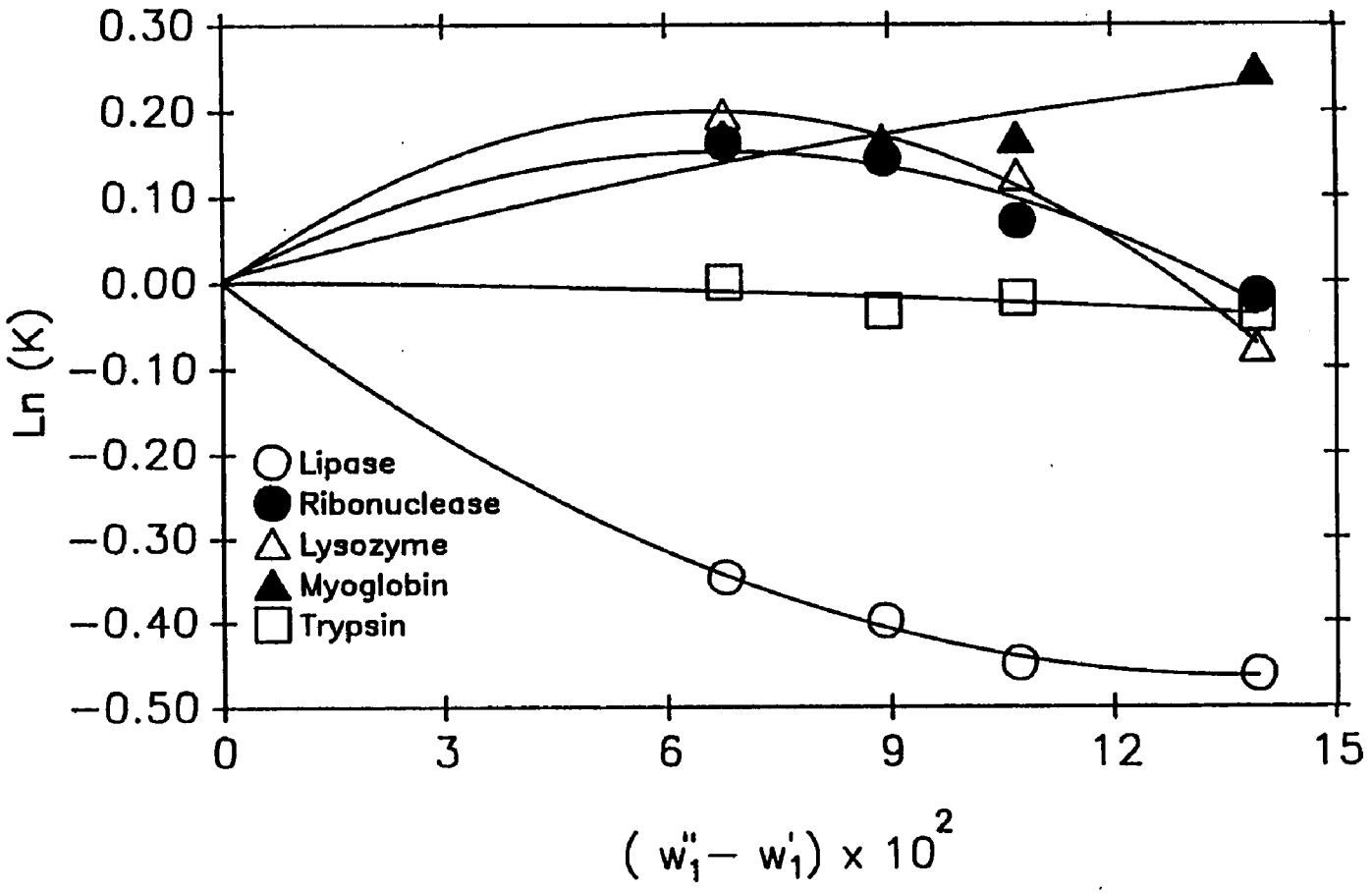

Figure 5.6 Correlation of Protein Partitioning According to Equation (4.1) in the Ficoll 400/Dextran T-500/Water System at 23°C.

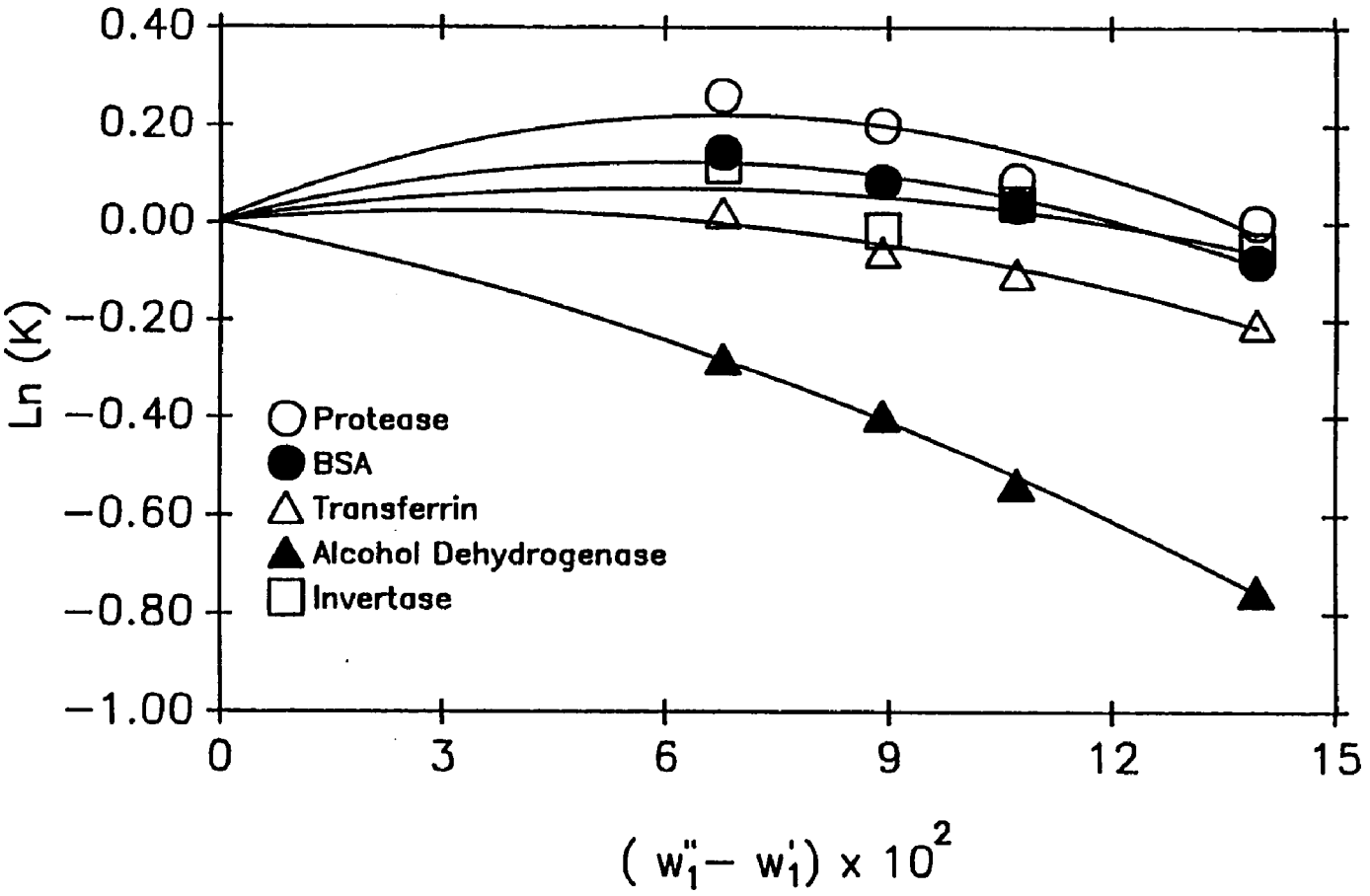

Figure 5.7 Correlation of Protein Partitioning According to Equation (4.1) in the Ficoll 400/Dextran T-500/Water System at 23°C.

partitioned in the PEG 8000/Dextran T-500/water system could be used in the other two systems for reasons of denaturation and precipitation at the interface. In particular, tie lines D and E of the PEG 3400/potassium phosphate/water system and tie lines C and D of the Ficoll 400/Dextran T-500/water system proved to be deleterious to many of the proteins, and therefore, the data are not reported.

Examination of Figure 5.1 reveals that the low molecular weight proteins, ribonuclease, lysozyme, and trypsin, exhibit relatively linear partitioning in the PEG 8000/Dextran T-500/water system and may be correlated according to equation (4.1). Cytochrome c and myoglobin are slightly nonlinear, while lipase exhibits a strong nonlinearity. Figures 5.2 and 5.3 reveal that the high molecular weight proteins exhibit nonlinear partitioning which was expected based on the data presented in Chapter IV). Interestingly, in Figures 5.1–5.3, a majority of the proteins favor the dextran phase (low partition coefficients) as the PEG concentration difference is increased, i.e., the polymer content of the phases increases. In other words the curves are concave downward. This may be due to a greater repulsion of the proteins for the hydrophobic PEG molecules at the high PEG concentration as compared to the dextran rich bottom phase. Futhermore, from these figures, by manipulating the $(w_1'' - w_1')$, these molecules can be adequately resolved based on the separation factor.

Figures 5.4 and 5.5 indicate that protein partitioning in the PEG/potassium phosphate/water system tends to be nonlinear regardless of protein molecular weight. The only protein that still shows linearity is lysozyme. At high PEG concentration differences, the proteins tend to favor the upper, PEG phase instead of the lower, potassium phosphate phase, which

is opposite the trend in the PEG/dextran/water system. In other words, the curves are concave up. This could be due to a salting out effect in which protein solubility is greater in the PEG phase rather than the highly concentrated potassium phosphate phase.

In Figures 5.6 and 5.7 it may be observed that proteins, regardless of molecular weight, exhibit nonlinear partitioning in the ficoll/dextran/water system as was exhibited in the PEG/potassium phosphate/water system. However, the partitioning curves may be concave upward or downward depending upon the protein. For proteins with ln(K) greater than zero, the curves are concave down, tending to favor the lower, ficoll phase at high dextran concentration difference, while for ln(K) less than zero, the curves are concave up. Interestingly, trypsin has an ln(K) close to zero over the range of dextran concentration difference and exhibits a linear, horizontal partition curve through the origin.

Since the majority of the proteins partitioned in the above systems proved to be nonlinear when correlated according to equation (4.1), this equation is too simple to describe the partition phenomena. Hence, the data were correlated according to the second order relation of equation (5.1) (Diamond and Hsu, 1990a,b). In Figures 5.8–5.10, protein partitioning in the PEG/dextran/water system presented in Figures 5.1–5.3 has been correlated according to the relationship of equation (5.1). Similarly, Figures 5.11 and 5.12 correspond to Figures 5.4 and 5.5 for the PEG/phosphate/water system, while Figures 5.13 and 5.14 correspond to Figures 5.6 and 5.7 for the ficoll/dextran/water system. The lines drawn through the data points in Figures 5.8–5.14 represent a first order regression, and the A^* and b^* parameters, along with protein molecular weight are recorded in Table 5.1. It

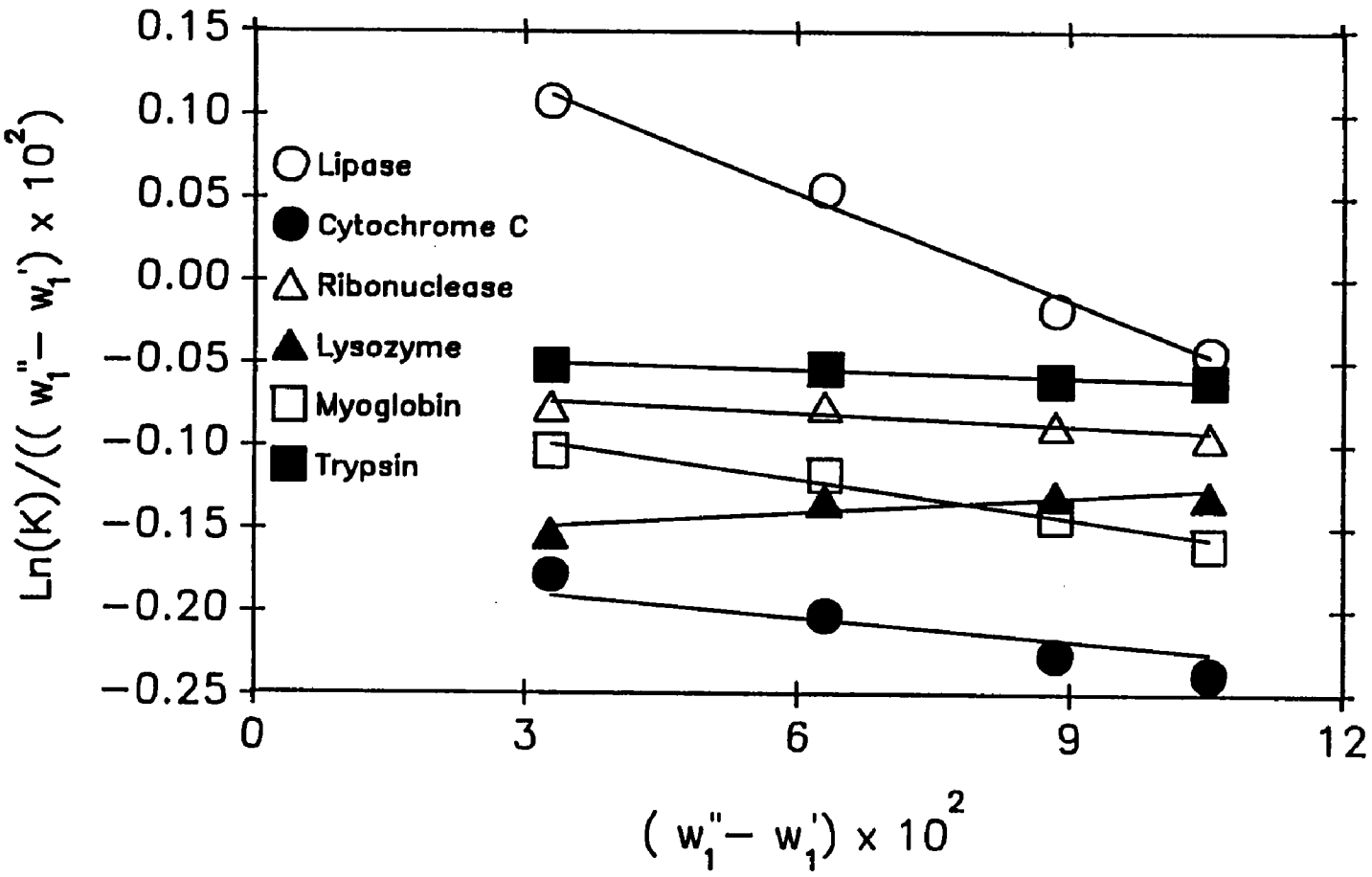

Figure 5.8 Correlation of Low Molecular Weight Protein Partitioning According to Equation (5.1) in the PEG 8000/Dextran T-500/Water System at 4°C.

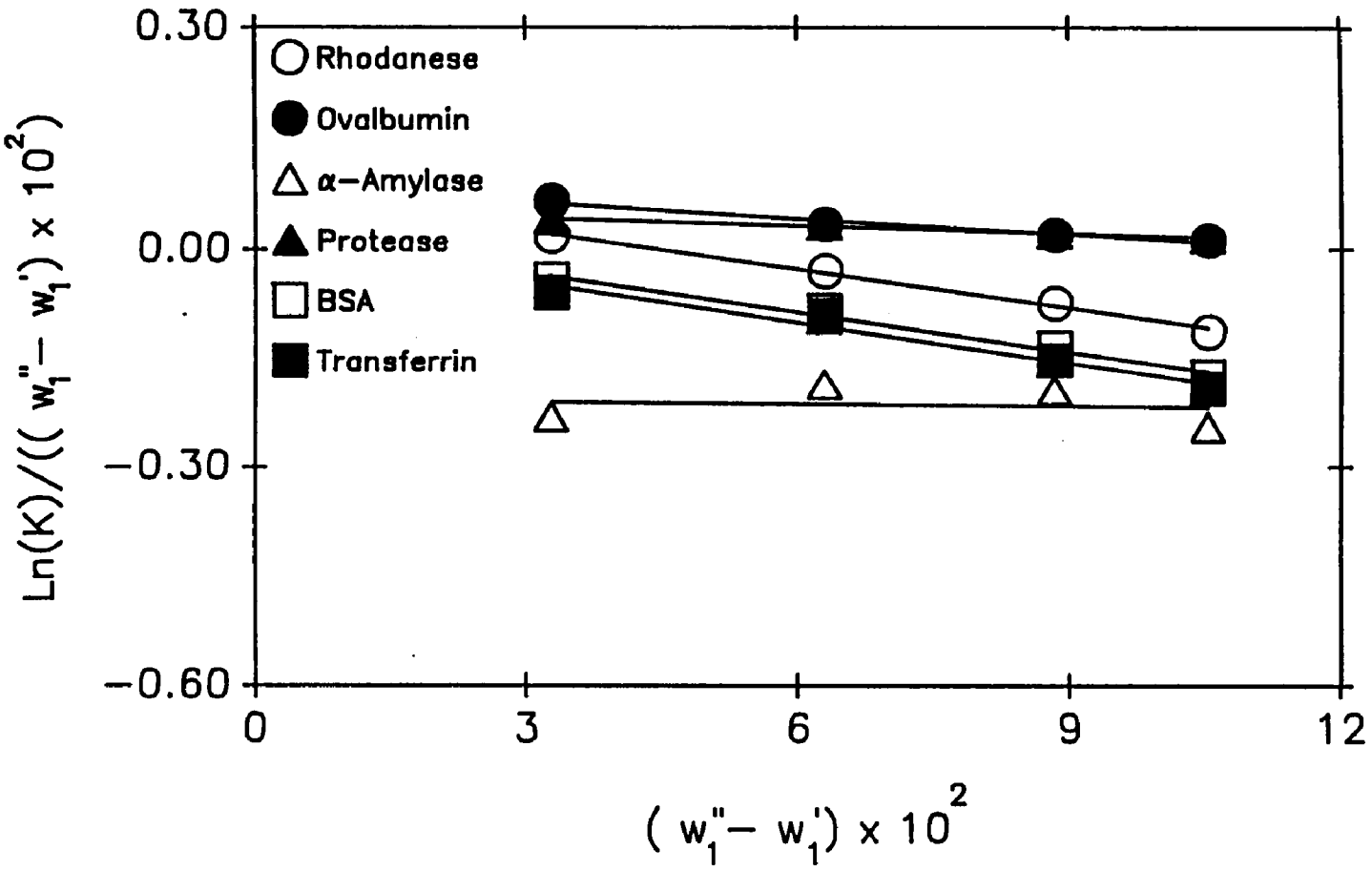

Figure 5.9 Correlation of High Molecular Weight Protein Partitioning According to Equation (5.1) in the PEG 8000/Dextran T-500/Water System at 4°C.

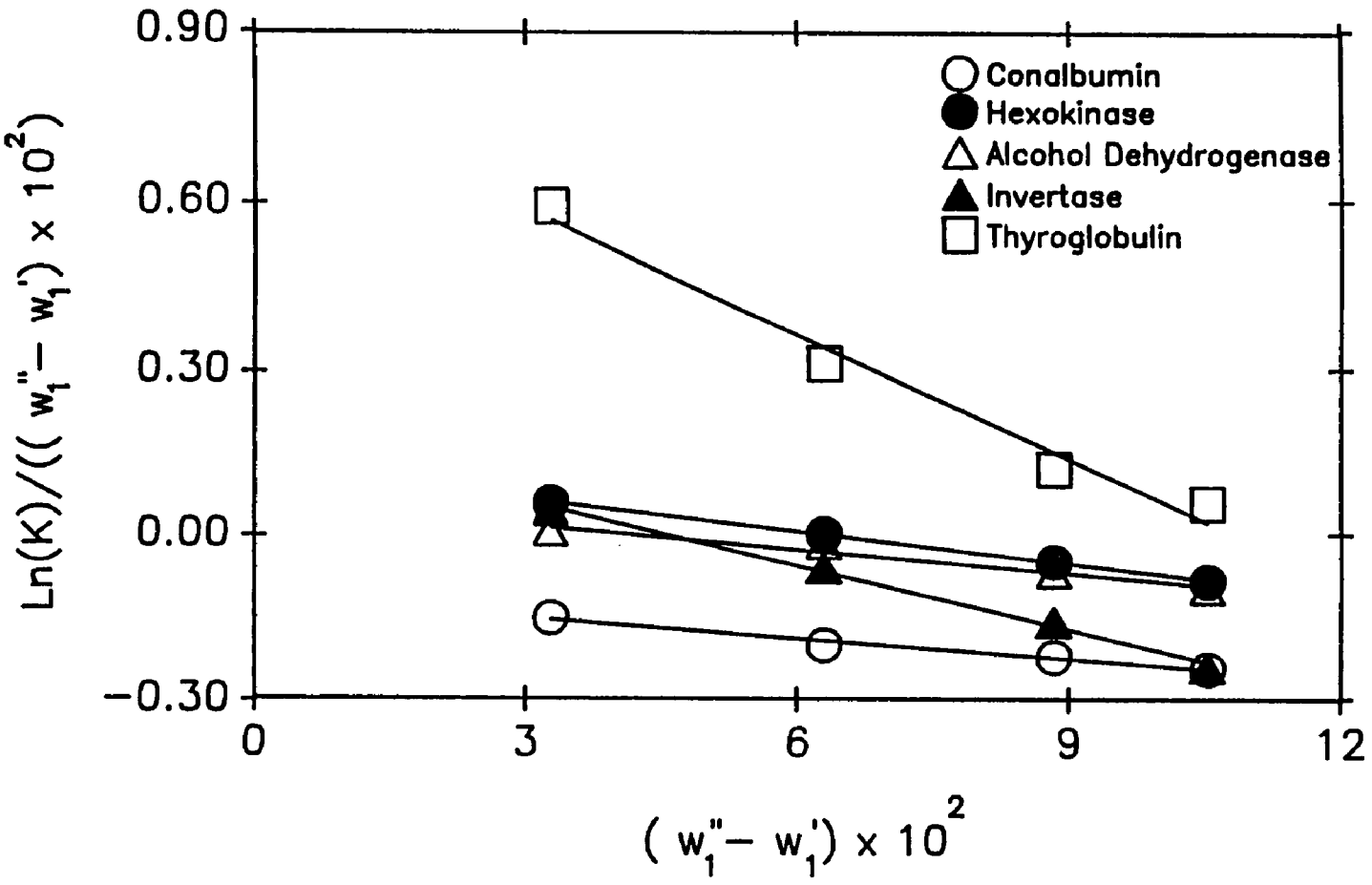

Figure 5.10 Correlation of High Molecular Weight Protein Partitioning According to Equation (5.1) in the PEG 8000/Dextran T-500/Water System at 4°C.

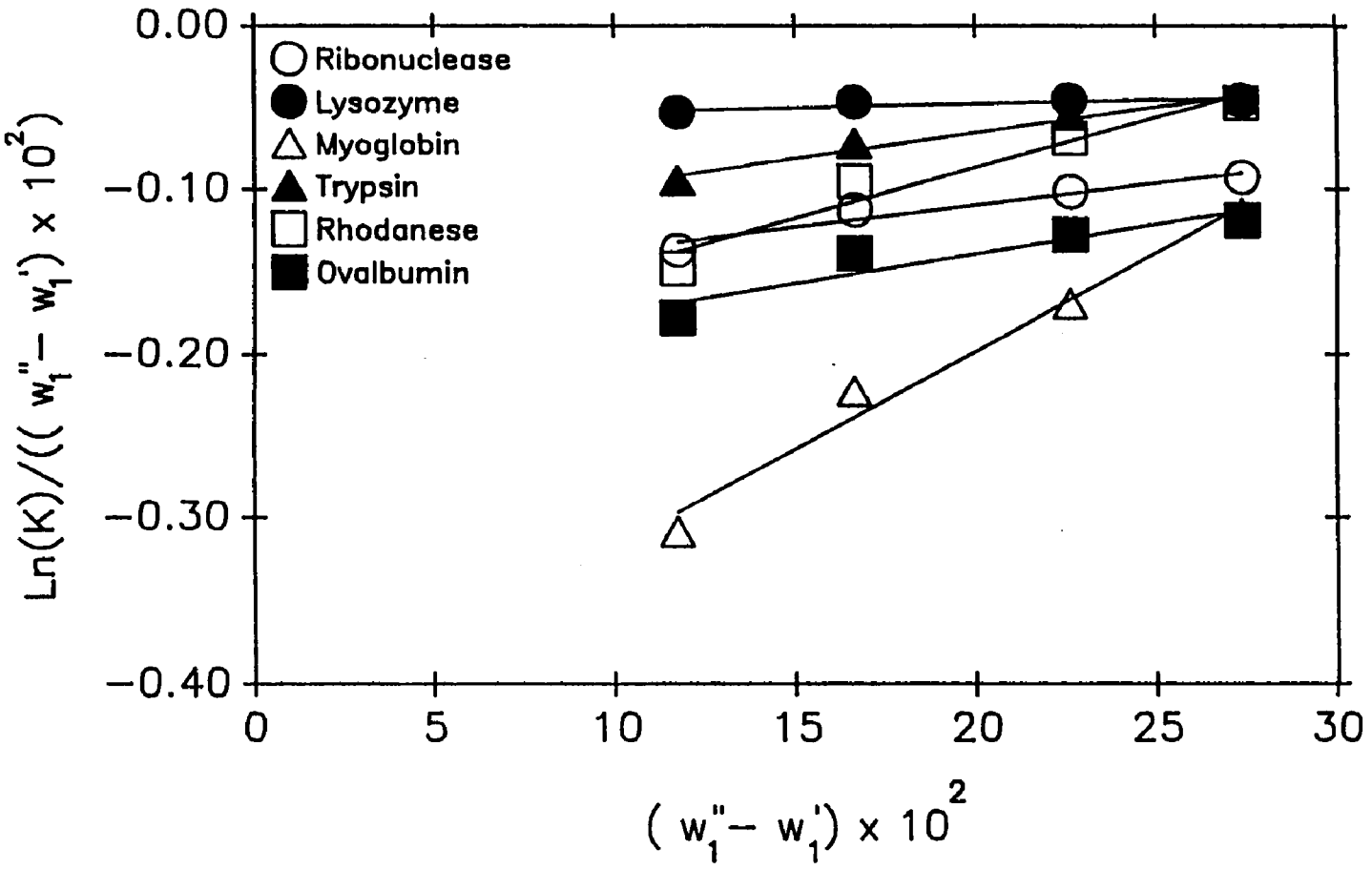

Figure 5.11 Correlation of Protein Partitioning According to Equation (5.1) in the PEG 3400/Potassium Phosphate/Water System at 20°C, pH 7.0.

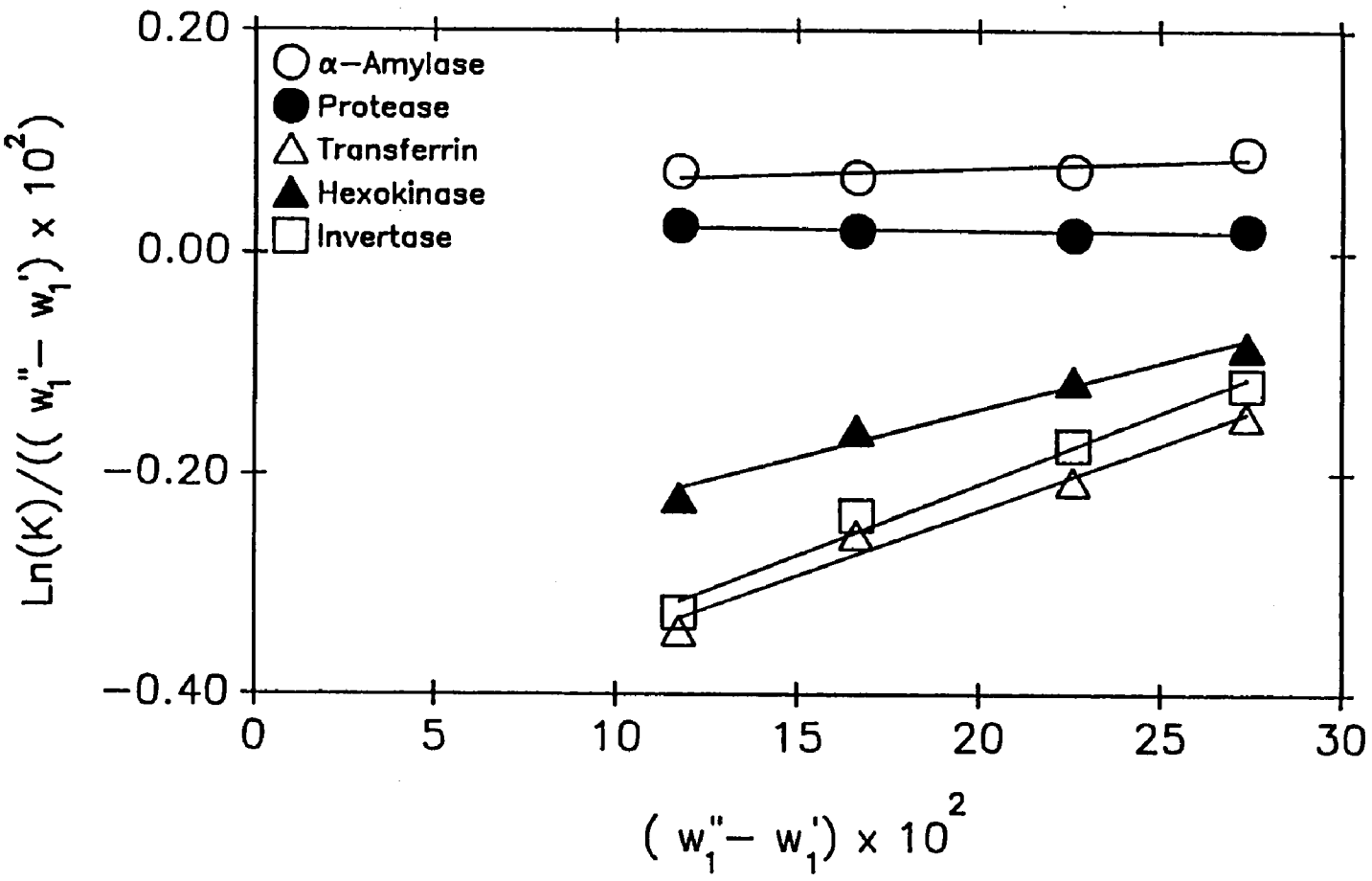

Figure 5.12 Correlation of Protein Partitioning According to Equation (5.1) in the PEG 3400/Potassium Phosphate/Water System at 20°C, pH 7.0.

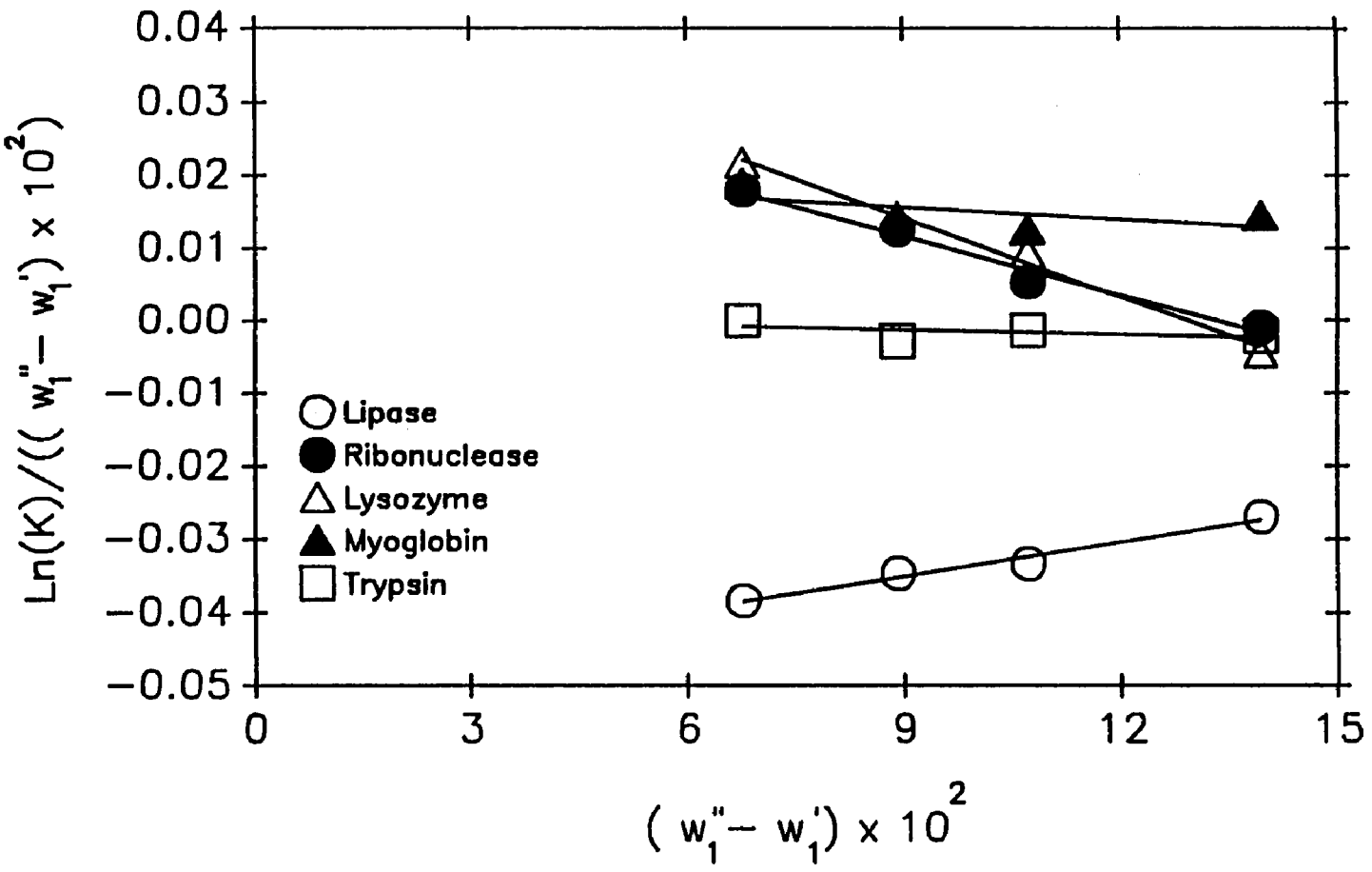

Figure 5.13 Correlation of Protein Partitioning According to Equation (5.1) in the Ficoll 400/Dextran T-500/Water System at 23°C.

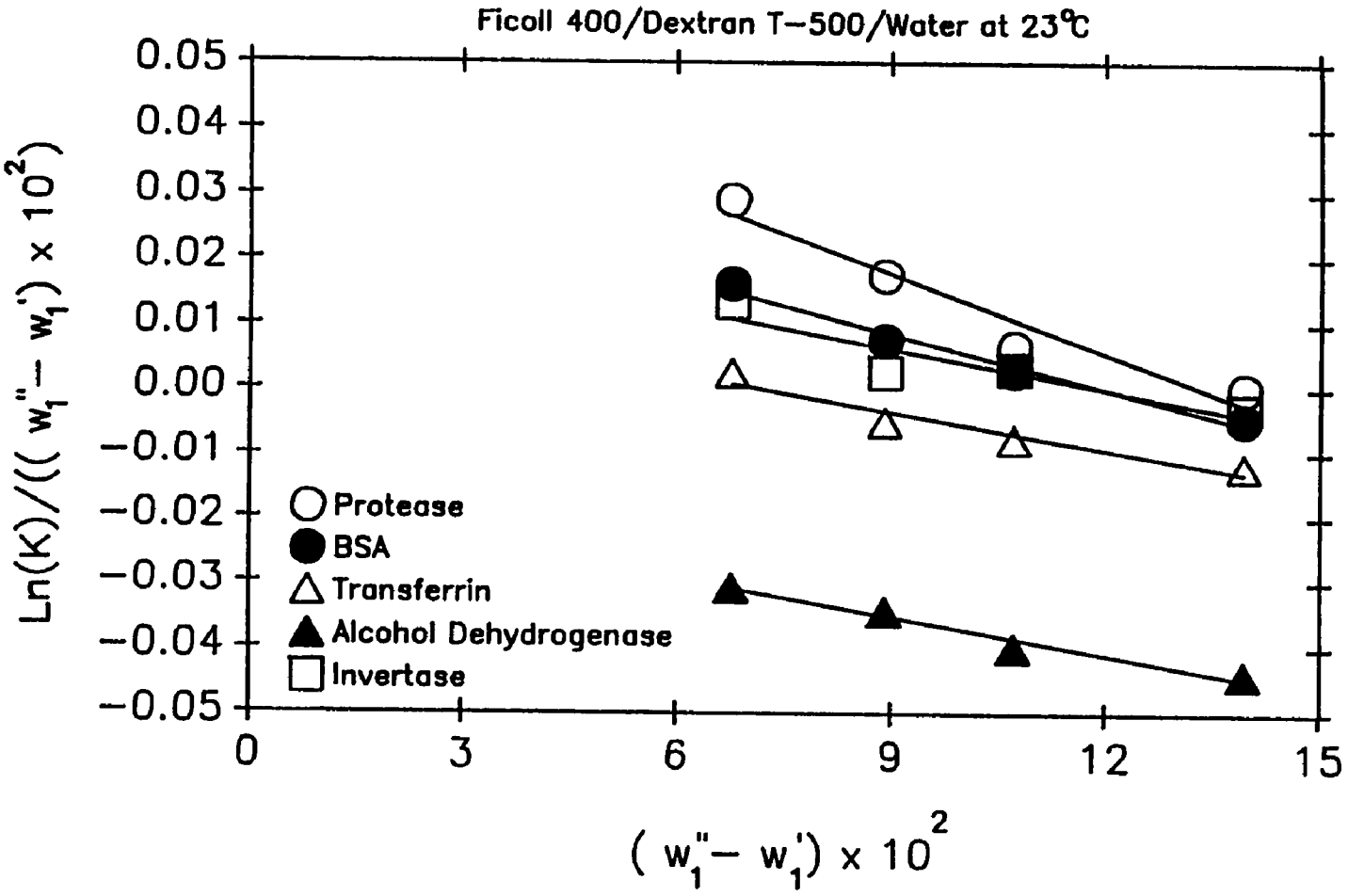

Figure 5.14 Correlation of Protein Partitioning According to Equation (5.1) in the Ficoll 400/Dextran T-500/Water System at 23°C.

Table 5.1 The Parameters A^* and b^* of Equation (5.1) for Protein Partitioning in the PEG 8000/Dextran T-500/Water System at 4°C, the PEG 3400/Potassium Phosphate/Water System at 20°C, and the Ficoll 400/Dextran T-500/Water System at 23°C.

		PEG/Dextran		PEG/Phosphate		Ficoll/Dextran	
Protein	Molecular Weight	A^*	b^*	A^*	b^*	A^*	b^*
Lipase	6,669	18.1	−217.0	---	---	−5.1	−13.7
Cytochrome C	12,400	−17.7	−47.9	---	---	---	---
Ribonuclease	12,600	−6.7	−25.3	−16.4	26.9	3.9	−24.0
Lysozyme	13,900	−16.1	31.3	−5.6	4.3	5.1	−32.1
Myoglobin	16,900	−7.6	−78.0	---	---	−2.1	−5.1
Trypsin	23,200	−4.8	−14.8	−12.9	31.8	0.0	−1.9
Rhodanese	37,570	−8.0	−178.0	−21.1	61.9	---	---
Ovalbumin	44,000	−8.7	−74.5	−21.0	35.3	---	---
α-Amylase	45,000	−20.8	−10.0	5.5	10.7	---	---
Protease	48,410	−5.5	−37.3	2.6	−3.1	6.0	−36.1
BSA	67,500	−2.4	−183.0	---	---	3.8	−25.3
Transferrin	77,000	1.1	−186.0	−47.3	120.0	1.6	−17.2
Conalbumin	86,810	−12.0	−122.0	---	---	---	---
Hexokinase	102,000	11.9	−194.0	−31.5	86.9	---	---
Alcohol Dehydrogenase	145,000	5.8	−147.0	---	---	−1.6	−16.7
Invertase	270,000	17.3	−387.0	−46.9	130.0	2.8	−18.6
Thyroglobulin	669,000	81.2	−753.0	---	---	---	---

should be noted that not all of the proteins partitioned in the PEG 8000/Dextran T-500/water system could be used in the other two systems for reasons of denaturation and precipitation at the interface. In particular, tie lines D and E of the PEG 3400/potassium phosphate/water system and tie lines C and D of the Ficoll 400/Dextran T-500/water system (the letters for the tie lines come form Albertsson (1986)) proved to be deleterious to many of the proteins, and therefore, the data are not reported.

In Chapter IV it was shown that a linear semilogarithmic relationship could be used to correlate the partitioning of some dipeptides and low molecular weight proteins in PEG/dextran/water systems, but high molecular weight proteins could not be correlated by this relation (Diamond and Hsu, 1989a). Therefore, it is expected that a line with a relatively small slope (small value of b) would be obtained when the data are regressed according to equation (5.1). Examination of Figure 5.8 and Table 5.1 indicates that, although not perfectly horizontal, the b values for the low molecular weight proteins are of relatively small magnitude. However, of the low molecular weight proteins, cytochrome c, myoglobin, and lipase, which exhibited the greatest deviation from linearity, have b values which differ the most from zero.

In Figures 5.9 and 5.10 it is seen that the relationship of equation (5.1) is also applicable to high molecular weight proteins in the PEG/dextran/water system. Examination of Table 5.1 reveals that although a simple relationship can not be established between the A^* values and protein molecular weight, A^* does tend to become less negative as molecular weight is increased. The major exceptions are lipase, which has a relatively high value of A^* in comparison with the remainder of the low molecular weight proteins, and α-amylase and conalbumin which have comparatively low values of A^*. It should be pointed

out that A^* does not correlate well with molecular weight because it is a function of protein-polymer, protein-water, and polymer-water interaction as well as protein molecular weight. Similarly, the b^* values, which are also a function of protein molecular weight, tend to become more negative as the molecular weight of the protein is increased.

Figures 5.11 and 5.12 indicate that the relationship of equation (5.1) is also applicable to the PEG/potassium phosphate/water system. The A^* values given in Table 5.1 tend to become more negative as protein molecular weight is increased, while the b^* values become more positive. This is opposite the trend of the PEG/dextran/water system, but is expected based on the concavity of the partitioning curves presented earlier.

Partitioning in the ficoll/dextran/water system may be correlated according to equation (5.1) as is indicated in Figures 5.13 and 5.14. From Table 5.1, it is appears as if there is no definite trend between A^* or b^* and protein molecular weight. A majority of the proteins seem to have positive A^* and negative b^* values, which is similar to the PEG/dextran/water system. However, the magnitude of the values does not cover the same range as the PEG/dextran/water system.

5.3.2 Correlation of Literature Data

In order to provide further proof of the applicability of our correlation, we attempted to apply it to data obtained from the literature. In Figure 5.15 we have plotted the partition data of Johansson and Andersson (1984) for the proteins glucose-6-phosphate dehydrogenase and alcohol dehydrogenase. The system conditions are 25 mM sodium phosphate buffer, pH 7.0 and 0°C. It is

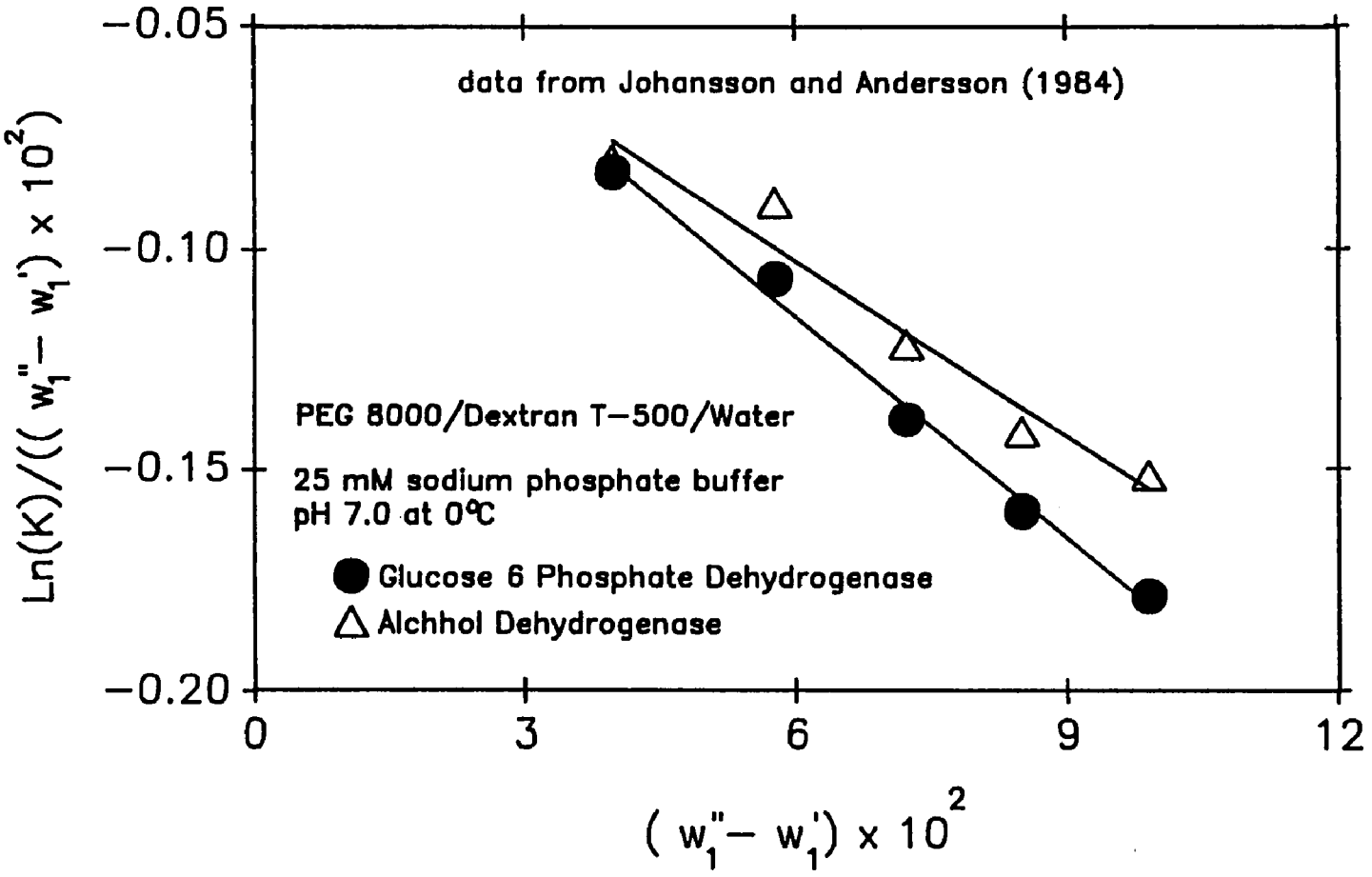

Figure 5.15 Correlation of Protein Partitioning Data from Johansson and Andersson (1984) According to Equation (5.1).

apparent that these two proteins follow the linear trend when correlated according to equation (5.1). It is also interesting to note that the two-phase system used in their study contained more than double the salt concentration of our systems. This indicates that our correlation can be applied to systems containing appreciable quantities of salt. In a similar fashion, we have plotted, according to equation (5.1), the protein partition data from King *et al.* (1988) in Figure 5.16. The data from King *et al.*, like that of Johansson and Andersson, show a linear trend. It should also be noted that King's data contained salt concentrations five times as great as our work, indicating, once again, the applicability of our relationship in salt-containing two-phase systems.

5.3.3 Molecular Weight Effect

In Chapter IV it was demonstrated that when the low molecular weight proteins lysozyme and trypsin were partitioned in the PEG 8000/Dextran T-40, PEG 8000/Dextran T-70, PEG 8000/Dextran T-500, and PEG 3400/Dextran T-500 aqueous systems at 4°C, a semilogarithmic linear trend was observed, according to equation (4.1), depending on the molecular weight of the phase forming polymers (Diamond and Hsu, 1989a). It should be pointed out that Dextran T-40, Dextran T-70, and Dextran T-500 have weight average molecular weights of 40,000, 70,000, and 500,000, respectively, while PEG 3400 and PEG 8000 have molecular weights of 3,400 and 8,000, respectively. The A values for each of the proteins increased as dextran molecular weight increased or PEG molecular weight decreased. In addition, BSA was partitioned in the four systems indicated above, and a series of curves obtained when $\ln(K_3)$ was plotted versus the PEG concentration difference. In Figure 5.17 the same BSA data have been replotted according to the relationship of equation (5.1). Each

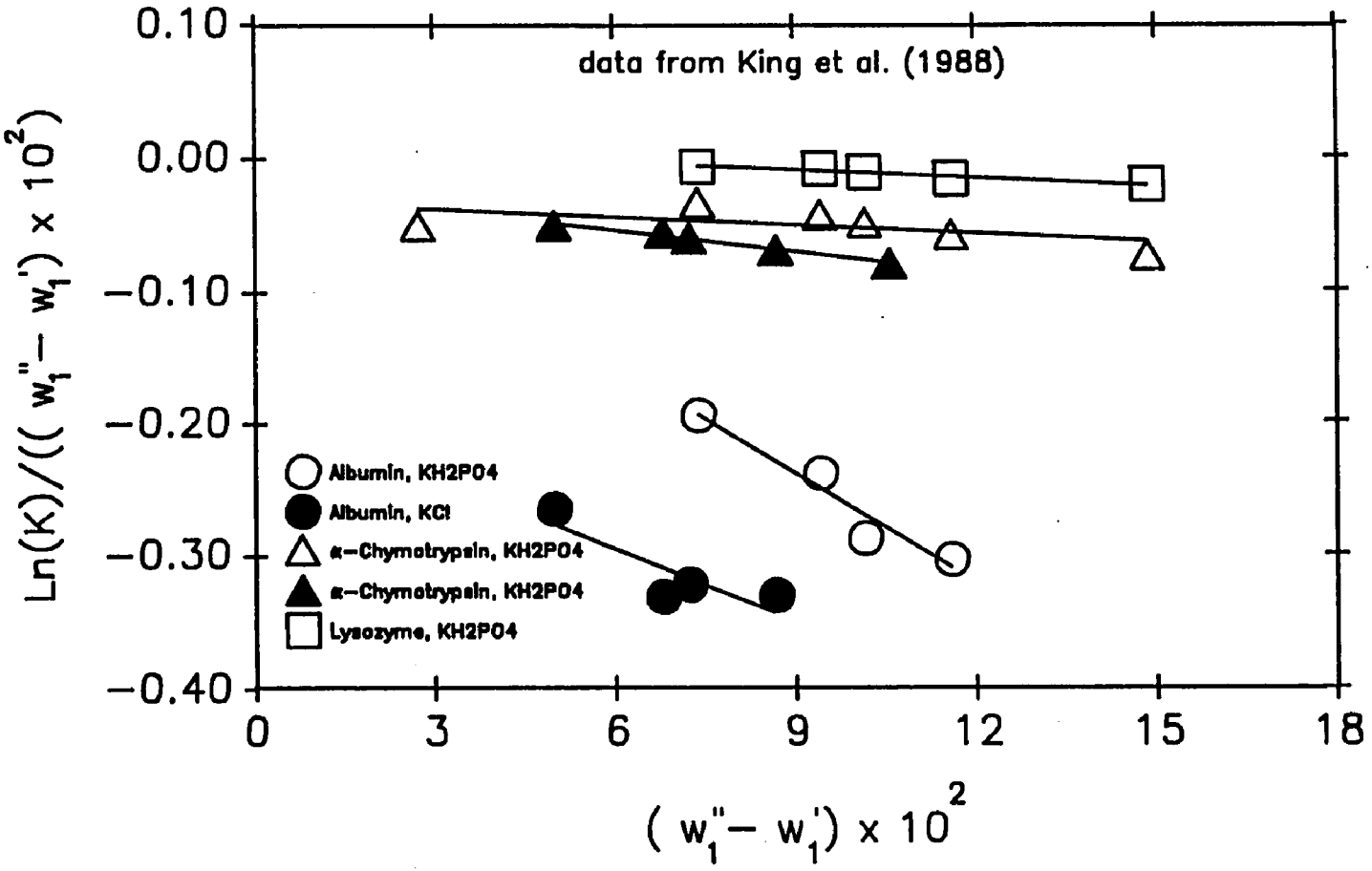

Figure 5.16 Correlation of Protein Partitioning Data from King *et al.* (1988) According to Equation (5.1). All Partition Data is at 25°C. Open Symbols Represent Partitioning in the PEG 3350/Dextran T-70/Water System. Closed Symbols Represent Partitioning in the PEG 8000/Dextran T-500/Water System.

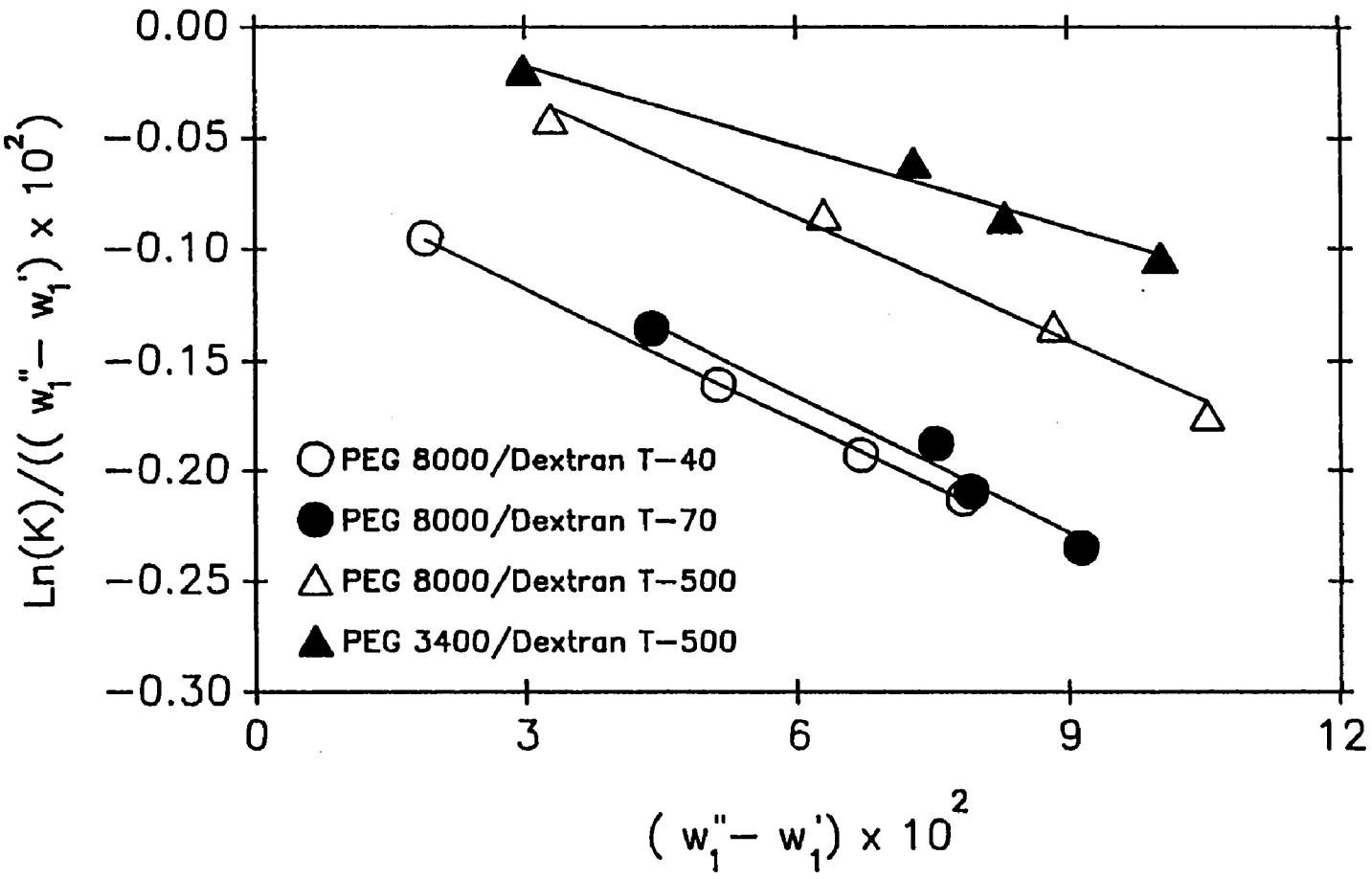

Figure 5.17 The Effect of PEG and Dextran Molecular Weight on the Partitioning of BSA in PEG/Dextran/Water Systems at 4°C.

phase system yields a different trend, with the values of A* being −5.8, −4.2, 2.4, and 1.9, and the b values being −199, −207, −183, and −121 for the above four systems, respectively. It can be seen that A* like A increased as dextran molecular weight was increased, while it also increased as PEG molecular weight was decreased from 8,000 to 3,400.

The effect of polymer molecular weight on A*, like A, is mainly due to the term $\left(\frac{\alpha_1}{m_1} + \frac{\alpha_2\phi}{m_2}\right)$. Since α_1, α_2, m_1, and m_2 are positive while ϕ is negative, then $\frac{\alpha_1}{m_1}$ is positive and $\frac{\alpha_2\phi}{m_2}$ is negative. Since the molar volume ratios of PEG and dextran, m_1 and m_2, are directly proportional to polymer molecular weight, then as dextran molecular weight is increased, $\frac{\alpha_2\phi}{m_2}$ becomes less negative, and A* increases. Similarly, as PEG molecular weight is increased, $\frac{\alpha_1}{m_1}$ becomes less positive, causing a decrease in A*. Both these trends were observed with the BSA partitioning. The effect of polymer molecular weight on b* is not as obvious as that of A*. The interaction parameters χ_{01} and χ_{02} should be functions of PEG and dextran molecular weight, but these functions are not yet known. However, from the data it can be seen that b* is relatively constant at dextran molecular weights of 40,000 and 70,000, and then increases as the dextran molecular weight is increased to 500,000. As PEG molecular weight is increased from 3400 to 8000, the value of b* becomes more negative.

5.3.4 Temperature Effect

The effect of temperature on A* and b* can be derived by considering the general form of the Flory-Huggins interaction parameters which comprise them (Flory, 1953):

$$\chi_{ij} = \frac{z\Delta w_{ij} m_i}{kT} \tag{5.4}$$

where Δw_{ij} is the change in energy for the formation of a contact between species i and j, z is the lattice coordinate number, and k, T and m_i have previously been defined. By introducing this definition into equations (5.2) and (5.3) and rearranging, the following relations can be obtained:

$$A^* = \gamma^* + \frac{\delta^*}{T} \tag{5.5}$$

and

$$b^* = \frac{\epsilon^*}{T} \tag{5.6}$$

where,

$$\gamma^* = m_3\left(\frac{\alpha_1}{m_1} + \frac{\alpha_2\phi}{m_2} - (\alpha_1 + \alpha_2\phi)\right) \tag{5.7}$$

and

$$\begin{aligned}\delta^* \quad = \quad & m_3\frac{z}{k}\Big((\alpha_1 + \alpha_2\phi)\Delta w_{03} - \alpha_1\Delta w_{13}m_1 - \alpha_2\phi\Delta w_{23}m_2 + \alpha_1\Delta w_{01} \\ & + \alpha_2\phi\Delta w_{02} + \frac{z_b F g}{m_3 z N_A}\Big)\end{aligned} \tag{5.8}$$

and

$$\epsilon^* = m_3\frac{z}{k}\left(\Delta w_{02}\alpha_2^2\phi^2 - \Delta w_{01}\alpha_1^2 + \frac{z_b F h}{m_3 z N_A}\right) \tag{5.9}$$

The parameters γ^*, δ^* and ϵ^*, as will be shown by experimental proof, are

essentially constant. This will be demonstrated by a plot of A^* versus reciprocal absolute temperature for a variety of proteins partitioned in PEG/dextran aqueous two-phase systems.

In order to verify the effect of temperature on partitioning, as indicated by the relationship of equations (5.5) and (5.6), the proteins cytochrome c, ribonuclease, lysozyme, myoglobin, trypsin, and BSA were partitioned in the tie line compositions of the PEG 8000/Dextran T-500 system at 0°C, 4°C, 10°C, and 22°C. In Figures 5.18–5.23, $\ln(K_3)/(w_1'' - w_1')$ at the four different temperatures is plotted versus $(w_1'' - w_1')$ for the above proteins, respectively. It is apparent from the data that for each temperature, the second order semilogarithmic relationship is obtained for a particular protein. In Figure 5.24, A^* is plotted versus (1/T) according to equation (5.5). The data indicate a linear trend suggesting that equation (5.5) is useful for summarizing the variation of A^* over the given temperature range. It is interesting to note that, for each of the proteins in Figure 5.24, the data point at 4°C consistently provides the greatest deviation from the linear trend. Although there is no definite explanation for this, it may be due to density changes occurring at the different temperatures. In Figure 5.25, b^* is plotted versus (1/T) according to equation (5.6). Although the data does not perfectly obey equation (5.6), i.e., at high temperatures b^* should approach zero, the linear trend is still apparent. This deviation may be due to the assumptions and simplifications inherent in the thermodynamic model.

5.4 Conclusions

Based on the relationship of equation (5.1), which was derived from a modified form of the Flory-Huggins theory, a simple means was devised for

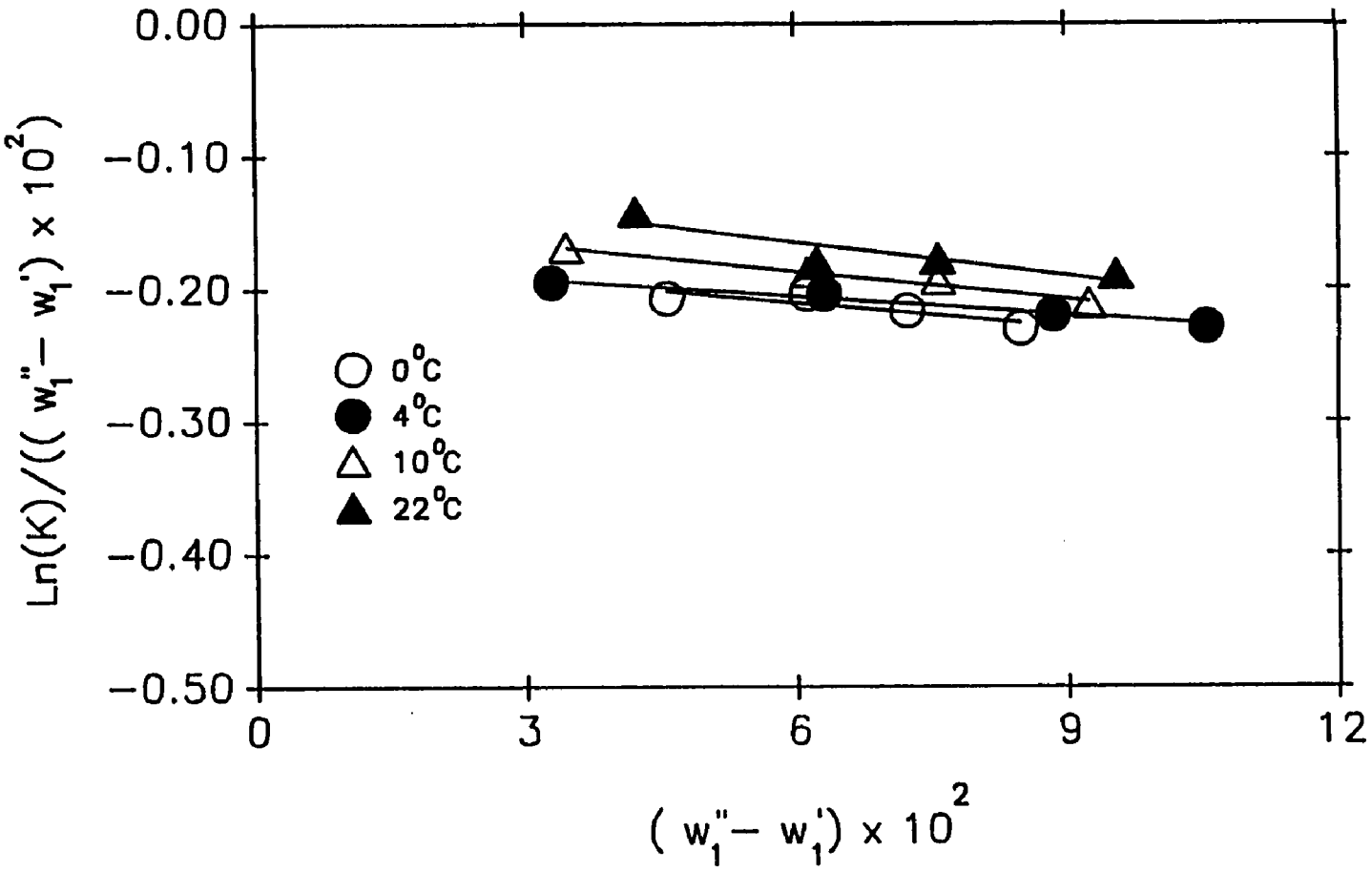

Figure 5.18 The Effect of Temperature on Cytochrome c Partitioning in the PEG 8000/Dextran T-500 System at 4°C.

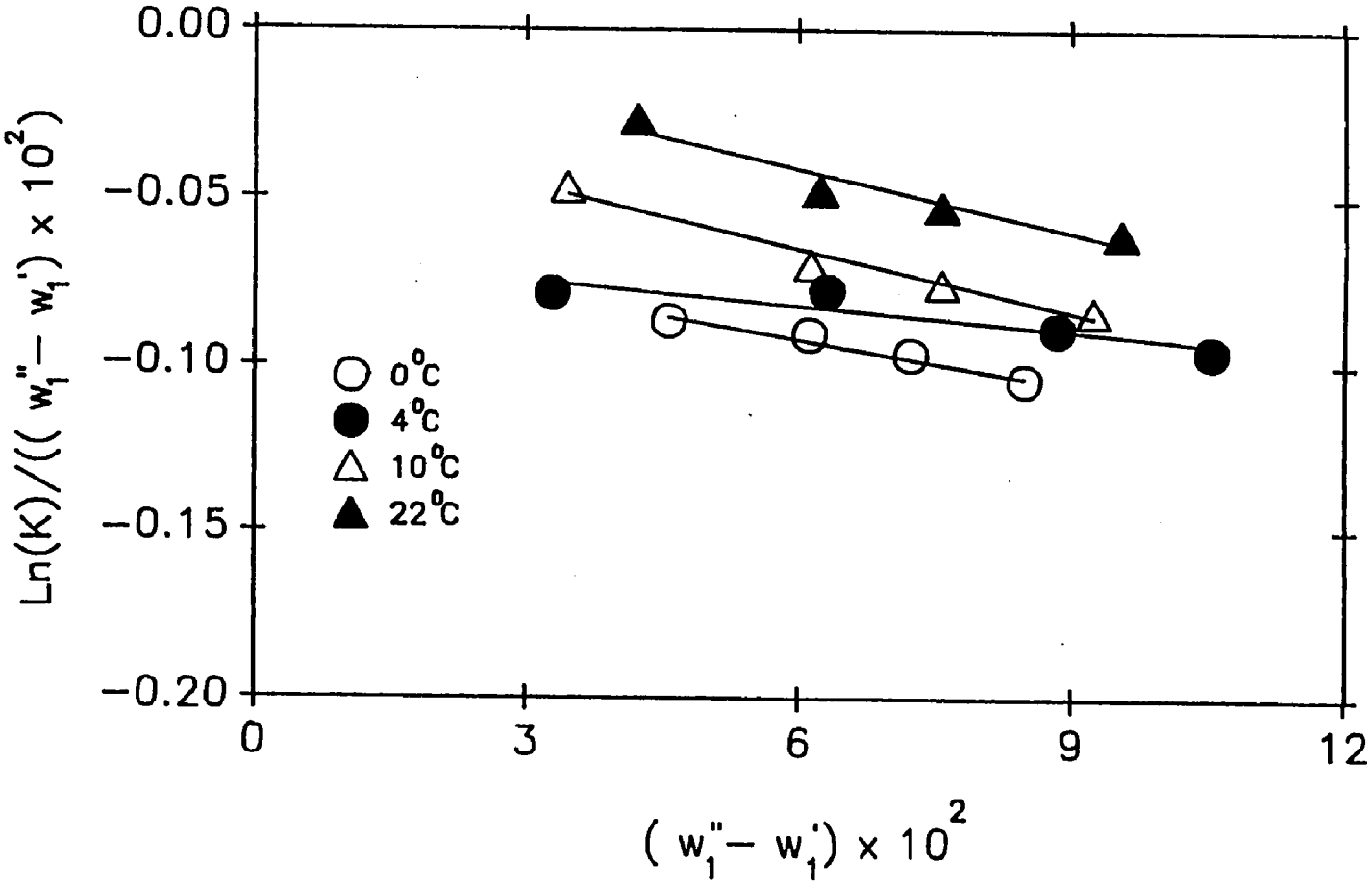

Figure 5.19 The Effect of Temperature on Ribonuclease Partitioning in the PEG 8000/Dextran T-500 System at 4°C.

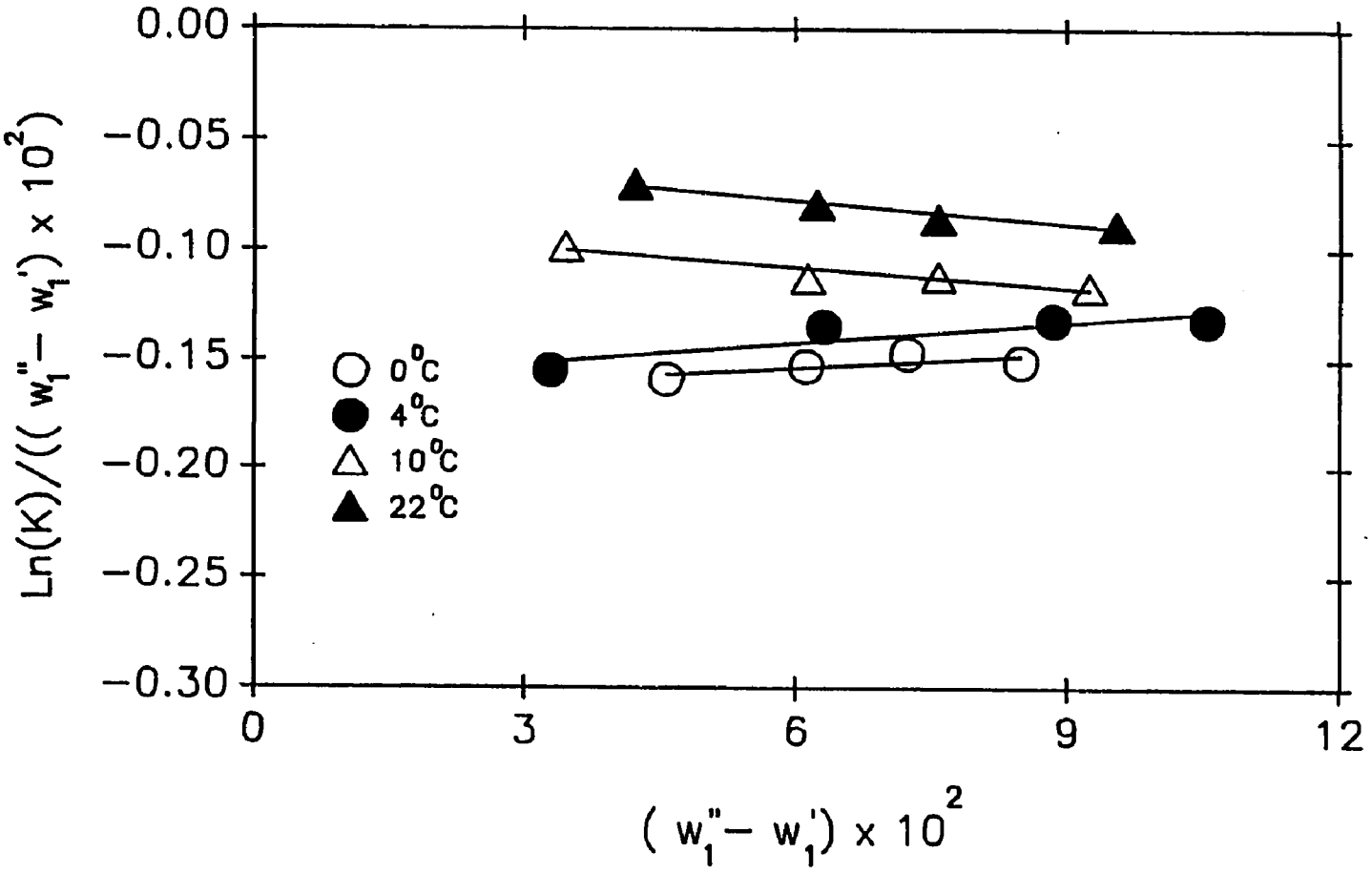

Figure 5.20 The Effect of Temperature on Lysozyme Partitioning in the PEG 8000/Dextran T-500 System at 4°C.

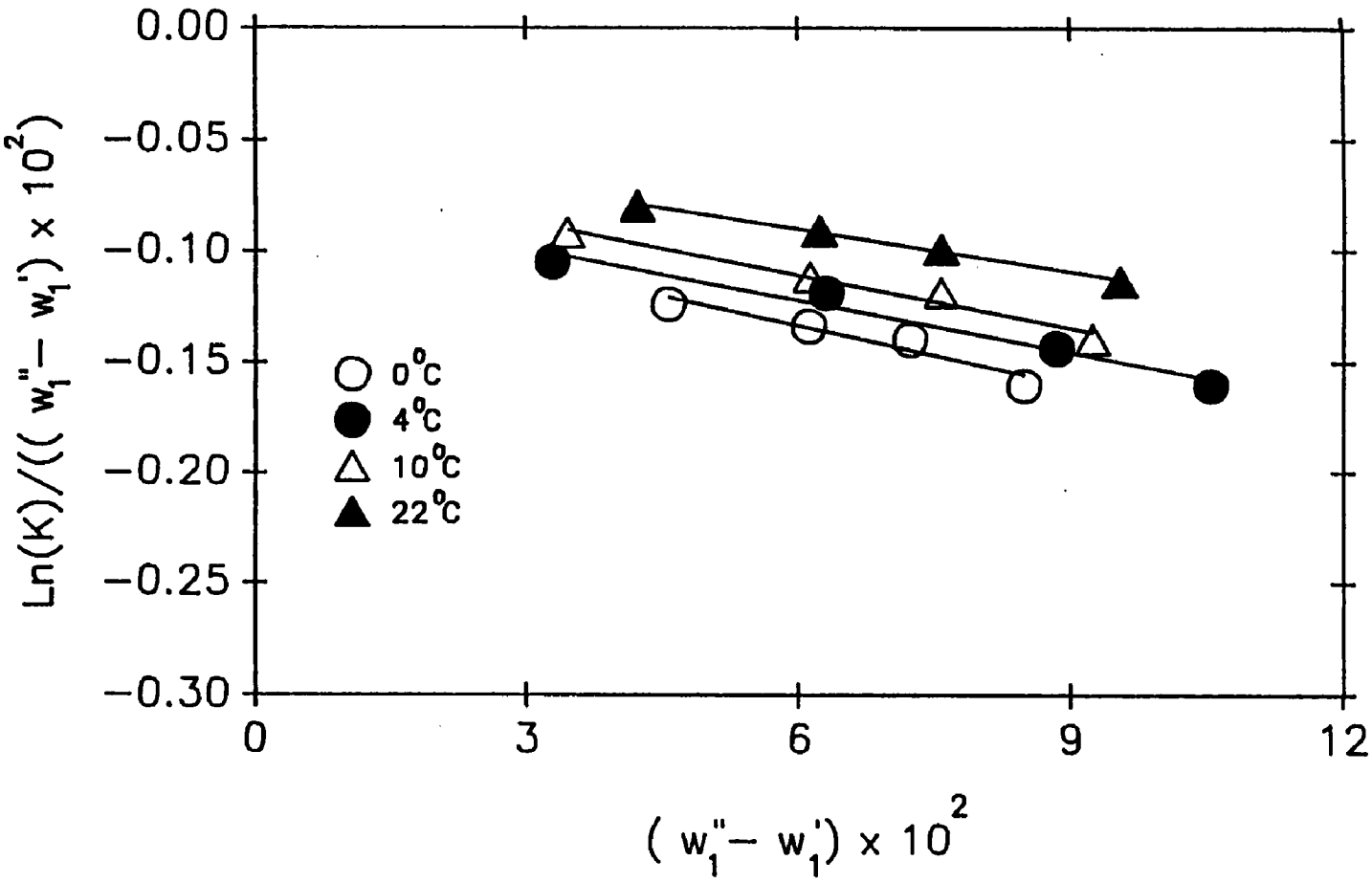

Figure 5.21 The Effect of Temperature on Myoglobin Partitioning in the PEG 8000/Dextran T-500 System at 4°C.

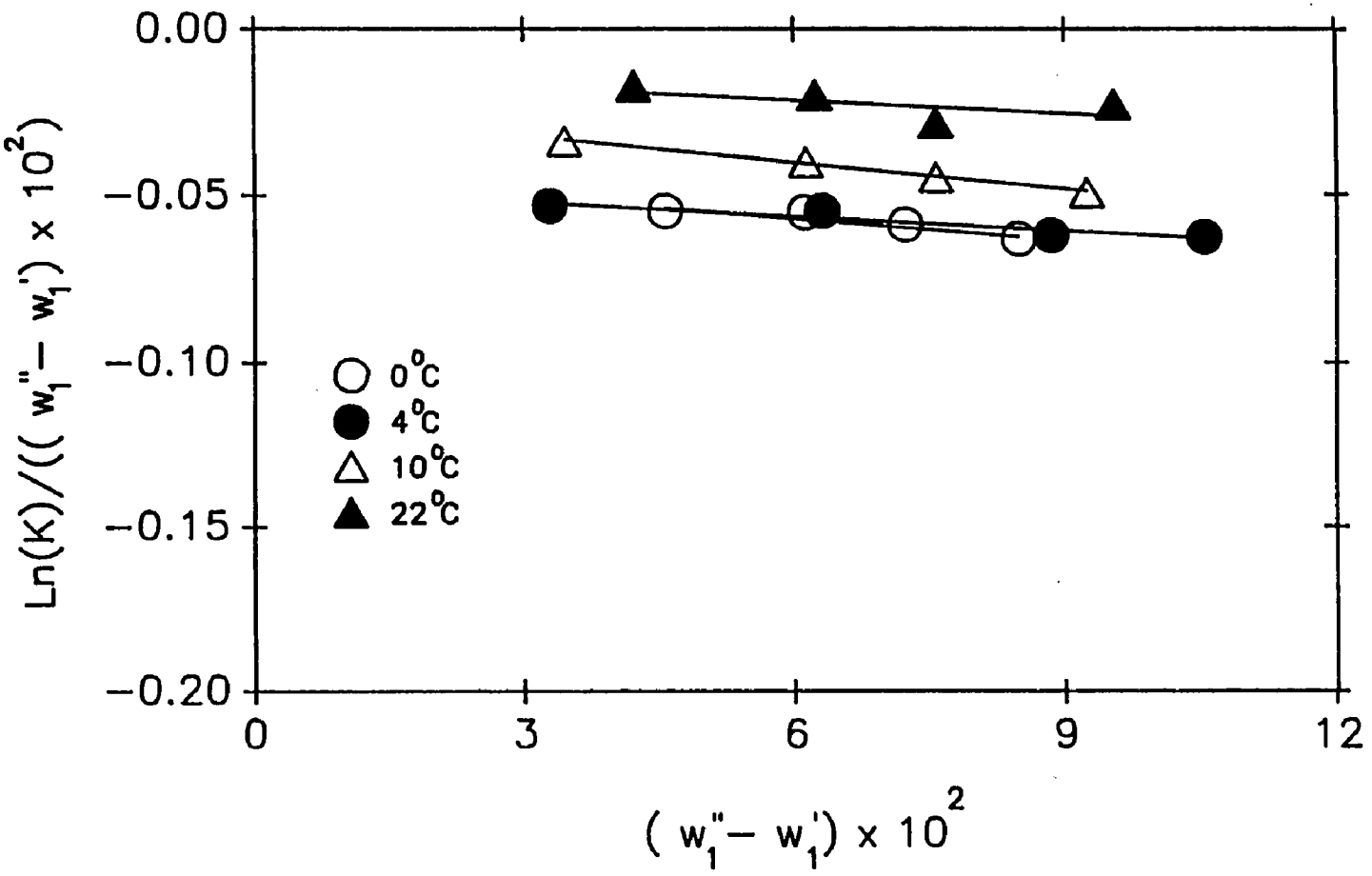

Figure 5.22 The Effect of Temperature on Trypsin Partitioning in the PEG 8000/Dextran T-500 System at 4°C.

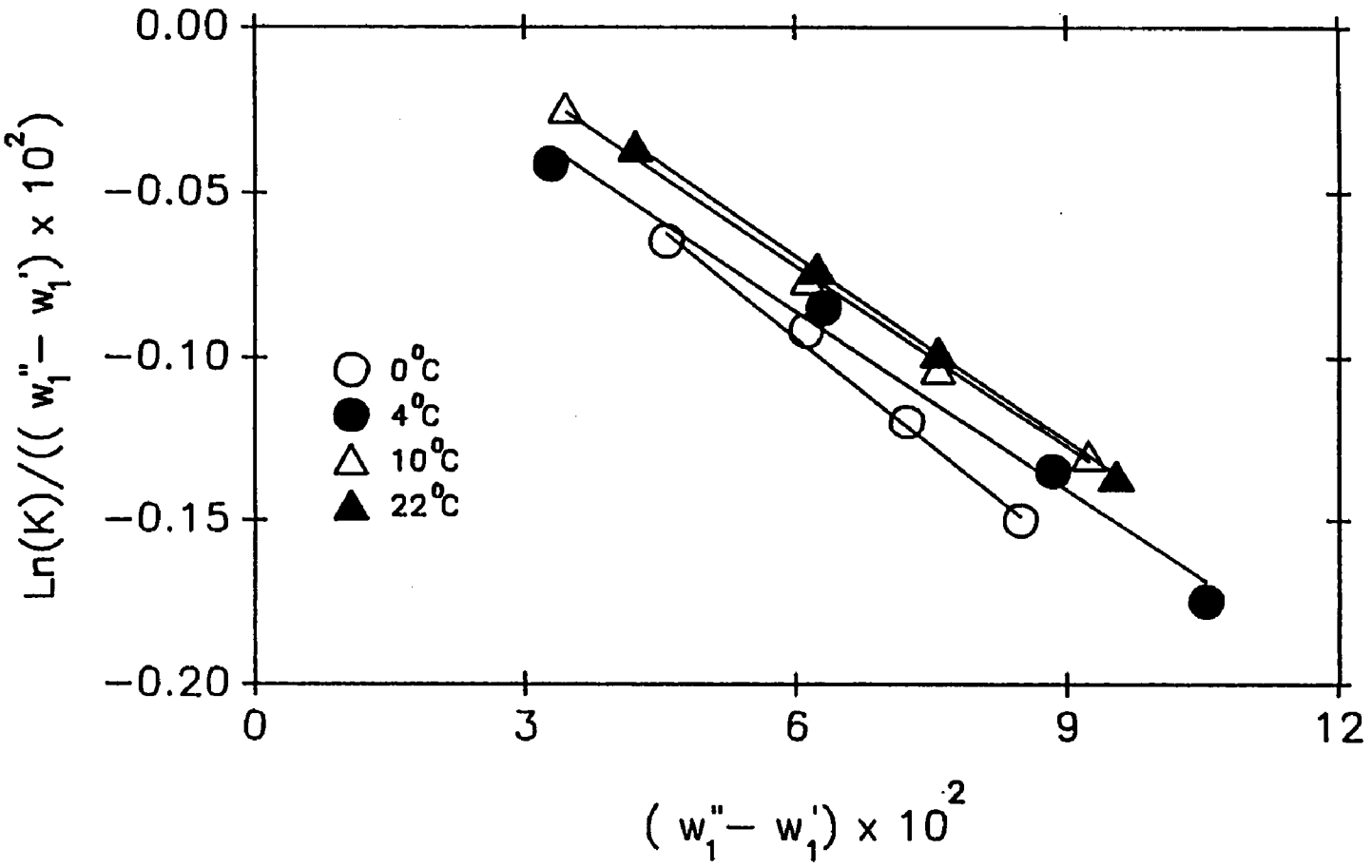

Figure 5.23 The Effect of Temperature on BSA Partitioning in the PEG 8000/Dextran T-500 System at 4°C.

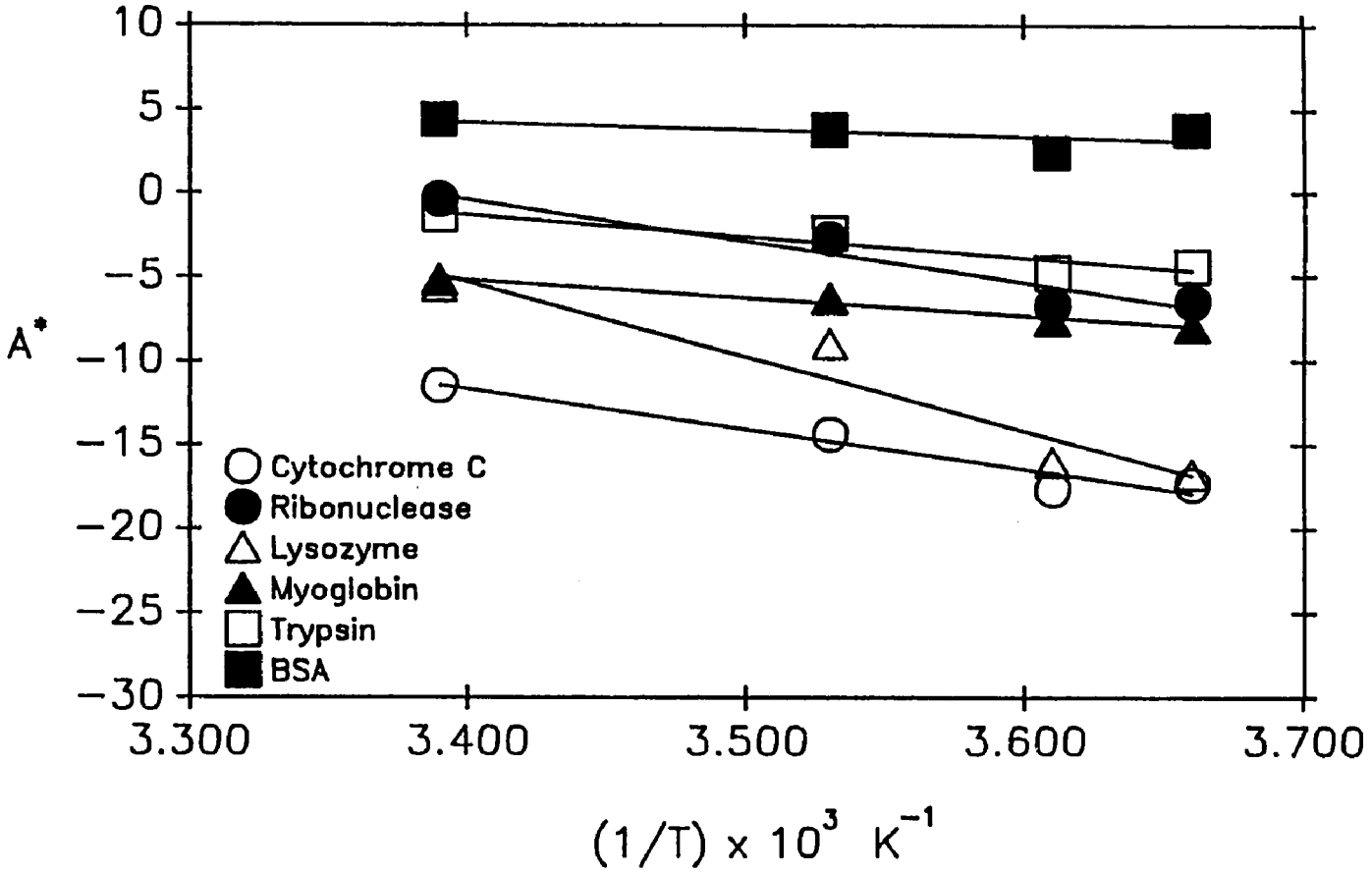

Figure 5.24 The Parameter A* as a Function of Temperature, Based on the Relationship of Equation (5.5).

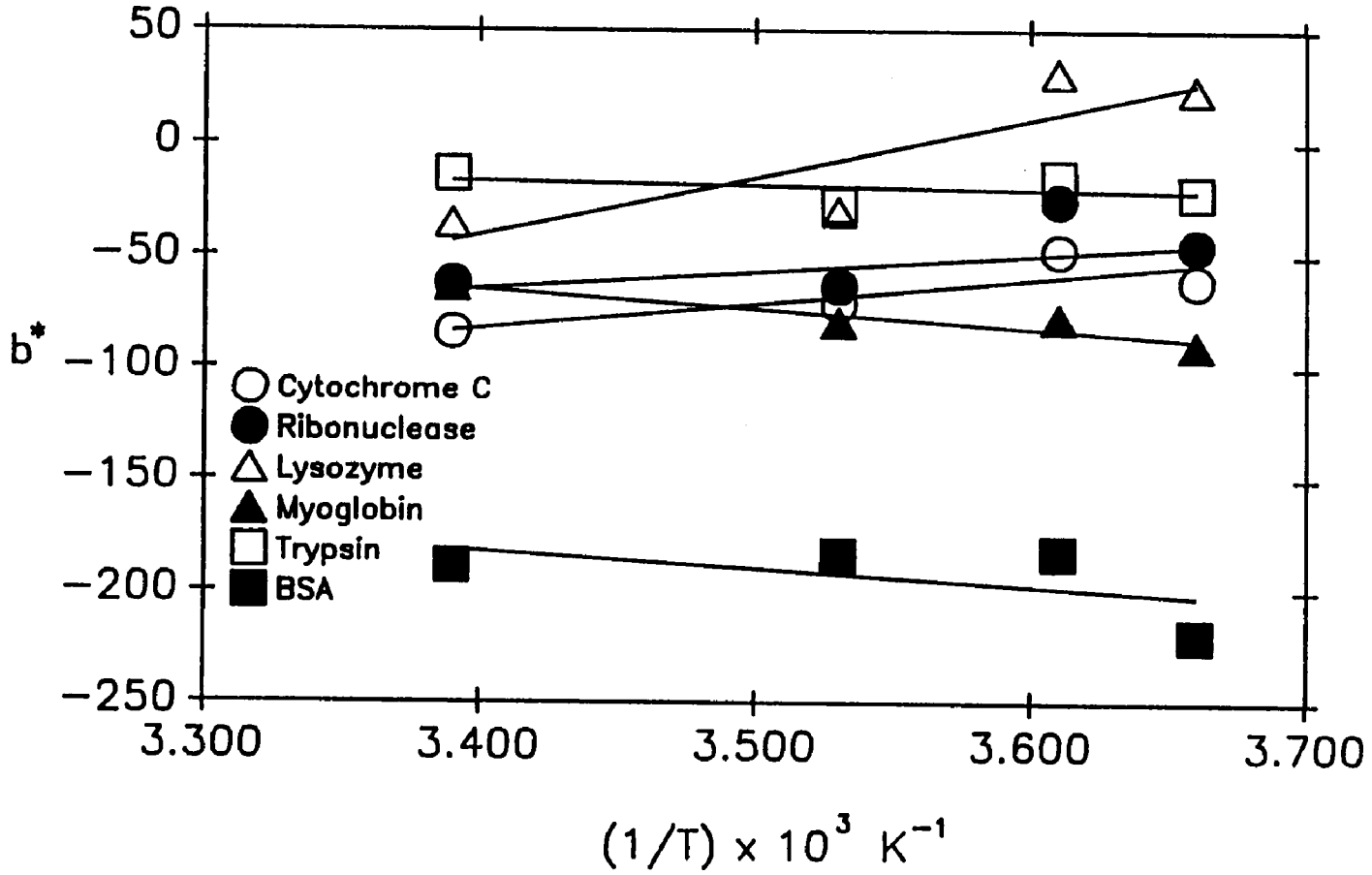

Figure 5.25 The Parameter b* as a Function of Temperature, Based on the Relationship of Equation (5.6).

correlating protein partitioning in aqueous polymer two phase systems. The relationship contained two parameters, A^* and b^*, and was verified for PEG/dextran/water, PEG/potassium phosphate/water and Ficoll 400/Dextran T-500/water systems utilizing seventeen proteins covering a broad range of molecular weight, along with protein partition data from the literature. The effect of phase forming polymer molecular weight on the parameters was investigated. A^* was shown to increase as dextran molecular weight increased, and increase as PEG molecular weight decreased. No definite molecular weight trend could be observed for b^*. The A^* and b^* parameters of the correlating equation were also shown to be linearly related to reciprocal absolute temperature. Equation (5.1) will simplify the selection of an appropriate aqueous two-phase system for protein purification since only two partition coefficients need to be measured in order to obtain the parameters of the equation, and thus have a clear picture of partition trends in an aqueous two-phase system.

CHAPTER VI
THE EFFECT OF PROTEIN STRUCTURE ON THE PARTITION COEFFICIENT

In this chapter, the effect of protein primary structure on the partition coefficient is correlated through the use of amino acids, which are the building block molecules of peptides and proteins. In addition, the sensitivity of aqueous two phase systems is explored through the use of reversed sequence peptides, homologous peptides and proteins, and reversed sequence dinucleotides.

6.1 Introduction

In the preceding two chapters, the effect of environmental conditions, such as phase forming polymer concentration, temperature and molecular weight, on protein partitioning had been investigated. In this chapter, light will be shed on the effect of protein structure on the partition coefficient. In particular, a theoretical model, which relates the effect of amino acid sequence on protein partition, will be developed and explored.

Sasakawa and Walter (1971, 1972, 1974) first examined the behavior in aqueous two-phase systems of some closely related proteins of known structure and chemical and physiological properties. They found that, while the molecular weights of homologous hemoglobins are essentially the same, significant differences in the partitioning of hemoglobins A and F as well as mammalian hemoglobins were evident in PEG/dextran/water systems. Human hemoglobin A had the highest K, 0.43; dog hemoglobin, 0.36; horse, 0.29; rabbit, 0.27 and pig hemoglobin the lowest, 0.20. While the primary structures

of human and rabbit hemoglobins differ to the greatest extent among the proteins studied (i.e., at least 16% of their amino acid sequence), the greatest difference in partition is between human and pig hemoglobin (which differ by at least 11%). Interestingly, the K values have no apparent relation to the relative electrophoretic mobility of the hemoglobins in question.

Previously, aqueous two-phase systems have been used to study protein secondary and tertiary structure. Andreasen (1981) had used aqueous two-phase partitioning to characterize the transformation process of the rat liver glucocorticoid receptor and to characterize aberrant receptor properties from cultured mouse lymphoma cells (Andreasen and Gehring, 1981). Recently, Hansen and Gorski (1985) have shown that the unoccupied estrogen receptor (ER) has a higher partition coefficient (more hydrophobic) than the nontransformed (without heat treatment) ER (1.0 vs 0.44) in the PEG 8000/Dextran T-500/water system. Interestingly, the transformed (with heat treatment) ER resulted in a lower partition coefficient, 0.17.

In this chapter, it will be shown that reversing the amino acid sequence of a dipeptide or the nucleotide sequence of a dinucleotide produces a distinct difference in how they partition between a PEG/potassium phosphate/water system (Diamond *et al.*, 1989, 1990). The partition coefficients of forty-six dipeptides (twenty-three pairs), and one pair of dinucleotides will be presented. From the results one may hypothesize that the size and location of the amino acid side chain play a significant role in effecting the dipeptide molecular structure and partitioning in PEG/potassium phosphate/water systems.

In order to further demonstrate the effect of amino acid sequence on protein partitioning, the similar proteins β-lactoglobulin A and B, along with

homologous insulins and cytochrome c, and the amino acids which make up the proteins, will be investigated in the PEG/potassium phosphate/water system These data, along with the dipeptide partition data, will be used to develop a model for predicting protein partitioning based on primary structure.

The effect of amino acid sequence on protein partitioning in aqueous two-phase systems is important to the field of protein engineering. A fundamental problem in protein engineering is the need to understand the relationship between amino acid sequence and a protein's three dimensional structure. The partitioning data may provide some insight into the effect of amino acid sequence on the hydrophobic and hydrophilic properties of a protein. Partition experiments may determine the protein's antigenic determinants, which are located on the hydrophilic region of a protein's surface (Hopp and Woods, 1981). Such antigenic determinants are used for synthetic vaccine development.

6.2 Materials and Methods

6.2.1 Polymers, Peptides, Proteins and Dinucleotides

PEG of molecular weight 3,400 (Lot 00304EV) was obtained from Aldrich Chemical Company, Milwaukee, WI. Potassium phosphate, both mono- and dibasic, were of A.C.S. reagent grade and also obtained from Aldrich.

The peptides gly-gly, triglycine, tetraglycine, pentaglycine, gly-ala-tyr, gly-tyr-ala, gly-ala, ala-gly, gly-val, val-gly, gly-leu, leu-gly, gly-phe, phe-gly, gly-trp, trp-gly, gly-met, met-gly, gly-pro, pro-gly, gly-ser, ser-gly, ser-leu, leu-ser, gly-tyr, tyr-gly, gly-asp, asp-gly, gly-lys, lys-gly, gly-his, his-gly, ala-trp,

trp-ala, ala-val, val-ala, ala-leu, ala-tyr, tyr-ala, ala-asp, asp-ala, val-asp, asp-val, leu-arg, arg-leu, val-lys, lys-val, asp-lys, and lys-asp were purchased from Sigma Chemical Company, St. Louis, MO. The dipeptides gly-ile, ile-gly, and leu-ala were purchased from U. S. Biochemical Corp., Cleveland, OH.

Glycine, along with the following l-amino acids were purchased from Sigma: tryptophan, phenylalanine, tyrosine, isoleucine, leucine, cysteine, methionine, valine, proline, glutamic acid, glutamine, alanine, threonine, aspartic acid, asparagine, serine, arginine, lysine and histidine.

Insulin from equine and porcine pancreas, cytochrome c from horse, pig and dog heart, and β-lactoglobulins A and B were also purchased from Sigma. It should be pointed out that individual A and B samples were purchased, not a mixture of the two.

6.2.2 Biomolecule Partitioning Method

Five hundred to one thousand milliliter samples of systems 1–4 of the PEG 3400/potassium phosphate/water phase diagram at 20°C were prepared according to the procedure of Albertsson (1986). The phase compositions of each of these systems were as follows (Albertsson, 1986):

1. Bottom Phase: 14.06% phosphate/4.23% PEG, Top Phase: 8.19% phosphate/15.96% PEG
2. Bottom Phase: 15.46% phosphate/2.54% PEG, Top Phase: 7.01% phosphate/19.16% PEG
3. Bottom Phase: 17.41% phosphate/1.30% PEG, Top Phase: 5.56% phosphate/23.90% PEG

4. Bottom Phase: 19.41% phosphate/0.78% PEG, Top Phase: 4.55% phosphate/28.15% PEG

The potassium phosphate utilized in this study consisted of a dibasic to monobasic weight ratio of 1.82, thus giving a pH of 7.0 in each of the four systems. The samples were placed in separatory funnels and allowed to settle at 20°C for 24 hours in the laboratory environment. The two phases were collected and then used as stock solutions for the partitioning studies.

5 mL of top and bottom phase were placed together into a 15 mL polypropylene centrifuge tube. 3 mg of either peptide, amino acid or dinucleotide, or 10 mg of β-lactoglobulin, insulin or cytochrome c was then added, and the tubes tightly sealed. The biomolecule was then dissolved by gently mixing the contents of the centrifuge tube with a vortex mixer. The systems containing the biomolecule were permitted to settle at 20°C for 24 hours. The phases were then separated. Peptide and β-lactoglobulin concentration was determined by measuring absorbance using a Shimadzu UV-Vis spectrophotometer according to the procedure of Sasakawa and Walter (1972, 1974). Absorbance at 220 nm was utilized for the peptides, while 280 nm was used for the β-lactoglobulins. Amino acid and insulin concentration was determined using the fluorescamine technique (Bohlen *et al.*, 1973). Cytochrome c concentration in the bottom phase was determined using absorbance at 280 nm, while concentration in the bottom phase was estimated using the fluorescamine technique. The concentrations determined for the top and bottom phases were then used to calculate the partition coefficient, K, which was defined as biomolecule concentration in the top phase divided by the concentration in the bottom phase.

6.3 Results and Discussion

6.3.1 Biomolecule Partitioning Results

Twenty-three dipeptide pairs were partitioned in systems 1–4 of the PEG 3400/potassium phosphate/water phase diagram at 20°C. The dipeptides that comprise a pair differ from one another by reversal of their amino acid sequence. Six categories of reversed sequence dipeptides were utilized in this study, with each category containing the following sidechain types: 1. uncharged polar and nonpolar sidechains, 2. uncharged polar sidechains, 3. uncharged polar and charged polar sidechains, 4. nonpolar sidechains, 5. nonpolar and charged polar sidechains, and 6. charged polar sidechains.

The dipeptide partition data from phase systems 1 and 2 are recorded in Table 6.1, while the partition data for phase systems 3 and 4 are recorded in Table 6.2. Examination of the dipeptide partition data for category 1 reveals that when glycine, a polar, uncharged amino acid, is at the N-terminal and is attached to an amino acid with a nonpolar side chain, i.e., alanine, valine, leucine, phenylalanine, proline, or methionine, the partition coefficient is lower than the reverse sequence. Interestingly, it can be seen that when a CH_2 group is added to the residue with a nonpolar sidechain, the difference between partition coefficients for the reverse pair increases, with the gly-leu/leu-gly pair showing the greatest difference. When serine (polar uncharged amino acid) is at the N-terminal and paired with leucine (nonpolar), its partition coefficient is higher than the reverse case. A similar situation is encountered when tyrosine is combined with alanine. This is opposite of what occurred when glycine was at the N-terminal and paired with a nonpolar residue. Hence, at present, a generalization can not be made as to which dipeptide will have a higher partition coefficient when polar and nonpolar residues are combined. However,

Table 6.1 Partition Coefficients of Dipeptides in Phase Systems 1 and 2 of the PEG 3400/Potassium Phosphate/Water Phase Diagram at 20°C.

Dipeptide	Phase System 1	2
I. Uncharged Polar and Non Polar Sidechains		
Gly-Ala	0.465	0.415
Ala-Gly	0.486	0.427
Gly-Val	0.593	0.541
Val-Gly	0.638	0.585
Gly-Leu	0.691	0.659
Leu-Gly	0.775	0.745
Gly-Ile	0.691	0.650
Ile-Gly	0.798	0.769
Gly-Phe	0.984	0.981
Phe-Gly	1.10	1.11
Gly-Trp	1.95	1.99
Trp-Gly	2.01	2.20
Gly-Pro	0.484	0.438
Pro-Gly	0.561	0.521
Gly-Met	0.627	0.578
Met-Gly	0.701	0.668
Ser-Leu	0.718	0.664
Leu-Ser	0.695	0.640
Tyr-Ala	1.13	1.16
Ala-Tyr	1.08	1.11
II. Uncharged Polar Sidechains		
Gly-Ser	0.394	0.331
Ser-Gly	0.428	0.363
Gly-Tyr	1.01	1.01
Tyr-Gly	1.12	1.13
III. Uncharged Polar and Charged Polar Sidechains		
Gly-Asp	0.372	0.323
Asp-Gly	0.504	0.432
Gly-Lys	0.276	0.213
Lys-Gly	0.299	0.239
Gly-His	0.334	0.300
His-Gly	0.453	0.404
IV. Non Polar Sidechains		
Ala-Val	0.657	0.613
Val-Ala	0.670	0.623
Ala-Leu	0.769	0.739
Leu-Ala	0.792	0.763
Ala-Trp	2.00	2.30
Trp-Ala	2.14	2.37
V. Non Polar and Charged Polar Sidechains		
Ala-Asp	0.436	0.382
Asp-Ala	0.555	0.500
Val-Asp	0.541	0.498
Asp-Val	0.688	0.663
Val-Lys	0.382	0.313
Lys-Val	0.396	0.341
Leu-Arg	0.559	0.532
Arg-Leu	0.593	0.554
VI. Charged Polar Sidechains		
Asp-Lys	0.305	0.254
Lys-Asp	0.273	0.222

Table 6.2 Partition Coefficients of Dipeptides in Phase Systems 3 and 4 of the PEG 3400/Potassium Phosphate/Water Phase Diagram at 20°C.

Dipeptide	Phase System 3	4
I. Uncharged Polar and Non Polar Sidechains		
Gly-Ala	0.348	0.274
Ala-Gly	0.363	0.290
Gly-Val	0.464	0.422
Val-Gly	0.511	0.483
Gly-Leu	0.592	0.542
Leu-Gly	0.687	0.662
Gly-Ile	0.581	0.537
Ile-Gly	0.714	0.680
Gly-Phe	0.975	0.982
Phe-Gly	1.14	1.20
Gly-Trp	2.40	2.70
Trp-Gly	2.55	3.01
Gly-Pro	0.372	0.301
Pro-Gly	0.449	0.377
Gly-Met	0.505	0.455
Met-Gly	0.623	0.573
Ser-Leu	0.625	0.557
Leu-Ser	0.577	0.522
Tyr-Ala	1.21	1.29
Ala-Tyr	1.11	1.16
II. Uncharged Polar Sidechains		
Gly-Ser	0.241	0.184
Ser-Gly	0.279	0.236
Gly-Tyr	0.990	0.970
Tyr-Gly	1.09	1.09
III. Uncharged Polar and Charged Polar Sidechains		
Gly-Asp	0.247	0.192
Asp-Gly	0.387	0.321
Gly-Lys	0.143	0.105
Lys-Gly	0.163	0.127
Gly-His	0.196	0.148
His-Gly	0.313	0.253
IV. Non Polar Sidechains		
Ala-Val	0.541	0.486
Val-Ala	0.565	0.503
Ala-Leu	0.688	0.616
Leu-Ala	0.734	0.679
Ala-Trp	2.55	3.30
Trp-Ala	2.87	3.52
V. Non Polar and Charged Polar Sidechains		
Ala-Asp	0.298	0.234
Asp-Ala	0.430	0.370
Val-Asp	0.426	0.343
Asp-Val	0.601	0.534
Val-Lys	0.234	0.175
Lys-Val	0.266	0.204
Leu-Arg	0.472	0.385
Arg-Leu	0.491	0.396
VI. Charged Polar Sidechains		
Asp-Lys	0.199	0.125
Lys-Asp	0.178	0.101

one may conjecture that such factors as side chain size and charge distribution are of importance.

The dipeptide partitioning from categories 2 (gly-ser/ser-gly, gly-tyr/tyr-gly) and 6 (asp-lys/lys-asp) each contain dipeptides composed of amino acids with similar sidechains. Examination of the data for these two categories indicates that gly-ser, gly-tyr, and lys-asp have lower partition coefficients than the reverse sequence. In the case of lys-asp/asp-lys, lysine contains a positively charged residue, while aspartic acid is negative. The lower partition coefficient occurs when the positively charged lysine is at the positive N-terminal, while the negative aspartic acid is at the negative C-terminal.

Examination of the dipeptide partition data of category 3, reveals that when glycine is paired with a residue containing a charged, polar sidechain, whether positive or negative, the partition coefficient is lower than the reverse. When two residues with nonpolar sidechains are combined, i.e., category 4, the partition coefficient is lower when the smaller of the two residues is at the N-terminal. When a polar residue such as alanine, valine, or leucine is at the N-terminal and paired with a charged residue, i.e., category 5, the partition coefficient is lower than the reverse case.

In order to further demonstrate the sensitivity of the PEG 3400/potassium phosphate/water systems, and the effect of amino acid sequence on protein partitioning, the two proteins, β-lactoglobulin A and B, were partitioned in systems 1–4. These two proteins have been selected since there is only a slight difference in their amino acid sequence, which is given in Figure 6.1 (Walstra and Jenness, 1984). Species A has aspartic acid and valine, while species B has glycine and alanine at residues 64 and 118, respectively (Walstra

H-Leu-Ile-Val-Thr-Gln-Thr-Met-Lys-Gly-Leu-Asp-Ile-Gln-Lys-Val-Ala-Gly-Thr-

Trp-Tyr-Ser-Leu-Ala-Met-Ala-Ala-Ser-Asp-Ile-Ser-Leu-Leu-Asp-Ala-Gln-Ser-

Ala-Pro-Leu-Arg-Val-Tyr-Val-Glu-Glu-Leu-Lys-Pro-Thr-Pro-Glu-Gly-Asp-Leu-

Glu-Ile-Leu-Leu-Gln-Lys-Trp-Glu-Asn-[Asp/Gly]-Glu-Cys-Ala-Gln-Lys-Lys-Ile-Ile-

Ala-Glu-Lys-Thr-Lys-Ile-Pro-Ala-Val-Phe-Lys-Ile-Asp-Ala-Leu-Asn-Glu-Asn-

Lys-Val-Leu-Val-Leu-Asp-Thr-Asp-Tyr-Lys-Lys-Tyr-Leu-Leu-Phe-Cys-Met-

Glu-Asn-Ser-Ala-Glu-Pro-Glu-Gln-Ser-Leu-[Val/Ala]-Cys-Gln-Cys-Leu-Val-Arg-

Thr-Pro-Glu-Val-Asp-Asp-Glu-Ala-Leu-Glu-Lys-Phe-Asp-Lys-Ala-Leu-Lys-Ala-

Leu-Pro-Met-His-Ile-Arg-Leu-Ser-Phe-Asn-Pro-Thr-Gln-Leu-Glu-Glu-Gln-Cys-

His-Ile-OH

Figure 6.1 Amino Acid Sequence of β-Lactoglobulins A and B. Species A has aspartic acid and valine, while species B has glycine and alanine at residues 64 and 118, respectively.

and Jenness, 1984). The proteins, which may be resolved by ion exchange chromatography or electrophoresis, have an isoelectric point difference of only 0.1 pH units (Righetti and Caravaggio, 1976). The partition results are presented in Figure 6.2 where the natural logarithm of the partition coefficient divided by the PEG concentration difference is plotted versus the PEG concentration difference according to equation (5.1) of Chapter V. The separation factor, defined as the partition coefficient of species A divided by that of B, was found to be 2.0. Although this separation factor is quite high, it should also be noted that the partition coefficients are very low, on the order of 10^{-2}.

The β-lactoglobulin A and B were partitioned in the PEG 8000/Dextran T-500/water phase diagram at 4°C and the results are presented in Figure 6.3. The two proteins showed a slight difference in partition, with a maximum separation factor of 1.09 being obtained in the tie line farthest away from the plait point. The data also reveal that the PEG 8000/Dextran T-500/water system is not as sensitive to changes in protein primary structure as is the PEG/potassium phosphate/water system.

Insulin from horse and pig pancreas were partitioned in phase system 2 of the PEG/potassium phosphate/water phase diagram. The amino acid sequences for these homologous proteins are provided in Figure 6.4 (Sober, 1968). The two proteins differ from one another at the ninth amino acid residue in the sequence, where the horse and pig species have glycine and serine respectively. However, the partition coefficients were found to show a significant difference, 21.2 and 19.4 for the two species, respectively.

Cytochrome c from horse, dog and pig heart were partitioned in phase systems 1 and 2 of the PEG 3400/potassium phosphate/water phase diagram,

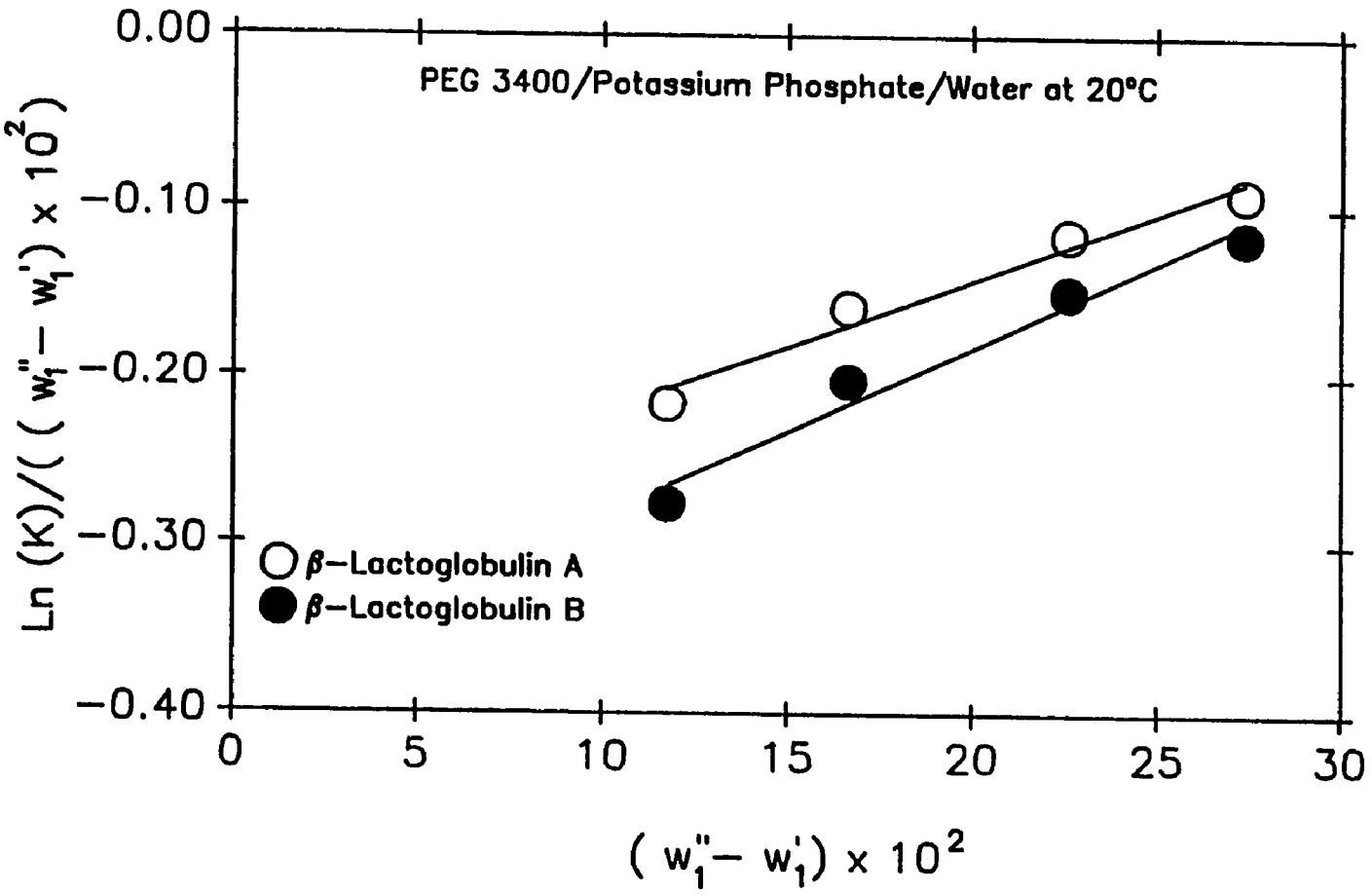

Figure 6.2 Partitioning of β-Lactoglobulins A and B in the PEG 3400/Potassium Phosphate/Water System at 20°C.

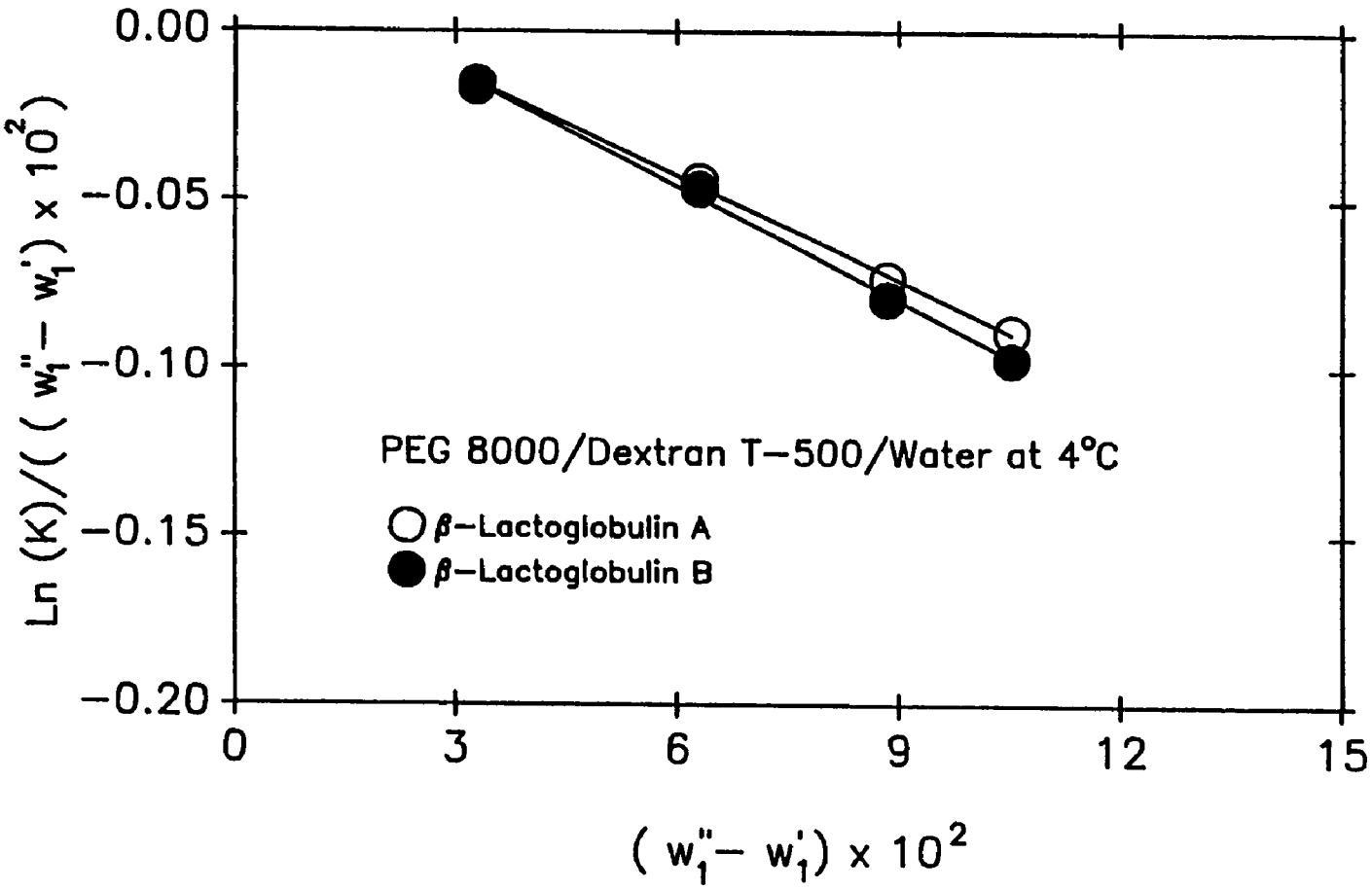

Figure 6.3 Partitioning of β-Lactoglobulins A and B in the PEG 8000/Dextran T-500/Water System at 4°C.

Insulin A Chain:
H-Gly-Ile-Val-Glu-Gln-Cys-Cys-Thr-[Gly/Ser]-Ile-Cys-Ser-Leu-Tyr-Gln-Leu-Glu-Asn-Tyr-

Cys-Asn-OH

Insulin B Chain:
H-Phe-Val-Asn-Gln-His-Leu-Cys-Gly-Ser-His-Leu-Val-Glu-Ala-Leu-Tyr-Leu-

Val-Cys-Gly-Glu-Arg-Gly-Phe-Phe-Tyr-Thr-Pro-Lys-Ala-OH

Figure 6.4 Amino Acid Sequence of Horse and Pig Insulin. The two differ at residue 9 of chain A, in which the horse and pig have glycine and serine, respectively.

and in the four tie lines of the PEG 8000/dextran T-500/water phase diagram. The amino acid sequences for the proteins, which are provided in Figure 6.5 (Sober, 1968), differ from one another at six locations. In system 1 of the PEG 3400/potassium phosphate/water phase diagram, the partition coefficients for the three proteins were found to be 0.0136, 0.0143 and 0.0142, respectively, while in system 2 they were 0.0074, 0.0284 and 0.0105, respectively. The data indicate that the dog cytochrome c consistently has the highest partition coefficient of the three, and the horse cytochrome c the least. The partition data for the PEG 8000/Dextran T-500/water phase diagram are provided in Figure 6.6. In this system it is apparent that the pig cytochrome c has the highest partition coefficient, while the horse and dog cytochrome c are both lower and exhibit essentially identical partition behavior.

The above results demonstrate the effect of amino acid and nucleotide sequence on biomolecule partitioning. By changing only one or two residues in a protein, its partition coefficient was dramatically altered in the

Horse Acetyl-Gly-Asp-Val-Glu-Lys-Gly-Lys-Lys-Ile-Phe-Val-Gln-Lys-Cys-Ala-Gln-Cys-
Pig Acetyl-Gly-Asp-Val-Glu-Lys-Gly-Lys-Lys-Ile-Phe-Val-Gln-Lys-Cys-Ala-Gln-Cys-
Dog Acetyl-Gly-Asp-Val-Glu-Lys-Gly-Lys-Lys-Ile-Phe-Val-Gln-Lys-Cys-Ala-Gln-Cys-

Horse His-Thr-Val-Glu-Lys-Gly-Gly-Lys-His-Lys-Thr-Gly-Pro-Asn-Leu-His-Gly-Leu-Phe-
Pig His-Thr-Val-Glu-Lys-Gly-Gly-Lys-His-Lys-Thr-Gly-Pro-Asn-Leu-His-Gly-Leu-Phe-
Dog His-Thr-Val-Glu-Lys-Gly-Gly-Lys-His-Lys-Thr-Gly-Pro-Asn-Leu-His-Gly-Leu-Phe-

Horse Glu-Arg-Lys-Thr-Gly-Gln-Ala-Pro-Gly-Phe-**Thr**-Tyr-Thr-Asp-Ala-Asn-Lys-Asn-
Pig Glu-Arg-Lys-Thr-Gly-Gln-Ala-Pro-Gly-Phe-**Ser**-Tyr-Thr-Asp-Ala-Asn-Lys-Asn-
Dog Gly-Arg-Lys-Thr-Gly-Gln-Ala-Pro-Gly-Phe-**Ser**-Tyr-Thr-Asp-Ala-Asn-Lys-Asn-

Horse Lys-Gly-Ile-Thr-Trp-**Lys**-Glu-Glu-Thr-Leu-Met-Glu-Asn-Pro-Lys-Lys-Tyr-Ile-Pro-
Pig Lys-Gly-Ile-Thr-Trp-**Gly**-Glu-Glu-Thr-Leu-Met-Glu-Asn-Pro-Lys-Lys-Tyr-Ile-Pro-
Dog Lys-Gly-Ile-Thr-Trp-**Gly**-Glu-Glu-Thr-Leu-Met-Glu-Asn-Pro-Lys-Lys-Tyr-Ile-Pro-

Horse Gly-Thr-Lys-Met-Ile-Phe-Ala-Gly-Ile-Lys-Lys-**Lys-Thr**-Glu-Arg-**Glu**-Asp-Leu-
Pig Gly-Thr-Lys-Met-Ile-Phe-Ala-Gly-Ile-Lys-Lys-**Lys-Gly**-Glu-Arg-**Glu**-Asp-Leu-
Dog Gly-Thr-Lys-Met-Ile-Phe-Ala-Gly-Ile-Lys-Lys-**Thr-Gly**-Glu-Arg-**Ala**-Asp-Leu-

Horse Ile-Ala-Tyr-Leu-Lys-Lys-Ala-Thr-Asn-**Glu**-OH
Pig Ile-Ala-Tyr-Leu-Lys-Lys-Ala-Thr-Asn-**Glu**-OH
Dog Ile-Ala-Tyr-Leu-Lys-Lys-Ala-Thr-Asn-**Lys**-OH

Figure 6.5 Amino Acid Sequence of Homologous Cytochrome c.

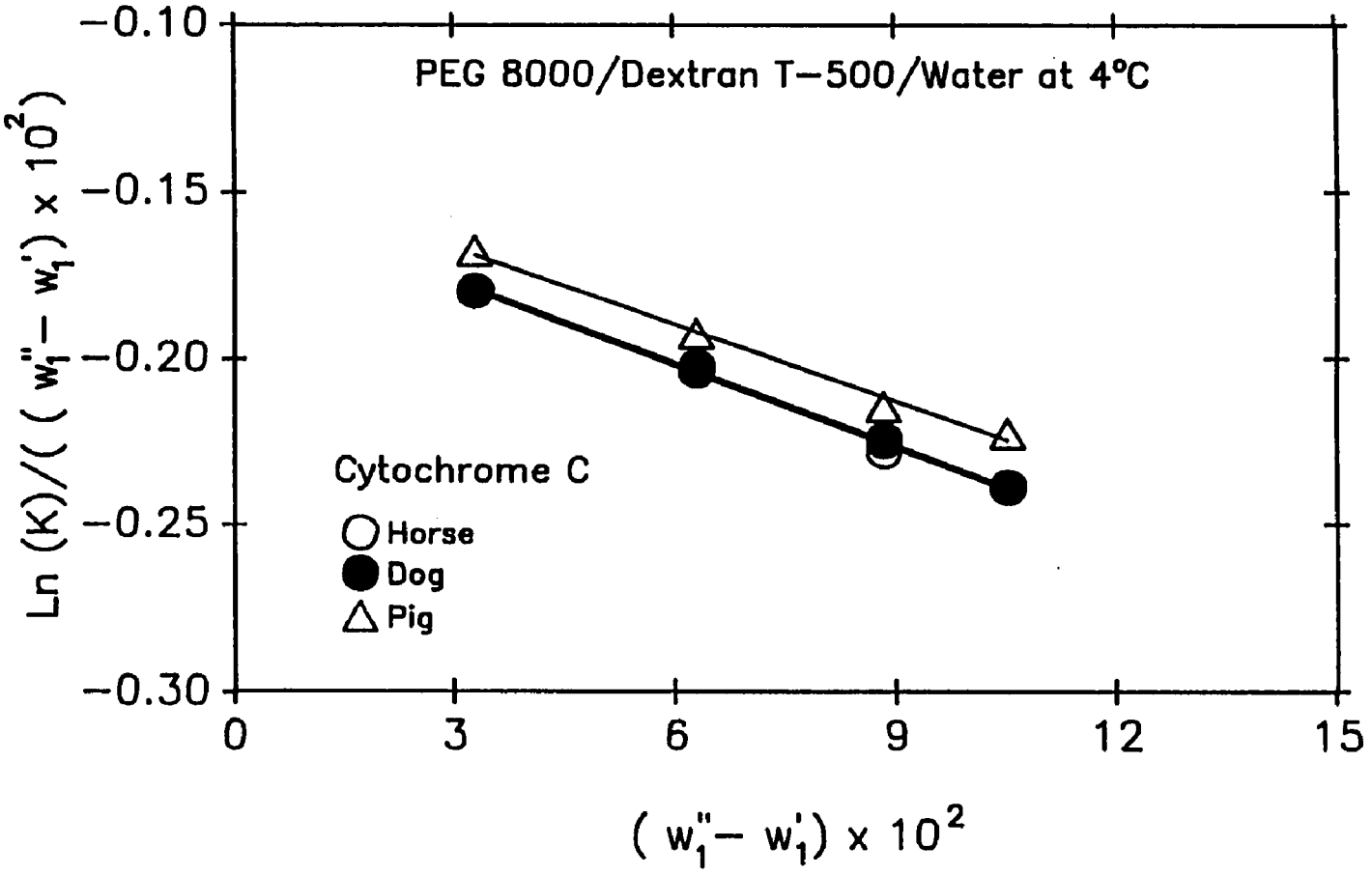

Figure 6.6 Partitioning of Homologous Cytochrome c in the PEG 8000/Dextran T-500/Water System at 4°C.

PEG/potassium phosphate/water systems. A quantitative explanation for this occurrence will be given later on in the chapter.

In order to gain a more fundamental understanding of peptide and protein separation in aqueous two-phase systems, the partition of their building blocks, the amino acids, is undoubtedly required. Twenty amino acids were partitioned in phase system 2 of the PEG 3400/potassium phosphate/water phase diagram at 20°C and the results are presented in Table 6.3 in the order of decreasing partition coefficient. Although this table by no means represents a hydropathy scale due to the many factors that influence partitioning in the PEG/potassium phosphate/water systems, it is of interest to compare these results with previously established scales, such as the hydropathy index of Kyte and Doolittle (1982). This index is presented in Table 6.3. In the case of the PEG/potassium phosphate/water systems, the upper, PEG rich phase may be considered more hydrophobic than the lower, salt rich phase. Kyte and Doolittle's scale has the charged, polar amino acids with the lowest (most negative) hydropathy, followed by the polar and then nonpolar amino acids. Similarly, the charged, polar amino acids have the lowest partition coefficient followed by the polar and then nonpolar amino acids.

6.3.2 Correlation of Biomolecule Partitioning

With knowledge of amino acid partitioning, the next logical step is to utilize the data for correlation and prediction of peptide partitioning. It is of interest to derive the partitioning behavior of peptides from their amino acid sequences. The correlation between individual amino acids and peptides is a revelation of the interaction between amino acids in the sequence and the nature of the peptide bond and may help to decipher the rules of peptide

Table 6.3 Partitioning Parameters for l-Amino Acids in Phase System 2 of the PEG 3400/Potassium Phosphate/Water Phase Diagram at 20°C.

l-Amino Acid	H*	K	E	δ^C	δ^N	ϵ
Tryptophan	−0.9	2.00	0.69	0.27	−1.04	1.46
Phenylalanine	2.8	1.14	0.13	0.31	−0.94	0.77
Tyrosine	−1.3	1.07	0.07	0.31	−1.08	0.84
Isoleucine	4.5	0.86	−0.15	0.35	−0.87	0.37
Leucine	3.8	0.84	−0.17	0.37	−0.92	0.38
Cysteine	2.5	0.78	−0.25	---	---	---
Methionine	1.9	0.71	−0.34	0.28	−0.96	0.34
Valine	4.2	0.70	−0.36	0.38	−0.93	0.19
Proline	−1.6	0.61	−0.49	0.35	−0.86	0.01
Glutamic Acid	−3.5	0.57	−0.56	---	---	---
Glutamine	−3.5	0.56	−0.58	---	---	---
Alanine	1.8	0.54	−0.62	0.40	−0.95	−0.06
Threonine	−0.7	0.53	−0.64	---	---	---
Aspartic Acid	−3.5	0.50	−0.69	0.26	−0.84	−0.11
Glycine	−0.4	0.48	−0.73	0.35	−1.00	−0.08
Asparagine	−3.5	0.50	−0.69	---	---	---
Histidine	−3.2	0.44	−0.82	0.24	−0.81	−0.25
Serine	−0.8	0.43	−0.84	0.25	−1.01	−0.09
Arginine	−4.5	0.37	−0.99	0.27	−0.96	−0.31
Lysine	−3.9	0.32	−1.14	0.33	−0.92	−0.55

* Kyte and Doolittle's hydropathy index (1982)

conformation.

The Gibbs free energy of transfer of a molecule between the two phases is determined by its partition coefficient:

$$\Delta G^{\circ} = -RT \ln(K) \tag{6.1}$$

where ΔG° is the free energy of transfer, R is the gas law constant T is absolute temperature and K the partition coefficient. Since the experiments were carried out at 20°C, RT remains constant. As a simplification, the quantity E may be defined as

$$E = \frac{-\Delta G^{\circ}}{RT} = \ln(K) \tag{6.2}$$

Thus, E is proportional to ΔG° and retains the sign. It can be regarded as the transfer free energy on a nondimensional scale, or, alternatively, the natural logarithm of the partition coefficient. E values for the twenty amino acids are listed in Table 6.3. In addition to the amino acids, the partition coefficient for the twenty-three dipeptide pairs partitioned in phase system 2 will also be utilized in this study.

An initial assumption was that the E of a dipeptide equaled that of the N-terminal amino acid plus that of the C-terminal amino acid minus a loss term, denoted by δ:

$$E_{BX} = E_B + E_X - \delta \tag{6.3}$$

where subscripts B and X refer to two arbitrary amino acids, and BX is the

dipeptide with B at the N-terminal. A correlation of phase system 2 data gives δ between 0.55 and 0.71. However, application of this result to prediction of dipeptide partitioning would produce a maximum error of 15%. In order to make predictions more accurate, δ is treated as a characteristic of an individual amino acid and is split into two components,

$$\delta_i = \delta_i^N + \delta_i^C \tag{6.4}$$

where superscripts N and C refer to the amino and carboxyl terminals, respectively, and subscript i refers to the amino acid in question. For dipeptide BX,

$$E_{BX} = E_B + E_X - \delta_B^C - \delta_X^N \tag{6.5}$$

where E_B and E_X in equation (6.5) are the E values for amino acids B and X, respectively. The parameter δ_B^C is a correction term which takes into account the fact that the first amino acid, in this case B, has lost an oxygen atom from its carboxyl terminal upon formation of the peptide bond. The parameter δ_X^N is a correction term which takes into account that the second amino acid, X, has lost two hydrogen atoms from its amino terminal upon formation of the peptide bond. Since fifteen different amino acids are present among the twenty-three dipeptide pairs used in the partitioning study, then there are fifteen unknown δ_i^N and δ_i^C for each amino acid for a total of thirty variables. For each dipeptide, an equation like that for XB may be written. Thus, from the published data, there are forty-six equations (arising from the twenty-three dipeptide pairs) with thirty variables. The δ_i^N and δ_i^C can be solved for by least square fit. The

δ_i^N and δ_i^C thus obtained are recorded in Table 6.3. It should be pointed out that these two parameters were not obtained for all of the amino acids due to the limitations of the dipeptide data.

Now that E_i, δ_i^N and δ_i^C values have been obtained for individual amino acids, a generalized expression for predicting the E value of a peptide (poly-amino acid) may be obtained by summing the E_i, δ_i^N and δ_i^C along the peptide chain:

$$E = \sum_{j=1}^{n} (E_j - \delta_j^N - \delta_j^C) + \delta_1^N + \delta_n^C = \sum_{j=1}^{n} \epsilon_j + \delta_1^N + \delta_n^C \qquad (6.6)$$

where j is the number of the amino acid in the sequence, counting from the N-terminal, n refers to the last amino acid in the sequence, and $\epsilon_j = E_j - \delta_j^N - \delta_j^C$. The δ_1^N and δ_n^C have been added to equation (6.6) since the first amino acid in the chain (i.e., amino acid 1) has not lost any hydrogen atoms, while the last amino acid (i.e., amino acid n) has not lost an oxygen atom. The parameter ϵ_j is of interest because it represents the ln(K) of the amino acid residue, i.e., the amino acid minus a water molecule. The ϵ values corresponding to the amino acids from which they were derived, are recorded in Table 6.3. It is the amino acid residue, instead of the amino acid itself, which determines the local behavior in a peptide or protein. The ϵ values, as will be demonstrated later in this chapter, can be used to compare the partitioning behavior of similar or homologous proteins.

Equation (6.6) may be applied to the dipeptide gly-ala by letting the subscripts 1 and 2 refer to glycine and alanine, respectively:

$$E_{\text{gly-ala}} = E_1 + E_2 - \delta_1^C - \delta_2^N \qquad (6.7)$$

The calculated value of $E_{gly\text{-}ala}$ is −0.75. Application of equation (6.7) gives a K value of 0.47, which agrees very well with the experimental value of 0.465. The predicted partition coefficients using equation (6.6) for the forty-six dipeptides in phase system 2 of the PEG 3400/potassium phosphate/water phase diagram are listed in Table 6.4 along with the actual K values. The dipeptides yielding the greatest percent error were ala-tyr and tyr-gly with errors of 5.6% and 8.0%, respectively, while for most dipeptides, the error was close to zero.

The experimental and predicted partition coefficients of the glycine peptides in phase system 2 of the PEG 3400/potassium phosphate/water phase diagram are listed in Table 6.5. As can be seen, they are fairly consistent and show the same trend of decreasing K with longer chains. In a similar manner, the tripeptides gly-tyr-ala and gly-ala-tyr were partitioned in phase system 2, and the experimental K values were 1.09 and 1.06, respectively. When equation (6.6) is used to predict the K values, the result is 1.09 and 1.00, respectively, which is in good agreement.

Examination of Table 6.5 reveals that the correlation gives large error as the number of glycine residues is increased, with pentaglycine giving the greatest error. This is most probably due to the fact that the database used for developing equation (6.6) contained solely amino acids and dipeptides. In addition, the secondary and tertiary structures begin to become factors for the larger peptides and proteins. Although these factors will undoubtedly arise when applying the predictive equations to proteins, it is interesting to see how they may predict the ratio of K values for two similar, or homologous proteins, such as β-lactoglobulins A and B, or insulin from different species.

Table 6.4 Comparison of Experimental and Predicted Partition Coefficients for Dipeptides in Phase System 2 of the PEG 3400/Potassium Phosphate/Water Phase Diagram at 20°C.

Dipeptide	$K_{Exper.}$	$K_{Pred.}$	Dipeptide	$K_{Exper.}$	$K_{Pred.}$
1. Uncharged Polar and Non Polar Sidechains			**3. Uncharged Polar and Charged Polar Sidechains**		
Gly-Ala	0.465	0.472	Gly-Asp	0.372	0.389
Ala-Gly	0.486	0.477	Asp-Gly	0.504	0.508
Gly-Val	0.593	0.595	Gly-Lys	0.276	0.270
Val-Gly	0.638	0.626	Lys-Gly	0.299	0.301
Gly-Leu	0.691	0.709	Gly-His	0.334	0.333
Leu-Gly	0.775	0.762	His-Gly	0.453	0.453
Gly-Ile	0.691	0.691	**4. Non Polar Sidechains**		
Ile-Gly	0.798	0.798	Ala-Val	0.657	0.643
Gly-Phe	0.984	0.984	Val-Ala	0.670	0.669
Phe-Gly	1.10	1.10	Ala-Leu	0.769	0.766
Gly-Trp	1.95	1.90	Leu-Ala	0.792	0.815
Trp-Gly	2.01	2.01	Ala-Trp	2.00	2.05
Gly-Pro	0.484	0.484	Trp-Ala	2.14	2.15
Pro-Gly	0.561	0.561	**5. Non Polar and Charged Polar Sidechains**		
Gly-Met	0.627	0.627	Ala-Asp	0.436	0.420
Met-Gly	0.701	0.701	Asp-Ala	0.555	0.543
Ser-Leu	0.718	0.703	Val-Asp	0.541	0.552
Leu-Ser	0.695	0.687	Asp-Val	0.688	0.685
Tyr-Ala	1.13	1.10	Val-Lys	0.382	0.383
Ala-Tyr	1.08	1.14	Lys-Val	0.396	0.406
2. Uncharged Polar Sidechains			Leu-Arg	0.559	0.559
Gly-Ser	0.394	0.398	Arg-Leu	0.593	0.593
Ser-Gly	0.428	0.437	**6. Charged Polar Sidechains**		
Gly-Tyr	1.01	1.06	Asp-Lys	0.305	0.311
Tyr-Gly	1.12	1.03	Lys-Asp	0.273	0.265

Table 6.5 Comparison of Experimental and Predicted Partition Coefficients for Polyglycines in Phase System 2 of the PEG 3400/Potassium Phosphate/Water Phase Diagram at 20°C.

Peptide	Experimental	Predicted
Diglycine	0.43	0.44
Triglycine	0.41	0.41
Tetraglycine	0.40	0.37
Pentaglycine	0.39	0.34

Utilizing equations (6.6), the ratio, ω, of K values for β-lactoglobulins A and B may be expressed as

$$\omega = \frac{K_A}{K_B} = \exp\ (\ E_A - E_B) \tag{6.8}$$

where E for β-lactoglobulin (which has 162 residues) may be expressed as

$$E = \sum_{j=1}^{162} \epsilon_j + \delta_1^N + \delta_n^C \tag{6.9}$$

and E_A and E_B differ at $n = 64$ and $n = 118$ as was previously discussed. Substituting equation (6.9) into (6.8) and simplifying gives:

$$\omega = \exp\left[(\epsilon_{asp} + \epsilon_{val}) - (\epsilon_{gly} + \epsilon_{ala})\right] \tag{6.10}$$

It is interesting to note that only values of ϵ, which represent the effect of an amino acid residue on the partition coefficient, remain in the partition ratio. As was mentioned earlier, it is the value of ϵ which will be used to compare the

partition coefficients of similar proteins. When the ϵ values for aspartic acid, valine, glycine, and alanine are substituted into equation (6.10) a predicted ratio of 1.25 is obtained. The actual partition coefficients of β-lactoglobulins A and B were found to be 0.079 and 0.039, respectively, giving an experimental ratio of 2.03. The error between experimental and predicted ratios is undoubtedly due to the complex nature of the proteins and the simplicity of the predictive method.

The predictive nature of equation (6.6) was again tested using the horse and pig insulin partitioned in phase system 2. The partition coefficient for the two species was found to be 21.2 and 19.4, respectively, thus giving a partition ratio, ω, of horse to pig insulin of 1.09. The two species differ at position 9, in which the horse and pig species have glycine and serine, respectively. In order to predict the ratio of horse to pig insulin, an equation similar to that used for the β-lactoglobulins may be written:

$$\omega = \frac{K_{horse}}{K_{pig}} = \exp\left(\epsilon_{gly} - \epsilon_{ser}\right) \tag{6.11}$$

Substituting the appropriate values of ϵ into equation (6.11) yields a predicted ratio of 1.00, which agrees well with the experimental value. This prediction, which is only 9% in error, is much improved over that of the β-lactoglobulins due to the fact that glycine and serine, which have similar partitioning behavior in the system, and which both have polar uncharged sidechains, are the only differing residues in the two insulins.

6.4 Conclusions

The effect of amino acid sequence on peptide partitioning was

investigated by partitioning twenty-three pairs of reversed sequence dipeptides, β-lactoglobulins A and B, horse and pig insulin, and horse, dog and pig cytochrome c in the PEG 3400/potassium phosphate/water phase diagram at 20°C and the PEG 8000/Dextran T-500/water phase diagram at 4°C. The dipeptide partition data along with the partition coefficients measured for twenty amino acids in the above system were utilized to obtain equation (6.6) for the prediction of peptide and protein partition coefficients. The equation, which takes into account the effect of the amino acid residues rather than the pure amino acids, was used to successfully predict the partition of homogeneous glycine peptides containing two to five residues, and several tripeptides. Although the correlation is too simple to predict protein partitioning, it provides a promising start for analyzing the effect of amino acid sequence. The ratio of β-lactoglobulin A and B partition coefficients, along with the ratio of horse to pig insulin partition coefficients were predicted and compared with experimental results.

CHAPTER VII
SUMMARY OF RESULTS AND CONCLUSIONS

7.1 Thermodynamic Expressions for Phase Separation and Biomolecule Partition

Utilizing the Flory-Huggins theory of polymer solution thermodynamics, expressions were derived in Chapter II for correlating phase diagram behavior and biomolecule partitioning in aqueous polymer two-phase systems. The Flory-Huggins theory is the simplest and most basic polymer solution theory and provides a good starting point for interpreting the aqueous two-phase phenomenon. The key assumptions that had to be made were that the phase forming polymers and partitioning solutes could be treated as linear and homogeneous polymeric species in which the tertiary structure is that of a random coil, the partitioning solute concentration is small relative to that of the phase forming polymers and water, and the phase compositions do not significantly change in the presence of the partitioning solute. The following two, rather simple, relationships were then obtained for phase separation:

$$\ln (K_1) = A_1(w_1'' - w_1') \tag{7.1}$$

and

$$\ln (K_2) = A_2(w_1'' - w_1') \tag{7.2}$$

Similarly, the following simple expressions were obtained for protein

partitioning:

$$\ln (K_3) = A(w_1'' - w_1') \tag{7.3}$$

and

$$\frac{\ln (K_3)}{(w_1'' - w_1')} = A^* + b^*(w_1'' - w_1') \tag{7.4}$$

The above expressions incorporate the polymer concentrations in the phases, the molecular weight of the species present, the interactions among the species present, and, in the case of the biomolecule correlations, the electrostatic potential difference between the phases. In Chapters III–V, these relationships were verified through the use of aqueous polymer phase diagrams, and dipeptide and protein partitioning.

7.2 Phase Diagrams

Phase diagram data were obtained for PEG/dextran/water systems at 4°C, 10°C and 22°C, and PEG/potassium phosphate/water systems at 4°C and pH 6.0, 7.0, 8.0 and 9.2., and the results were recorded in Chapter III. Since purification of labile biomolecules frequently occurs at low temperatures, the data at 4°C and 10°C are of extreme importance for biochemical research. The data at 22°C are also extremely valuable since aqueous two-phase systems may be used at room temperature without endangering the activity of biomolecules (due to the stabilizing effect of the polymers on the biomolecule). This phase diagram data are in agreement with experimental phase diagrams and qualitative predictions available in the literature. The PEG/dextran/water,

PEG/potassium phosphate/water phase diagram data presented in Chapter III, and Ficoll 400/Dextran T-500/Water data obtained from the literature were shown to correlate well with equations (7.1) and (7.2). For the PEG/dextran/water systems the slope A_1 was not significantly effected by dextran molecular weight but increased slightly as PEG molecular weight increased. The slope A_2 decreased when either dextran molecular weight or PEG molecular weight increased. An increase in temperature of a PEG 8000/Dextran T-500/water system had no effect on A_1 while A_2 became more negative.

For the PEG/potassium phosphate/water systems, the slope A_2 was found to be independent of PEG molecular weight. The slope A_1 was shown to deviate slightly from equation (7.1), most probably due to the high interfacial potential which exists in these systems.

7.3 Linear Semilogarithmic Partitioning of Biomolecules

Based on the linear semilogarithmic relationship of equation (7.3), which was derived from the Flory-Huggins theory, a simple means was devised (in Chapter IV) for correlating low molecular weight solute and protein partitioning. The relationship was verified for PEG/dextran/water systems utilizing dipeptides and proteins as partitioning solutes. From the dipeptide partitioning, it was found that knowledge of the partition coefficient in only one of the PEG/dextran/water systems, regardless of polymer molecular weight, enabled prediction of the coefficient in all of the systems. The values of the slope A for the dipeptides permitted the determination of the Gibbs free energy of transfer for a CH_2 group and thus, the hydrophobicity in the PEG/dextran/water systems. As the tie line length increased the

hydrophobicity was shown to increase. In addition, the effect of a CH_2 group on dipeptide partitioning could be qualitatively explained in terms of the interaction parameter, χ_{ij}. As a CH_2 group was added to the c-terminal residue, the slope A became less negative due to a small increase in χ_{13} (interaction between PEG and dipeptide) and a large increase in χ_{03} (interaction between water and dipeptide) and χ_{23} (interaction between dextran and dipeptide).

Protein distribution indicated that the relationship of equation (7.3) holds up to a molecular weight of approximately 25,000, above which nonlinearities become important. The parameter A was shown to increase as dextran molecular weight increased, and increase as PEG molecular weight decreased. For the low molecular weight proteins, knowledge of the partition coefficient at one tie line composition of a phase diagram enabled determination of the coefficient at other tie lines of the same diagram.

7.4 Generalized Partition Expression

Based on the relationship of equation (7.4), which was derived from a modified form of the Flory-Huggins theory, a simple means was devised (in Chapter V) for correlating both low and high molecular weight protein partitioning in aqueous polymer two phase systems. The relationship was verified for PEG/dextran/water, PEG/potassium phosphate/water and Ficoll 400/Dextran T-500/water systems utilizing seventeen proteins covering a broad range of molecular weight, along with protein partition data from the literature. The effect of phase forming polymer molecular weight on the parameters was investigated. The A^* parameter of the correlating equation was shown to increase as dextran molecular weight increased, and increase as PEG molecular

weight decreased. No definite molecular weight trend could be observed for b^*. In addition, A^* and b^* were shown to be linearly related to reciprocal absolute temperature. Equation (7.4) will simplify the selection of an appropriate aqueous two-phase system for protein purification since only two partition coefficients need to be measured in order to obtain the parameters of the equation, and thus have a clear picture of partition trends in an aqueous two-phase system.

7.5 Protein Structural Effect on the Partition Coefficient

The effect of amino acid sequence on peptide partitioning was investigated in Chapter VI by partitioning twenty-three pairs of reversed sequence dipeptides, β-lactoglobulins A and B, horse and pig insulin, and horse, dog and pig cytochrome c in the PEG 3400/potassium phosphate/water phase diagram at 20°C and the PEG 8000/Dextran T-500/water phase diagram at 4°C. In addition, the sensitivity of the PEG 3400/potassium phosphate/water phase diagram was further demonstrated by the partitioning of reversed sequence dinucleotides. The dipeptide partition data along with the partition coefficients measured for twenty amino acids in the above system were utilized to obtain the following equation:

$$E = \sum_{j=1}^{n} (E_j - \delta_j^N - \delta_j^C) + \delta_1^N + \delta_n^C = \sum_{j=1}^{n} \epsilon_j + \delta_1^N + \delta_n^C \qquad (7.5)$$

for the prediction of peptide and protein partition coefficients. The equation, which takes into account the effect of the amino acid residues rather than the pure amino acids, was used to successfully predict the partition of homogeneous glycine peptides containing two to five residues and several tripeptides.

Although the correlation is too simple to predict protein partitioning, it provides a promising start for analyzing the effect of amino acid sequence. The ratio of β-lactoglobulin A and B partition coefficients, along with the ratio of horse to pig insulin partition coefficients, were predicted and compared rather favorably with experimental results.

CHAPTER VIII
RECOMMENDATIONS FOR FUTURE WORK

Aqueous polymer two-phase technology is a relatively new area for both basic and applied research to be performed by scientists and engineers. Not only can the systems be used for the purification and analysis of biomolecules, they can be applied to any substance which has solubility in water. For this reason, there is an unlimited number of applications for these systems. With this in mind, the possible areas for future research have been divided into five areas.

1. The most fundamental data for any type of liquid-liquid extraction process is the phase diagram. For this reason it is suggested that more phase diagrams be determined, in particular for the PEG/salt/water systems, which are highly effective two-phase extraction systems. In addition, multicomponent phase diagrams should be determined, i.e., water (0)/polymer (1)/polymer or salt (2)/proteins (3). This data will be extremely interesting since the presence of a protein or proteins will alter the phase equlibrium compositions of the three component system (absence of protein). Such data will be helpful for the eventual scale-up of aqueous two-phase extraction processes.

2. In this dissertation and in the literature, partition coefficients have been measured primarily for pure biological materials. Thus, there is a need for fundamental multicomponent protein partition data. Studies are needed to determine how the presence of a variety of proteins effect the partition

coefficient of a protein of interest.

3. One of the obstacles plaguing the widespread use of aqueous two-phase systems is the need for a methodology to select an optimal system for the purification of a desired biological material. Future research should involve the development of advanced thermodynamic models which would facilitate the selection of appropriate two-phase systems. Such models should adequately describe the partition phenomenon, and enable the prediction of binodials and partition coefficients with a minimum of experimental data.

4. In Chapter II it was shown that the electrostatic potential difference ($\Delta\psi$) is needed in order to correlate biomolecule partition coefficients in aqueous two-phase systems. The $\Delta\psi$ results from the fact that anions and cations will have different affinities for the two phases, although there is a requirement of electroneutrality in each phase. These two competing phenomena result in $\Delta\psi$. Electrostatic potential difference data are, at present, scarce in the literature. Therefore it is proposed that $\Delta\psi$ measurements be performed for a variety of two-phase systems at a variety of environmental conditions. In particular it would be interesting to find out if the second order relationship proposed in Chapter II between $\Delta\psi$ and the polymer concentration difference between the phases is valid for systems other than the PEG/dextran/water systems.

5. One way to improve productivity of enzymatic conversions is to continuously extract product, thus altering the environment to favor greater conversion. This extractive bioconversion may be accomplished through the use of, for example, organic solvents or aqueous two-phase systems. Aqueous two-

phase systems provide an excellent system for bioconversion because not only can the product be continuously extracted, the phase forming polymers have a tendency to stabilize and even enhance biocatalytic activity. Future research would be to study extractive bioconversions using aqueous two-phase systems. The goals of this research should be to develop a model and determine the kinetic and extraction parameters for the bioconversion and their sensitivity. Using these parameters, a theoretical estimate can be made for productivity increase. In addition, estimation of kinetic criteria for further development and large-scale production should be explored.

NOMENCLATURE

$A = m_3\left(\alpha_1\left(\frac{1}{m_1} - 1 + \chi_{03} - \chi_{13} + \chi_{01}\right) + \alpha_2\phi\left(\frac{1}{m_2} - 1 + \chi_{03} - \chi_{23} + \chi_{02}\right)\right)$

$A_1 = m_1\left(\alpha_1\left(\frac{1}{m_1} - 1 + 2\chi_{01}\right) + \alpha_2\phi\left(\frac{1}{m_2} - 1 + \chi_{01} + \chi_{02} - \chi_{12}\right)\right)$

$A_2 = m_2\left(\alpha_2\phi\left(\frac{1}{m_2} - 1 + 2\chi_{02}\right) + \alpha_1\left(\frac{1}{m_1} - 1 + \chi_{02} + \chi_{01} - \chi_{12}\right)\right)$

$A^* = A + \frac{z_b F g}{RT}$

$b = m_3(\chi_{02}\alpha_2^2\phi^2 - \chi_{01}\alpha_1^2)$

$b^* = b + \frac{z_b F h}{RT}$

$E = \ln(K_i)$

$E_i = \ln(K_i)$

F = Faraday constant

g = regression parameter in the relation between ψ and $(w_1'' - w_1')$

h = regression parameter in the relation between ψ and $(w_1'' - w_1')$

K = v_i''/v_i', partition coefficient for species i

K_i = v_i''/v_i', partition coefficient for species i

k = Boltzman's Constant

m_i = molar volume ratio of species i to that of water

M = molarity

m = molality

N_A = Avagadro's number

N_{CH_2} = number of CH_2 groups on the c-terminal residue of a dipeptide

n_i = number of molecules of species i

n = number of amino acid residues in a polypeptide or protein

P = pressure

R = gas law constant

T = absolute temperature

$\overline{V}_i$ = partial specific volume of species i, ml/g

v_i = volume fraction of species i

w_i = weight fraction of species i

z = lattice coordinate number

z_b = charge of a biomolecule

Greek Letters

α_i = $\rho\overline{V}_i$, proportionality factor between volume and weight fraction for species i

γ^* = $m_3\left(\frac{\alpha_1}{m_1} + \frac{\alpha_2\phi}{m_2} - (\alpha_1 + \alpha_2\phi)\right)$

ΔG° = standard state Gibbs free energy change

ΔG_m = Gibbs free energy of mixing

$\Delta G_{tr}^{CH_2}$ = Gibbs free energy of transfer of a CH_2 group, J/mol

ΔH_m = enthalpy change on mixing

ΔS_m = entropy change on mixing

Δw_{ij} = energy change for the formation of a contact between species i and j

$\Delta\psi$ = electrostatic potential difference between the phases

$$\delta^* = m_3\frac{z}{k}\Big((\alpha_1 + \alpha_2\phi)\Delta w_{03} - \alpha_1\Delta w_{13}m_1 - \alpha_2\phi\Delta w_{23}m_2 + \alpha_1\Delta w_{01} + \alpha_2\phi\Delta w_{02} + \frac{z_b F g}{m_3 z N_A}\Big)$$

δ_j^C = C-terminal correction factor for amino acid j

δ_j^N = N-terminal correction factor for amino acid j

$$\epsilon^* = m_3\frac{z}{k}\left(\Delta w_{02}\alpha_2^2\phi^2 - \Delta w_{01}\alpha_1^2 + \frac{z_b F h}{m_3 z N_A}\right)$$

$\epsilon_j = E_j - \delta_j^C - \delta_j^N$

μ_i = chemical potential for species i

μ_i° = standard state chemical potential for species i

ρ = density

$$\phi = \frac{w_2'' - w_2'}{w_1'' - w_1'}$$

χ_{ij} = Flory-Huggins interaction parameter between species i and j

ψ = electrostatic potential

ω = K_i/K_j, ratio of partition coefficients of two species

Superscripts

" = top phase

' = bottom phase

Subscripts

0 = water

1 = PEG in the PEG/dextran/water and PEG/potassium phosphate/water systems; dextran in the ficoll/dextran/water system.

2 = dextran in the PEG/dextran/water system; potassium phosphate in the PEG/potassium phosphate/water system; ficoll in the ficoll/dextran/water system

3 = biomolecule

B = amino acid B

BX = dipeptide composed of amino acids B and X

i = component i

j = component j

X = amino acid X

REFERENCES

1. **Abbot**, N. L., and T. A. Hatton, "Liquid-Liquid Extraction of Biomolecules," *Chem. Eng. Prog.*, **84**, 31 (1988).

2. **Abrams**, D. S., and J. M. Prausnitz, "Statistical Thermodynamics of Liquid Mixtures: A New Expression for the Excess Gibbs Energy of Partly or Completely Miscible Systems," *AIChE J.*, **21**(1), 116 (1975).

3. **Albertsson**, P.-Å., *Partition of Cell Particles and Macromolecules*, 2nd ed., John Wiley & Sons, New York (1971).

4. **Albertsson**, P.-Å, "History of Aqueous Polymer Two-Phase Systems," *Partitioning in Aqueous Two-Phase Systems. Theory, Methods, Uses and Applications to Biotechnology*, H. Walter, D. E. Brooks, and D. Fisher, eds., Academic Press, Orlando (1985).

5. **Albertsson**, P.-Å., *Partition of Cell Particles and Macromolecules*, 3rd ed., John Wiley & Sons, New York (1986).

6. **Albertsson**, P.-Å., A. Cajarville, D. E. Brooks, and F. Tjerneld, "Partition of Proteins in Aqueous Polymer Two-Phase Systems and the Effect of Molecular Weight of the Polymer," *Biochim. Biophys. Acta*, **926**, 87 (1987).

7. **Albertsson**, P.-Å., S. Sasakawa, and H. Walter, "Cross Partition and Isoelectric Points of Proteins," *Nature* (London), **228**, 1329 (1970).

8. **Andreasen**, P. A., "A Specific Adenine Nucleotide Effect on the Rat Liver Glucocorticoid Receptor, Demonstrated by Aqueous Two=Phase Partitioning," *Biochim. Biophys. Acta*, **676**, 205 (1981).

9. **Andreasen**, P. A., and Gehring, U. "Activation and Partial Proteolysis of Variant Glucocorticoid Receptors, Studied by Two-Phase Partitioning," *Eur. J. Biochem.*, **120**, 443 (1981).

10. **Bamberger**, S., G. V. F. Seaman, J. A. Brown, and D. E. Brooks, "The Partition of Sodium Phosphate and Sodium Chloride in Aqueous Dextran Poly(ethylene glycol) Two-Phase Systems," *J. Colloid Interface Sci.*, **99**, 187 (1984).

11. **Baskir**, J. N., T. A. Hatton, and U. W. Suter, "Thermodynamics of the Separation of Biomaterials in Two-Phase Aqueous Polymer Systems: Effect of Phase Forming Polymers," *Macromolecules*, **20**, 1300 (1987).

12. **Baskir**, J. N., T. A. Hatton, and U. W. Suter, "Protein Partitioning in Two-Phase Aqueous Polymer Systems," *Biotech. Bioeng.*, **34**, 541 (1989).

13. **Beijerinck**, M. W., "Ueber une Eigentumlichkeit der loslichen Starke," *Zbl. Bakt.*, **2**, 627 (1896).

14. **Beijerinck**, M. W., "Ueber Emulsionsbildungbei der vermischung wässeriger Lösunger gewisser gelatinierender Kolloide," *Kolloid-Z.*, 7, 16 (1910).

15. **Bohlen**, P., W. Dairman, and S. Udenfriend, "Fluormetric Assay of Proteins in the Nanogram Range," *Arch. Biochem. Biophys.*, **155**, 213 (1973).

16. **Brooks**, D. E., K. A. Sharp, S. Bamberger, C. H. Tamblyn, G. V. F. Seaman, and H. Walter, "Electrostatic and Electrokinetic Potentials in Two Polymer Aqueous Phase Systems," *J. Colloid Interface Sci.*, **102**, 1 (1984).

17. **Brooks**, D. E., K. A. Sharp, and D. Fisher, "Theoretical Aspects of Partitioning," *Partitioning in Aqueous Two-Phase Systems. Theory, Methods, Uses and Applications to Biotechnology*, H. Walter, D. E. Brooks, and D. Fisher, eds., Academic Press, Orlando (1985).

18. **Carlson**, A., "Factors Influencing the Use of Aqueous Two-Phase Partition for Protein Purification," *Sep. Sci. Tech.*, **23**(8&9), 785 (1988).

19. **Craig**, L. C., and D. Craig, in *Techniques of Organic Chemistry, Vol. III*, A. Weissberger, ed., Interscience, NY (1956).

20. **Diamond**, A. D., and J. T. Hsu, "Fundamental Studies of Biomolecule Partitioning in Aqueous Two-Phase Systems," *Biotech. Bioeng.*, **34**, 1000 (1989a).

21. **Diamond**, A. D., and J. T. Hsu, "Phase Diagrams for Dextran-PEG Aqueous Two-Phase Systems at 22°C," *Biotech. Techn.*, **3**, 119 (1989b).

22. **Diamond**, A. D., X. Lei, and J. T. Hsu, "Reversing the Amino Acid Sequence of a Dipeptide Changes its Partition in an Aqueous Two-Phase System," *Biotech. Techn.*, **3**, 271 (1989).

23. **Diamond**, A. D., and J. T. Hsu, "Protein Partitioning in PEG/Dextran Aqueous Two-Phase Systems," *AIChE J.*, **36**(7), 1017 (1990a),

24. **Diamond**, A. D., and J. T. Hsu, "Correlation of Protein Partitioning in Aqueous Two-Phase Systems," *J. Chromatogr.*, **513**, 137 (1990b).

25. **Diamond**, A. D., K. Yu, and J. T. Hsu, "The Effect of Amino Acid Sequence on Peptide and Protein Partitioning in Aqueous Two-Phase Systems," *ACS Symposium Series*, **427**, 52 (1990).

26. **Dobry**, A., and F. Boyer-Kawenoki, "Phase Separation in Polymer Solution," *J. Polym. Sci.*, **2**, 90 (1947).

27. **Edmond**, E., and A. G. Ogston, " An Approach to the Study of Phase Separation in Ternary Aqueous Systems," *Biochem. J.*, **109**, 569 (1968).

28. **Fisher**, D. and A. Sutherland, eds., *Separations Using Aqueous Phase Systems. Applications in Cell Biology and Biotechnology*, Plenum Press, NY, 1989.

29. **Flory**, P. J., "Thermodynamics of High Polymer Solutions," *J. Chem. Phys.*, **9**, 660 (1941).

30. **Flory**, P. J., *Principles of Polymer Chemistry*, Cornell University Press, Ithaca, NY (1953).

31. **Gustafsson**, Å., and H. Wennerström, "The Nature of Phase Separation in Aqueous Two-Polymer Systems," *Polymer*, **27**, 1768 (1986).

32. **Hansen**, J. C., and J. Gorski, "Conformational and Electrostatic Properties of Unoccupied and Ligated Estrogen Receptors Determined by Aqueous Two-Phase Partitioning," *Biochem.*, **24**, 6078 (1985).

33. **Hopp**, T. P., and K. R. Woods, "Prediction of Protein Antigenic Determinants from Amino Acid Sequences," *Proc. Natl. Acad. Sci. USA*, 78, 3824 (1981).

34. **Huggins**, M. L., "Solutions of Long Chain Compounds," *J. Chem. Phys.*, **9**, 440 (1941).

35. **Hustedt**, H., K. H. Kroner, W. Stach, and M.-R. Kula, "Procedure for Simultaneous Large Scale Isolation of Pullulanase and 1,4-α-Glucan Phosphorylase from *Kebsiella pneumoniae* Involving Liquid-Liquid Separations," *Biotech. Bioeng.*, **20**, 1989 (1978).

36. **Hsu**, C. C., and J. M. Prausnitz, "Thermodynamics of Polymer Compatibility in Ternary Systems," *Macromolecules*, 7, 320 (1974).

37. **Johansson**, G., "Partition of Salts and their Effects on Partition of Proteins in a Dextran-Poly(ethylene glycol)-Water Two-Phase System," *Biochim. Biophys. Acta*, **221**, 387 (1970).

38. **Johansson**, G., "Partition of Proteins and Micro-organisms in Aqueous Biphasic Systems," *Molec. Cell Biochem.*, **4**, 169 (1974).

39. **Johansson**, G., and M. Andersson, "Parameters Determining Affinity Partitioning of Yeast Enzymes Using Polymer-Bound Triazine Dye Ligands," *J. Chromatogr.*, **303**, 39 (1984).

40. **Kang**, C. H., and S. I. Sandler, "Phase Behavior of Aqueous Two-Polymer Systems," *Fluid Phase Equil.*, **38** (1987).

41. **King**, R. S., H. W. Blanch, and J. M. Prausnitz, "Molecular Thermodynamics of Aqueous Two-Phase Systems for Bioseparations," *AIChE J.*, **34** (10), 1585 (1988).

42. **Kroner**, K. H., H. Hustedt, and M.-R. Kula, "Evaluation of Crude Dextran as Phase-Forming Polymer for the Extraction of Enzymes in Aqueous Two-Phase Systems in Large Scale," *Biotech. Bioeng., 24, 1015 (1982).*

43. **Kroner**, K. H., H. Hustedt, and M.-R. Kula, "Extraction Enzyme Recovery: Economic Considerations," *Process Biochem.*, **19**, 170 (1984).

44. **Kyte**, J., and R. F. Doolittle, "A Simple Method for Displaying the Hydropathy Character of a Protein," *J. Mol. Biol.*, **157**, 105 (1982).

45. **Lehninger**, A. L., *Principles of Biochemistry*, Worth Publishers, Inc., New York (1982).

46. **Lei**, X., A. D. Diamond, and J. T. Hsu, "Equilibrium Phase Behavior of the Polyethylene Glycol/Potassium Phosphate/Water Two-Phase System at 4°C," *J. Chem. Eng. Data*, **35**, 420 (1990).

47. **Righetti**, P. G., and T. J. Caravaggio, "Isoeletric Points and Molecular Weights of Proteins, a Table," *J. Chromatogr.*, **127**, 1 (1976).

48. **Sasakawa**, S., and H. Walter, "Blood Clam (*Anadara inflata) Red Cells.* Partition in Aqueous Two-Polymer Phase Systems," *Biochim Biophys. Acta*, **244**, 452 (1971).

49. **Sasakawa**, S., and H. Walter, "Partition Behavior of Native Proteins in Aqueous Dextran-Poly(ethylene glycol) Phase Systems," *Biochem.*, **11**, 2760 (1972).

50. **Sasakawa**, S., and H. Walter, "Partition Behavior of Amino Acids and Small Peptides in Aqueous Dextran-Poly(ethylene glycol) Phase Systems," *Biochem.*, **13**, 29 (1974).

51. **Scheutjens**, J. M. H. M., and G. J. Fleer, "Statistical Theory of the Adsorption of Interacting Chain Molecules. 1. Partition Function, Segment Density Distribution, and Adsorption Isotherms," *J. Phys. Chem.*, **83**, 1619 (1979).

52. **Scheutjens**, J. M. H. M., and G. J. Fleer, "Statistical Theory of the Adsorption of Interacting Chain Molecules. 2. Train, Loop, and Tail Size Distribution," *J. Phys. Chem.*, **84**, 178 (1980).

53. **Schürch**, S., D. F. Gerson, and D. J. L. McIver, "," *Biochem. Biophys. Acta*, **640**, 557 (1981).

54. **Shanbhag**, V. P., and C. G. Axelsson, "Hydrophobic Interaction Determined by Partition in Aqueous Two-Phase Systems. Partition of Proteins in Systems Containing Fatty-Acid Esters of Poly(ethylene glycol)," *Eur. J. Biochem.*, **60**, 17 (1975).

55. **Sober**, H. A., ed., *CRC Handbook of Biochemistry. Selected Data for Molecular Biology*, The Chemical Rubber Co., Cleveland, OH (1968).

56. **Svehla**, G., ed., *Comprehensive Analytical Chemistry, Vol. XIV*, Elsevier Pub. Co., NY (1982).

57. **Tjerneld**, F., G. Johansson, and M. Joelsson, "Affinity Liquid-Liquid Extraction of Lactate Dehydrogenase on a Large Scale," *Biotech. Bioeng.*, **30**, 809 (1987).

58. **Walstra**, P., and R. Jenness, *Dairy Chemistry and Physics*, John Wiley and Sons, New York (1984).

59. **Walter**, H., E. J. Jrob, and D. E. Brooks, "Membrane Surface Properties other than Charge Involved in Cell Separation by Partition in Polymer, Aqueous Two-Phase Systems," *Biochem.*, **15**, 2959 (1976).

60. **Walter**, H., D. E. Brooks, and D. Fisher, eds., *Partitioning in Two-Phase Aqueous Systems. Theory, Methods, Uses and Applications to Biotechnology*, Academic Press, Orlando (1985).

61. **Zaslavsky**, B. Yu., L. M. Miheeva, N. M. Mestchkina, V. M. Pogorelov, and S. V. Rhogozhin, "General Rule of Partition Behaviour of Cells and Soluble Substances in Aqueous Two-Phase Polymeric Systems," *FEBS Lett.*, **94**, 77 (1978).

62. **Zaslavsky**, B. Yu., L. M. Miheeva, and S. V. Rhogozhin, "Relative Hydrophobicity of Surfaces of Erythrocytes from Different Species as Measured by Partition in Aqueous Two-Polymer Phase Systems," *Biochim. Biophys. Acta*, **588**, 89 (1979).

63. **Zaslavsky**, B. Yu., L. M. Miheeva, N. M. Mestechkina, and S. V. Rogozhin, "Physico-Chemical Factors Governing Partition Behavior of Solutes and Particles in Aqueous Polymeric Biphasic Systems. I. Effect of Ionic Composition on the Relative Hydrophobicity of the Phases," *J. Chromatogr.*, **253**, 139 (1982a).

64. **Zaslavsky**, B. Yu., L. M. Miheeva, N. M. Mestechkina, and S. V. Rogozhin, "Physico-Chemical Factors Governing Partition Behavior of Solutes and Particles in Aqueous Polymeric Biphasic Systems. II. Effect of Ionic Composition on the Hydration Properties of the Phases," *J. Chromatogr.*, **253**, 149 (1982b).

65. **Zaslavsky**, B. Yu., L. M. Miheeva, N. M. Mestechkina, and S. V. Rogozhin, "Physico-Chemical Factors Governing Partition Behavior of Solutes and Particles in Aqueous Polymeric Biphasic Systems. III. Features of Solutes and Biological Particles Detected by the Partition Technique," *J. Chromatogr.*, **256**, 49 (1983).

66. **Zaslavsky**, B. Yu., and L. M. Miheeva, "Effect of Polymer Composition on the Relative Hydrophobicity of the Phases of the Biphasic System Aqueous Dextran-Poly(Ethylene Glycol)," *J. Chromatogr.*, **404**, 123 (1987).

67. **Zaslavsky**, B. Yu., T. O. Bagirov, A. A. Borovskaya, N. D. Gulaeva, L. H. Miheeva, A. U. Mahmudov, M. N. Rodnikova, "Structure of Water as a Key Factor of Phase Separation in Aqueous Mixtures of Two Nonionic Polymers," *Polymer*, **30**, 2104 (1989).

VITA

Alan Diamond, son of Mr. and Mrs. Marvin Diamond was born on October 18, 1964, in Manhattan, NY. His undergraduate studies were done at the Georgia Institute of Technology, where, in June of 1986 he received a bachelor of science degree in chemical engineering with highest honors. In September of 1986, he began his graduate research at Lehigh University. During his studies at Lehigh, he received an Air Products Research Fellowship and a National Institutes of Health Fellowship. In addition, he published seven papers in peer reviewed journals and presented five papers at internationally recognized conferences.

J. T. Hsu and A. D. Diamond, "Fundamental Studies of Peptide Separation by Aqueous Two-Phase Systems," presented at the AIChE Annual Meeting, Washington, D. C., Nov. 22–Dec. 2 (1988).

A. D. Diamond and J. T. Hsu, "Fundamental Studies of Biomolecule Partitioning in Aqueous Two-Phase Systems," *Biotechnology and Bioengineering*, **34**, 1000 (1989).

A. D. Diamond and J. T. Hsu, "Phase Diagrams for Dextran-PEG Aqueous Two-Phase Systems at 22°C," *Biotechnology Techniques*, **3**(2), 119 (1989).

A. D. Diamond, X. Lei, and J. T. Hsu, "Reversing the Amino Acid Sequence of a Dipeptide Changes its Partition in an Aqueous Two-Phase System," *Biotechnology Techniques*, **3**(4), 271 (1989).

A. D. Diamond and J. T. Hsu, "Fundamental Studies of Protein Separation in Aqueous Two-Phase Systems," presented at the International Conference on Separations Technology, Davos, Switzerland, May 14–19 (1989).

A. D. Diamond and J. T. Hsu, "Fundamental Studies of Protein Separation in Aqueous Two-Phase Systems", presented at the 6th International Conference on Partitioning in Aqueous Two-Phase Systems, ABmannshausen/Rhein, West Germany, August 27 – September 1 (1989).

J. T. Hsu and A. D. Diamond, "The Effect of Amino Acid Sequence on Protein Partitioning in Aqueous Two-Phase Systems," presented at the ACS Meeting, Miami Beach, FL, September 10–15 (1989).

A. D. Diamond and J. T. Hsu, "Protein Partitioning in PEG/Dextran Aqueous Two-Phase Systems," *AIChE Journal*, **36**(7), 1017 (1990).

Diamond, A. D., K. Yu, and J. T. Hsu, "The Effect of Amino Acid Sequence on Peptide and Protein Partitioning in Aqueous Two-Phase Systems," *ACS Symposium Series*, **427**, 52 (1990).

A. D. Diamond and J. T. Hsu, "Correlation of Protein Partitioning in Aqueous Polymer Two-phase Systems," *Journal of Chromatography*, **513**, 137 (1990).

X. Lei, A. D. Diamond, and J. T. Hsu, "Equilibrium Phase Behavior of the Polyethylene Glycol/Potassium Phosphate/Water Two-Phase System at 4°C," *Journal of Chemical and Engineering Data*, **35**, 420 (1990).

A. D. Diamond and J. T. Hsu, "Generalized Correlation of Protein Partitioning in Aqueous Polymer Two-Phase Systems," presented at the AIChE Annual Meeting, Chicago, IL, Nov. 11–16 (1990).